

HOST DEFENSE PEPTIDES AND COPPER(II) IONS: NOVEL THERAPEUTIC OPPORTUNITIES

Jasmin Portelinha,^{†,‡} Searle S. Duay,^{†,¶,‡} Seung I. Yu,[¶] Kara Heilemann,[†] M. Daben J. Libardo,[†] Samuel A. Juliano,[†] M. Jonathan L. Klassen,^{*,†} Alfredo M. Angeles-Boza^{*,†,§}

[†]These authors contributed equally.

[†]Department of Chemistry, University of Connecticut, 55 N. Eagleville Road, Storrs, CT 06269

^{*}Chemistry Department, Adamson University, 900 San Marcelino St., Ermita, Manila, Philippines 1000

[¶]Department of Molecular and Cell Biology, University of Connecticut, 91 N. Eagleville Road, Storrs, CT 06269

[§]Institute of Material Science, University of Connecticut, 55 N. Eagleville Road, Storrs, CT 06269

CONTENTS

1. Introduction

1.1 Antimicrobial Peptides

1.2 Introduction to the Mechanism of Action of AMPs

1.3 Role of Copper in the Immune System

2. Biophysical Methods for Characterization of AMPs

2.1 Circular dichroism (CD)

2.2 UV-Vis titration

2.3 Isothermal Titration Calorimetry (ITC)

2.4 Fluorescence Microscopy

2.5 Determination of Three-Dimensional Structure of AMPs

2.6 Molecular Dynamics (MD) Simulations

2.6.1 Equilibrium simulations

2.6.2 Non-equilibrium simulations

2.6.3 Molecular Dynamics of ATCUN-containing AMPs

3. The Amino Terminal Copper and Nickel (ATCUN) Binding Motif and its Role in Immunity

3.1 BLAST sequence homology network

3.2 Ixosin and other insect AMPs

3.3. Piscidins: archetypal metalloAMPs

3.4 Peptides from tunicates

3.4.1 Metal-binding peptides from tunicates

3.4.2 Clavanins

3.5 Human Peptides

3.6 Amphibian ATCUN-AMPs

3.6.1 Tachykinin and neuro-active peptides

3.6.2 Limnonectins

3.6.3 Nigroains

3.6.4 Temporins

3.6.5 Other amphibian ATCUN-peptides

3.7 Mussel AMPs

3.7.1 Myticins

3.7.2 Mytilins

3.7.3 Mytimycins and Mytichitins

3.7.4 Myticusin

3.7.5 Defensins and Big Defensins

3.7.6 Mytimacins

3.8 AMPs from Bacteria: Bacteriocins

4. Designing ATCUN-AMPs

5. Outlook and Challenges

ABSTRACT

The emergence of new pathogens and multidrug resistant bacteria is an important public health issue that requires the development of novel classes of antibiotics. Antimicrobial peptides (AMPs) are a promising platform with great potential for the identification of new lead compounds that can combat the aforementioned pathogens due to their broad-spectrum antimicrobial activity and relatively low rate of resistance emergence. AMPs of multicellular organisms made their debut four decades ago thanks to ingenious researchers who asked simple questions about the resistance to bacterial infections of insects. Questions such as “Do fruit flies ever get sick?”, combined with pioneering studies, have led to an understanding of AMPs as universal weapons of the immune system. This review focuses on a sub-class of AMPs that feature a metal binding motif known as the Amino Terminal Copper and Nickel (ATCUN) motif. One of the metal-based strategies of hosts facing a pathogen, it includes wielding the inherent toxicity of copper and deliberately trafficking this metal ion into sites of infection. The sudden increase in the concentration of copper ions in the presence of ATCUN-containing AMPs (ATCUN-AMPs) likely results in a synergistic interaction. Herein, we examine common structural features in ATCUN-AMPs that exist across species, and we highlight unique features that deserve additional attention. We also present the current state of knowledge about the molecular mechanisms behind their antimicrobial activity and the methods available to study this promising class of AMPs.

1. Introduction

Antibiotics are the most successful form of chemotherapy in modern human medicine. However, concern over the emergence of antibiotic-resistant bacterial strains has led to increased interest in developing agents with unique modes of action. In his 1945 Nobel lecture, Alexander Fleming was already warning humanity on the possibility of microbes becoming resilient to antibiotics.¹ Now, 75 years later, we fear that we are at the edge of the antibiotic era due to the rapid emergence of resistant microorganisms.^{2,3} The problem of resistance is compounded by the fact that few antibiotics have been licensed for clinical use in recent years.⁴ As our society flirts with a post-antibiotic era, some estimates indicate that in 2050, 10 million people are expected to die annually due to antibiotic-resistant microbial infections. It is therefore imperative to evaluate new chemistries.⁵

1.1 Antimicrobial Peptides (AMPs)

Due to their broad-spectrum activity, antimicrobial peptides (AMPs) have arisen as an important model for the design of novel antibiotics.^{6,7} AMPs are also known as host defense peptides, a term reserved for naturally occurring peptides that are essential innate host defense effector molecules in a variety of tissues and cell types of virtually every form of life, from bacteria and fungi to invertebrates, plants, and vertebrates.⁸ The diversity of AMP sequences is salient, likely a consequence of adaptation strategies by both hosts and pathogens that have evolved over millions of years. Indeed, AMPs belong to the most rapidly evolving families of biosynthetic products,⁹ but the reasons behind AMP diversity are poorly understood.¹⁰ Understanding how this ancient arm of host immunity remains effective against pathogenic microbial communities is of the utmost importance, as it resembles our current crisis managing the emergence of antibiotic resistance via new drug development for the treatment of bacterial infections.

The field of AMP research started with a basic question about why fruit flies do not get sick.¹¹ Boman and colleagues eventually studied the giant silk moth *Hyalophora cecropia* due to its inducible immunity, ease to work with, and ability to yield large volumes of hemolymph.¹¹ The first AMPs, cecropin A and B, were discovered in the hemolymph of *H. cecropia* and were called inducible bacteriolytic proteins.¹² The original cecropins are 37-amino acid peptides that have 66% sequence homology with a basic N-terminus and a hydrophobic center.¹³ Both AMPs were found to be active against several Gram-negative bacteria, including *Escherichia coli* and *Pseudomonas aeruginosa*, and Gram-positive bacteria, where cecropin B was most active against *Bacillus subtilis*.^{12,13} Shortly after the discovery of the cecropins, two defensins were isolated in rabbit alveolar macrophages by the Lehrer group.¹⁴ They went on to study six other defensins from rabbit granulocytes that had broad-spectrum activities.¹⁵ Three human neutrophil defensins were found in humans and were similar to the rabbit defensins, in that they had six conserved Cys residues that formed three disulfide bonds and shared a total of 11 conserved residues including several Arg residues.¹⁶ Subsequent studies soon revealed more AMPs in vertebrates after an observation that frogs could avoid infection and heal wounds despite being in a non-sterile water tank.¹⁷ From *Xenopus laevis* skin, Zasloff isolated magainin 1 and 2, which are 23 residue AMPs that have broad-spectrum activity.¹⁷ Magainin 2 has been heavily studied as an α -helical membrane active peptide and has an analog peptide called pexiganan that was developed as a topical treatment for diabetic foot ulcers.¹⁸⁻²⁴ The subsequent discovery of tachyplesin was one of the first AMPs that were discovered in invertebrate species. Horseshoe crab *Tachypleus tridentatus* hemocytes

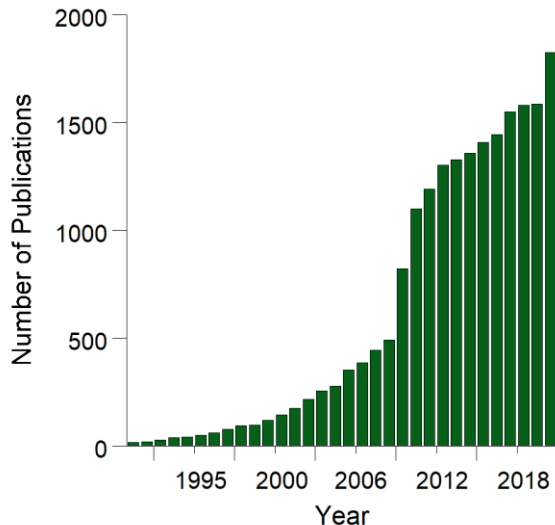


Figure 1. The number of publications from 1990 to 2020 resulting from a search using the keywords “antimicrobial peptides” in SciFinder® shows the increase of interest in the field. Search date: January 12, 2021.

contained tachyplesin, a 17 residue, C-terminally amidated AMP.²⁵ Tachyplesin had a high affinity for binding lipopolysaccharides (LPS) but showed activity against both Gram-negative and -positive bacteria.²⁵ Nuclear magnetic resonance (NMR) spectroscopy revealed a unique antiparallel β -sheet structure with two disulfide bonds.²⁶ These families and the large number of peptides that have been subsequently identified have exponentially expanded after the discovery of this initial set of AMPs. The amount of publications and interest in the area of AMPs has steadily increased since the 1990’s (Figure 1). The intensive study and search for AMPs in all six kingdoms of life have revealed characteristic traits among the majority of AMPs. Structural diversity is an important feature that can inform on the potential mode of action of the AMP. AMPs can form α -helical, β -sheet, loop, cyclic, and disordered structures.^{17,25,27-33} The diversity of AMPs is not limited to sequence and structure, as a wide range of mechanisms have been studied, some of which are more specific than others.

1.2 Introduction to the Mechanism of Action of AMPs

Mechanistic studies show that the majority of AMPs irreversibly damage cell membranes to kill pathogens; however, several new modes of action have also been discovered. Numerous hypotheses for the mechanism of membrane disruption have been proposed and some of them are

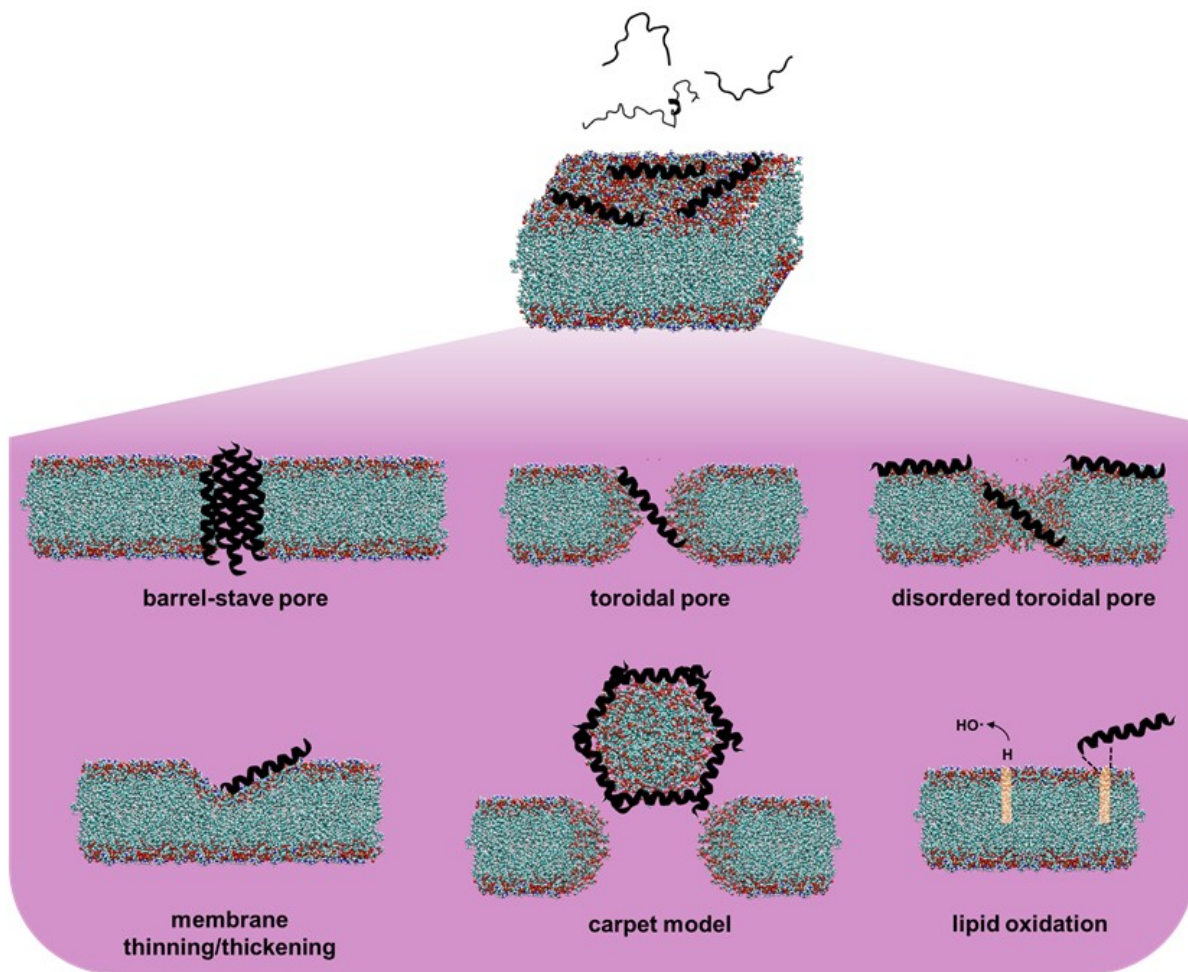


Figure 2. Selected models of membrane disruption. Peptides are depicted in an helical conformation, but they do not need to have that secondary structure.

illustrated in Figure 2. Transmembrane pore formation can occur via either a toroidal pore or barrel stave model. In order to form a transmembrane pore and span the bilayer, the peptide must be ~22 residues long as an α -helix, and ~8 residues long as a β -sheet.³⁴ The toroidal pore model proposes that the curvature of the membrane is affected when the peptide integrates perpendicular to the

membrane in a favorable manner.³⁵ This curvature disrupts the membrane and causes separation of the lipid tails and polar head groups.³⁵ The barrel stave mode of action begins with peptide accumulation on the surface of the membrane, followed by perpendicular insertion to the bilayer and self-association to form a pore.^{35,36} Once a pore is formed, there is recruitment of more peptides that eventually lead to the leakage of cellular contents and death. Dissipation of membrane potential through an ion gradient can be another consequence of pore formation.³⁷ Membrane depolarization has been observed in two peptide toxins, melittin and alamethicin, and may be their main mode of action.^{35,38} The site of pore formation is more likely to occur at sites of membrane curvature or septa of dividing cells because of the lower lipid to peptide ratio requirement at the newly synthesized bilayer, the shape of the curve, and the type of lipid at the septa or poles of bacteria.³⁹⁻⁴¹ Transmembrane models have been suggested as the mode of action for a myriad of AMPs including magainin 2, which is hypothesized to span the membrane, aggregate, and form water-filled pores that can depolarize the membrane.^{42,43} When magainin 2 becomes α -helical and starts to form a pore, lipid flip-flopping occurs that can lead to lipid asymmetry and contribute to depolarization of the membrane.^{42,43} Recently, the piscidins have been studied using neutron and X-ray diffraction techniques.^{44,45} It was revealed that partitioning into the membrane is accompanied by thinning of the bilayer and reorganization of lipids.^{44,45} Although many peptides are thought to form pores, it has been debated whether transmembrane pores can be formed. Wimley and colleagues have argued that using vesicles can lead to deceiving results. Simulations show that a single channel in the vesicle can cause leakage of all of the vesicle contents in less than a second.³⁵ Additionally, total leakage from vesicles is usually incomplete, which leads to the conclusion that no pores are forming or that they may just form transiently.³⁵ The carpet or detergent model was first proposed by Shai *et al.* and describes a loss of integrity of the membrane

due to peptide accumulation on the membrane where there is a high peptide to lipid ratio.^{46,47} The peptides arrange themselves parallel to the membrane, where the hydrophilic side of the peptide faces the headgroups and the hydrophobic portion faces the lipid tails. A density of AMPs must accumulate, where the peptide:lipid ratio needed for disruption is between 1:1000 and 1:100.³⁵ Once a threshold of peptides are present, this accumulation leads to a lack of structural integrity and cell content leakage.⁴⁷ Peptides do not need to oligomerize in or on the membrane but do need to reach a threshold to cause lysis of the cell.³⁶ Further, an AMP does not need to have a certain secondary structure or be able to enter the bilayer to induce disintegration of the membrane by the carpet model.³⁶ The mechanism of action of aurein 1.2, a 13 residue AMP from *Litoria aurea*, a tree frog, has been well-studied and is an ideal example of a carpet model. Due to the short length of aurein 1.2, it is unlikely that this peptide can span the membrane as a monomer and form a transmembrane pore. Confocal microscopy was utilized to image giant unilamellar vesicles (GUVs) with differently sized fluorophores and examine the leakage upon peptide interaction. At a high peptide:lipid ratio, there was immediate rupture of GUVs that indicates a lytic carpet mechanism.⁴⁸ Solid state NMR (ssNMR) and surface plasmon resonance were used to ascertain that there was increased headgroup disorder in the presence of dimyristoylphosphatidylcholine (DMPC) lipids, while the lipid tails were almost unaffected by the presence of peptide.⁴⁹ A concentration higher than 10 μ M was needed to fully lyse a DMPC lipid bilayer.⁵⁰ This supports the notion that aurein 1.2 attacks membranes by using a carpet mechanism that disintegrates the membrane. A more recent study used NMR and neutron reflectometry to reinforce the notion that aurein 1.2 binds to the phospholipid headgroups, while only partially inserting into the lipid tails.⁵⁰ It was also found that there were greater membrane defects, greater headgroup disorder, and thinner lipid tail regions in membranes composed of anionic lipids.⁵⁰ As indicated above, multiple

forms of interactions can occur when AMPs encounter membranes. These molecular events are directed by the physical features of both the AMPs and the membrane constituents.

AMPs can also translocate into bacterial cells without disrupting the membranous environment. Intracellular components have been targeted by many AMPs including buforin II, tachyplesin I, apidaecin, indolicidin, PR-39, and clavanin A.^{26,51-57} When an AMP enters a cell, electrostatic interactions can cause binding to DNA, RNA, ribosomes, and other cellular components, which can lead to cellular death. Translocation into the cell can occur spontaneously with little membrane perturbation, specifically if the peptide is Arg-rich, reminiscent of cell-penetrating peptides, or through protein channel transport.^{56,58-60} For example, *E. coli* expresses an inner membrane protein called SmbA that is part of an ABC transporter that can import Pro-rich AMPs.⁶¹ One of those AMPs is PR-39, which is composed of almost 50% Pro residues. PR-39 can be rapidly transported into bacterial cells, inhibit DNA synthesis, and cause protein degradation.⁵⁶ Another Pro- and Arg-rich peptide that can translocate into cells is apidaecin. Entry into the cell has been postulated to rely on a transporter that may be a chaperone protein that the peptide binds to when interacting with LPS.^{55,62} The mode of action of apidaecin was found to be stereospecific through the comparison of activity between L-amino acid and D-amino acid versions of apidaecin, and has an effect on protein synthesis, most likely via binding to ribosomes.^{55,63} Apidaecin can also directly bind to the bacterial heat shock protein DnaK with sequence specificity, while it nonspecifically binds the chaperone GroEL.⁶² This activity was specific to bacterial DnaK and not its homolog in human cells.⁶² AMPs that can spontaneously translocate are typically Arg-rich.⁵⁶ Buforin II is a highly active, broad-spectrum AMP from the N-terminus of the histone H2A from the stomach of *Bufo gargarizans*.⁶⁴ Even at five times the minimum inhibitory concentration (MIC) of buforin II, there is no cell lysis observed and it seems

to have a wholly intracellular mode of action.⁶⁴ The unique helix-hinge-helix structure and the DNA binding moiety at the C-terminus of buforin II specifically targets DNA and RNA to cause cell death.^{64,65} Similar to buforin II, indolicidin is a short 13 residue AMP from bovine neutrophils that can rapidly translocate cells at three times the MIC without causing any cell membrane damage.^{52,53} Indolicidin has a multi-hit mode of action that includes inhibition of DNA synthesis, inhibition of DNA processing enzymes, direct binding to abasic DNA sites, ssDNA, and dsDNA, and DNA crosslinking.^{53,66,67} At high concentrations, indolicidin can also halt protein synthesis.⁵³ AMPs that are thought to be only membrane active may also have activity against intracellular components for a multi-hit mechanism. This is the case for tachyplesin I, which has a concentration-dependent mechanism of action. Membrane disruption is the primary target, but sublethal doses can influence esterase activity and lead to cell death, albeit more slowly than via membrane disruption.^{68,69} The most recent developments regarding AMP-induced DNA damage features the metal-mediated mode of action of clavanin A, an AMP from the tunicate *Styela clava*. It was previously shown that clavanin A potentiates its antimicrobial activity when combined with Zn²⁺ ions, even against antibiotic-resistant strains of Gram-negative bacteria.^{28,57} Although the major mode of action of clavanin A was previously hypothesized to be pore formation, it was later shown that clavanin A has multiple mechanisms of action including a novel DNA hydrolysis mechanism.^{28,57} Through the use of quantum mechanics/molecular mechanics, it was shown that the hydrophilic side of holo-clavanin A was bound to the major groove of DNA by hydrogen bonding.⁵⁷ DNA cleavage was mediated by a Zn²⁺-bound hydroxyl nucleophile, similar to the mechanism of metallohydrolases.^{57,70}

A more recent development has been the discovery of nanonet formation by AMPs, not to be confused with NETosis (Neutrophil Extracellular Traps). Nanonets are fibrillated structures

formed by AMPs that can trap bacteria.⁷¹ The formation of nanonets has been observed in at least two different groups of peptides in humans and mollusks.⁷¹⁻⁷³ Interestingly, nanonet formation seems to be triggered by the presence of bacteria, as they are not observed in the absence of bacteria. At the molecular level, nanonets show crosslinking through Cys residues, although the details of their nature remain to be elucidated.⁷² Human α -defensin 6 (HD6) was the first AMP observed to form nanonets.⁷¹ HD6 is expressed in Paneth cells of the small intestine, where several defensins are expressed.⁷¹ Importantly, HD6 does not directly kill bacteria, but it was found to block the invasion of *Salmonella* Typhimurium into intestinal epithelial cells.⁷¹ Self-association of HD6 forms fibrillated nets on non-specific bacterial surfaces that obstruct bacterial invasion into intestinal cells.⁷¹ Mussel defensins also form nanonet structures and are discussed in detail later in this review.^{72,73}

Organisms produce several AMPs, many of them with similar sequences that are deployed to the same area of infection. It is proposed that these different AMPs possess synergistic interactions; however, the issue has not yet been settled.⁷⁴⁻⁷⁶ Clearly, synergy among two or more AMPs would allow a host to reduce the AMP concentrations needed to combat a pathogen.⁷⁷ Synergy is commonly characterized by the fractional inhibitory concentration (FIC), although other susceptibility assays are possible. The FIC is evaluated by $\frac{MIC\ A}{MIC\ C} + \frac{MIC\ B}{MIC\ C}$ where MIC C represents the MIC of compounds A and B together. If the FIC is <0.5 , the interaction is said to be synergistic. Interactions with an FIC of 0.5 to 1.0 are additive, an FIC of 1.0 to 4.0 means that there is indifference, and interactions that are >4.0 are antagonistic. The first example of synergism between AMPs was published in 1995 and is still being investigated today.⁷⁸ Magainin 2 and PGLa are both found in the skin of *X. laevis* and are membrane active peptides, where PGLa interacts with LPS on the surface of Gram-negative bacteria, in addition to forming pores.^{79,80} The

synergistic interaction between PGLa and magainin 2 lead to a stronger permeabilization effect when the peptides were in a 1:1 ratio.⁸¹ It was later confirmed that heterodimer formation between PGLa and magainin 2 can occur in a lipid bilayer, and this accounts for the larger permeabilizing effect when there is a 1:1 ratio of peptide.^{82,83} ssNMR was used to confirm that this heterodimer formed in a lipid bilayer and lead to more stable transmembrane pore formation.⁸³ This may provide one reason why a variety of AMPs are found in the same tissues, in this case the skin, because they can be active alone but even more potent together. This example of synergy also shows that AMPs do not need to have different modes of action to have synergy. Synergy has been studied in the context of a *Drosophila* model through the deletion of a combination of up to ten groups of AMPs using CRISPR technology.⁷⁴ Importantly, it was found that certain groups of AMPs target Gram-positive bacteria and fungi, and many groups of AMPs were identified to have additive or synergistic effects.⁷⁴ This is supported by work showing that *Drosophila* can induce expression of different antibacterial or antifungal peptides depending on which pathogen they are infected with.⁸⁴ Further, it was revealed that with even one AMP knockout, the *Drosophila* became more susceptible to infection.⁷⁴ More *in vivo* studies should be conducted to see whether these observations are relevant to other species. Several examples of synergy between antibiotics and AMPs⁸⁵⁻⁸⁷, along with AMPs that synergize with each other, show that unique combinations can lead to more effective killing and may be useful in the clinic to fight antibiotic resistance.

Another emerging paradigm in the field of AMPs are metal-sequestering host defense peptides in humans.⁸⁸⁻⁹⁰ An interesting example is calprotectin, which has been implicated in growth inhibition through Fe²⁺, Mn²⁺, Cu²⁺, Ni²⁺, Ca²⁺, and Zn²⁺ sequestration and plays a role in nutritional immunity.⁸⁸ Calprotectin is released by neutrophils, where there are also abundant metal ions, at the site of infections and as much as 40-60% of the cytoplasmic space in neutrophils

contains calprotectin.^{91,92} The heterodimeric protein consists of two subunits called S100A8 and S100A9 and there are two metal binding sites on calprotectin, 1) a hexa-His sequence and 2) a tri-His-Asp site that has been seen to bind Zn²⁺ with picomolar affinity and other metal ions with lower affinity.⁹³ Interestingly, Zn²⁺, which binds to both sites, has Kd₁=240 pM and Kd₂=10 pM, however, this high affinity seems to rely on the presence of Ca²⁺ because without Ca²⁺ the Kd values were reduced to nM and high pM levels.^{93,94} This phenomenon is similar to Mn²⁺ and Fe²⁺ binding at site 1.⁹⁵⁻⁹⁷ Importantly, this work concluded that Zn²⁺ binding is tuned so that within neutrophils the Zn²⁺ binding of calprotectin is lower than when the protein is released in the presence of Ca²⁺ at the site of infections.⁹³ Moreover, Ni²⁺ was shown to bind at high affinity to both sites, where it was more thermodynamically favorable for Ni²⁺ to bind to site 1 than Zn²⁺.⁹⁸ A crystal structure revealed that Ni²⁺ exhibited unique coordination at both sites. Ni²⁺ at the first site was coordinated by all six His residues through Nε2 atoms, similar to Mn²⁺ coordination at this site.⁹⁸ Site 2 exhibited tetrahedral binding through three His Nε2 atoms and one Asp residue.⁹⁸ Ni²⁺ sequestration showed biological relevance by inhibiting bacterial urease activity and growth.⁹⁸ Recently, Cu²⁺ sequestrations, in addition to Zn²⁺ sequestration, were observed to be important to *Candida albicans* growth *in vitro* and *in vivo* in a mouse model.⁹¹ Zn²⁺ import was upregulated after calprotectin sequestered Zn²⁺, however, *C. albicans* was still able to regulate and maintain the intracellular concentration of Zn²⁺ stores.⁹¹ More surprisingly, Cu²⁺ sequestration occurred at sub-picomolar concentrations and caused the induction of a stress response that lasted over 72 hours.⁹¹ Fe²⁺ sequestration by calprotectin is also able to starve *P. aeruginosa* of Fe²⁺ under aerobic and anaerobic conditions.⁹⁹ Calprotectin is a promiscuous metal binding protein that can lead to growth inhibition through the sequestration of metal ions at the sites of infections.

In this review, we will focus on a family of AMPs with a putative copper binding motif known as Amino Terminal Copper and Nickel (ATCUN) binding motif.¹⁰⁰ Interestingly, although almost 5% of the reported AMPs contain an ATCUN motif, the role of copper ions in the mechanism of action of these peptides has been largely undetermined. We are interested in this binding motif since, despite the aforementioned variability among AMP sequences, the ATCUN motif has remained present in every phylum from which AMPs have been isolated. What advantage does the ATCUN motif provide? Although this is an exciting question, we believe there is not enough information in the literature of AMPs to provide a complete answer. Herein, we will explore possible answers and draw conclusions based on the available information. Although other metal ions, such as Zn^{2+} ,²⁸ can synergize with AMPs, this work is limited to copper-binding peptides containing the ATCUN motif. This review is also a call for more studies on these exciting classes of peptides, which we call metalloAMPs. We believe that the drug development community can use this knowledge to develop new antimicrobial strategies based on these binding motifs and meet the challenge of antimicrobial resistance.

1.3 Role of copper in the immune system

Transition metal ions are frequently found in metalloproteins that function either in redox- and non-redox catalysis, storage and/or transport, transcriptional regulation, and signal transduction.^{101–103} Because of the essentiality of transition metals, pathogenic microbes have evolved elegant (and sometimes redundant) mechanisms to acquire metals from their host.^{104,105} Indeed, this tug-of-war for metal ions in the host-pathogen interface highlights the host's effort to limit microbial growth and the pathogen's need for survival in a hostile environment. To prevent infection, the host relies on two major and contrasting strategies involving distinct groups of metals (Figure 3). First, the host limits the availability of iron, manganese and zinc in regions containing

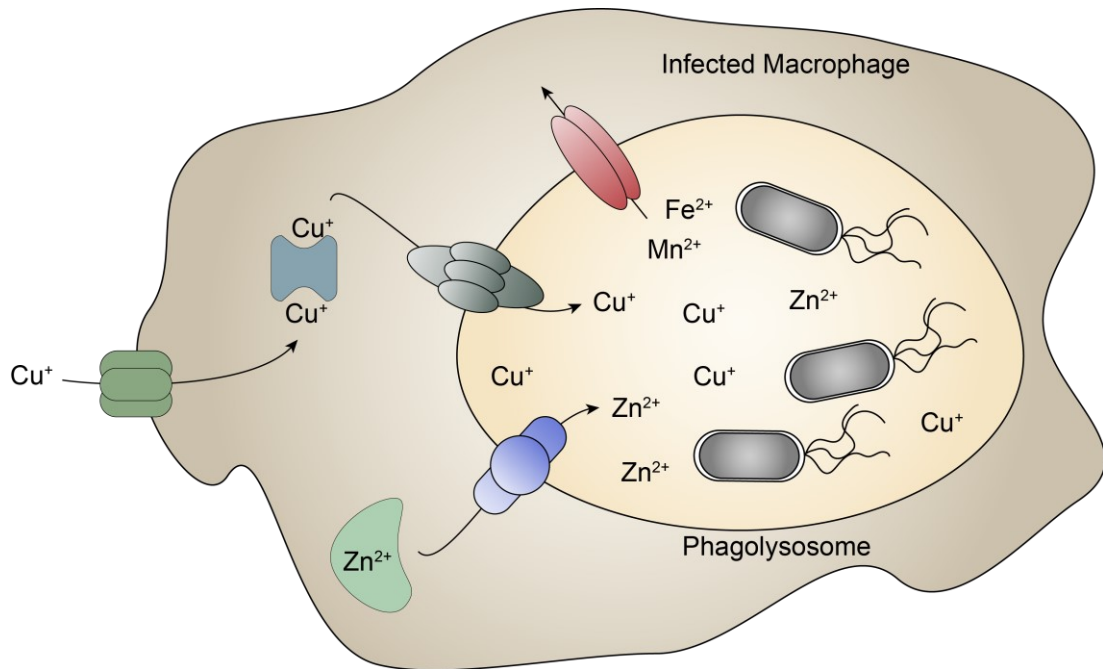


Figure 3. Depiction of the two strategies by the host in which metal ions are involved. In a common strategy against most pathogens, Fe^{2+} and Mn^{2+} ions are removed from the phagosomes. Alternatively, in cases such as *Mycobacteria* infections, Cu^+ and Zn^{2+} ions are rushed into the phagocytic environment.

bacteria by expressing high-affinity metal binding proteins.^{103–105} Termed nutritional immunity, this withholding mechanism effectively starves pathogens of these essential micronutrients.¹⁰³ Second, the host leverages the inherent toxicity of copper and zinc, and deliberately traffics these metals into sites of infection.^{106–108} The sudden increase in concentration of these toxic metals, which can be as high as $800 \mu M$, causes pleiotropic effects (*vide infra*) that result in microbial killing.^{106,109,110} It is not difficult to imagine that in these environments in which AMPs and copper ions are found in large concentrations, they interact synergistically. Multiple trafficking mechanisms involving a variety of immune effectors ensure that copper levels in sites of infection are enriched. In phagocytic cells like macrophages, infection triggers overexpression of copper transporters (Ctr1 and ATP7A) and chaperones (Atox1), resulting in increased copper uptake.^{109,111} ATP7A, a Golgi-resident transporter, gets trafficked into phagosomes and delivers copper into the

lumen of bacteria-containing vesicles. In fact, during *Mycobacterium tuberculosis* infections, the phagosomal copper concentration was measured to be 10 – 800 μM .¹¹² Extracellular levels of copper increase during infections as well. Serum copper levels progressively rise during infection, irrespective of the agent (viral, bacterial, fungal), mainly due to the upregulation of the cuproprotein ceruloplasmin.^{113,114} While the exact reason why this happens is still unknown, it's reasonable to assume that ceruloplasmin, which can bind up to six copper atoms, helps to deliver copper into sites of infection.¹¹⁰ Indeed, granulomas from *M. tuberculosis*-infected guinea pigs were found to contain markedly higher copper concentrations.¹¹⁵ A significant accumulation of copper in the urine of patients infected with uropathogenic *E. coli* was also observed.¹¹⁶ Furthermore, the observation that increased salivary Cu^{2+} concentrations are associated with lowered amounts of tooth decay or caries is clinically important.¹¹⁷ It is apparent that boosting copper concentration at sites of infections is advantageous due to the inherent antimicrobial activity of this metal, as well as its ability to synergize with other molecules, including peptides.^{118–120}

The classical view of copper's antimicrobial activity is based on its ability to form deleterious hydroxyl radicals via a Fenton-like mechanism.¹²¹ This direct production of reactive oxygen species (ROS) not only covalently damages multiple biomolecules but also depletes bacterial antioxidants. Recent evidence shows that low molecular weight thiols like glutathione can bind to and inactivate the cycling of copper between its +1 and +2 states.¹²² This makes copper intoxication via direct ROS formation less likely. Nevertheless, induction of ROS detoxifying genes occurs upon exposure of bacteria to lethal levels of copper. Recent work shows that bacterial susceptibility to copper arises from one or any combination of the following mechanisms. First, copper can replace cofactors in metalloproteins, leading to inactivation of enzymatic activity (in

the case of catalytic metals) or significant structural perturbation (in the case of structural metals).¹⁰⁷ Next, iron-sulfur clusters of metalloproteins collapse following exposure to copper due to Cu¹⁺ displacement of Fe²⁺. This liberates free ferrous ions, which can then catalyze the Fenton reaction.¹²³ The first two routes of copper toxicity can largely be explained by the metal's position in the Irving-Williams series: Mn(II) < Fe(II) < Co(II) < Ni(II) < Cu(II) > Zn(II).¹²⁴ From a chemical standpoint, donor atoms from proteins preferentially bind Cu²⁺ because it yields the highest complex stability.¹²⁵ Copper can therefore easily replace less competitive metals in the series. Finally, copper impairs membrane function by peroxidizing lipids in the bilayer.¹²⁶ Invading bacteria often mount multiple modes of detoxification in response to the influx of copper ions to sites containing pathogens. Copper-responsive transcription factors in bacteria detect minute changes in cytosolic copper concentration and activate the expression of genes that function in copper detoxification.¹²⁷ Membrane bound exporters in *E. coli*, *Salmonella* spp., *Streptococcus* spp., and *M. tuberculosis* have been widely studied.¹²¹ These efflux pumps utilize energy from ATP hydrolysis or electrochemical gradients to pump copper from the bacterial cytosol back to the phagosomal lumen. Bacteria also express protein- or small molecule-based copper chelators that bind to cytosolic or periplasmic copper.^{128,129} In addition, some small molecules bind to copper and act as enzyme mimics (superoxide dismutase) to minimize secondary toxic effects of copper.^{130,131} Finally, expression of multicopper oxidases that convert the more toxic Cu¹⁺ to the less toxic Cu²⁺ act to prevent the Fenton reaction.^{132,133} All of these mechanisms work in concert to ensure that concentration of “free” copper in the cytosol is maintained below picomolar levels.¹³⁴ While some of these bacterial defenses are redundant within any single pathogen, some detoxification modes are more dominant than others. Indeed, bacteria that cannot neutralize the toxicity of copper are more susceptible to copper-related toxicity of macrophages.^{111,115}

2. Biophysical Methods for Characterization of ATCUN-AMPs

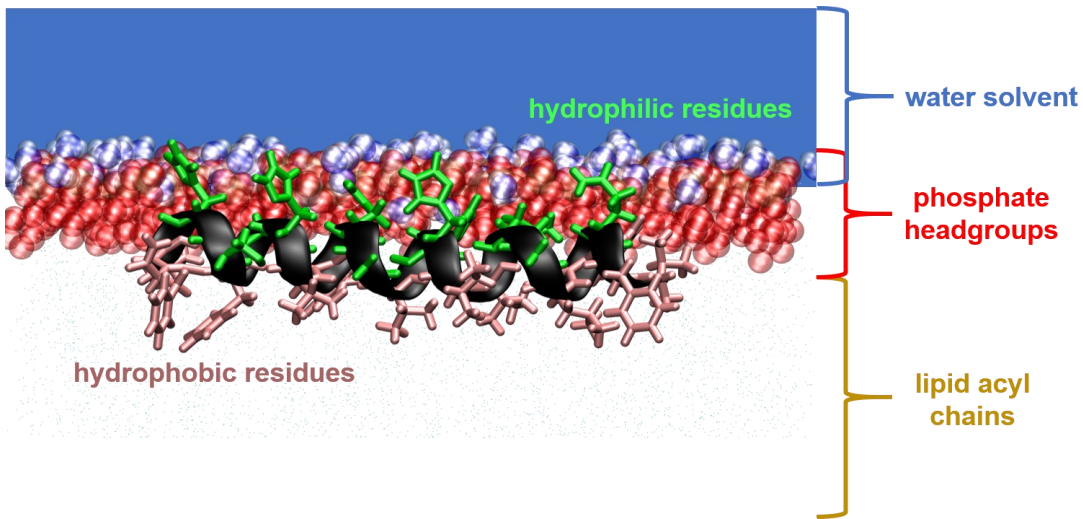


Figure 4. Schematic depiction of a typical interaction between an amphipathic peptide and a double-layer membrane. The hydrophilic residues (green) of the peptide (black) interact with the polar headgroups of the lipid bilayer, while the hydrophobic residues (pink) get buried within the hydrophobic acyl chains (not shown).

Understanding the mechanism of action of ATCUN-AMPs can potentially allow for their development as therapeutic agents. This can be done by using a battery of biophysical techniques. Like enzymes, the relationship between the structure of an AMP and its function is often, if not always, correlated. An important difference is that because of the shorter nature of AMPs, they cannot easily maintain an ordered structure in solution because they often do not have the mechanism of burying its nonpolar residues in a hydrophobic core, as enzymes usually do. The ability of AMPs to form and stabilize secondary or tertiary structures requires the presence of a cell membrane or oligomerization among two or more AMPs.¹³⁵ For amphiphilic AMPs in the presence of a membrane, electrostatic interactions between the polar/charged residues and the polar lipid headgroups, and hydrophobic interactions between the nonpolar residues and the nonpolar lipid tails, stabilize the formation of an α -helix (Figure 4).¹³⁵⁻¹³⁸

2.1 Circular dichroism (CD)

AMPs can be classified based on their secondary structures (Figure 5). A quick way to evaluate its secondary structure is by utilizing CD spectroscopy. Briefly, CD is the difference in sample absorption of left-handed and right-handed circularly polarized light.¹³⁹ CD can be measured across a spectrum of wavelengths, and characteristic bands are obtained for specific secondary structures. α -helical character can be determined from negative bands at around 222 nm and 208 nm and a positive band at around 193 nm.¹⁴⁰ Anti-parallel β -sheets are characterized by a negative band at around 218 nm and a positive band at around 195 nm.¹⁴¹ Low ellipticity at around 210 nm and negative bands at around 195 nm indicate disorder in the protein structure.¹⁴² It is also possible to use CD to study the interaction of peptides with *E. coli* cells. Recently, Romanelli and co-workers recorded CD spectra of magainin 2 and cecropin A in 10 mM phosphate buffer acting with *E. coli* cells. Changes in the spectra corresponding to structural changes of the peptide driven by the components of the bacterial membrane were reported, demonstrating that one can follow the folding of AMPs in the presence of cells.¹⁴³

CD has been used to study the interactions and possible structural changes of ATCUN-AMPs and metal ions. Interestingly, there is an example of a penta-coordinate ATCUN motif, where Trp is in the fifth position engaged in a weak π -cation interaction.¹⁴⁴ This binding can be observed using CD, where a peak at 223 nm can be observed when Cu^{2+} or Ni^{2+} are added.¹⁴⁴

Secondary structure changes such as slight increase in α -helical structures upon binding metal ions can also be detected from the CD spectra but are not common for ATCUN-AMPs. Histatins,

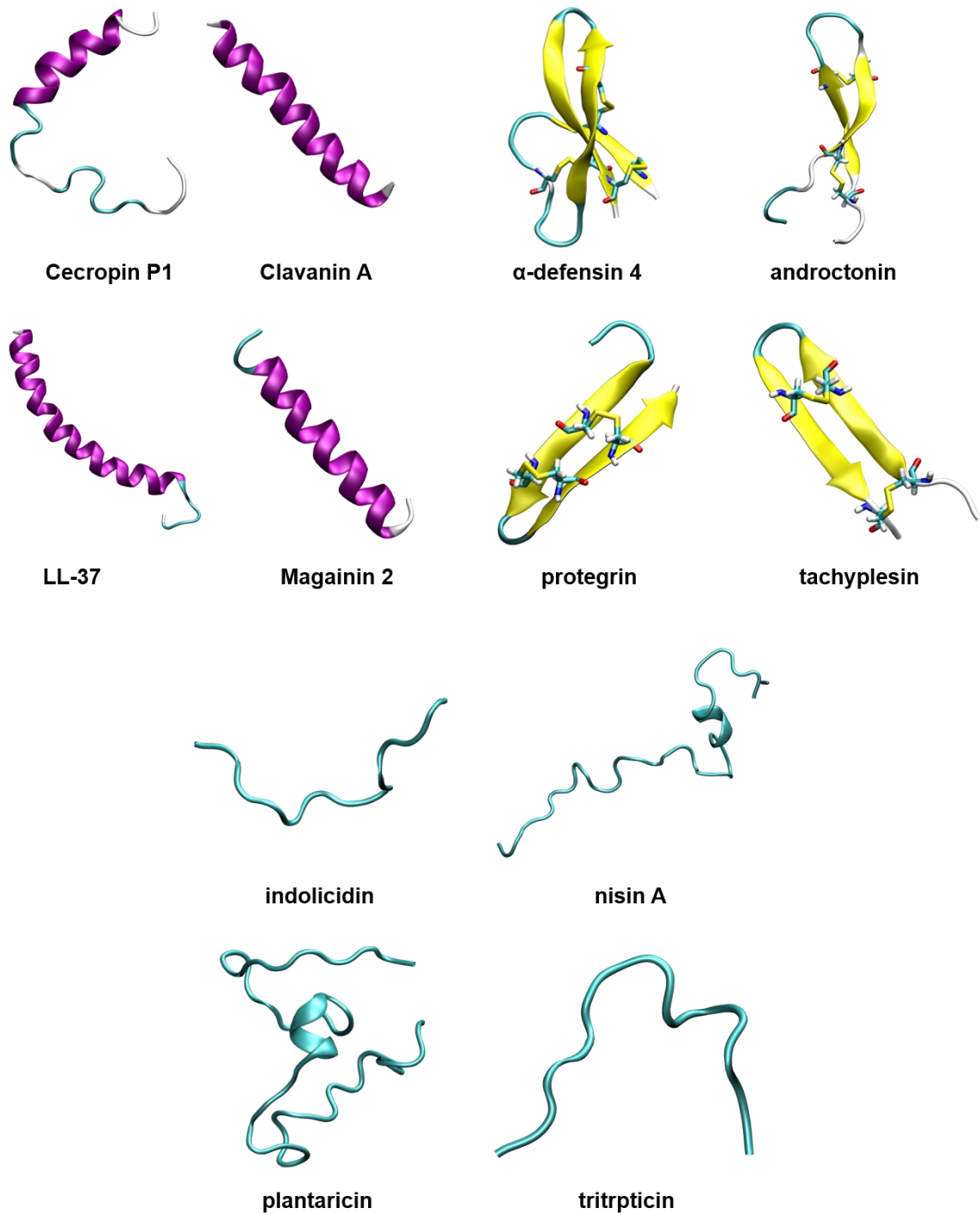


Figure 5. Examples of AMPs classified based on their secondary structures. α -helices are shown in purple, β -sheets are shown in yellow, while disordered AMPs are shown in cyan.

piscidins, and CM-15 ATCUN-AMPs, as well as AMPs with added ATCUN motifs have all been shown to not exhibit a change in secondary structure.¹⁴⁵⁻¹⁴⁷ In the case of histatin 3 and 5, which can bind to multiple divalent cations, there was no change in secondary structure in the presence of Cu²⁺, Ni²⁺, and Zn²⁺ and could not induce an α -helix in 5 mM potassium phosphate buffer.¹⁴⁵ In addition, clavanin A, which binds to Zn²⁺, exhibits similar behavior, where the helicity only increases by 5% in the presence of excess Zn²⁺.²⁸ The presence of absorption bands at around 500 nm and characteristic fingerprint-like split patterns of d-d bands in the CD spectrum confirmed the geometry of Cu²⁺ binding to the N-terminus of the ATCUN-containing hepcidin at higher pH, as the metal ion replaces the four protons from the titratable residues in that region.¹⁴⁸

2.2 UV-Vis titration

Metal binding and binding constants of metal ions to metalloAMPs are usually obtained by doing spectrophotometric titrations with small molecule ligands that compete with the AMPs. Significant changes in the absorption profile of the AMP at the UV-Vis region will be observed upon binding of metal ions. In the direct titration of Cu²⁺ with the ATCUN-containing histatin 5, an increase in absorbance at around 240 to 260 nm and presence of an absorption band at 530 nm were observed.^{149,150} Competitive ligand titrations can be used to determine apparent binding constants in buffer, where the other component should have a known binding constant for Cu²⁺. When utilizing competitive binding titrations, it is useful to carry out reverse titrations to confirm the apparent binding constants of peptide to Cu²⁺ and ensuring that there would be no excess Cu²⁺ ions in solution by using a ratio of 1:0.8 chelator:Cu²⁺. Competitive ligand titration with nitrilotriacetic acid allowed the determination of the apparent binding affinity, the dissociation constant (K_d), of Cu²⁺ to histatin 5, which is about 8 pM.¹⁵⁰ For a better understanding of the

different competitive models that can be used to determine the binding affinity of metal ions to proteins, a comprehensive review by Xiao and Wedd is available.¹⁵¹

2.3 Isothermal Titration Calorimetry (ITC)

Another titration technique that is useful to study the interactions of AMPs with lipid bilayers as well as metal ions is ITC.^{152–154} In ITC, the thermodynamic properties of binding can be evaluated by quantitating the heat flow associated with a binding event.¹⁵⁵ From the ITC thermograms generated, the K_d and change in enthalpy (ΔH) upon binding can be determined.¹⁵⁵ Indirectly, the change in Gibbs' free energy (ΔG) is calculated from the K_d ($\Delta G = -RT \ln K_d$), followed by the calculation of the change in entropy ($\Delta S = \frac{\Delta H + \Delta G}{T}$). There are advantages to using ITC compared to UV-Vis to determine K_d including the facile determination of thermodynamic properties of binding including ΔG , ΔS , ΔH , and stoichiometry constants of binding. Additionally, when using ITC the temperature and stirring can remain constant and the use of software can make it easier to fit to binding models and determine thermodynamic constants. The K_d of Zn^{2+} and Cu^{2+} to the AMP histatin 5 were determined to be 83 μM and 38.5 nM, respectively.¹⁴⁹ The value obtained for Cu^{2+} using ITC shows a weaker binding affinity for Cu^{2+} to histatin 5 compared to the value obtained using the competitive ligand titration mentioned earlier.¹⁴⁹ This is because ITC can only measure binding affinities up to the nanomolar range when direct titration is carried out.¹⁵⁶ To be able to measure picomolar binding affinities, competitive titration should be done using ITC.^{157,158} For example, the tripeptide GHK and tetrapeptide DAHK bind Cu^{2+} ions with femtomolar binding affinity, as shown by competitive titration with glycine using ITC.¹⁵⁹ On the other hand, the advantage of using ITC over other spectrophotometric techniques is that it can measure binding affinities at multiple sites of the AMP. In histatin 5, three binding affinities each were measured for Zn^{2+} and Cu^{2+} , implying that there are three binding sites for these metal ions

in histatin 5.¹⁴⁹ ITC can also be used to identify the affinity of AMP binding to model membranes.¹⁶⁰ Common model membranes used are multilamellar vesicles, small unilamellar vesicles, and large unilamellar vesicles with varying lipid compositions. To avoid aggregation in some AMPs, the titrant in the experiment is usually the model membrane, as they can be stable in higher concentrations.¹⁶⁰ The AMP is in the sample cell, where the concentration can be relatively dilute.¹⁶⁰ The model membranes are continuously titrated until all AMPs are bound to the model membranes, and a binding isotherm is generated. The cationic AMP β -17 was evaluated for its binding affinity with zwitterionic and anionic lipids.¹⁶¹ It was observed that there is very little heat generated when β -17 is titrated with the zwitterionic phosphatidylcholine (PC), while there is a significant amount of heat generated when titrated with anionic 1-palmitoyl-2-oleoyl-*sn*-glycero-3-phosphoglycerol (POPG), or when POPG was mixed with PC.¹⁶¹ This indicates the strong binding interaction due to the electrostatics between the cationic AMP and the anionic lipids. This was also observed when the AMP NK-2 was titrated against zwitterionic 1,2-dioleoyl-*sn*-glycero-3-phosphocholine and anionic 1,2-dioleoyl-*sn*-glycero-3-phosphoglycerol.¹⁶² Interestingly, pore formation and micellation can be observed in ITC as a superposition of individual calorimetric heat traces generated by the processes involved in pore formation and micellation.¹³³ The method was shown to work reversibly, that is, the same results were obtained when the peptide was titrated to the lipid as when the lipid was titrated to the peptide.¹³³

2.4 Fluorescence Microscopy

Fluorescence microscopy, particularly single-cell microscopy, is a powerful technique to study the time-resolved mechanism of action for AMPs.¹⁶³⁻¹⁶⁷ Peptides with commercially available fluorescent labels, including rhodamine B and 5(6)-carboxyfluorescein, can be easily synthesized at low cost. For ATCUN-AMPs an N-terminal fluorescent tag should not be used, as

this can impair metal binding.¹⁰⁰ For example, a model peptide of human Ctr1, MDHSHHMGMGSYMD, decreased its Cu²⁺ apparent binding constant at pH 7.4 by two orders of magnitude when it was acetylated in the amino-terminal amine.¹⁶⁸ The fluorophore can be attached to other positions of the peptide; however, one must keep in mind that Cu²⁺ binding will lead to quenching of the fluorescence of the tags. This property can be used to produce chemosensors for Cu²⁺ ions.^{169,170} A family of pentapeptides containing three different fluorophores illustrate the quenching activity of Cu²⁺ binding when the fluorophore is attached to

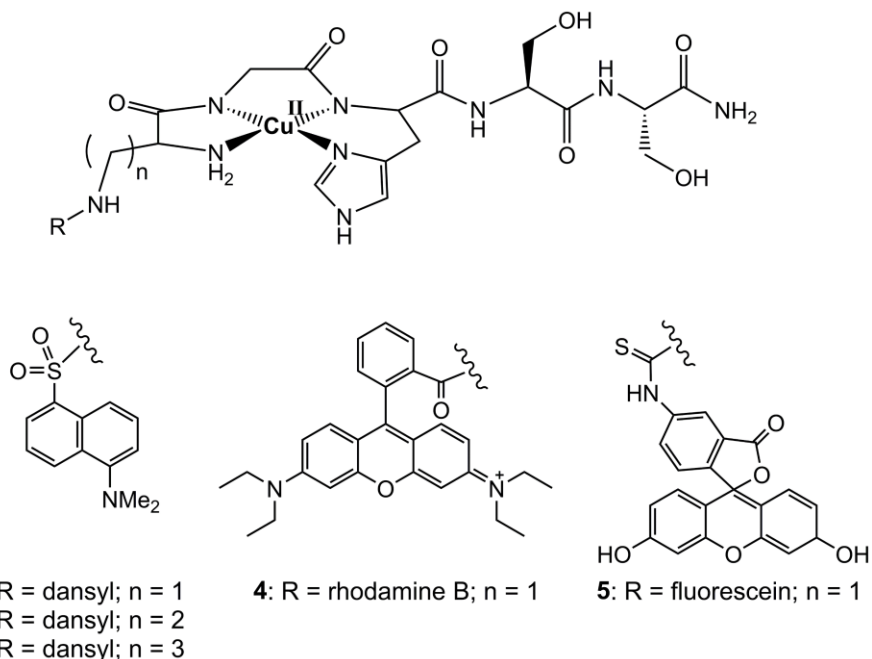


Figure 6. Family of ATCUN-containing pentapeptides attached to three different fluorophores: dansyl, rhodamine B, and fluorescein.^{171,172}

the first amino acid in the ATCUN sequence (Figure 6).^{171,172} Compounds **1**, **2**, and **3**, containing dansyl, show a decrease in fluorescence of 85%, 75%, and 70%, respectively, when one equivalent of Cu²⁺ was titrated.¹⁷¹ The difference is explained by the increase in distance between the

fluorophore and the metal ion. When rhodamine B and fluorescein are used instead of dansyl, as in compounds **1**, **4**, and **5**, the percent quenching of fluorescence is the same, ~85%. The distance between the fluorophore tag and the Cu²⁺ ion can also be increased by locating the fluorophore in the C-terminal region of the peptide. For example, a decrease in quenching efficiency from 85% to 30% is observed between the tetramer SGHK-dansyl and the dodecamer SGHAAAAAAAK-Dansyl.¹⁷³ For these reasons, the fluorescent tag should be placed on C-terminus of the peptide to diminish quenching of the fluorophore when in proximity to the ATCUN motif. Although in some cases, it could be beneficial to have the fluorophore close to the ATCUN motif. Libardo *et al.* took advantage of the larger quenching efficiency of Cu²⁺ when a fluorophore is close to the ATCUN motif to study the mechanism of action of the icosamer _DVIHRAGLQFPVGRVHRLRK-NH₂ (DAB-10). Two peptides were synthesized containing the pH-insensitive fluorophore tetramethylrhodamine (TMR), one with the tag in position 4, DAB-10-K₄(TMR), and the second one with TMR in position 20, DAB-10-K₂₀(TMR).¹⁷⁴ Whereas DAB-10-K₄(TMR) showed a decrease in emission intensity of 35% when exposed to 1 equivalence of Cu²⁺, DAB-10-K₂₀(TMR) did not diminish its fluorescence. These differences were used to demonstrate that DAB-10 binds to Cu²⁺ ions inside the phagosomes of RAW264.7 macrophages.

A possible drawback of using fluorescent labels is that depending on the peptide sequence, these dyes can perturb the activity due to the bulkiness and hydrophobicity of the fluorophore and the mechanism of the peptide.¹⁷⁵⁻¹⁷⁷ Several examples of modified localization of cell penetrating peptides has been observed after conjugation to fluorophores.^{175,176} Seven fluorophores with different sizes and charge were conjugated to penetratin, a cell penetrating peptide, and revealed that charged fluorophores can effect fluorescent intensity, translocation, and membrane binding properties.¹⁷⁶ While cationic, hydrophobic fluorophores reduced membrane binding, there was an

increased cytotoxicity against mammalian cells.¹⁷⁶ Conjugation to fluorophores can impact the depth of penetration into the lipid bilayer, where conjugated penetratin resulted in a deeper penetration into the core of the lipid bilayer.¹⁷⁵ A membrane thinning effect was also observed with conjugated penetratin, suggesting that conjugation to fluorophores may affect the perceived mode of action of peptides.¹⁷⁵ Moreover, a recent article compared four commonly used fluorophores with slightly varied properties to investigate the effects on the biological activity of AMPs.¹⁷⁷ It was concluded that more hydrophobic and positively charged fluorophores can increase hemolysis of human red blood cells compared to negatively charged fluorophores such as 5(6)-carboxyfluorescein.¹⁷⁷ There were also differences observed in the fluorescence intensity, where 5(6)-carboxyfluorescein had the lowest fluorescent intensity of the four tested fluorophores.¹⁷⁷ Overall, the advantages and disadvantages of certain fluorophores, including increased toxicity or alteration on biological activity, should be weighed before using them. However, a labeled peptide is not always required, as techniques such bacterial cytological profiling allow the identification of cellular pathways within bacterial cells using unlabeled peptides.^{57,164-166}

2.5 Determination of Three-Dimensional Structures of AMPs

Three-dimensional structures of AMPs in different environments can be studied via NMR spectroscopy. One of the earliest AMPs that was structurally elucidated using two-dimensional NMR was magainin 2, dissolved in a mixture of perdeuterated trifluoroethanol (TFE) and water.¹⁷⁸ In determining the structure of a protein using NMR, unique fingerprint cross-peaks at distinct chemical shifts contain the information that allows the structure elucidation. Different methods are available, such as Nuclear Overhauser Effect (NOE) Spectroscopy and Total Correlated Spectroscopy, that correlate protons interacting through space and through bonds, respectively. As

a substitute for lipid bilayer environments, TFE is commonly added to the solvent mixture to mimic the environment by reducing the solvent polarity. It stabilizes intramolecular hydrogen bonds in the peptide, particularly between the carbonyl oxygen of the *i*-th residue and the amine hydrogen of the (*i* + 4)-th residue, responsible for the α -helical conformation.¹⁷⁸ The metal binding of AMPs can be probed using NMR techniques. Due to the paramagnetic character of Cu^{2+} , it will directly influence the chemical shifts and relaxation rates of resonances that are in close proximity to it and cause severe peak broadening, which is why Ni^{2+} is commonly used as a proxy for Cu^{2+} to investigate ATCUN-AMPs. Heteronuclear single-quantum correlation (HSQC) NMR experiments are run in the absence of metal ions and then metal is titrated into solution and run again. The peak shifting and broadening is compared to the HSQC data with and without metal ions to determine which residues/regions of the peptide may be interacting with metal ions. Typically, small amounts of metal (0.5 equivalents) is titrated to avoid peak broadening to such an extent that the proton peaks are no longer there.

Further, NMR can be used to determine the structure of the metal binding site to ATCUN-containing AMPs. Recently, Rai *et al.* used ssNMR to characterize piscidin 3 (p3) bound to DMPC/DMPG lipid bilayer and coordinated to Cu^{2+} ions.¹⁷⁹ Due to the paramagnetic character of Cu^{2+} , it will directly influence the chemical shifts and relaxation rates of resonances that are in close proximity to it and cause severe peak broadening, which is why Ni^{2+} was used for the ssNMR experiment.¹⁷⁹ The study revealed that a square-planar geometry is present in the metal-binding site complex, where the metal ion is coordinated with the first three residues of p3.¹⁷⁹ The other ligand coordinated to the Ni^{2+} , however, was not detected. It is possible that the metal is also coordinating to the lipid headgroup of the bilayer, facilitating the insertion of the N-terminal region of the peptide into the bilayer.¹⁷⁹ Two-dimensional NMR has also been used to probe the ATCUN

binding of ixosin. Again, Ni^{2+} was used as a proxy for Cu^{2+} to avoid peak broadening. Upon metal titration there was peak broadening at the N-terminus consistent with Ni^{2+} binding to the ATCUN motif including broadening of proton peaks on the imidazole ring of His3 and proton peaks for Gly1 and Lys4.¹¹⁸ A similar study was conducted with hepcidin 5 using an N-terminal fragment of the peptide and the entire peptide sequence.¹⁸⁰ Similar results were achieved, showing significant broadening after titration with Ni^{2+} for the first three residues, indicating metal binding.¹⁸⁰ There was also less significant peak shifting for residues 4, 5, and 6 around the metal center.¹⁸⁰

X-ray crystallography is another technique that can be used to obtain a three-dimensional structure of AMPs. As compared to structures determined using NMR, the structures determined from X-ray crystallography are usually higher in resolution (around 2.0 to 2.5 Å) due to the static nature of the crystals. However, sample preparation in X-ray crystallography requires crystallization, which is more challenging than solubilizing AMPs in solution NMR. These two methods can be used together to provide a clearer picture of the mechanism of action for an AMP. In dermcidin, X-ray crystallography studies revealed the hexameric bundle formed by α -helical dermcidins (Figure 7).¹⁸¹ This bundle is stabilized by salt bridges and Zn^{2+} ions that were seen to intercalate between two of the helices. It has a high charge density inside the channel due to 96 ionizable residues oriented towards the interior of the channel.¹⁸¹ This makes it easier for the hexamer to be dissolved in water. Outside the channel, there is a region which is exclusively hydrophobic allowing it to be soluble also when membrane-bound.¹⁸¹

While biophysical experiments are significant in determining the structure and providing some mechanistic insights of AMPs, each technique has their own limitations. Thus, it is important to do as many biophysical studies as possible to have a more plausible mechanism of action for

AMPs. CD spectroscopy can only provide an ensemble average of the secondary structure present in the given sample. It cannot determine which specific residues or regions of the peptide contain the secondary structure. This can be solved by determining the structure of the peptides using more sophisticated techniques such as NMR spectroscopy or X-ray crystallography, as described earlier. X-ray crystallography can provide high resolution structures, but it cannot be used to study the dynamics of the peptide at a high resolution. NMR spectroscopy allows the dynamics of the AMP to be studied as it interacts with different membrane environments, but it cannot provide high-resolution dynamics.

2.6 Molecular Dynamics (MD) Simulations

Molecular dynamics (MD) simulations are a powerful tool to visualize how the AMPs interact with lipid bilayers, or with themselves (in cases of multiple peptide interactions), in an atomistic scale on timescales ranging from picoseconds to hundreds of microseconds. To briefly describe an MD simulation, each atom or a group of atoms is modeled as a bead, while each covalent bond between the atoms or groups of atoms is modeled as a spring. The potential energy of each atom is calculated from a chosen set of force field parameters. From these energies, the

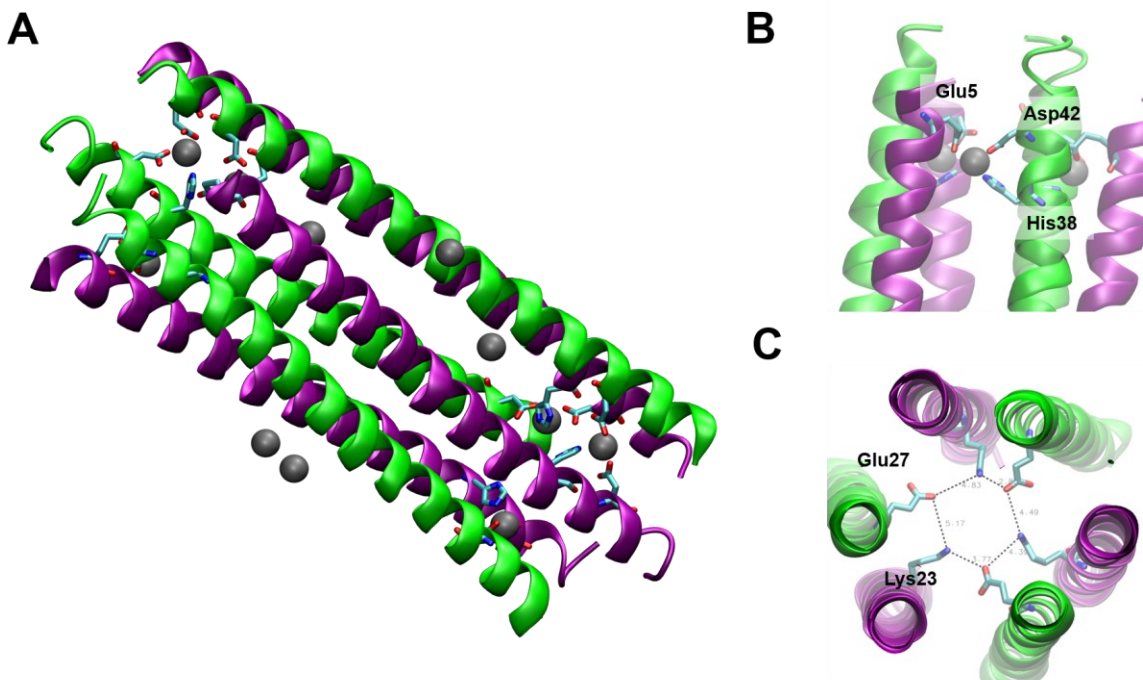


Figure 7. (A) Hexameric bundle (trimer of dimers) of α -helical dermicidins. Each dimer is depicted by one green helix and one purple helix. (B) One of the Zn^{2+} (gray spheres) complex that stabilizes the dimer are formed by coordination to Glu5, Asp42, and His38. (C) One of the salt bridges that stabilize the hexamer are formed by between Glu27 and Lys23.

velocities of each atom are calculated based on the theory of classical mechanics. The system is advanced for one timestep, usually about 1 to 2 femtoseconds for all-atom simulations, and each atom moves according to its velocity. New potential energies and velocities are calculated, and the process is repeated for a million to a billion times to generate nanosecond to microsecond trajectories, consisting of consecutive frames describing the coordinates, velocities, and forces of each atom in the system.

2.6.1 Equilibrium simulations

The simplest and most common MD simulation is equilibrium simulation, wherein no additional bias energies are introduced in the system, and the simulation is run for a long time until

the desired properties of the system are equilibrated. The properties of AMP-lipid bilayer systems that can be studied are: (1) the order of the lipid acyl chains in each bilayer leaflet, (2) membrane curvature, (3) membrane thickness, and (4) water orientation and penetration into the bilayer. Commonly, amphipathic AMPs that are surface-bound to the membrane are initiated from a configuration that corresponds to the “wedge” model (Figure 8).^{182,183} Melittin is one of the most widely-studied AMPs using MD simulations. It is a 26-amino acid AMP isolated from the venom of the honeybee.¹⁸³⁻¹⁸⁵ When it was surface-bound to a DMPC bilayer, the lipid perturbation by melittin lead to an approximately 30 percent reduction of membrane thickness along the hydrophobic core.¹⁸⁶ The order of the acyl chains in the leaflet where melittin is bound was significantly reduced.¹⁸⁶ This indicates that the lipids in this leaflet can easily adopt conformations that will accommodate the insertion of melittin and will avoid creating a large cavity beneath the peptide.¹⁸⁶ In an MD simulation of melittin where it was initially oriented transmembrane to the

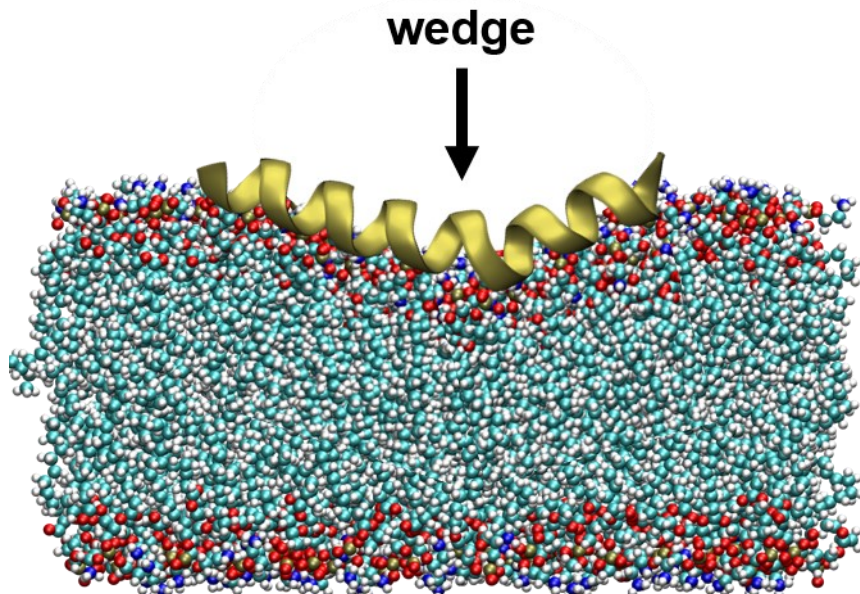


Figure 8. Wedge-bound model of a melittin that is surface-bound to a lipid bilayer. The planar region of the bilayer gets distorted as melittin interacts with the lipid headgroups.

bilayer and the N-terminus was in the leaflet closer to the intracellular side, the intracellular side of the leaflet was more disordered, opposite the observation from the surface-bound simulation. The asymmetry in the disorder between the two leaflets when the melittin is oriented transmembrane to the bilayer suggests that the favored orientation of the melittin might not be a full transmembrane orientation.¹⁸⁷

The effect of AMP insertion into the bilayer on the water molecules surrounding it and the water molecules on the solvent-bilayer interface is another property that can be studied using MD simulations. In melittin, Lys7 is the residue responsible for water penetration from the extracellular

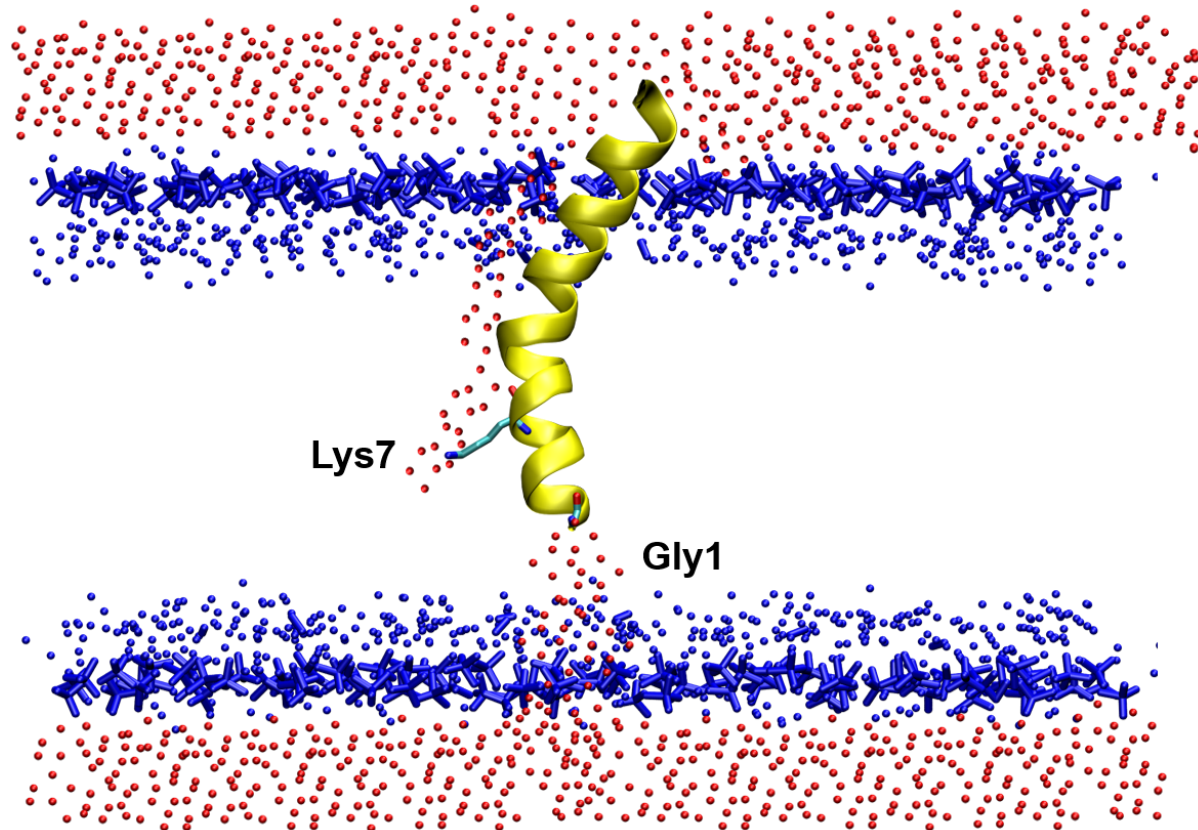


Figure 9. Melittin orientation when it is inserted into the bilayer. Water molecules from the extracellular side can penetrate up to the Lys7 residue, while those from the intracellular side can penetrate up to the positively charged N-terminus.

side of the membrane, while the protonated N-terminus is responsible for water penetration from the intracellular side (Figure 9).^{186,188} Combining the surface-bound and transmembrane MD simulations in melittin allows the description of a plausible mechanism in which melittin binds with an unprotonated N-terminus. Once bound, it gets protonated, allowing water to penetrate the bilayer. As water molecules cross the bilayer, it helps the charged N-terminus in crossing the hydrophobic core of the bilayer, putting the peptide in an inserted orientation where the N-terminus is closer to the intracellular side of the bilayer. The presence of multiple transmembrane melittins in the bilayer induces pore formation, and therefore the lytic activity of the melittin.

2.6.2 Non-equilibrium simulations

Equilibrium simulations do not allow the system to cross high energy barriers and explore metastable states that might lead to discovering other conformations in a local minimum energy well. Transitions between states occur on a timescale greater than microseconds; thus, these transitions are considered as rare events in equilibrium simulations. In this light, bias interactions may be introduced into the system to allow such rare events to be explored on a shorter timescale. A more recent study on melittin introduced a bias force that created membrane defects by pulling randomly selected groups of lipid headgroups at a rate of 0.001 nm/ps towards the bilayer center.¹⁸⁹ When the bias was removed without a peptide inserting into the membrane defect, the defect is short-lived and the membrane goes back to its normal state.¹⁸⁹ However, whenever a membrane defect is formed closer to the N-terminus of the peptide, the N-terminus inserts into the defect and does not allow the membrane to heal.¹⁸⁹ This was followed by the N-terminus of the other peptides also inserting into the stable membrane defect, which eventually became a small pore that remained stable throughout the simulation.¹⁸⁹

2.6.3 Molecular Dynamics of ATCUN-containing AMPs

Among the MD simulation studies of ATCUN-AMPs reported in the literature, just a few of them take into account the metal ion. The main challenge in the field is the selection of an appropriate methodology that will accurately model the binding of ATCUN motif to the metal ion. Currently, quantum mechanics/molecular mechanics (QM/MM) simulations are being employed in proteins that contain a metal ion cofactor to better understand the mechanistic role of the latter in the protein function.¹⁹⁰⁻¹⁹² In these cases, *i.e.* QM/MM simulations of metal-bound proteins, the structure is known experimentally for such metal-protein systems, which allows calibration of the method. Unfortunately, solved structures of their metal-bound state are not known common for ATCUN-AMPs.

In a QM/MM study of two piscidins (p1 and p3, discussed in section 3.3) interactions with DNA, Cu²⁺ ion was not included in the model.¹¹⁹ Due to the lack of solved DNA-bound piscidins, the systems were prepared by refining the DNA duplex structure with MD simulations, and by searching for the bound structures with Haddock docking. The advantage of using QM/MM is that it better captures the electronic properties of the hydrogen bonding interactions at the binding site. This cannot be accurately depicted using a purely classical mechanics simulation due to the fixed charge implementation of most force fields. On the other hand, modelling the system completely using quantum mechanics has a very high computational cost and can potentially compromise the sampling of the system. It was shown in the study that p3 requires lower binding energy to DNA than p1 does, and this is attributed to the more extensive network of DNA-p3 interactions, which was also observed from the same study.

The interactions of an ATCUN-containing truncated version of buforin II (*sh*-buforin, RAGLQFPVGRVHRLRK-NH₂) with DNA were studied using MD simulations, in tandem with molecular docking using the software VINA.¹⁹³ This approach required less computational power

than QM/MM simulations as it does not do any quantum chemical calculations. In this method, Adaptive Poisson-Boltzmann Solver (APBS) software was employed to calculate the binding energies of the AMP-DNA complexes every 2 ns from the MD simulations.^{194,195} There were four different variants of *sh*-buforin included in the study, with two of them containing a different sequence of ATCUN motif: L-*sh*-buforin, D-*sh*-buforin (_DRAGLQFPVGRVHRLRK-NH₂), Cu^{II}-L-VIH-*sh*-buforin (VIHRAGLQFPVGRVHRLRK-NH₂), and Cu^{II}-L-RTH-*sh*-buforin (RTHRAGLQFPVGRVHRLRK-NH₂). The difference in the charges of ATCUN motif sequences appended to *sh*-buforin led to difference in their respective binding positions of the Cu^{II}-ATCUN moiety within the DNA sequence. In the VIH-containing *sh*-buforin, the metallated ATCUN moiety is oriented equatorially to the negatively charged phosphate backbone of DNA, while in the more positive RTH-containing *sh*-buforin, the same fragment is oriented axially. It was observed that most of the hydrogen bonding interactions that stabilize the binding of these peptides with DNA originate from the basic residues present in the parent sequence, *i.e.* the residues other than the ATCUN motif, highlighting the importance of the non-ATCUN sequence to target a specific biopolymer, a theme that we will observe repeating itself throughout this review. The presence of Arg and Thr in Cu^{II}-L-RTH-*sh*-buforin extends this hydrogen bonding network, resulting to an increased binding affinity of the peptide to the negatively charged DNA backbone. This supports the experimentally observed enhancement of antimicrobial activity when an ATCUN motif is added to *sh*-buforin, as the proposed mechanism of action for this family of peptides is DNA cleavage.

3. The Amino Terminal Copper and Nickel (ATCUN) Binding Motif and its Role in Immunity

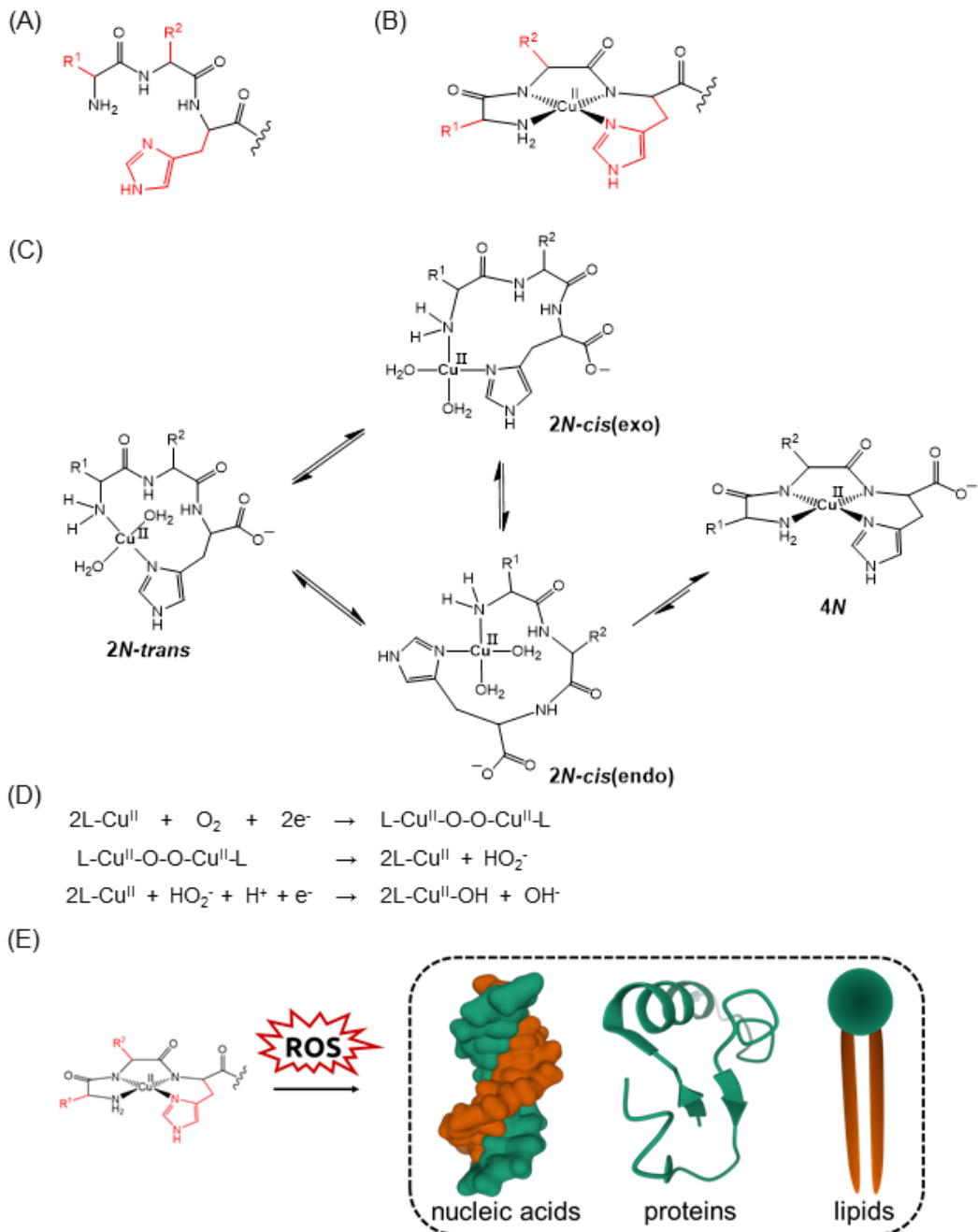


Figure 10. (A) Amino Terminal Copper and Nickel (ATCUN) binding motif. (B) Schematic representation of a Cu²⁺-ATCUN complex. The nitrogen atoms bound to Cu²⁺ form a distorted square planar geometry. (C) Sequence of steps hypothesized by Bal *et al.* leading to the formation of the Cu²⁺-ATCUN complex via bis-aquo intermediates.¹⁹⁸ (D) Mechanism proposed by Cowan *et al.* for the formation of reactive oxygen species. Two-electron reduction of O₂ produces diffusible H₂O₂ that subsequently produces a copper-bound hydroxyl radical, the formal highly oxidizing reactive species (ROS).¹⁹⁷ (E) ROS from the Cu²⁺-ATCUN complex can damage nucleic acids, proteins and lipids.

biology,^{100,196} is composed of the sequence H₂N-XXH found in the N-terminus, where the XX component of the motif can be any amino acid other than Pro.¹⁰⁰ Cu²⁺ and Ni²⁺ can bind to the motif in a distorted square planar geometry through the backbone of the two deprotonated N_{amide} atoms and the imidazole ring of the His (Figure 10).^{100,197,198} The ATCUN motif is ubiquitous in nature as it is part of human serum albumin (HSA), histatin, and protamine P2a, to name but a few examples.¹⁰⁰ Over 250 ATCUN-containing AMPs or putative AMPs can be found in species from 12 different phyla, with the most being identified in the phylum Chordata (Table 1). However, the biophysical characteristics of the ATCUN motif in large proteins such as HSA cannot be directly correlated to that of its truncated forms or shorter analogs with high sequence homology to the parent protein. For example, the binding affinity of the ATCUN-containing tetrapeptides Asp-Ala-His-NH₂ and Asp-Ala-His-Lys-NH₂ found in the native HSA sequence have higher binding affinities than HSA itself.¹⁹⁹ It is important to realize how the presence of other residues in large proteins can affect the accessibility of the ATCUN motif, or any metal-binding motif, especially upon protein folding. The ATCUN motif can coordinate Cu²⁺ and Ni²⁺ with high affinity. The strongest Cu²⁺ binding reported for an ATCUN binding motif is for human hepcidin or Hep-25, with a logK_d of 14.4 and a sequence of DTH.¹⁴⁸ Other ATCUN peptides have been reported to have μM to pM binding affinity.^{149,150,200} The affinity of binding can be influenced by the basicity of the side chains of the residues preceding His3 and steric hindrances.^{201,202} When the amide nitrogen is more acidic, the residue is more easily deprotonated, potentially due to the electron withdrawing ability of the acidic residue.²⁰¹ Increased hydrophobicity of the side chains in the first, second, and fourth positions can protect the holo-peptide from hydrolysis reactions and stabilize the complex by forming a hydrophobic fence.^{201–203} VIH is one of the strongest metal binders due to this hydrophobic fence formation.²⁰³ Basic residues at the N-terminus can also lead to increased

stability and basicity of the other N atoms that form the complex.²⁰⁴ Aromatic residues can contribute to the thermodynamic stability of the holo-peptide via d-π interactions.²⁰⁵ Complexes of Cu²⁺ can produce ROS and the Cu²⁺-ATCUN complexes are no different.^{172,197,206–213} These ROS species can damage any molecules in close proximity, including the ROS generator itself. In the case of ATCUN-AMPs, the ROS form will target nucleic acids, proteins, and lipids (Figure 10E). The ATCUN sequence acts as the cargo whereas the rest of the sequence has the important function of localizing the cargo close to the target molecule.^{212,214}

Table 1. Summary of ATCUN-AMPs, including putative sequences

Peptide	Sequence	Species
Arthropoda		
Tenecin-3 ²¹⁵	DHHDGHLGGHQTGHQGGQQGGHLGG HQGGQPGGHLGGHQGGIGGTGGQQHG QHGP GTGAGHQGGYKTHGH	<i>Tenebrio molitor</i>
LSer-PCecL2 ²¹⁶	HHHHRFGKIGHELHKGVKKVEKVTHD VNKVTSGVKVASSIEKAKNV	<i>Lucilia sericata</i>
LSer-PCecL3 ²¹⁶	HHHFGRIGHELHKGVKKVEKVTSDVN KVTNGVKQVANGIAKAKTVIEAGSIAG AVAAAAA	<i>Lucilia sericata</i>
LSer-PCecL5 ²¹⁶	HHHLFGHVGHEVERSLHKVGHKLEHA CHEVHKTAKKVQK	<i>Lucilia sericata</i>
Ixosin ¹¹⁸	GLHKVMREVLGYERNSYKKFFLR	<i>Ixodes sinensis</i>

Metchnikowin ²¹⁷	HRHQGPIDTRSPFNPQPRPGPIY	<i>Drosophila melanogaster</i>
HIcyst-2 ²¹⁸	RLHDPSNSPKYLELAHFAISQQTHTVLK LVKVETQVVAGINNYRPTNCPVNEKYS IENCKPTTNHATVYERPWENYRELTTSR	<i>Haemaphysalis longicornis</i>
	CP	
Periplanetasin-4 ²¹⁹	LRHKVYGYCVLGP	<i>Periplaneta americana</i>
ISGCock_contig02_37	KLHEFKLGYPLATNYACAIARDLILHKI	<i>Periplaneta americana</i>
34 ²²⁰	YIIHFLHRLRKKLSHY	<i>Periplaneta americana</i>
ISGCock_contig01_37	PPHMQSPLCAPCKIQGRSIVFRSIVLVN	<i>Periplaneta americana</i>
7 ²²⁰	LN	<i>Periplaneta americana</i>
ISGCock_contig16_20	SIHNHLTAASITHVKNRGKYIYMHLKFR	<i>Periplaneta americana</i>
60 ²²⁰	KTNVLI	<i>Periplaneta americana</i>
ISGCock_contig13_43	YAHLSNIPIFQVCVCSKVYYIHKHFTNY	<i>Periplaneta americana</i>
05 ²²⁰	LRVSKQNC	<i>Periplaneta americana</i>
Midgut defensin ²²¹	ACHAHCQSVGRRGGYCGNFRMTCYCY	<i>Haemaphysalis longicornis</i>
Def-Acaa(Def-1)	VNHALCAAHCIARRYRGGYCNSKAVC	<i>Anopheles gambiae</i>
	VCR	
Def-Daa (Def-1)	WNHTLCAAHCIARRYRGGYCNSKAVC	<i>Anopheles gambiae</i>
	VCR	

Carpenter	Ant	VNHSACAAHCILRGKTGGRCNSNAVCV	<i>Camponotus</i>
Defensin ²²²	CR		<i>floridanus</i>
Diptericin ²²³	DLHIPPPDNKINWPQLSGGGGGSPKTGY	<i>Sarcophaga</i>	
	DININAQQK		<i>peregrin</i>
AclasinN ²²⁴	LCHNSISCALGGDNVCNNVCVRQGND	<i>Nasonia vitripennis</i>	
	NGGRCLPRDGCPGYDICACYPRS		
AfusinN ²²⁴	FCHNSISCMMGGDSTCNNVCVRQGNP	<i>Nasonia vitripennis</i>	
	NGGRCLPRDGCPGYDICACYPNN		
Nefisin-2N ²²⁴	LCHNSISCMMGGDSTCNNVCVRQGNPS	<i>Nasonia vitripennis</i>	
	GGRCLPRDGCPGYDICACYPNS		
Nefisin-1N ²²⁴	FCHNSISCALGGDSTCNNVCVRQGNPH	<i>Nasonia vitripennis</i>	
	GGRCLPRDGCPGYDICACYPNN		
AorsinN ²²⁴	FCHDSISCMVGGDNVCNNVCVRQGNP	<i>Nasonia vitripennis</i>	
	NGGRCLPRDGCPGNDICACYPQS		
Aflasin-1N ²²⁴	FCHDSISCMVGGDNVCNNVCVRQGNP	<i>Nasonia vitripennis</i>	
	NGGRCLPRDGCPGNDICACYPQS		
Psabaecin*	DTHTLLTHRIRLPNGPGYGPFNPHQPWP	<i>Pseudomyrmex</i>	
	IPWPNNNG	<i>gracilis</i>	
Atabaecin-2*	DIHTLSTHKIRLPNGPGYGPFNPHQPWI		
	PWPNNNG	<i>Atta colombica</i>	
Cyabaecin*	DTHTFSTHKIRLPNGPGYGPFNPHQPWP	<i>Cyphomyrmex</i>	
	IPWPW	<i>costatus</i>	

Trabaecin*	DTHALPKHRFLPSGPGYGPFPNPQQPW PVPWPNNNG	<i>Trachymyrmex</i> <i>cornetzi</i>
Acabaecin*	DTHTLSTHRIRLPSGPGYGPFPNPQHQPWL ISWPQNQ	<i>Acromyrmex</i> <i>echinatior</i>
Tachylectin-5B ²²⁵	DVHHHAACSTVCSLKGILDSVSDLTDL AKERLATLQNPICSKDKAFYMETYTNV TQNKAEKNGLPINCATVYQQGNRTSGI YMIWPLFLNHPISVFCDMETAGGGWTV IQRRGDFGQPIQNFYQTWESYKNGFGN LTKEFWLGNDIIFVLTNQDSVVLVDLE DFEGGRRYAEAVEFLVRSEIELYKMSFK TYKGDAAGDSLSQHNNMPFTTKDRDND KWEKNCAEAYKGGWWYNACHHSNLN GMYLRGPHEESAV	<i>Tachypleus</i> <i>tridentatus</i>
Sickin2.4 ²²⁶	ENHDASTAACQTRQTCKRTSDCCDGL VCVKHAWICVPDEEPPY	<i>Solenopsis invicta</i>
Sickin2.3 ²²⁶	GNHEASTSACVHTSLPCKQTSDCCDGL MCEPHARICIPNKKNSHFG	<i>Solenopsis invicta</i>
Atabecin2 ²²⁶	DTHTFSTHKIRLPNGPGYGPFPNPHQSWP IPWPNNNG	<i>Atta cephalotes</i>
Aeabaecin2 ²²⁶	DIHTLSTHKIRLPNGPGYGPFPNPHQPWPI PWPNNNG	<i>Acromyrmex</i> <i>echinatior</i>

Pobabaecin2 ²²⁶	DTHALPKHRLRLPGGGPGYGPFNPRLP WPIPLPNRDH	<i>Pogonomyrmex</i> <i>barbatus</i>
Siabaecin2 ²²⁶	DTHALPEHRPRLPEGPGYVLFNPRQPW PVPWPNHGR	<i>Solenopsis invicta</i>
Wasabaecin*	DTHTLSTHRIRLPNGPGYGPFNPHQSWP IPLPNNG	<i>Wasemannia</i> <i>europunctata</i>
Attacin-E ²²⁷	DAHGALTLDGTSGAVVKVPFAGND KNIVSAIGSVDLTDRQKLGAATAGVAL DNINGHGLSLTDTHIPFGDKMTAAGK VNVFHNDNHDTAKAFATRNMPDIANV PNFNTVGGGIDYMFKDKIGASASAHT DFINRNDYSLDGKLNLFKTPDTSIDFNA GFKKFDTDFMKSSWEPNFGFSLSKYF	<i>Hyalophora</i> <i>cecropia</i>
Attacin-F ²²⁷	DAHGALTLDGTSGAVVKVPFAGND KNIVSAIGSVDLTDRQKLGAATAGVAL DNINGHGLSLTDTHIPFGDKMTAAGK VNVFHNDNHDTAKAFATRNMPDIANV PNFNTVGGGIDYMFKDKIGASASAHT DFINRNDYSLDGKLNLFKTPDTSIDFNA GFKKFDTDFMKSSWEPNFGFSL	<i>Hyalophora</i> <i>cecropia</i>

Chordata

Piscidin-1 ²²⁸	FFHHIFRGIVHVGKTIHRLVTG	<i>Morone saxatilis</i> x <i>M. chrysops</i>
----------------------------------	------------------------	---

Piscidin-2 ²²⁸	FFHHIFRGIVHVGKTIHKLVTG	<i>Morone saxatilis</i> x <i>M. chrysops</i>
Piscidin-3 ²²⁸	FIHHIFRGIVHAGRSIGRFLTG	<i>Morone saxatilis</i> x <i>M. chrysops</i>
Sablefish Piscidin ²²⁹	FIHHIFNGLVKVGKSIHGLIRRHHG	<i>Anoplopoma fimbria</i>
Yellowtail Kingfish	FFHHILSGIFHVGKMIHGAIQRRRH	<i>Seriola lalandi</i>
Piscidin ²²⁹		
Sea Bass Piscidin ²²⁹	FIHHIFRGIIINAGKSIGRFITGGKA	<i>Dicentrarchus labrax</i>
Striped Beakfish	FFHHIFNGLVGVGKTIHRLITGGRN	<i>Oplegnathus fasciatus</i>
Piscidin ²²⁹		
Japanese Amberjack	FFHHILSGIFHVGKMIHGAIHRRRH	<i>Seriola quinqueradiata</i>
Mandarin Fish	IFHHIFKGIVHVGKTIHRLVTG	<i>Siniperca chuatsi</i>
Moronecidin ²³⁰		
Almaco Jack	FIHHIIGIFHIGKMIHSAINRRRHG	<i>Seriola rivoliana</i>
Piscidin**		
Greater Amberjack	FIHHIIGIFHIGKMIHSAINRRRHG	<i>Seriola dumerili</i>
Piscidin**		
Gaduscidin-1 (pis-1)	FIHHIIGWISHGVRAIHRAIH	<i>Gadus morhua</i>
231,232		
Gaduscidin-2 (pis-2)	FLHHIVGLIHHGLSLFGDRAD	<i>Gadus morhua</i>
231,232		

Pis-2β [57]	FLHHIVGLIHHGKLDMYRSNN	<i>Gadus morhua</i>
Pteroicidin-α ²³³	FIHHIIGGLFHVGVKSIHDLIR	<i>Pterois volitans</i>
Myxinidin ²³⁴	GIHDILKYGKPS	<i>Myxine glutinosa</i>
Dicentracin ²³⁵	FFHHIFRGIVHVGVKSIHKLVGT	<i>Dicentrarchus labrax</i>
Oreoch-1 ²³⁶	FIHHIIGGLFSVGKHIHGLIHGHH	<i>Oreochromis niloticus</i>
Oreoch-2 ²³⁶	FIHHIIGGLFSAGKAIHRLIRRRRR	<i>Oreochromis niloticus</i>
TP3 ²³⁷	FIHHIIGGLFSVGKHIHSЛИGH	<i>Oreochromis niloticus</i>
TP4 ²³⁷	FIHHIIGGLFSAGKAIHRLIRRRRR	<i>Oreochromis niloticus</i>
AJHba ²³⁸	FAHWPDLGPSPSVKKHGKVIM	<i>Anguilla japonica</i>
Clavanin C ²³⁹	VFHLLGKIIHHVGNFVYGFHV	<i>Styela clava</i>
Plicatamide (PL-101)	FFHLHFHY (Y is dc Δ DOPA)	<i>Styela plicata</i>
240		
Rainbow trout β-defensin 3 ²⁴¹	SLHLCFISGGGCRNRLCLAPGGTNIGK MGCTWPNVCC	<i>Oncorhynchus mykiss</i>
SA-Hepcidin ²⁴²	QSHLSMCRYCCNCCRNNKGCGFCCKF	<i>Scatophagus argus</i>
Mud-loach Hamp-1 ²⁴³	QSHLSMCRYCCKCCRNNKGCGFCCKF	<i>Misgurnus mizolepis</i>
Blunt Snout Bream	QSHLSLCRYCCNCCRNNKGCGYCC	<i>Megalobrama amblycephala</i>
LEAP-1 ²⁴⁴		

cm-Hep ²⁴⁵	QSHISLCRYCCKCCCKTGCGFCCSF	<i>Channa maculata</i>
Minnow Hepcidin ²⁴⁶	QSHISLCRYCCKCCRNKGCGYCCKF	<i>Gobiocypris rarus</i>
Om-hep1 ²⁴⁷	QSHLSMCSVCCNCCKNYKGCGFCCRF	<i>Oryzias melastigma</i>
Cod Hepcidin ²⁴⁸	QSHLALCRWCCNCCRNQKGCGICCKF	<i>Gadus morhua</i>
Human LEAP-1/Hep-25 ²⁴⁹	DTHFPICIFCCGCCRSKCGMCCKT	<i>Homo sapiens</i>
Hepcidin TH2-3 ²⁵⁰	QSHLSLCRWCCNCCRSNKGC	<i>Oreochromis mossambicus</i>
Sheep Hepcidin ²⁵¹	DTHFPICIFCCGCCRKGTGCGICCKT	<i>Ovis aries</i>
Salmon Hepcidin ²⁵²	QIHLSLCGLCCNCCHNIGCGFCCKF	<i>Salmo salar</i>
Bovine Hepcidin ²⁵²	DTHFPICIFCCGCCRKGTGCGMCCKT	<i>Bos taurus</i>
Rabbit Hepcidin ²⁵³	DTHFPICIGCCSCCRNSKCGICCKT	<i>Oryctolagus cuniculus</i>
Dog Hepcidin ²⁵⁴	DTHFPICIFCCGCCCKTPKGCLCCKT	<i>Canis lupus familiaris</i>
Pig Hepcidin ²⁵⁵	DTHFPICIFCCGCCRKAIKGMCCKT	<i>Sus scrofa</i>
Chimpanzee Hepcidin	DTHFPICIFCCGCCRSKCGMCCKT	<i>Pan troglodytes</i>
255		
HAMP-1 Seabass ²⁵⁶	QSHLSLCRWCCNCCRGNKKGCGFCCKF	<i>Dicentrarchus labrax</i>
Gibbon Hepcidin ²⁵⁷	DTHFPICIFCCGCCRSKCGMCCKT	<i>Hylobates concolor</i>
Japanese Macaque	DTHFPICIFCCGCCRSKCGMCCKT	<i>Macaca fuscata</i>
Hepcidin ²⁵⁷		

Grivet Hepcidin ²⁵⁷	DTHFPICIFCCGCCHRSKCGMCCRT	<i>Cercopithecus aethiops</i>
Bornean Orangutan Hepcidin ²⁵⁷	DTHFPICIFCCGCCHRSKCGMCCKT	<i>Pongo pygmaeus</i>
Dusty Leaf Monkey Hepcidin ²⁵⁷	DTHFPICIFCCGCCHRSKCGMCCRT	<i>Presbytis obscurus</i>
Gorilla Hepcidin ²⁵⁷	DTHFPICIFCCGCCHRSKCGMCCKT	<i>Gorilla</i>
Buffalo Hepcidin ²⁵⁷	DTHFPICIFCCGCCHRSKCGMCCKT	<i>Bubalus bubalis</i>
Bat Hepcidin ²⁵²	DTHFPICIFCCGCCYPSKCGICCKT	<i>Myotis lucifugus</i>
Mole Rat Hepcidin ²⁵²	DTHFPICVFCCGCCKNARCGICCKT	<i>Heterocephalus glaber</i>
Orangutan Hepcidin 1 ²⁵²	DTHFPICIFCCGCCRQSNCGMCCKT	<i>Pongo</i> spp.
Orangutan Hepcidin 2 ²⁵²	DTHFPIYIFCCGCCHQSNCGMCCKT	<i>Pongo</i> spp.
Fox Hepcidin ²⁵²	DTHFPICIFCCGCCYKSKCGIGGKT	<i>Pteropus alecto</i>
Marmoset Hepcidin ²⁵²	DTHFPICIFCCGCCRQSNCGMCCKT	<i>Callithrix jacchus</i>
Baboon Hepcidin ²⁵²	DTHFPICIFCCGCCHRSKCGMCCRT	<i>Papio papio</i>
Horse Hepcidin ²⁵¹	DTHFPICTLCCGCCNKQKCGWCCKT	<i>Equus caballus</i>
Panda Hepcidin ²⁵⁸	DTHFPICLFCCGNKSKCGICCKT	<i>Ailuropoda melanoleuca</i>

Camel Hepcidin ²⁵⁹	DTHFPICVFCCGCCCHKSKGMCCKT	<i>Camelus dromedarius</i>
Yak Hepcidin ²⁵⁹	DTHFPICIFCCGCCRKGTCCMCCRT	<i>Bos grunniens</i>
Cat Hepcidin ²⁵⁹	DTHFPICIFCCGCCKKARCGMCCKT	<i>Felis catus</i>
Donkey Hepcidin ²⁵⁹	DTHFPICTLCCGCCNKQKCGWCCKT	<i>Equus asinus</i>
Painted Turtle	NSHFPICTYCCKCCRNQGCGFCCRT	<i>Chrysemys picta</i>
Hepcidin ²⁵⁸		
Three-spined	QSHLSMCRWCCCKCRSYKGCGYCKF	<i>Gasterosteus</i>
Stickleback Hamp1 ²⁶⁰		<i>aculeatus</i>
Sailfin Molly Hamp1	QSHLSLCRYCCNCCKNGCGFCCRF	<i>Poecilia latipinna</i>
260		
Burton's	QSHLSLCRWCCNCCRSNKKGCGFCCFK	<i>Haplochromis</i>
Mouthbrooder		<i>burtoni</i>
Hamp1 ²⁶⁰		
Western Clawed Frog	QSHLSICVHCCNCCKYKGCGKCCLT	<i>Xenopus tropicalis</i>
Hepcidin ²⁵²		
Flounder Hepcidin ²⁶¹	ISHISLCRWCCNCCKANKCGFCCKF	<i>Pseudopleuronectes americanus</i>
Notothenioid	QSHLSLCRWCCNCCKGNGGCCFCCRF	<i>Antarctic</i>
Hepcidin ²⁶²		<i>notothenioid</i>
Lizard Hepcidin ²⁶³	NSHISICTYCCNCCKNGCSFCCRT	<i>Anolis carolinensis</i>
Alligator Hepcidin ²⁶³	NSHFPICTSYCCNCCHNKKGCGFCCRT	<i>Alligator mississippiensis</i>

SmHep1P ²⁶⁴		QSHISLCRWCCNCCKANKGCGFCKF	<i>Scophthalmus</i> <i>maximus</i>
Longtooth Grouper		QSHLSMCRWCCNCCKGNKGCGPCCKF	<i>Epinephelus</i> <i>moara</i>
Hepc5 ²⁴⁵			
Smallmouth Bass		QSHLSLCRWCCNCCKGNKGCGFCCRF	<i>Micropterus</i>
Hepcidin ²⁴⁵			<i>dolomieu</i>
Pacific Mutton		QSHLSLCRWCCNCCKGNKGCGFCKF	<i>Alphestes</i>
Hamlet Hepcidin ²⁴⁵			<i>immaculatus</i>
Redbanded Seabream		QSHISMCYWCCNCCKRANKGCGYCKF	<i>Pagrus</i> <i>auriga</i>
Hepcidin ²⁴⁵			
Javanese Ricefish		QSHLSMCSVCCNCCKNYKGCGFCCRF	<i>Oryzias</i> <i>javanicus</i>
Hepcidin ²⁴⁵			
Rainbow Trout		QSHLSLCRWCCNCCHNKGCGFCKF	<i>Oncorhynchus</i>
Hepcidin ²⁴⁴			<i>mykiss</i>
Turbot Hepcidin ²⁴⁴		QSHISLCRWCCNCCKANKGCGFCKF	<i>Scophthalmus</i> <i>maximus</i>
Nile Tilapia Hepcidin		QSHLSLCRWCCNCCKRSNKGCGFCCRF	<i>Oreochromis</i>
244			<i>niloticus</i>
LEAP-2 (4Cys) ²⁶⁵		MWHLKLCAVLMIFLLLLGQIDGSPipeV SSAKRRPRRMTPFWRGVSLRPIGASCR DDSECITRLCRKRRCSLSVAQE	<i>Homo sapiens</i>
Smallmouth Bass		QSHLSMCRWCCNCCKGNKGCGFCCRF	<i>Micropterus</i>
Hepcidin ²⁴⁴			<i>dolomieu</i>

Largemouth	Bass	QSHLSLCRWCCNCCRGNKCGFCCRF	<i>Micropterus</i>
Hepcidin ²⁴⁴			<i>salmoides</i>
Large Yellow Croaker		QSHLSLCRWCCNCCSNKCGFCCRF	<i>Larimichthys crocea</i>
Hepcidin ²⁴⁴			
Weather	Loach	QSHLSMCRYCCKCCRNKGCGFCCKF	<i>Misgurnus mizolepis</i>
Hepcidin ²⁴⁴			
Zebrafish Hepcidin ²⁴⁴		QSHLSLCRFCCKCCRNKGCGYCCKF	<i>Danio rerio</i>
Olive Barb Hepcidin		QSHLSLCRYCCNCCRNKGCGYCCKF	<i>Puntius sarana</i>
244			
Common	Carp	QSHLSLCRYCCNCCRNKGCGYCCKF	<i>Cyprinus carpio</i>
Hepcidin ²⁴⁴			
Grass Carp Hepcidin		QSHLSLCRYCCNCCRNKGCGYCCKF	<i>Ctenopharyngodon</i>
244			<i>idella</i>
Wuchang	Bream	QSHLSLCRYCCNCCRNKGCGYCCKF	<i>Megalobrama</i>
Hepcidin ²⁴⁴			<i>amblycephala</i>
Chinese Rare Minnow		QSHISLCRYCCKCCRNKGCGYCCKF	<i>Gobiocypris rarus</i>
Hepcidin ²⁶⁶			
Ragged	Bigscale	QSHLSMCRYCCKCCRNKGCCFCCKF	<i>Scopelogadus</i>
Hepcidin ²⁶⁶			<i>mizolepis</i>
Richardson's Willow		QSHLSLCRYCCNCCRNKGCGYCCKF	<i>Salix richardsonii</i>
Hepcidin ²⁶⁶			
Silver Carp Hepcidin		QSHLSLCRYCCNCCRNKGCGYCCKF	<i>Hypophthalmichthys</i>
266			<i>molitrix</i>

Buff-throated	QSHISLCRWCCNCCKANKGCGFCKF	<i>Saltator maximus</i>
Saltator Hepcidin ²⁶⁶		
Hamp-1	Yellowtail	QSHLSMCRWCCNCCTANKGCGFCCRF
		<i>Seriola lalandi</i>
Kingfish ²²⁹		
Hamp-1	Amazon	QSHLSLCRYCCNCCKNKGCGFCCRF
		<i>Poecilia formosa</i>
Molly ²²⁹		
Channel	Catfish	QSHLSLCRYCCNCCKNKGCGFCCRF
		<i>Ictalurus punctatus</i>
Hepcidin ²⁶⁷		
Atlantic	Salmon	QSHLSLCRWCCNCCHNKGCGFCKF
		<i>Salmo salar</i>
Hepcidin ²⁶⁶		
Longtooth	Grouper	QSHLSMCRWCCNCCKGNKGCGGLCKF
		<i>Epinephelus moara</i>
Hepcidin ²⁶⁶		
Japanese	Rice	QSHISMCTMCCNCCKNYKGCGFCCRF
	Fish	<i>Oryzias latipes</i>
Hepcidin ²⁶⁶		
Brown	Trout	QSHLSLCRWCCNCCHNKGCGFCKF
		<i>Salmo trutta</i>
Hepcidin ²⁶⁸		
Siberian	Tiamen	QSHLSLCRWCCNCCHNKGCGFCKF
		<i>Hucho taimen</i>
Hepcidin ²⁶⁸		
Coho	Salmon	QSHLSLCRWCCNCCHNKGCGFCKF
		<i>Oncorhynchus</i>
Hepcidin ²⁶⁸		<i>kisutch</i>
Hamp-1		MSHLSVCVYCCDCCHKKTCGICCKF
		<i>Chiloscyllium</i>
Bambooshark ²²⁹		<i>plagiosum</i>
Hamp-1 Fugu ²²⁹		QSHLSLCTLCCNCCKGNKGCGFCCRF
		<i>Takifugu rubripes</i>

Hamp-1	Rainbow	QSHLSLCRWCCNCCHNKGCGFCKF	<i>Oncorhynchus</i>
Trout ²²⁹			<i>mykiss</i>
Brown-headed Spider		DTHFPICIFCCGCCRQPNCGMCCKT	<i>Ateles fusciceps</i>
Monkey Hepcidin ²⁵⁵			
Sumatran Orangutan		DTHFPIYIFCCGCCHRSKCGMCCKT	<i>Pongo abelii</i>
Hepcidin ²⁶⁹			
Human LEAP-2 ²⁷⁰		MWHLKLCAVLMIFLLLLGQIDG	<i>Homo sapiens</i>
Rhesus	Macaque	MWHLKLCAVLMIFLLLLGQTDG	<i>Macaca mulatta</i>
LEAP-2 ²⁷⁰			
Bovine LEAP-2 ²⁷⁰		MWHLKLFAVLMICLLLQAQVDG	<i>Bos taurus</i>
Pig LEAP-2 ²⁷⁰		MWHLKLFAVLVICLLLAVQVHG	<i>Sus scrofa</i>
Sperm	Whale	DTHFPICVFCCKCCRKGMCGLCCRT	<i>Physeter catodon</i>
Hepcidin ²⁵³			
Saddleback		QSHLSLCRWCCNCCKGNKGCGFCCRF	<i>Pogonophryne scotti</i>
Plunderfish Hepcidin			
253			
Spiny-head	Croaker	QSHISLCRYCCNCCKGNKGCGFCCRF	<i>Collichthys lucidus</i>
Hepcidin ²⁵³			
ATCUN-C16 ²⁷¹		DSHAGYKRKFHEKHHSHRGY	Histatin-5 analog
Ubiquicidin (UBI 1-		KVHGSLARAGKVRGQTPKVAKQEKKK	<i>Homo sapiens</i>
59) ²⁷²		KKTGRAKRRMQYNRRFVNVPPTFGKK	
		KGPNANS	

Gorilla Histatin 1	²⁷³	DSHEKRHHGYRRKFHEKHHSHIEFPFY	<i>Gorilla</i>	<i>gorilla</i>
		GDYGTNYLYDN		<i>gorilla</i>
Gorilla Histatin 3	²⁷³	DSHEKRHHGYKRKSHEKHHSHRGYRS	<i>Gorilla</i>	<i>gorilla</i>
		NYLYDN		<i>gorilla</i>
Silver-leaf Monkey		DSHEEKHHGRGHHEYGRKFQEKHYS	<i>Trachypithecus</i>	
Histatin 3	²⁷³	HRGYRSNYLYGN		<i>cristatus</i>
Crab-eating Macaque		DSHKGKHHGHRRKFHEKHHSH		<i>Macaca fascicularis</i>
Histatin 1	²⁷³			
Crab-eating Macaque		DSHEERRQGRGHHEYGRKFHEKHS		<i>Macaca fascicularis</i>
Histatin 3	²⁷³	HRGYRSNYLYGN		
Crab-eating Macaque		DSHEERRQGRGHHEYGRKFHEKHS		<i>Macaca fascicularis</i>
Histatin 5	²⁷³	HRGY		
Crab-eating Macaque		DSHEERHHGRGHHKYGRKFHEKHS		<i>Macaca fascicularis</i>
Histatin	²⁷⁴	HRGYRSNYLYDN		
Rhesus Macaque		DSHKGKHHGHRRKFHEKHHSH		<i>Macaca mulatta</i>
Histatin	²⁷³			
Silver-leaf Monkey		DSHKGKHHGHRRKFHEKHSHEFPSYG	<i>Trachypithecus</i>	
Histatin	²⁷³	GYRSNYLYYN		<i>cristata</i>
Sumatran Orangutan		DSHEKRHEHRRKFHEKHHSHRGYRSN	<i>Pongo abelii</i>	
Histatin 5	²⁷³	YLDEN		
Human MUC7 20-	LAHQKPFIRKSYKCLHKRCR		<i>Homo sapiens</i>	
Mer	²⁷⁵			

Human Histatin 1 ²⁷⁶	DSHEKRHHGYRRKFHEKHHSHREFPFY GDYGSNYLYDN	<i>Homo sapiens</i>
Human Histatin 3 ²⁷⁶	DSHAKRHHGYKRKFHEKHHSHRGYRS NYLYDN	<i>Homo sapiens</i>
Human Histatin 4 ²⁷⁷	KFHEKHHSHRGYRSNYLYDN	<i>Homo sapiens</i>
Human Histatin 5 ²⁷⁶	DSHAKRHHGYKRKFHEKHHSHRGY	<i>Homo sapiens</i>
Human Histatin 6 ²⁷⁷	DSHAKRHHGYKRKFHEKHHSHRGYR	<i>Homo sapiens</i>
Human Histatin 8 ²⁷⁷	KFHEKHHSHRGY	<i>Homo sapiens</i>
Human Histatin 10 ²⁷⁷	KFHEKHHSHRGYR	<i>Homo sapiens</i>
Human Histatin 11 ²⁷⁷	KRHHGYKR	<i>Homo sapiens</i>
Human Histatin 12 ²⁷⁷	KRHHGYK	<i>Homo sapiens</i>
Grivet Histatin 1 ²⁷³	DSHEEKHHGHRRKHHGKHHSH <i>Chlorocebus aethiops</i>	
Grivet Histatin 3 ²⁷³	DSHEERHHGRHHGYGRKFHEKHS HRGYRSNYLYGN <i>Chlorocebus aethiops</i>	
Gibbon Histatin 1 ²⁷³	DSHEKRHEHRRKFHEKHHSHREYPFY GYYR <i>Nomascus leucogenys</i>	
Scorpion Ctry2459- H3 ²⁷⁸	FLHFLHHLP <i>Chaerilus tryznai</i> and <i>Chaerilus tricostatus</i>	
15kDa protein ²⁷⁹	IPHRLRLRYEEVVAQALQFYNEGQQGQP LFRLLEATPPPSLNSKSRIPLNFRIKETVC IFTLDRQPGNCAFREGGEERICRGAFVR <i>Oryctolagus cuniculus</i>	

		RRRVRALTLRCDRDQRRQPEFPRVTRP	
		AGPTA	
Rainbow Trout 40S	KVHGSLARAGK		<i>Oncorhynchus</i>
ribosomal protein S30			<i>mykiss</i>
280			
Human 40S ribosomal protein S30	KVHGSLARAGKVRGQTPKVAKQEKKK		<i>Homo sapiens</i>
	KKTGRAKRRMQYNRRFVNVVPTFGKK		
	KGPNANS		
Medaka 40S	KVHGSLARAGKVRGQTPNVDKHEEKE		<i>Oryzias latipes</i>
ribosomal protein S30	EEDGRAKRRIQYNRRFVNVVPTFGKK		
280	GANANS		
Shrimp 40S ribosomal protein S30	KVHGSLSRAGKVKGHTPKV X KKEKRK		<i>Litopenaeus</i>
	SKTGRAKRRI X YNRRFVN X ASFGKKR		<i>setiferus</i>
	GPNNSNS		
Chimpanzee Beta- defensin 134	EMHKKCYKNGICRLEYSEMLVAYC		<i>Pan troglodytes</i>
	MFQLECCVKGNPAP		
DEFB109P	EGHCLNLSGVCRDVCKVVEDQIGACR		<i>Pan troglodytes</i>
	RRMKCCRAW		
CAMP-t2 Beta- defensin	PIHRRIPPRWPRLKRRW		<i>Gallus gallus</i>
	281		
Chimpanzee Beta- defensin 107A**	AIHRALISKRMEGHCEAECLTFEVKTGG		<i>Pan troglodytes</i>
	CRAELAPFCCKNRKKH		

Human Beta-defensin	AIHRALISKRMEGHCEAECLTFEVKIGG	<i>Homo sapiens</i>
107**	CRAELAPFCCKNRKKH	
Beta-defensin 107A**	AIHRALICKRMEGHCEAECLTFEVKIGG	<i>Pongo pygmaeus</i>
	CRAELAPFCCKNRKKH	
White-handed Gibbon	AIHRALICKRMEGHCEAECLTFEVKIGG	<i>Hylobates lar</i>
Beta-defensin 107A**	CRAELAPFCCKNRKKH	
Dog	Beta-defensin	
119**	KHHILRCMGNTGICRPSCRKTEQPYLYC LNYQSCCLQSYMRISISGREEKDDWSQ QNRWPKIS	<i>Canis lupus familiaris</i>
Human Beta-defensin	KRHILRCMGNSGICRASCKKNEQPYLY	<i>Homo sapiens</i>
119**	CRNCQSCCLQSYMRISISGKEENTDWSY EKQWPRLP	
Rhesus macaque Beta-defensin 119**	KRHILRCMGNSGICRASCKKNEQPYLY CRNYQACCLQSYMRISISGKEENTDWS YEKQWPRLP	<i>Macaca mulatta</i>
Crab-eating Macaque	KRHNLRCMGNSGICRASCKKNEQPYLY	<i>Macaca fascicularis</i>
Beta-defensin 119**	CRNYQACCLQSYMRISISGKEENTDWS YEKQWPRLP	
Chimpanzee	Beta-	
defensin 119**	KRHILRRMGNSGICRASCKKNEQPYLY CRNYQSCCLQSYMRISISGKEENTDWS YEKQWPRLP	<i>Pan troglodytes</i>

Low-land gorilla Beta- defensin 119**	KRHILRCMGNSGICRASCKNEQPYLY CRNYQSCCLQSYMRISISGKEEDTDWS YEKQWPRLP	<i>Gorilla</i>	<i>gorilla</i>
White-handed Gibbon	KHHILRCMGNSGICRASCKNEQPYLY	<i>Hylobates lar</i>	
Beta-defensin 119**	CRNYQHCCLQSYMRISISGEEENTDWS YEKQWPRLP		
Bovine Beta-defensin 119**	RRHMLRCMGDLGICRPACRQSEEPYLY CRNYQPCCLPFYVRIDISGKEGKNDWS RENRWPKVS	<i>Bos taurus</i>	
Rhesus Macaque α- defensin 11²⁸⁴	ICHCRIGGCSRTEYSRICILRGQVARLC CRRAS	<i>Macaca mulatta</i>	
Chimpanzee	α - ICHCRVLYCLFGEHLGGTCFIHGERYPIC	<i>Pan troglodytes</i>	
defensin 13²⁸⁴	CY		
Rhesus Macaque α- defensin 18²⁸⁴	ICHCRVLYCLFGEHPGGTCFIHGEHYPIC CY	<i>Macaca mulatta</i>	
Human α-defensin²⁸⁴	TCHCRRSCYSTEYSYGTCTVMGINHRF CCL	<i>Homo sapiens</i>	
Chimpanzee	α - TCHCRRSCYSTEYSYGTCTVMGINHRF	<i>Pan troglodytes</i>	
defensin 1²⁸⁴	CCL		
Bornean Orangutan	TCHCRRSCYSTEYSYGTCTVMGINHRF	<i>Pongo pygmaeus</i>	
α-defensin²⁸⁴	CCL		
Human Furin²⁸⁵	YYHFWHRGVTKRSLSPHRPRHSRLQR	<i>Homo sapiens</i>	

PG-KI ²⁸⁶	EPHPDEFVGLM	<i>Pseudophryne</i> <i>giintheri</i>
PG-KIII ²⁸⁶	EPHPNEFVGLM	<i>Pseudophryne</i> <i>giintheri</i>
Electrin 3 ²⁸⁷	FVHPM	<i>Litoria electrica</i>
Schmackerin-F1 ²⁸⁸	VDHLWQVWLPR	<i>Odorrana</i> <i>schmackeri</i>
Limnonectin-1Fb ²⁸⁹	SFHVFPPWMCKSLKKC	<i>Limnonectes</i> <i>fujianensis</i>
Nigroain-D1 ²⁹⁰	CVHWQTNPARTSCIGP	<i>Rana nigrovittata</i>
Nigroain-D2 ²⁹⁰	CVHWQTNPARTSRIGP	<i>Rana nigrovittata</i>
Nigroain-D3 ²⁹⁰	CVHWQTNTARTSCIGP	<i>Rana nigrovittata</i>
Nigroacin-D-RK1 ²⁹¹	CMHWQTGPARTSCIGP	<i>Limnonectes kuhlii</i>
Pleurain-R1 ²⁹²	CVHWMTNTARTACIAP	<i>Rana pleuraden</i>
Temporin-GHb ²⁹³	FIHHIIGALGHLF	<i>Hylarana guentheri</i>
Gallinacin-7 ²⁹⁴	RYHMQCGYRGTFCTGKCPYGNAYLGL CRPKYSCCRWL	<i>Gallus gallus</i>
Caseicin A ²⁹⁵	IKHQGLPQE	<i>Bos taurus</i>
Chicken AvBD4 ²⁹⁶	RYHMQCGYRGTFCTPGKCPYGNAYLG LCRPKYSCCRWL	<i>Gallus gallus</i>
Histidine-rich glycoprotein, GHH20	GHHPHGHHPHGHHPHGHHPH	<i>Homo sapiens</i>

AHH24	²⁹⁸	AHHAAHAAHAAHHAAHAAHAAHAAHAA	<i>Homo sapiens</i>
Human	kininogen-	HKHGHGHGKHKKNKGKKNGKH	<i>Homo sapiens</i>
derived	peptide,		
HKH20	²⁹⁹		
Cystatin-1	³⁰⁰	DTHISEKIIDCNDIG	<i>Capra hircus</i>
Cystatin-2	³⁰⁰	DTHISEYIIDCNDIG	<i>Capra hircus</i>
YR26, Human furin-		YYHFWHRGVTKRSLSPHRPRHSRLQR	<i>Homo sapiens</i>
prodomain	²⁸⁵		
RV23, Human furin-		RKHGFLNLQGIFGDYYHFWHRGV	<i>Homo sapiens</i>
prodomain	²⁸⁵		
SR30, Human furin-		SPHRPRHSRLQREPQVQWLEQQVAKRR	<i>Homo sapiens</i>
prodomain	²⁸⁵	TKR	
YR23, Human furin-		YYHFWHRGVTKRSLSPHRPRHSR	<i>Homo sapiens</i>
prodomain	²⁸⁵		
YR20, Human furin-		YYHFWHRGVTKRSLSPHRPR	<i>Homo sapiens</i>
prodomain	²⁸⁵		
YR17, Human furin-		YYHFWHRGVTKRSLSPH	<i>Homo sapiens</i>
prodomain	²⁸⁵		
YR14, Human furin-		YYHFWHRGVTKRSL	<i>Homo sapiens</i>
prodomain	²⁸⁵		
YR12, Human furin-		YYHFWHRGVTKS	<i>Homo sapiens</i>
prodomain	²⁸⁵		

Mollusca

Myticin A ³⁰¹	HSHACTSYWCGKFCGTASCTHYLCRVL	<i>Mytilus</i>
	HPGKMCACVHCSR	<i>galloprovincialis</i>
Myticin B ³⁰¹	HPHVCTSYYCSKFCGTAGCTRYGCRNL	<i>Mytilus</i>
	HRGKLCFCLHCSR	<i>galloprovincialis</i>
Myticusin-1 ³⁰²	TDHQMAQSACIGVSQDNAYASAIPRDC	<i>Mytilus coruscus</i>
	HGGKTCEGICADATATMDRYSDTGGPL	
	SIARCVNAFHFYKRRGEENVSYKPFVV	
	SWKYGVAGCFYTHCGPNFCCCIS	
Myticin 1**	HSHACASYYCSKFCGTASCTHYLCRVL	<i>Mytilus coruscus</i>
	HPGKLCVCVNCNSRVKNPFRATQDAKSI	
	NELDYTPLMKSMEMLDNGMDML	
Myticin 2**	HSHACTSYYCAKFCGTAKCTHYLCRVL	<i>Mytilus coruscus</i>
	HPGKLCVCVNCNSKVKNPFRATQDAKSI	
	NELDYTPLMKSMEMLDNGMDML	
Myticin 3**	HSHACTSYYCAKFCGAAKCTHYLCRVL	<i>Mytilus coruscus</i>
	HPGKLCVCVNCNSKVKNPFRATQDAKSI	
	NELDYTPLMKSMEMLDNGMDML	
Myticin 4**	HSHACTSYYCAKFCGTASCTHYLCRVL	<i>Mytilus coruscus</i>
	HPGKLCVCVNCNSKVKNPFRATQDAKSI	
	NELDYTPLMKSMEMLDNGMDML	

Myticin 6**	HSHACASYYCSKFCGTASCTHYLCRVL	<i>Mytilus coruscus</i>
	HPGKLCACVNCSRVKNPFRATQDAKSI	
	NELDYTPLMKSMENLDNGMDML	
Myticin 7**	HSHACTSYYCSKLCGTASCTHYLCRVL	<i>Mytilus coruscus</i>
	HPGKLCVCANCSRVKNPFRATQDAKSV	
	NELDYTPIMKSMENVDNGMDML	
Myticin 8**	HSHACTSYYCSKFCGTASCTHYLCRVL	<i>Mytilus coruscus</i>
	HPGKLCVCANCSRVKNPFRATQDAKSV	
	NELDYTPIMKSMENVDNGMDML	
Myticusin-beta-1 ³⁰³	SDHQMAQSACMGLAQDAAYASAIPRT	<i>Mytilus coruscus</i>
	CSGGKTCESICADATSTMNKYSTAGGP	
	LSTARCVDAFHIYSRRGQENVPYQPYV	
	VSWKYGVKGCFQTSCGPNFCCCIV	
Myticusin-beta-2 ³⁰³	SDHQMAQSACMGLAQDAAYASAIPRT	<i>Mytilus coruscus</i>
	CSGGKTCESICADATSTMNKYSTGGGP	
	LSTARCVDAFHIYSRRGQENVPYQPYV	
	VSWKYGVKGCFQTNCGPNFCCCIV	
Myticusin-beta-3 ³⁰³	SDHQMAQSACMGLAQDAAYASAIPRT	<i>Mytilus coruscus</i>
	CSGGKTCESICADATSTMNKYSTGGGP	
	LSTARCVDAFHIYSRRGQENVPYQPYV	
	VSWKYGVKGCFQTSCGPNFCCCIV	

Firmicutes

Enterocin A ³⁰⁴	TTHSGKYYGNGVYCTKNKCTVDWAK	<i>Enterococcus</i>
	ATTCIAGMSIGGFLGGAIPGKC	<i>faecium CTC492</i>
Garvieacin Q ³⁰⁵	EYHLMNGANGYLTRVNGKTVYRVTKD	<i>Lactococcus</i>
	PVSAVFGVISNCWGSAGAGFGPQH	<i>garvieae</i>
Plantaricin 163 ³⁰⁶	VFHAYSARGNYYGNCPANWPSCRNNY	<i>Lactobacillus</i>
	KSAGGK	<i>plantarum</i>
Planticarin F ³⁰⁷	VFHAYSARGVRNNYKSAVGPADWVIS	<i>Lactobacillus</i>
	AVRGIHG	<i>plantarum</i>
Bacteriocin acidocin 8912 ³⁰⁸	KTHYPTNAWKSLWKGFWESLRYTDGF	<i>Lactobacillus acidophilus</i>
Other Phyla		
Theromyzin ³⁰⁹	DHHHDHGDDHEHEELTLEKIKEKIKD	Annelida
	YADKTPVDQLTERVQAGR DYLLGKGA	(<i>Theromyzon</i>
	RPSHLPARVDRHLSKL TAAEKQELADY	<i>tessulatum</i>)
	LLTFLH	
cPcAMP1/26 ³¹⁰	PPHKKKLA VYPVFLFYLFLSWFSLIV	Ciliophora
		(<i>Paramecium</i>
		<i>caudatum</i>)
Serracin-P 43 kDa subunit ³¹¹	DYHHGVRVL	Proteobacteria
		(<i>Serratia</i>
		<i>plymuthicum</i>)

Shepherin II ³¹²	GYHGGHGGHGGGYNGGGHGGHGG YNGGGHHGGGGHG	Tracheophyta (<i>Capsella bursa-pastoris</i>)
SPP-12 ³¹³	FCHLCEDLIKDGKEAGDVALDVWLDEE IGSRCKDFGVLAECFKELKVAEH DIAI DQEIPEDKTCKEAKLC	Nematoda (<i>Caenorhabditis elegans</i>)
Holothuroidin 2 ³¹⁴	ASHLGHHALDHLLK	Echinodermata (<i>Holothuria tubulosa</i>)
EeCentrocin 2 ³¹⁵	WGHKL RSSWNKVKA VKKGAGYASG ACRVLGH	Echinodermata (<i>Echinus esculentus</i>)
P4 ³¹⁶	VLHTGYRKFLHRSKRFFHLR	Rumen of bacteria
Mannose-specific lectin ³¹⁷	DNHLLPGERLNPGNFLKQDRYMLIMQE DCNLVLYNLNKPEWATKTANQGSRCF VTLQSDGNFVIYDEHEQEGRNEAIWAS KTDGENGNVIIILQKDGNLVLYSKPIFA TGTNRFGSTAVVVAKRNRKAHFGVEQ NIIEVTTNL	Asparagales (<i>Dendrobium findleyanum</i>)

*Indicates that the sequences were found on ClustalO v1.2.4

**Indicates that the sequences were found on UniProt

Although both Cu²⁺ and Ni²⁺ ions are found in host and microbial environments, Cu²⁺ is probably the most likely element to interact with ATCUN-containing AMPs (ATCUN-AMPs), given the role of this metal ion in immunity. Cu²⁺ has been observed at high concentrations in the

phagocytic milieu as a response to infections by the human pathogens *Mycobacterium tuberculosis* and *Mycobacterium avium*, or by avirulent *Mycobacterium smegmatis*.¹¹² Cu²⁺ ions within phagolysosomes of peritoneal macrophages were found at high micromolar concentrations.¹¹² Additional indirect evidence for the presence of Cu ions in the intracellular stand-off against microbes include the observation that in IFN- γ and LPS-activated macrophages, the levels of the Ctrl Cu importer are elevated.¹¹¹ In addition, the Cu pump ATP7A is overexpressed and localized to the phagolysosome, suggesting transport of Cu into this vesicle.¹¹¹ Other indirect evidence includes the observation that *Salmonella* Typhimurium-infected macrophage exposure to the intracellular Cu chelator tetrathiomolybdate resulted in increased survival of the microbe.³¹⁸ Besides the phagocytic environment, there are other sites of microbial infection in which Cu²⁺ ions are found at concentrations that can impact the activity of antimicrobial agents. Cu²⁺ ions have been found at higher levels during urinary tract infection by the pathogens *Proteus mirabilis* and *Klebsiella pneumoniae*.¹⁰⁸ Interestingly, *in vivo* studies have shown that Cu-deficient mice are more susceptible to uropathogenic *E. coli* infection, indicating that Cu²⁺ ions are an important antimicrobial effector in urine.¹⁰⁸ Other bodily fluids such as saliva and sweat have been shown to be essential host defense effectors against bacteria. For example, Cu²⁺ concentrations ranging from 4.6 ± 0.4 μM to 20 ± 10 μM have been found in sweat, and human saliva contains Cu²⁺ ranging from 1.6 μM to 7.5 μM.^{319,320}

Clearly, Cu²⁺ ions are an important antimicrobial effector, and interactions with AMPs are plausible during infections. Peptides can acquire Cu²⁺ from places other than oxidative compartments, as mentioned above, including from the microbes themselves. There is a labile pool of Cu²⁺ in the periplasm of *E. coli* where peptides can chelate metals.¹²² Moreover, a peptide can be post-translationally modified with Cu²⁺ if they are carboxy-amidated as a post-translational

modification by peptidoglycine α -amidating monooxygenase, which occurs in the Golgi apparatus where metal ions can also be acquired.³²¹

The Cu²⁺-ATCUN complex can catalytically produce ROS. It has been hypothesized that this ROS production happens through the redox cycling of the uncommon Cu²⁺/Cu³⁺ redox pair,¹⁹⁷ although the exact mechanism by which ROS are produced from this catalytic cycling remains to be elucidated.³²² Despite this lack of mechanistic details, one can imagine how ROS production can potentiate the activity of AMPs. A holo-AMP (*i.e.* the Cu²⁺-bound AMP) can be localized on the membrane or find an internal target (*e.g.* DNA or the chaperone DnaK), as many AMPs have been shown to do, and when close, *in situ* generate and deliver its deadly ROS cargo. Several artificial catalytic metallodrugs containing the ATCUN motif have been reported in the literature.^{197,212,323–325}

In the following sections, we will focus on selected ATCUN-AMP members for which evidence exists concerning the involvement of the ATCUN motif in their mechanism of action. Other examples are included to help us and the readers identify broad trends in the chemistry and biology of these keystone molecular species. We have also compiled an exhaustive table of known ATCUN-AMPs, therefore allowing other researchers to delve into these peptides.

3.1 BLAST sequence homology network

A sequence similarity network showing the BLAST homology between ATCUN-AMP sequences was used to develop a classification scheme for ATCUN-AMPs (Figure 11).³²⁶ A total of 260 AMP sequences were compared to each other using BLASTp (v.2.6.0) with default parameters.³²⁷ We iteratively filtered this dataset to exclude false-positive links with the script available at https://github.com/klassen-lab/BLAST_parser_for_cytoscape, using clustalOmega

(v1.2.4; default parameters used) multiple sequence alignments of representative network clusters to confirm homology relationships.³²⁸ Our optimized parameters included sequences that shared more than 40% identity, higher than 10% alignment of the shorter sequence to the longer one, and an e-value (which describes the statistical likelihood of a false-positive match) less than 0.0264.

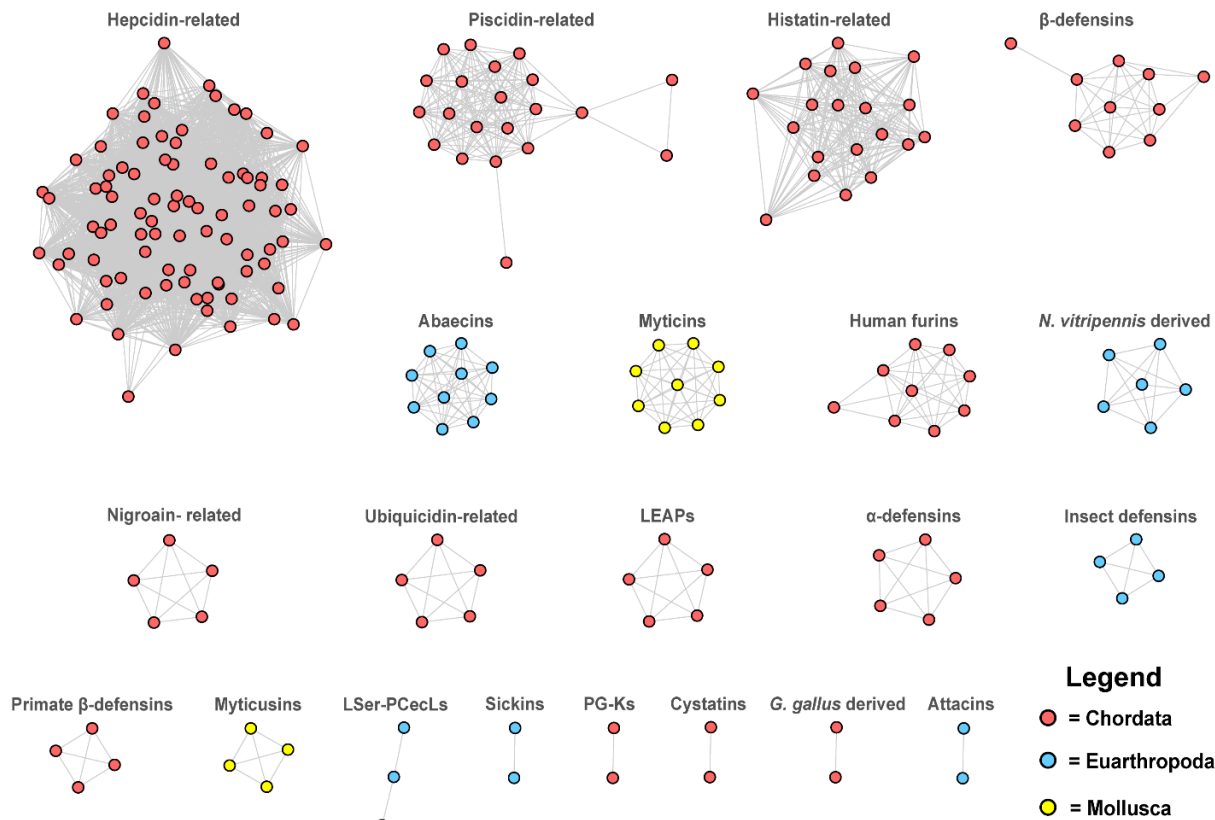


Figure 11. Sequence similarity network of 216 ATCUN-containing AMPs. Nodes (circles) represent individual AMP sequences, and are colored by their phylum of origin. Edges (lines connecting the nodes) represent homology relationships between AMPs.

The resulting BLAST homology network contains 21 clusters that together included 216 ATCUN-AMPs, with the remaining 44 AMPs representing singleton clusters that lacked relationships with the other sequences in the dataset. Of the 21 clusters containing at least 2 sequences, five clusters contained more than 10 sequences. Each cluster contained only sequences that were encoded by members of a single phylum, and the phylogenetic distributions of clustered

ATCUN-AMPs approximated that in the input dataset. Of the 21 clusters, 13 included sequences from Chordates, six included sequences from Arthropods, and two included sequences from Mollusks. The remaining 44 singleton sequences are ATCUN-AMPs from Firmicutes, Arthropods, Chordates, and other phyla with limited representation in our dataset.

Most of our clusters defined based on sequence homology included ATCUN-AMPs with similar annotations. The largest cluster (Cluster 1) included 86 sequences that were mostly annotated as hepcidin AMPs. Cluster 2 included has 21 sequences that are primarily annotated as piscidins, and Cluster 3 included 20 sequences that were all annotated as histatins, except for one that was annotated as ATCUN-C16. Clusters 4 and 5 both included 10 sequences that were all annotated as β -defensins and abaecins, respectively. Cluster 6 contained nine myticins, and Cluster 7 contained nine furins. The remaining 14 clusters have six or fewer sequences, which limits the generalizability of their annotations. As more naturally occurring AMPs are discovered and studied, there may be additions to the clusters that will expand the information available for these families of AMPs.

3.2 Ixosin and other insect AMPs

The peptide ixosin (GLHKVMREVLGYERNNSYKKFFLR-NH₂) has been isolated from the saliva of the tick *Ixodes sinensis* and identified as a saliva immunogenic peptide in *Amblyomma americanum*.³²⁹ ¹H-¹⁵N HSQC, ¹H-¹³C HSQC, and ESI-MS was used to show that ixosin binds to one equivalent of Cu²⁺ ions via the ATCUN motif and is capable of producing ROS and oxidizing membrane lipids.¹¹⁸ Removing the ATCUN motif by deleting the first three amino acids had a detrimental effect on its antimicrobial and antifungal activity. In susceptibility assays, the addition of the copper chelators triethylenetetramine and penicillamine to *E. coli* cells treated with ixosin partially rescued the growth of bacteria, demonstrating that this AMP has at least two

mechanisms of action, one that involves Cu²⁺ binding and a metal-free mechanism. Depletion of O₂ in susceptibility assays also led to increased survival of cells. This result was interpreted as a consequence of lower levels of ROS being produced by the ixosin-Cu²⁺ complex. However, mutating His3 to Ala only affected its antifungal activity. Organisms often encode more than one AMP, and in the case of *I. sinensis* a second AMP, ixosin B (QLKVDLWGTRSGIQPEQHSSGKSDVRRWRSRY-NH₂), that does not possess an ATCUN motif, has also been isolated from its salivary glands. Synergy studies between ixosin and ixosin B have provided insights into one of the many roles of ATCUN-AMPs. Synergy between ixosin and ixosin B was shown to occur only with an *E. coli* strain containing elevated levels of unsaturated fatty acids in its membrane. The synergy was abolished when the ATCUN motif was removed (by either deleting the first three residues or through an H3A mutation) or prevented from binding Cu²⁺ ions.¹¹⁸ These results indicate that the ATCUN motif is imperative in eliciting a synergistic interaction between ixosin and ixosin B. When *E. coli* were treated with ixosin B alone, the peptide was found to localize in the cytosol. Interestingly, when the bacteria were co-treated with ixosin and ixosin B, the latter was found localized to the *E. coli* membrane. Ixosin B localization was restored when a mutant of ixosin with abolished Cu-binding activity (and in effect, ROS formation) was used.¹¹⁸ These studies agree with recent reports in literature suggesting that oxidized phospholipids in bacteria are potential targets for antibiotic intervention.^{330,331} These findings are relevant to the development of treatments of *Borrelia burgdorferi*, the causative agent of Lyme disease transmitted by ticks, as this pathogen possesses membranes enriched with polyunsaturated fatty acids that are particularly sensitive to attack by ROS.³³² Intriguingly, the saliva of *A. americanum* has been shown to contain ixosin and has borrelicidal activity but this tick is not a vector for the disease.³³³ These studies on ixosin and its ability to assist other AMPs

by damaging bacterial membranes are also relevant in the context of phagocytic killing of bacteria, since (1) phagosomal ROS can oxidize certain bacterial lipids and turn them into better targets for AMPs, and (2) AMPs can disrupt the bacterial membrane to allow ROS to access the bacterial cytosol. High-resolution, spatiotemporal monitoring of the progress of phagocytic killing is desirable to address this ambiguity.^{330,331}

It is not surprising that ixosin acts as an antimicrobial effector to assist other AMPs since other AMP pairs have shown synergy, although its mechanism is indeed unique. A long-standing idea to explain the diversity among AMPs is that they work as a chemical cocktail in which the different components provide assistance to each other. This hypothesis has been supported by a number of reports, particularly from insect AMPs. A competing hypothesis is that the AMP diversity has emerged as a response to the variety of pathogens that invade a host and that AMPs specifically target subsets of these invaders.^{334,335} The latter thesis has been supported by evolutionary studies that show AMPs experience positive selection in selected organisms. In an aforementioned study, the deletion of 14 AMP genes in fruit flies demonstrated AMP specificities for controlling different types of infections.⁷⁴ Yet, a third hypothesis can be proposed in which both hypotheses are correct. For example, in *Drosophila melanogaster*, where high specificity in the activity of AMPs has been observed, the AMP metchnikowin, an ATCUN-containing AMP, was overexpressed when the organism was challenged with fungi, Gram-negative and -positive bacteria.⁸⁴ Diptericin, cecropin A, attacin, drosomycin, and drosocin only responded to one or two challenges but never to three of them. These results seem to indicate that metchnikowin can assist in the stand-off between the other AMPs and the invading pathogens.

Several other insect ATCUN-AMPs have been reported (Table 2) but besides ixosin, none of the studies have delved into the role of Cu²⁺ binding. We would like to introduce one more

family of insect ATCUN-AMPs, since their study could help dissect strategies that underlie the expression and conservation of ATCUN-containing AMPs. Abaecins are an important class of insect AMPs and are a representative example of gene duplication. In the ancestor of Hymenoptera, an abaecin gene was duplicated, forming the type 1 and type 2 abaecins. Type 1 is vertically inherited by bees, wasps, and five ant species. Type 2 has been lost in bees, wasps, and three ant species. Type 1 abaecins do not have significant antimicrobial activity against Gram-negative bacterial pathogens. Abaecin (FVPYNPPRPGQSKPFPSPGPGFNPQPKIQWPYPLPNPGH) alone did not exhibit any activity against *E. coli*, even at concentrations higher than its physiological concentration in

Table 2. Ant ATCUN-AMPs that contain a predicted DnaK binding motif.

Peptide	Sequence	Organism
Atabaecin ²²⁶	DTHTFSTHKIRLPNGPGYGPFPNPHQSWPIPWPNNNG	<i>Atta cephalotes</i>
Aeabaecin ²²⁶	DIHTLSTHKIRLPNGPGYGPFPNPHQPWPIPWPNNNG	<i>Acromyrmex echinatior</i>
Pobabaecin ^c ²²⁶	DTHALPKHRLRLPGGGPGYGPFPNPRLPWPIPLPNRDH	<i>Pogonomyrmex barbatus</i>
Siabaecin ²²⁶	DTHALPEHRPRLPEGPGYVLFNPRQPWPVPWPWNHGR	<i>Solenopsis invicta</i>
Trabaecin ^a	DTHALPKHRFRRLPSGPGYGPFPNPPQWPWPWPWNNG	<i>Trachymyrmex cornetzi</i>
Acabaecin ^a	DTHTLSTHRIRLPSPGPGYGPFPNPHQPWLISWPNNQ	<i>Acromyrmex echinatior</i>
Atabaecin-2 ^a	DIHTLSTHKIRLPNGPGYGPFPNPHQPWPIPWPNNNG	<i>Atta colombica</i>
Cyabaecin ^a	DTHTFSTHKIRLPNGPGYGPFPNPHQPWPIPWPNN	<i>Cyphomyrmex costatus</i>
Psabaecin ^{a,c}	DTHTLLTHRIRLPNGPGYGPFPNPHQPWPIPWPNNNG	<i>Pseudomyrmex gracilis</i>
Wasabaecin ^{a,c}	DTHTLSTHRIRLPNGPGYGPFPNPHQSWPIPLPNNG	<i>Wasmannia auropunctata</i>

^a Retrieved using BLAST searches of GenBank.

^b Highlighted in bold are the His residues. Underlined is the predicted DnaK binding motif.

^c Predicted heptapeptides for DnaK binding are overlapping. THRIRLP and RIRLPNG for Psabaecin and Wasabaecin. KHRLRLP and HRLRLPG for Pobabaecin.

insects.³³⁶ However, when it was co-incubated with hymenoptaecins, abaecins achieved cell growth inhibition and killing, suggesting synergism between the two AMPs.³³⁶ The two peptides have complementary mechanisms of action, hymenoptaecins being pore-formers and abaecins being DnaK binders, which may have caused their synergistic antimicrobial activity. In particular, hymenoptaecins form the pores that allow abaecins to easily enter the cell and effectively inhibit protein folding by binding to DnaK.³³⁶ Interestingly, other pore-forming AMPs found in different insect species, namely stomoxyn and cecropin A, exhibit potentiation of antimicrobial activity when present together with abaecins.³³⁷ Of particular interest to the current review are the type 2 abaecins from fungus-growing ants, as they have a conserved ATCUN motif in their mature peptide sequences and act in a complex ecosystem that includes fungal gardens. By doing a BLAST search against the NCBI database, we were able to identify conserved sequences of type 2 abaecins from different ant species (Table 2). Six of these ant species are fungus-growing (two *Acromyrmex*,³³⁸ *Cyphomyrmex*,³³⁹ *Trachymyrmex*, and two *Atta*³⁴⁰).^{341,342} Using the molecular chaperone binding site prediction Limbo (<http://limbo.switchlab.org/>), all the type 2 abaecin peptides are predicted to be DnaK binders, with heptapeptides dominated by Arg, Lys, and Pro residues as the predicted motif for DnaK binding (Table 2). Notably, the peptide siabaecin was predicted to have a DnaK binding motif that does not have any Arg nor Lys residues, but it has Pro residues, which could decrease the flexibility of the peptide and reduce entropy loss upon binding to DnaK.³³⁶ Furthermore, the peptides psabaecin, wasabaecin, and poabaecin have more than one heptapeptide predicted to be DnaK binding. Two heptapeptides in psabaecin and wasabaecin are overlapping, namely THRIRLP and RIRLPNG, while two of three heptapeptides in poabaecin are also overlapping, namely KHRLRLP and HRLRLPG. We hypothesize that type 2 abaecin peptides also act by binding DnaK, and that their activity is potentiated by binding Cu²⁺

to the ATCUN motif. Given their environment, the ant type 2 abaecins probably mediate symbiotic interactions with fungus-growing ants and may explain its presence in several ant species.

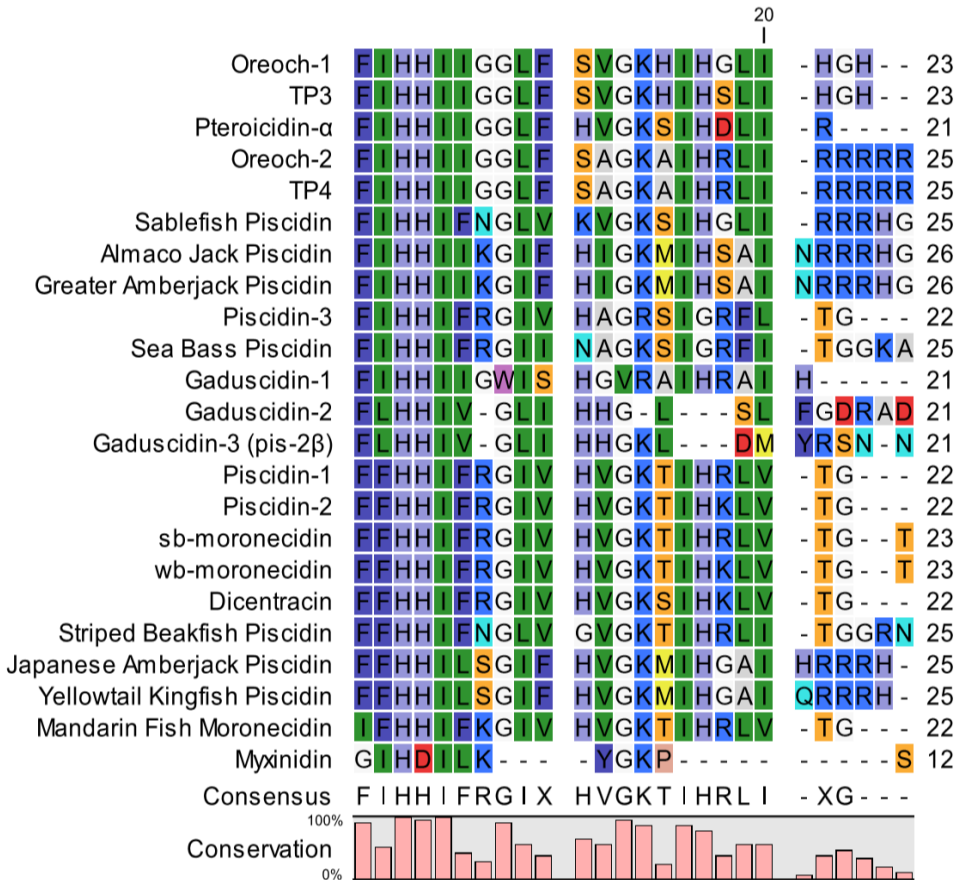
3.3 Piscidins: archetypal metalloAMPs

Piscidins are a class of α -helical, His-rich AMPs from teleost fish that were originally isolated from mast cells and granules of hybrid striped bass (*Morone saxatilis x M. chrysops*).^{343,344} Since the elucidation of the first piscidins, multiple others have been identified from teleost fish, more specifically from the Perciformes order.^{344,345} Pleurocidins, moronecidins, gaduscidins, myxinidin, epinecidin, chrysophsins, and dicentracin have all been designated as piscidins. The different piscidins range from 12 to 44 residues, with the majority having 22 residues (Figure 12). Piscidins can exist in an amidated or non-amidated form, where amidation can mediate proteolytic effects, however, this feature does not seem to change the secondary structure or orientation in the bilayer.³⁴⁶ Piscidins have low C-terminal sequence homology but a highly conserved N-terminus with His, Phe, and Ile residues, as well as a highly conserved propeptide region. Piscidin peptides are all α -helical to some extent and are characterized by a four exon/three intron gene sequence, with few exceptions. A sequence alignment with several piscidins reveals that His3, His4, His11, and His17 are all conserved residues, along with Gly8 and Gly13 (Figure 12). It has been hypothesized that the large number of His residues in the sequence leads to the higher antimicrobial

activity at low pH due to an increase in the charge of the peptide upon protonation of the His residues ($pK_a = 6.0$). The increase in activity as the pH is lowered, however, is not always the case.³⁴⁷ Coincidentally, piscidins have often been found in acidophilic granules and phagocytic cells, suggesting that the pH-dependent activity is biologically important.^{343,344,348} The isolation of piscidin-1, -2, and -3 (p1, p2, and p3, respectively) was the first report of AMPs in immunologically relevant cells.³⁴⁴ p1, p2, and p3 are transported to the phagosomes upon ingestion of bacteria, hinting at an intracellular role, in addition to extracellular modes of action.³⁴³

The first piscidins (p1, p2, p3) have a highly conserved N-terminal region with His, Phe, and Ile residues, where p2 is identical to p1 with the exception of an Arg to Lys mutation (Figure 12).³⁴⁴ All three piscidins are 22 residues long and have an ATCUN motif (FFH in p1 and p2, and

Figure 12. Piscidin AMP alignment, showing conserved N-terminus region.



FIH in p3). Hydrophobic and bulky residues, such as Phe, Ile, and His, around His3 are expected to enhance the stability of the Cu²⁺ complex in piscidins.¹⁷⁹ These bulky residues, coupled with the loss of a positive charge upon metal binding, have been suggested to have a role in insertion of the N-terminus into the bilayer.¹⁷⁹ Using ssNMR, the Cotten group showed that His4 is not significantly perturbed upon Ni²⁺ binding.¹⁷⁹ The structure of the first six residues of p3 bound to Ni²⁺, used as a proxy for the paramagnetic Cu²⁺ ion, was determined using DFT calculations and ssNMR data. It shows that Ni²⁺ binds in a square planar manner, and that the side chains of Ile2 and His4 surround the metal center.¹⁷⁹

Piscidins have been found to be only moderately hemolytic, while retaining activity in high salt conditions and at low pH.³⁴⁹ Furthermore, piscidins have therapeutic potential due to their activity against fish pathogens and parasites,^{232,345,349} human related pathogens,^{344,350} fungi,^{34,351} and viruses³⁵². When p1 and p3 were tested against *Trichosporon beigelii* and *C. albicans*, they had better activity than amphotericin B, an antifungal antibiotic, showing their broad reach as therapeutic agents.³⁴ It was found that p1 acted against fungi by disrupting the membrane.³⁴ p1 is more active than p3 against Gram-negative bacteria, but have similar activity with Gram-positive species.³⁵⁰ This difference could be due to p1 having four times more membranolytic activity than p3, possibly because of the increased hydrophobicity of p1 causing more perturbations/defects in the bilayer.³⁵⁰ p1 and p3 also tilt into the membrane and this may facilitate their transfer into the cell.³⁵⁰ Interestingly, many of the piscidin peptides have Arg or Lys residues at the middle and C-terminus of the peptide that could indicate that these peptides have different roles. For example, it is known that Arg rich peptides enter cells more easily and can have strong DNA binding interactions, which coincides with these peptides' flexibility to bind to multiple targets. Intracellular mechanisms have also been probed. Using confocal microscopy, p1 and p3 can

accumulate at the septum of bacteria and co-localize with the nucleoid region, suggesting that DNA may be bound by these peptides.³⁵⁰ This increased DNA interaction is potentially due to having three rather than two Arg residues and a Gly17 rather than His17 that yields a more flexible C-terminus.³⁵⁰ Interestingly, ssNMR experiments show that the ATCUN motif of p1 and p3 adopt conformations simultaneously poised for DNA and metal-ion binding.¹¹⁹ MD simulations have also been used to study piscidin and DNA interactions. The MD simulation system included a short duplex of DNA and piscidin (either p1 and p3), solvated with TIP3P water molecules.¹¹⁹ It was calculated that the binding energy of p3 to DNA is more negative than the binding energy of p1 to DNA, implying stronger binding for p3 with DNA.¹¹⁹ This can be due to the greater number of H-bonding interactions observed between p3 and DNA. Furthermore, the hydrophilic residues of both p1 and p3 prefer to interact to the DNA phosphate backbone than to the water solvent, exposing the hydrophobic residues to the water solvent.¹¹⁹ Due to this, the aggregation of piscidin-DNA complexes is favorable, evident from the more negative binding energy for the aggregated piscidin-DNA complex than for the monomeric piscidin-DNA complex.

One known mechanism of piscidins is to kill their bacterial target by disrupting the cell membrane. This has been shown experimentally and through MD simulations using microsecond-long simulations of multiple p1 peptides interacting with a heterogeneous bilayer of POPC and POPG.^{44,45,350,353,354} Here, the pores were placed in the starting structure of the simulation and, eventually, the peptides tilted to a surface-bound orientation, indicating that tetramers or hexamers were not able to stabilize the pore.³⁵³ The surface-bound state of p1 was stabilized by orienting its hydrophobic residues towards the hydrophobic core of the bilayer, specifically the Phe residues, thereby, maximizing the hydrophobic moment of the α -helix.³⁵³ In the same study, 16 peptides were bound to the surface of the POPC:POPG bilayer and membrane defects were seen to be

formed transiently.³⁵³ Once a peptide was inserted into the membrane defect, it resulted in stabilization of the defect and the peptide being on a tilted conformation.^{44,353} This occurred for about 10 to 20 ns before the peptide goes back into the surface-bound state and the C-terminus preferred to insert into the membrane defects over insertion of the N-terminus.^{44,353} While the lifetime of membrane defects may be shorter than the lifetime of a typical membrane pore, the preference of the p1 to insert into such defects, rather than spontaneously forming a pore, allows water permeation and can potentially initiate the membrane disruption mechanism of piscidins.^{44,353} Another type of defect with a longer lifetime (~100 ns) was found to be inserted with two C-terminal regions of p1 and one N-terminal region of p1.⁴⁴ These defects were described to be funnel-like, facilitating water leakage through the bilayer.^{44,353}

The role of Cu²⁺ in the activity of p1 and p3 is not limited to its bactericidal activity. p1 and p3 induce chemotaxis by utilizing formyl peptide receptors 1 and 2 (FPR1 and FPR2).³⁵⁵ FPR1 and FPR2 are receptors on neutrophils that, when activated by bacterial peptides, can trigger phagocytosis, degranulation, and ROS production.³⁵⁶ Using FPR-transfected cell lines and knockout mice, it was shown that p1 and p3 use FPR1 and FPR2 to induce chemotaxis and that p1-Cu²⁺ and p3-Cu²⁺ reduces chemotaxis induction.³⁵⁵ The authors suggest that an XVGK in the middle of the peptide sequence is a possible commonality that these piscidins share with other FPR-binding peptides such as pleurodicin and LL-37.³⁵⁵ Notably, our alignment in Figure 12 shows a conserved HVGK sequence among the ATCUN piscidins, suggesting that piscidins as a class can act as FPR binders. Additionally, the lower binding observed by p3 may be explained due to an Arg rather than a Lys residue being in the fourth position of the suspected binding sequence, or His17 in p1, where there is a Gly in the same position in p3.³⁵⁵

Many other piscidins have been reported; however, the role of the ATCUN motif have not been studied. For example, p2 has been found to have partial synergism with CuSO₄, which is commonly added to fish farms to prevent bacterial infections,³⁵⁷ in susceptibility assays against the fish parasites *Saprolegnia* spp. and *Tetrahymena pyriformis*.¹²⁰ Recently, five peptides were isolated from the teleost fish nile tilapia (*Oreochromis niloticus*) and were named TP1-TP5.²³⁷ These peptides range from 18 to 26 residues and they were all predicted to be α -helical.²³⁷ TP3 and TP4 have high sequence homology to the original piscidins and contain the FIH ATCUN sequence.²³⁷ TP3 and TP4 were also independently reported and named oreoch-1 and oreoch-2 respectively by Acosta *et al.*²³⁶ TP3 and TP4 were isolated in immunologically relevant tissues including the gills, epidermis, head kidney, intestines, heart, brain, kidneys, spleen, and gut.^{236,237} Under bacterial challenge, TP4 expression was increased 10- to 60-fold in the head, kidney, gills, and spleen, while TP3 expression was not affected.²³⁷ The structure of TP4 was determined using NMR and indicated the importance of the Phe, Ile, and Leu residues in the center of the peptide for the formation of an α -helix.³⁵⁸ Importantly, like p1, p3, and other piscidins, TP4 also has a G(X)₄G motif in the middle of the sequence that may confer additional conformational flexibility, which might be a requirement for the multiple functions of piscidins. More relevant to the metal-binding chemistry that we are trying to illustrate in this review is that mutations to the TP4 sequence have revealed that the bis-His motif (His3 and His4) at the N-terminus of piscidins is necessary for the antifungal properties of the peptide. When these residues were substituted for Ala, there was a complete loss in activity against fungi, indicating that His4 and the ATCUN motif may be necessary for fungicidal activity.³⁵⁸ Intriguingly, histatin 5, a human salivary peptide (*vide infra*), requires the bis-His motif to be active against *C. albicans* and may imply that the piscidins can also bind to Cu¹⁺, and not just Cu²⁺ ions.¹⁵⁰

The aforementioned bis-His motif is quite common among fish AMPs, suggesting that the presence of His3 and His4 provide an advantage. Pteroicidin- α (FIHHIIIGGLFHVGVKSIHDLIR) was isolated from the skin of *Pterois volitans*, the lion fish, as a mixture of amidated and nonamidated forms.²³³ The lion fish is widely distributed through the Indo-Pacific reef and has become an invasive species in the Western Atlantic and Mediterranean Sea with few or no predators. Dicentracin, isolated from the head kidney leukocytes of sea bass, was also found in leukocytes in the peripheral blood and in the peritoneal cavity where there are a high abundance of neutrophils and macrophages.²³⁵ Acute stress increases levels of dicentracin in the gills, and to some extent the epidermis, suggesting that the peptide also has a role in stress regulation besides its known role as an immune effector.³⁵⁹ Whether its role in stress response is modulated by metal ions or not remains to be determined.

The Atlantic cod (*Gadus morhua*) expresses three different piscidins, gaduscidin-1 (gad-1), gaduscidin-2 (gad-2), and gaduscidin-2 β (gad-2 β), where gad-2 β is a splice variant (alternatively named pis1, pis2, and pis2- β).^{231,232} In our recent studies, we have shown using ESI-MS that gad-1 was able to bind to two Cu²⁺ ions through an ATCUN motif and an HXXXH motif.³⁶⁰ Gad-1 was able to bore pores in the membrane, in addition to being able to significantly increase the amount of lipid peroxidation in *E. coli* membranes in the presence of Cu²⁺.³⁶⁰ We are continuing to study the implications of the multiple Cu²⁺ binding sites of gad-1 and the implications on the activity of the peptide. Both gad-1 (FIHHIIIGWISHGVRAIHRAIH[G]) and gad-2 (FLHHIVGLIHHGLSLFGDR[AD]) contain bis-His motifs, with gad-2 containing a second bis-His motif in the center of the sequence. The presence of these His pairs could influence how Cu²⁺ ions are handled. It is also possible that the bis-His motifs do not handle metal ions at all, since MD studies on gad-1 and gad-2 show the bis-His motifs interacting with the membrane

phospholipids where there was curvature.³⁶¹ MD simulations where POPC lipid molecules and a gad peptide were placed randomly inside a cubic simulation box. Throughout the simulation, the lipid bilayer would self-assemble with the peptide, revealing that when a pore is formed, His17 and Arg18 from gad-1 interacted with the planar part of the bilayer but to a lesser extent than the HH pairs.^{361,362} This indicates that the lipid interaction is not purely due to the charge of the His pair. Having a charged particle bound on the ATCUN site may drive stronger dipole-dipole interactions between the metal ion and the polar lipid headgroup and, if anionic lipids are present, it can even form stronger interactions via electrostatics. His3 interacted with the rim of the lipids in the pore when the peptide was protonated, reinforcing the idea that the His residues are important to the activity of these peptides whether they are metal bound or not.³⁶¹

Table 3. MIC of Myxinidin mutants against Gram-negative pathogens.^{363,364}

Myxinidin		MIC Values (μM)				
Variant		<i>S. aureus</i>	<i>E. coli</i>	<i>P. aeruginosa</i>	<i>S. typhimurium</i>	<i>K. pneumoniae</i>
Myxinidin		10	5	30	20	10
H3A		20	>50	15	10	30
H3R		10	5	20	5	5
H3K		15	10	30	5	10

At this point, it is important to note that it is possible that the activity engendered by the presence of the ATCUN motif, as it relates to metal binding, might be dependent on the bacterial strain. This is not surprising as many antibiotics and antimicrobial molecules show selective activity.³⁶⁵⁻³⁶⁷ The case of myxinidin (GIHDILKYGKPS), an AMP isolated from the epidermal mucus of the hagfish *Myxine glutinosa* L.,²³⁴ can be illustrating. Myxinidin has been reported to be active against Gram-negative and Gram-positive bacteria, fungi, and fish pathogens.²³⁴ Although the role of Cu²⁺ ions in the activity of this AMP has not been probed, an Ala walk was

utilized to determine the essential residues. None of the mutants dramatically changed secondary structure, as all were ~60% helical in TFE.³⁶⁴ Due to the decreased MIC against *K. pneumoniae*, *P. aeruginosa*, and *S. Typhimurium*, the authors stated that His3 was not essential to the activity of the peptide.³⁶⁴ However, substitutions of the His3 residue did have an effect on the MIC against *E. coli*, *Staphylococcus aureus*, and *K. pneumoniae* (Table 3).³⁶⁴

The body of research on piscidin peptides gives some perspective on how these peptides work in the natural system and how these peptides can be utilized as therapeutic agents. Piscidins are found ubiquitously in the tissue and are localized in acidophilic granules and phagocytic cells that allow the peptides to be protonated and highly charged, interact with labile Cu²⁺ ions and heparin, and activate immune cells through receptors.^{343,344,348,355} These features all contribute to the antimicrobial activity of this class of peptides. Although we know that some piscidins synergize with Cu²⁺ to potentiate their antimicrobial activity, more studies of piscidin peptides and metal ions need to be conducted to further understand the crucial role that metal ions have on their immunomodulatory and antimicrobial activities. Due to their broad-spectrum activity, piscidins have great potential to be utilized as therapeutic agents in both humans and fish. The N-terminal sequence homology should also be further investigated. All of the ATCUN piscidin peptides have a His in the 4th position, with the exception of myxinidin, and conserved His residues in the 3rd, 11th, and 17th positions. The N-terminus has many hydrophobic residues that form a “fence” and induce strong metal binding abilities. This may be crucial to the ability to bind metal ions outside of the phagocytic compartments, where labile Cu²⁺ may be scarce. An interesting similarity is to gonadotropin-releasing peptide hormones (GnRH) that are found in mammals and invertebrates and functions to regulate reproduction by triggering hormone release.³⁶⁸ GnRH peptides bind to G-coupled receptors, in part facilitated by the ability of the peptide to bind Cu²⁺.³⁶⁸ Binding in

most mammalian GnRHs is modulated by a pEH motif at the N-terminus, and the binding coordination involves the His N_{im}, pyro N, and a solvent molecule.³⁶⁹ Intriguingly, invertebrates, specifically the starfish *Asterias rubens*, have GnRHs that bind Cu²⁺ using an ATCUN motif.³⁶⁸ When comparing the ATCUN motif, the pEH motif found in mammals, and the pEXH ATCUN motif, there was a stronger Cu²⁺ binding affinity for the ATCUN motif by three orders of magnitude that may be explained by the lack of Cu²⁺ in seawater where starfish are found.³⁶⁸ The other GnRH peptides that contain an ATCUN motif are also found in the ocean, including in other echinoderms and mollusks. Although starfish are in the echinoderm phyla and piscidins are found in chordates, this may apply to piscidin peptides as well and explain why they have such a hydrophobic and conserved N-terminus. Other conserved residues are also important for peptide flexibility, such as the G(X)₄G motif, where Gly is in the 8th and 13th positions. However, gad-1 is the only peptide that has shifted Gly residues and this was found to have been positively selected for.³⁷⁰ The conserved, hydrophobic nature of the N-terminus of these peptides may be specifically conserved to stabilize Cu²⁺ binding at the ATCUN motif. His4 is in very close proximity to the metal binding site, but based on ssNMR evidence it does not seem that this residue binds to the metal ion and it may only be there as a hydrophobic fence to stabilize metal binding (Figure 13).¹⁷⁹ While there have been suggestions about the role of these residues, more work must be done to understand why they are conserved in this family of peptides. Other piscidin peptides have more than one metal binding motif, e.g. HXXXH (*vide infra*) and bis-His motifs, that could point to a central role of the synergistic interaction of piscidins and metal ions in phagocytic compartments. Additionally, the unique roles of each peptide or the possibility for synergy with multiple AMPs

that utilize Cu²⁺ needs to be investigated. Many other AMPs localize to phagocytic compartments and may interact with piscidin peptides or other small molecules.

3.4 Peptides from tunicates

The tunicates are invertebrates classified within the phylum Chordata due to the presence of a larval notochord in their early development.³⁷¹ Tunicates are of great interest, as they are the closest relatives of vertebrates, yet are developmentally far simpler. As such, studies on their

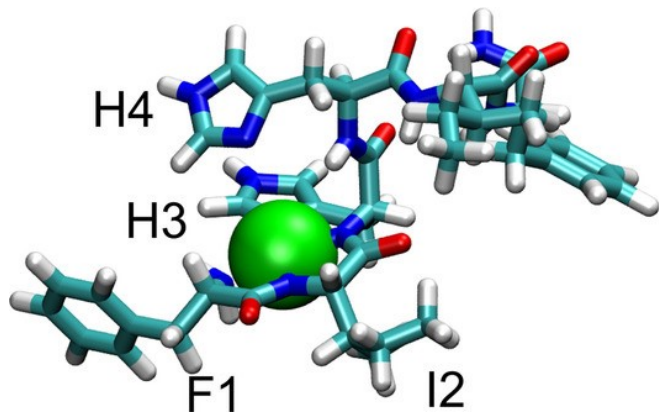


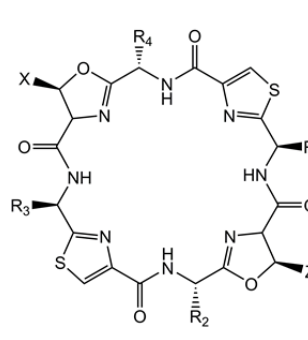
Figure 13. The ATCUN motif forms the hydrophobic fence that stabilizes the binding of metal ion. Reproduced with permission from Ref. 179. Copyright 2019 John Wiley and Sons.

immune system and embryo development are abundant.^{372,373} The tunicates are represented by *c.a.* 3,000 species, commonly divided into four classes: Appendicularia, Ascidiacea, Sorberacea, and Thaliacea. Tunicate metabolites have been isolated for almost 50 years, since many of these molecules have been shown to be biologically active.^{374,375} A variety of peptides, both cyclic and linear, have been isolated from these organisms, particularly from the Ascidiacea class. The ascidians are rich in peptides containing D- and L-amino acids, as well as modified residues such as 3,4-dihydroxyphenylalanine (DOPA) and 3,4,5-trihydroxyphenylalanine (TOPA). One can also

encounter oxazole, thiazole, oxazoline, and thiazoline rings among the different isolated compounds from the *Ascidiae*.^{373,374}

3.4.1 Metal-binding peptides from tunicates

Several cyclopeptides have been isolated from a symbiotic cyanobacteria associated to *Lissoclinum patella*.³⁷⁶⁻³⁷⁹ The patellamides and lissoclinamides are two examples of the peptide



Name	X	Z	R ₁	R ₂	R ₃	R ₄
patellamide A	Me	H	D-Val	L-Ile	D-Val	L-Ile
patellamide B	Me	Me	D-Ala	L-Leu	D-Phe	L-Ile
patellamide C	Me	Me	D-Ala	L-Val	D-Phe	L-Ile
patellamide D	Me	Me	D-Ala	L-Ile	D-Phe	L-Ile
patellamide E	Me	Me	D-Val	L-Val	D-Phe	L-Ile
patellamide F	H	Me	D-Ala	L-Val	D-Phe	L-Val
ascidiacyclamide	Me	Me	D-Val	L-Ile	D-Val	L-Ile

Figure 14. Depictions of selected patellamides containing thiazole and oxazoline rings. These moieties can bind metal ions with high affinity.

families isolated from *L. patella*, and a few of them are shown in figure 14. The patellamides are cyclooctapeptides characterized by the presence of two thiazole and two oxazoline rings, common metal binding ligands.^{380,381} Patellamide D forms mono- and di-nuclear Cu²⁺ complexes, whereas patellamides A, B, and E bind Cu²⁺ and Zn²⁺ but not Mg²⁺ and Ca²⁺.³⁸² Patellamides A, B, and E can bind two metal ions per molecule. By titrating solutions of CuCl₂ and ZnCl₂ into methanol solutions of the three aforementioned patellamides, Freeman and coworkers determined the metal binding affinity of the three cyclopeptides.³⁸² The first binding domain has a binding constant in the ranges 1.5×10^4 - 3×10^5 , and 3×10^4 - 8×10^4 for Cu²⁺ and Zn²⁺, respectively. The second binding site in patellamide B has binding constants of 230 and 20 for Cu²⁺ and Zn²⁺, respectively. The X-ray structure has been reported for a dinuclear Cu²⁺ complex of ascidiacyclamide, a closely related tunicate cyclooctapeptide (Figure 15).³⁸³ Interestingly, *L. patella*, as well as many other

tunicates, are known to concentrate many transition metal ions several times the concentration found in the local marine environment.^{240,384,385}

Linear AMPs have been isolated from the hemocytes of *Halocynthia roretzi*, *Styela plicata* and *S. clava*.^{386–388} Many of these peptides contain DOPA residues derived from post-translational modification of Tyr (Figure 16).^{386–388} Polyhydroxyphenylalanines such as DOPA, TOPA, and their derivatives are well-known metal-binding moieties and are found in metallophores, enzymes, and adhesion proteins.^{389–395} Plicatamide (FFHLHFH-dcΔDOPA, where dcΔDOPA represents decarboxy-(E)-α,β-dehydro3,4-dihydroxyphenylalanine), is the most thoroughly studied AMP in this class, although more studies are needed to get a full picture of its antimicrobial activity. So far, the evidence suggests that plicatamide targets the bacterial cell membrane and distorts ionophore gating.²⁴⁰ Whether it binds transition metal ions such as Fe³⁺ or Cu²⁺ remains to be elucidated.

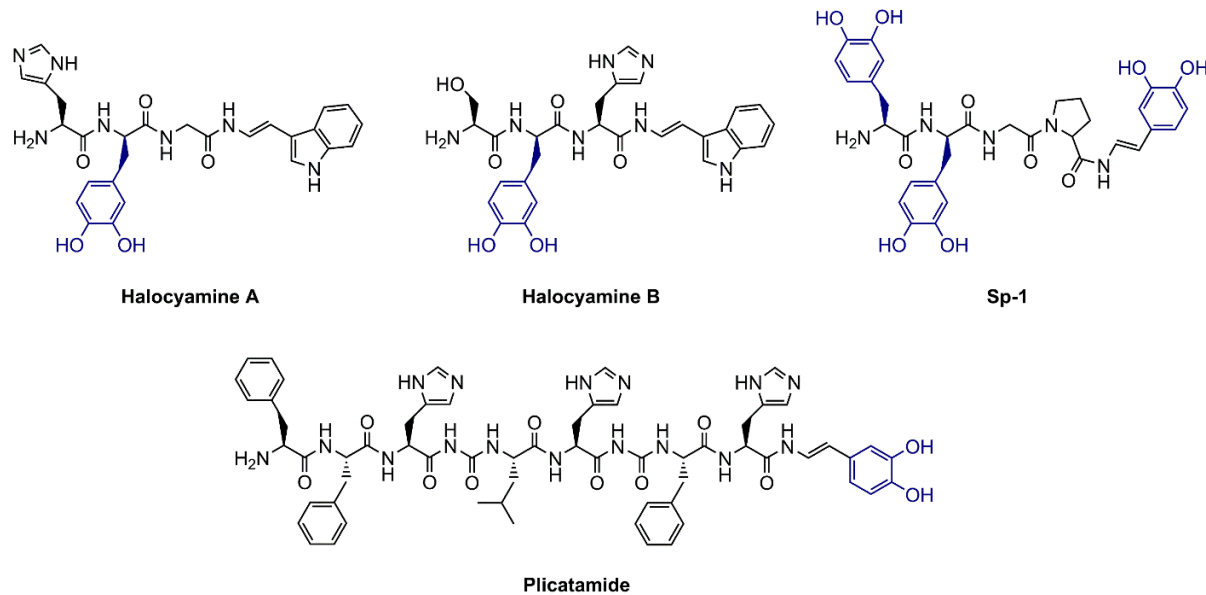


Figure 16. DOPA-containing peptides. Dihydroxyphenyl residues are shown in blue.

Figure 15. Crystal structure of ascidiacyclamide (CSD Entry: POHKOM)³⁸³

3.4.2 Clavanins

The clavanin family of cationic, α -helical AMPs was isolated from phagocytic hemocytes of *S. clava*,²³⁹ suggesting that these AMPs constantly interact with metal ions relevant to the immune system. The family contains six members with roughly 80% sequence homology, and a sixth member with only ~50% similarity that was discovered through the homology of the prepropeptide region of its genome (Table 4).^{239,396,397} Clavanin A is by far the most studied member of the family, appearing in at least 15 publications across five different laboratories, while each of the other members of the family have only appeared in the publication in which they were first reported.^{28,239} Clavanin B is nearly identical to clavanin A, with the only difference being an Arg in place of a Lys at position 7, though this is a conserved mutation as both residues are positively charged at biologically relevant pH values. Clavanins C and D were discovered to be the most active members of the clavanin family against not only Gram-negative and Gram-positive bacteria, but fungi as well.²³⁹ Despite this potency and broad-spectrum activity, clavanins C and D have never been studied in depth, likely due to the modified Tyr residue in the sequence, which was originally believed to be a methyl-Tyr, although the discovery of the styelin family of peptides has indicated that the modified Tyr may actually be a DOPA residue.³⁹⁸ Additionally, clavanin C contains an ATCUN motif which is likely capable of binding Cu^{2+} , although the role of copper binding in the activity of clavanin C has never been explored.

Table 4. Sequences of the clavanin family of peptides.^{396,397}

Peptide	Sequence
Clavanin A	VFQFLGKIIHHVGNFVHGFSHV
Clavanin B	VFQFLGRIIHHVGNFVHGFSHV
Clavanin C	VFHLLGKIIHHVGNFVÝGFSHV ^a

Clavanin D	AFKLLGRIIHVG ^Y GNFV ^Y GSFHV ^a
Clavanin E	LFKLLGKIIHHVG ^Y GNFVHGFSHV ^F
Clavaspirin	FLRFIGSVIHGIGHLVHHIGVAL

^a ^Y represents a post translationally modified Tyr residue

As a result of the lack of general attention for the other members of the clavanin family, clavanin A is the only member for which anything is known beyond relative antibacterial activity.^{28,57,135,239,399-402} Clavanin A was initially thought to act on the membrane, with two distinctly different activities depending on the pH of the peptide.^{403,404} This pH dependence is not surprising given the relatively high quantity of His residues found in its sequence. Using bacterial cytological profiling, we have recently demonstrated that clavanin A uses a multipronged approach that includes Zn²⁺-based DNA hydrolysis in addition to the aforementioned membrane targeting.⁵⁷ The potential for the use of clavanin A as a novel antibiotic has been well-explored. It has been studied *in vitro* in murine wound infection models, wherein clavanin A-treated *S. aureus* wounds showed improved healing and eradication of bacteria from the wound.⁴⁰⁰ Additionally, in systemic infection models, clavanin A treatment resulted in increased survival for both *E. coli*- and *S. aureus*-infected mice. Clavanin A has also proven effective against biofilms, preventing the formation of *E. coli* and *S. aureus* biofilms and perturbing preformed *K. pneumoniae* biofilms.⁴⁰⁵ In addition to the study of unmodified clavanin A as a potential therapeutic, it has also been conjugated to the surface of iron oxide nanoparticles and coated onto central venous catheters.³⁹⁹ Clavanin A-Fe₃O₄ coated catheters were capable of reducing adhesion of both Gram-positive (~50%) and Gram-negative (70-90%) bacteria, and modestly reducing the amount of planktonic bacteria by up to 20%.³⁹⁹ While more studies of clavanin A is certainly necessary, it appears to be an excellent framework for the development of novel, peptide-based antimicrobials in the future.

Another motif of interest in the clavanin family is the HXXXH motif, which can bind Zn²⁺ ions by coordinating Zn²⁺ to the nitrogen atoms of the His residues. Clavanin A is an AMP that was found to bind Zn²⁺ ions with a significant increase in activity as compared to the clavanin A free of Zn²⁺.²⁸ In one of our papers, we have looked at the effect of binding Zn²⁺ to clavanin A on the structure of the AMP, and its interaction with a POPE:POPG lipid bilayer, a simplified model of the *E. coli* outer membrane.¹³⁵ Zn²⁺ binding to the HXXXH motif provided stability to the α -helical structure of the C-terminal region of the peptide where the HXXXH motif is situated.¹³⁵ Though the structure-activity relationship for clavanin A has not yet been established, the provided conformational stability of the C-terminal region might have a role in helping the AMP potentiate its activity, thereby increasing its antimicrobial activity against *E. coli* when Zn²⁺ is bound. The interaction of the C-terminal region with the lipid bilayer was also significantly increased due to the increase in the net charge of the peptide at that region.¹³⁵ Interestingly, anionic POPG lipids preferentially interact and cluster around the Zn²⁺-bound region, neutralizing the positive charge from Zn²⁺.¹³⁵ This phenomenon of POPG clustering around a positive charge was also observed in piscidins, but for their cationic residues. These observations from MD simulations support the idea that a lot of known AMPs are cationic in character because it helps them to be selective towards bacterial membranes, which are more anionic than most membranes of mammalian cells.⁴⁰⁶⁻⁴⁰⁸

3.5 Human AMPs

ATCUN-AMPs are also present in humans and some of them may actually be Cu-binding peptides. Hepcidin or LEAP-1 exists in three forms: 20 residues (Hep-20, ICIFCCGCCHRSKCGMCCKT), 25 residues (Hep-25, DTHFPICIFCCGCCHRSKCGMCCKT), and the minority in a 22-amino acid form (Hep-22, FPICIFCCGCCHRSKCGMCCKT).²⁶¹ LEAP-

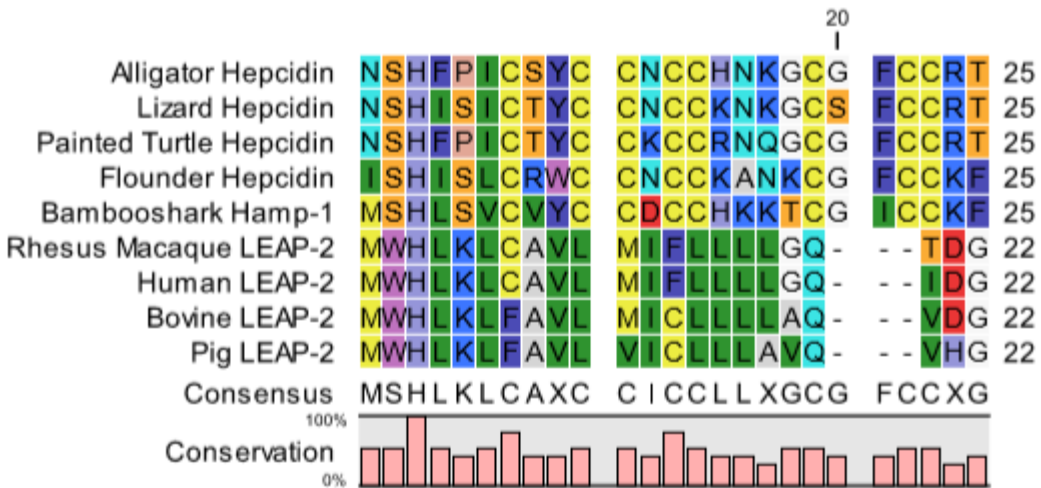


Figure 17. Hepcidin alignment from other hepcidin peptides that are not in the Mammalia or Acoipterygii class.

1 has been detected in the human liver, and to a smaller extent the heart and brain, and it also circulates in blood plasma.²⁴⁹ Hep-25 has also been isolated from urine.²⁶¹ These peptides are translated from the *HAMP* gene as an 84-amino acid prepropeptide and are modified to become amidated and shortened to either Hep-20 or Hep-25, which is not unlike other ATCUN peptides.^{255,261} Hep-25 has a disordered β-sheet, loop conformation in 50:50 TFE:phosphate buffer and in phosphate buffer alone using CD, with four disulfide bonds at positions Cys7–Cys23, Cys11–Cys19, Cys10–Cys13, and Cys14–Cys22.^{261,409} The peptide is not significantly cytotoxic towards K562 mammalian cells at concentrations up to 30 μM and has activity against *E. coli* and Gram-positive pathogens, including *Staphylococcus* and *Streptococcus* spp.²⁶¹ It is active at high salt concentration, 150 mM, which is consistent with its inclusion in blood plasma.²⁶¹ Similar to the human hepcidin, many animal hepcidins with ATCUN motifs exist and include fish, primate, pig, and dog hepcidin. These peptides share a conserved N-terminus sequence of DTHFPICIFCCGCC for the majority of the species that are classified in the class Mammalia (Figure 17 and 18). Notably, humans,²⁴⁹ buffalos,²⁵⁷ gorillas,²⁵⁷ orangutan,²⁵⁷ gibbon,²⁵⁷ and

chimps²⁵⁵ all express Hep-25 with the same sequence. The N-terminus of the class Acintopterygii (ray finned fish) is differently conserved (QSHLSLCRWCCNCC) but still contains an ATCUN motif (Figure 19). Hepcidin regulates blood plasma iron concentration and the tissue distribution of iron in humans.⁴¹⁰ Moreover, it controls iron recycling by macrophages and intestinal iron absorption.⁴¹¹ The mechanism of iron regulation is through Hep-25 binding to ferroportin, an iron

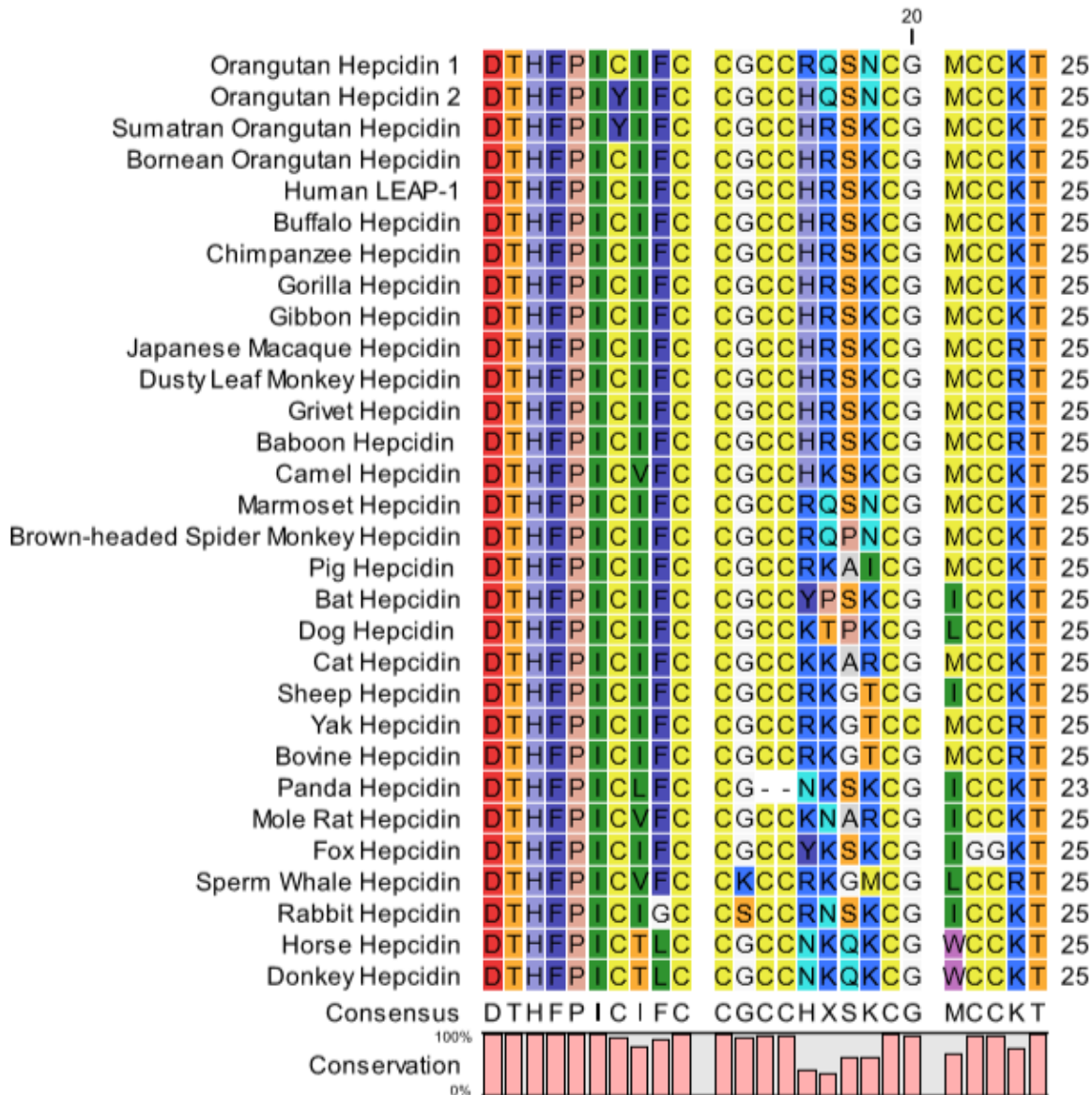


Figure 18. Hepcidin alignment from the class Mammalia, showing the conserved sequence DTHFPICIFCCGCC.

exporter, internalizing it, and degrading it, leading to less exported iron.⁴¹⁰ More recently, the ATCUN motif of Hep-25 was studied using 2D NMR techniques and mass spectrometry (MS). Hep-25 was isolated as Hep-25:Cu²⁺, Hep-25:2Cu²⁺, and apo-Hep-25 using MS.¹⁸⁰ It is important to note that the doubly bound state did not exist at physiological pH but at pH 11.¹⁸⁰ Using a hexapeptide and full length Hep-25, 2D NMR experiments including ¹D-¹H, ¹H-¹³C HSQC, ¹H,

¹H-TOCSY, and ¹H, ¹H-ROESY, were utilized to reveal that both Cu²⁺ and Ni²⁺ could bind to the first three residues based on chemical shift perturbations.¹⁸⁰ Holo-Hep-25 caused the N-terminus of the peptide to extend away from the C-terminus.¹⁸⁰ The carboxylate group of Asp1 may also bind the metal and form a modified version of the ATCUN.^{100,412} Structure-activity relationship studies show that the N-terminus is important for ferroportin binding, with His3, Phe4, and Ile6 being the most important for peptide binding.⁴¹³ The activity of Hep-25 against *P. aeruginosa* and *S. aureus* increases significantly with added Cu²⁺, whereas Hep-20 does not change its activity in the presence of the metal ion, suggesting a potentiation of activity in the presence of Cu²⁺ due to the presence of the ATCUN motif.⁴¹⁴ An H3A mutation hindered metal binding and abolished biological activity by decreasing the ability of Hep-25 to decrease ferroportin expression.^{415,416} Interestingly, Hep-25 may not have a solely membrane-based activity, but may also act intracellularly and promote DNA damage via ROS formation.⁴¹⁷ Hep-25 can bind to Cu²⁺, Ni²⁺, and Zn²⁺, in that order of affinity, while Fe²⁺ and Fe³⁺ did not bind.⁴¹⁵ Multiple binding constants have been reported for Hep-25 and Cu²⁺, including a logK_d of 7.7²⁵² and an estimated K_d of less than 1 μM,⁴¹⁵ however, using potentiometry and the hexapeptide, DTHFPI-NH₂, a logK_d of 14.66 was determined.¹⁴⁸ This is the strongest ATCUN binding constant found to date and is 457 times greater than the Cu²⁺ binding affinity of HSA, making hepcidin able to compete for labile Cu²⁺ in blood.¹⁴⁸

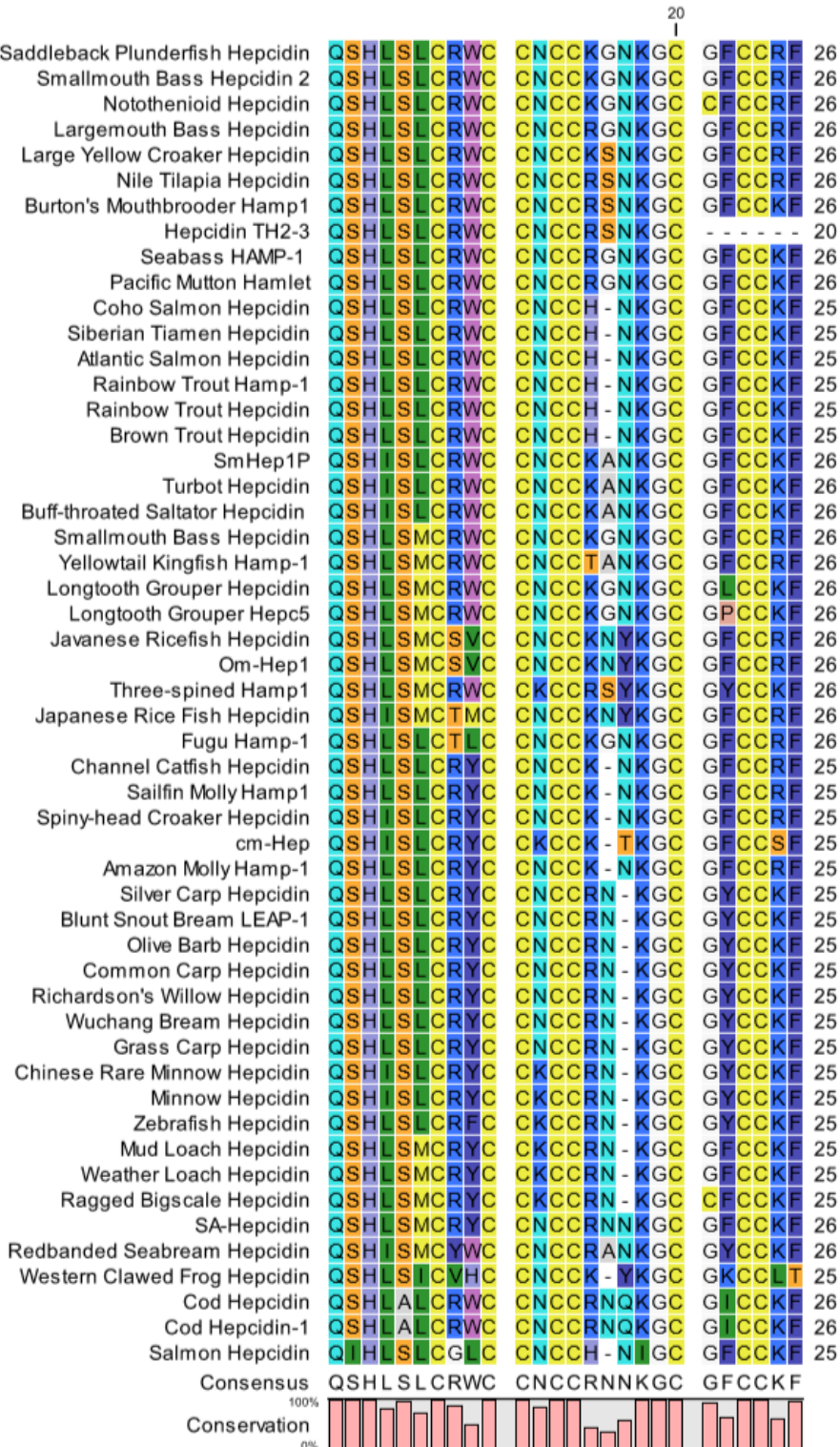


Figure 19. Hepcidin alignment of conserved sequences, all from the class Acintopyterygii (ray finned fish), except for the Western Clawed Frog and Richardson's Willow hepcidins.

A second family of human ATCUN-AMPs are the salivary peptides known as histatins (see Table 1 for sequences). Multiple reviews have covered the role of metal binding in histatins and the therapeutic potential of these ATCUN-AMPs.^{277,416,418} Human histatins are produced in the parotid and submandibular gland and secreted into the saliva. Histatins are His-rich peptides that almost always include an ATCUN motif, one to two bis-His motifs, and HEXXH or HXXXH motifs that can all bind to metal ions. Human histatin 1, 3, and 5 were active against *C. albicans*, of which histatin 5 was the most active and important to oral health in humans.²⁷⁶ The activity of histatin-5 against fungi was driven by intracellular targets, likely the mitochondria, but membrane lysis also occurred to some extent.⁴¹⁹ Histatin 1 and histatin 2 are major wound-closing factors in human saliva. Interestingly, the D-enantiomer of histatin 2 does not induce wound closure, hinting at the importance of the stereochemistry.⁴²⁰ MS determined that Fe^{2+} and Ca^{2+} did not bind to histatin 3 or 5, which is important because of the large level of Ca^{2+} in saliva that can saturate the binding sites of histatins.^{145,149} It has been determined that there are multiple Cu^{2+} binding sites on histatin 5 using ITC, with one high affinity site ($K_d = 2.6 \times 10^7 \text{ M}^{-1}$), likely the ATCUN site.¹⁴⁹ This value, however, was not corrected for TRIS buffer interactions. Correction is necessary since TRIS is known to coordinate metal ions.¹⁵⁵ With a correction for TRIS buffer interactions the binding affinity would be $8.81 \times 10^{-9} \text{ M}$, which is more consistent with other ATCUN-peptides in humans and with the presence of the Asp1 on the peptide.^{148,155,204} It has been hypothesized that Cu^{2+} binding leads to ROS production, and that this is the main contributor to the anti-fungal activity of the histatins. ROS has been found to be produced by histatin 5 and histatin 8 bound to Cu^{2+} and Cu^{1+} .⁴²¹ The mechanism is suggested to specifically target the mitochondria, where the peptide accumulates, to cause cell death.⁴¹⁹ Fungicidal activity has been postulated to be driven by

Cu binding by the bis-His motif in positions 7 and 8 via ROS,¹⁵⁰ and potentially by ROS formed at the ATCUN site.

3.6 Amphibian ATCUN-AMPs

Amphibians have been a plentiful source of peptides and other compounds of medicinal interest, including alkaloids.⁴²²⁻⁴²⁵ The skin specifically yields many biologically relevant peptides and AMPs due to its role as the major barrier between the organism and pathogens.²⁹¹ Peptides from amphibian skin have a diverse range of action, including acting as signal transmitting, antipathogenic, antioxidant, skin healing, insulin-releasing, immunomodulatory, and myotropic compounds, and have other purposes as well.^{286,291,292,422,426,427} A list of over 2000 amphibian peptides and varied activities have been recently reviewed.^{291,422} A limited few of this large library are ATCUN-peptides and/or His-containing peptides. Some His-containing amphibian peptides have been reported to be antioxidants.²⁹² This may be because His residues coordinated to some transition metals or alone can have antioxidant effects.⁴²⁸ Additionally, there is ample Cu²⁺ in different tissues of amphibians that can be used by AMPs to potentiate antimicrobial activity. For instance, *Rana ridibunda* has anywhere from 6-11 nmol/g of copper ions in its skin and up to 190 nmol/g in other tissues.⁴²⁹ It is likely that ATCUN-peptides in amphibians may have diverse roles including antioxidant, antipathogenic, and signal transmitting roles.

Amphibian peptide families including bombesin-like, tryptophyllins, tachykinin, cholecystokinins, and caeruleins all contain at least one member with a pyroglutamic acid (pGlu) residue at the N-terminus, where bombesin-like peptides and caeruleins have the largest number of pGlu containing peptides.²⁹¹ Interestingly, most AMPs do not have these residues, with some exceptions, including the spider derived AMP gomesin,⁴³⁰ but these modified residues have been found in many neuropeptides and hormone peptides.⁴³¹ Some pGlu residues may be a product of peptide isolation, as acidic conditions can trigger pGlu formation.⁴³² A pGlu residue can be post-translationally modified through an intramolecular cyclization of either a Gln or Glu residue at the N-terminus of a peptide, although Gln is almost always the residue that converts to a pGlu residue (Figure 20).⁴³² These pGlu residues can be modified from Gln spontaneously at a slow rate or, more typically, enzymatically using either glutamyl cyclotransferases or cyclases.⁴³¹ Cleverly, these enzymes are found in neurological regions of the amphibians, where the cyclization is too slow otherwise, resulting in a specific action of the peptide.⁴³¹ The Gln deamidation reaction occurs at alkaline or neutral pH. However, under low pH conditions, cyclization competes with protonation of the side chain amino group.⁴³³ Dehydration of Glu can also lead to pGlu formation.⁴³³ pGlu formation has been implicated in resistance to protease degradation, similar to C-terminal amidation, and will elongate circulation time for neuropeptides. Amyloid- β peptides

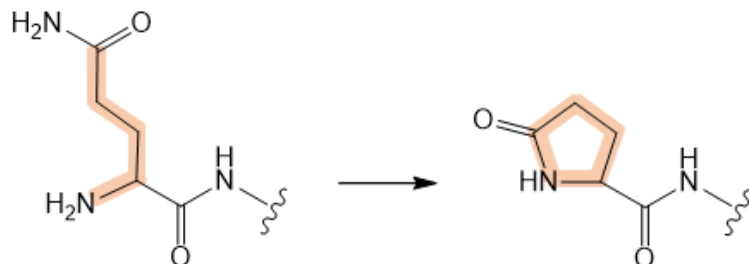


Figure 20. Glu cyclization to a pyroGlu (pGlu) residue at the N-terminus of a peptide. Important atoms are shown highlighted.

with pGlu residues have been reported to have a role in plaque formation and may play a role in Alzheimer's disease.⁴³⁴

3.6.1 Tachykinin and neuro-active peptides

Tachykinin AMPs and neuropeptides can contain pGlu residues with ATCUN motifs. Tachykinins have a conserved C-terminus region of FXGLM-NH₂ where X is a branched aliphatic or aromatic residue.⁴²⁷ The conserved C-terminus is important to the neuropeptide-receptor interaction and activity because the C-terminus is the part of the peptide that activates neuropeptides.⁴³⁵ The Australian frog, *Pseudophryne guntheri*, produces two tachykinin peptides, PG-KI and PG-KIII.²⁸⁶ Both peptides have a unique ATCUN sequence due to the inclusion of a pGlu residue in the first position, and PG-KI and PGK-III both contain Met residues that may additionally be able to coordinate metal ions. These peptides have not been well-studied but both were tested for their myotropic activity. PG-KI exists in either a C-terminally amidated and a deamidated form, where the deamidated version caused the peptide to become unable to cause smooth muscle contractions.²⁸⁶ PGK-III was only found with a free C-terminus and had a reduced ability to cause muscle contractions, leading to the conclusion that the C-terminal amidation may be important to myotropic ability.²⁸⁶ The C-terminus of PG-KI and PG-KIII are conserved for interactions with neuropeptides that leads to the hypothesis that PG-KI and PG-KIII are neuropeptides. Despite the inclusion of the pGlu residue in the ATCUN motif, these peptides may still be able to bind to Cu²⁺ and Ni²⁺ (Figure 21), although this binding still needs to be demonstrated. This has been shown with hormone peptides that have a pEIH ATCUN motif and has been reported to characteristically bind to Cu²⁺ with an affinity of 5.2×10⁻¹² M.³⁶⁸ There is potential for PG-KI and PG-KIII to act as neuropeptides that may have antioxidant properties, and this should be further studied. Understanding the chemistry of ATCUN binding is important to

identify a relationship between metal-binding and activity. PG-KI and PG-KIII can be used as a lesson to design neuropeptides that can be neuroprotective through Cu²⁺ binding.

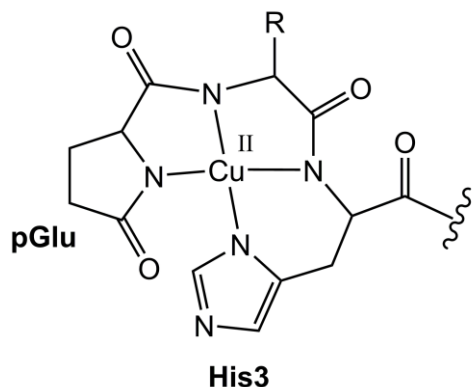


Figure 21. Hypothesized Cu²⁺ binding of an ATCUN motif containing a pGlu residue.

Other tachykinin peptides with ATCUN motifs have antioxidant properties, such as pleurain R1 and neurokinin B (NKB). The Pleurain family was derived from *Rana pleuraden* skin. However, out of the 34 discovered peptides, pleurain R1 was the only one with an ATCUN motif.²⁹² Several members of this family have been shown to have antimicrobial and/or antioxidant abilities to prevent skin infection and aging.²⁹² Pleurain R1 had antimicrobial activity against Gram-negative and -positive bacteria, and *C. albicans*, with MICs varying from 25-100 µg/mL. However, no metal-potentiated activity was investigated.²⁹² Equally interesting was the *in vitro* antioxidant activity that was observed. Pleurain R1 was able to effectively scavenge free radicals produced by nitric oxide, 2,2-diphenyl-1-picrylhydrazyl, and 2,2-azinobis(3-ethylbenzothiazoline-6-sulfonic acid. Substitution of 4th, 5th, and 16th residues with a Gly residue caused a reduction in scavenging ability, but no His3 substitution was tested.²⁹² This antioxidant activity may stem from metal sequestration by the peptide, a mechanism used by metallothionein proteins. The peptide may use the ATCUN motif, Cys, and Met residues to sequester metal and protect against ROS mediated damage. Antioxidant activity of pleurain R1 may be as important as the antimicrobial

activity of these peptides for the anti-aging properties of *R. pleuraden* skin, and the antioxidant properties of other amphibian AMPs derived from the skin should be tested. Several amphibian neuropeptides have ATCUN motifs, including neuromedin C (GNHWAVG^HLM) and neuromedin K (DMHDFFVGLM), have been confirmed to bind Cu²⁺ and Ni²⁺.⁴³⁶ Metal binding of neuropeptides can be important for the activity and conformation of the peptide. Specifically for neuromedin C, there is a conformational change when bound to metal that modifies receptor interactions⁴³⁶ Further, the neuropeptides NKB (DMHDFFVGLM-NH₂), neurokinin A (NKA), neuropeptide gamma (NPG), and substance P all have a conserved C-terminus that is also seen in tachykinins, while NKB is the only peptide of the group that has an ATCUN motif.⁴²⁷ NKA (HKTDSFVGLM-NH₂), NKB, and NPG (DAGHGQISHKRHKTDSFVGLM-NH₂) all have His residues in different positions and can bind to Cu²⁺ using different types of coordination. The Cu²⁺ binding of NKB has been investigated and is incredibly novel for ATCUN-peptides. NKB binds to Cu²⁺ as a dimer by utilizing both His3 imidazole residues and both free N-termini amines, which caused the peptide to become less helical.⁴³⁷ Intriguingly, Ni²⁺ was able to bind in a manner similar to a typical ATCUN motif, but Cu²⁺ preferred to form this dimeric structure.⁴³⁷ Antimicrobial

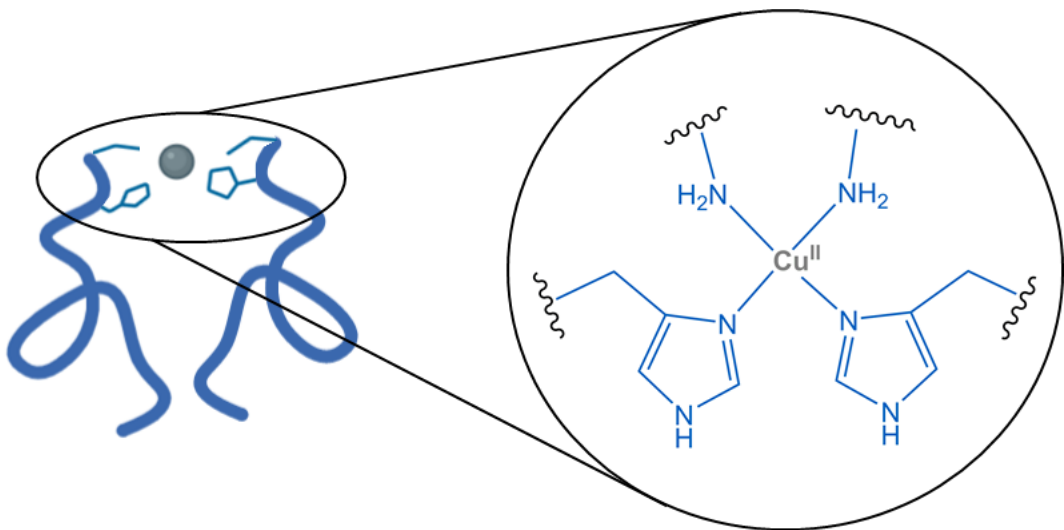


Figure 22. Dimerization of NKB using Cu^{2+} binding to His3 and the N-terminus of both peptides.

activity was not investigated; however, it is likely that the role of this peptide is as a neuropeptide or signal carrier that may have a neuroprotective role similar to other tachykinins. NKB bound to Cu^{2+} did not affect its affinity for neural receptors, and caused the release of calcium from astrocytoma cells but inhibited entry of Cu^{2+} into neural cells.⁴³⁷ Another fascinating feature of NKB is that it binds to Cu^{1+} using Met2, Met10, and His3, which is an unusual coordination for Cu^{1+} .⁴³⁸ This binding completely disrupts the helical structure of the peptide, but its effect on receptor binding was not examined. It was suggested that NKB plays a role in Cu homeostasis in different redox environments because Cu^{1+} exists in neuronal cells, and that its Cu^{2+} binding may compete with amyloid- β peptides that cause neurodegenerative diseases.⁴³⁸ Unlike NKB, NKA binds to Cu^{2+} in both a monomeric and dimeric state.⁴³⁵ NKA did not have the same neuroprotective role as NKB because it was shown that in the presence of H_2O_2 , ROS could be produced by Cu^{2+} -bound peptide, and that the peptide could be cleaved.⁴³⁵ Lastly, NPG is similar to NKA and can produce ROS and be cleaved through oxidation reactions when Cu^{2+} is bound.⁴³⁹ It is certainly interesting that NKA, NKB, and NPG all bind to Cu^{2+} in a different coordination and

seemingly have different roles, despite being in the same family of neuropeptides. ATCUN-peptides may not only confer heightened antimicrobial activity, but they may also have other roles in relieving antioxidative stress and metal sequestration. The study of the antioxidant properties of ATCUN-containing peptides found specifically in the skin of amphibians should be more fully investigated.

3.6.2 Limnonectins

A unique class of amphibian AMPs are the limnonectins that were discovered in the skin secretions of *Limnonectes fujianensis*.²⁸⁹ Limnonectin-1Fa (SFPFFPPGICKRLKRC) and -1Fb (SFHVFPWMCKSLKKC) are 16 residue peptides with 63% sequence homology to each other. However, limnonectin-1Fb has an ATCUN motif and -1Fa does not.²⁸⁹ Both peptides contain an intramolecular disulfide bond between Cys10 and Cys16 residues, where CXXXXXC is known as a Rana box in amphibian AMPs.^{289,440} Several examples show that the Rana box motif is not essential to AMP activity, but the function of the motif has been speculated.⁴⁴¹ Several amphibian AMPs including brevinin 1E and amurin-9KY did not require the Rana box for antimicrobial activity and further, the hemolytic effects and secondary structures of the peptides were not significantly affected by the removal of the motif.^{442,443} Other AMPs such as nigrocin-HL have shown increased helicity, lower cytotoxicity, and remarkably more antimicrobial activity against fungi, Gram-negative, and -positive bacteria, including MRSA, when the Rana box was removed.⁴⁴⁴ B1CTcu5, a brevinin AMP, showed increased hemolysis when the disulfide bond was present, and when the C-terminal region was removed the antimicrobial activity was significantly decreased.⁴⁴¹ It was suggested that the disulfide bond may be present to impart resistance to proteolytic degradation and increased circulation time of the AMP, whereas the C-terminal Rana box region may be needed for membrane targeting.⁴⁴¹ The structure of gaegurin 4, an AMP with a

Rana box, was studied using NMR, and when the Cys residues for the Rana box were replaced by Ser there was little change in the structure other than a more flexible C-terminus, which would be expected when the disulfide bond is not present.⁴⁴⁵ Gaegurin 4 has a helix-loop-helix structure where the N-terminus embeds in the bacterial membrane, while the C-terminus is not likely embedded in the membrane and may be on the membrane surface (Figure 23).⁴⁴⁵ The antimicrobial activity of gaegurin 4 was unchanged in the presence of dithiothreitol, again reinforcing that the disulfide bond does not have antimicrobial functionality.⁴⁴⁵ Several other AMPs have been studied where the Rana box motif and disulfide bonding did not significantly change antimicrobial activity.^{446,447} The function of the Rana box is still not well understood and the utility of the motif has remained debated. The secondary structure of the limnonectins wasn't probed using CD. However, both peptides have a Pro-rich N-terminus that is most likely disordered due to Pro not being able to induce an α -helix via hydrogen bonding. Both peptides had no detectable hemolytic activity against horse erythrocytes up to concentrations of 160 μ M.²⁸⁹ The limnonectins were tested

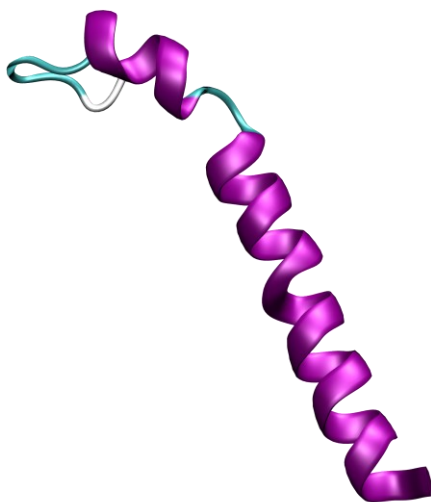


Figure 23. The helix-loop-helix structure of gaegurin 4, where the first helix spans from residues 2-10 and the second from residues 16-32 (PDB: 2G9L).

against *E. coli*, *S. aureus*, and *C. albicans*, but were only active against *E. coli*, where -1Fa had an MIC of 35 μ M and -1Fb had an MIC of 70 μ M.²⁸⁹ The MIC was tested in MHB media, which should have sufficient amount of Cu²⁺ for -1Fb to be metallated⁴⁴⁸ but the activities of -1Fa and -1Fb were almost the same. Curiously, amphibian AMPs typically are not selective towards either Gram-negative or -positive bacteria, and more information should be gathered about their secondary structure, the role of the Rana box motif on activity, and the mode of action of the limnonectins. Specifically, it would be of interest to study the role of Cu²⁺ and examine whether it enhances antimicrobial activity, or whether -1Fb could have another role that involves Cu²⁺ sequestration.

3.6.3 Nigroains

Another class of amphibian AMPs where several of the AMPs form disulfide bonds and can have Rana box sequences are the nigroains. The nigroain class of AMPs is large and includes nigroain-B to E, -I, and -K, where a full set is listed in a recent review.²⁹¹ The ATCUN-AMPs nigroain- D1, -D2, and -D3 were isolated from *Rana nigrovittata*, while nigroain-D-RK1 was isolated from *Limnonectes kuhlii* and is 88% homologous to nigroain-D1.^{290,291} Nigroain-D1, -D3, and -RK1 all form a 13 residue disulfide ring. However, nigroain-D2 has a mutation at position 13 where Arg is substituted for Cys and does not form a disulfide bridge. A 13 residue disulfide bond is uncommon for amphibian AMPs, which typically have either seven or nine residues.^{290,449} Most other nigroains have a Rana box that has a seven residue disulfide bridge.²⁹⁰ To our knowledge, there are only four other amphibian AMPs produced by *Odorrana grahami* and *Hyalarana spinulosa* that have either 11 or 13 residue disulfide rings.^{450,451} Metal binding has not been investigated for these peptides, but nigroain-D3 was tested on *C. albicans* and *B. subtilis* and had MICs of 110 and 55 μ g/mL, respectively.²⁹⁰ Nigroain-D3 was also only 6% hemolytic using a 100

$\mu\text{g/mL}$ dose.²⁹⁰ The other peptides were not tested for antimicrobial or hemolytic activity, and the implications of the disulfide bridge on the activity has not been determined. The ATCUN motif is within this Cys loop, and nigroain-D AMPs are some of the only ATCUN-AMPs with this feature. To our knowledge, there have not been any natural ATCUN-AMPs studied for metal binding that also have a Cys bridge at the N-terminus of the peptide. It is likely that metal ions would still be able to bind in conjunction with disulfide bond formation, but this should be investigated further. Nigroain-D2 could be used as a negative control for such experiments due to the Cys to Arg substitution. Although this constricted ATCUN motif has not been studied, the ATCUN motif in cyclic peptides have been studied by the Kritzer group using synthetic AMPs, showing that short cyclic ATCUN-AMPs can still bind to Cu^{2+} and Ni^{2+} .⁴⁵²

3.6.4 Temporins

The temporin group is one of the largest groups of amphibian AMPs that are devoid of a Rana box motif and disulfide bonds. Temporins have been isolated from over 44 amphibian species and can have insulin releasing, immunomodulatory, and antimicrobial effects.⁴⁵³⁻⁴⁵⁵ Although there have been many temporins discovered, they have little sequence homology. However, temporins are typically short (10-19 residues), C-terminally amidated peptides with a low net neutral charge (0 to 3+).⁴⁵⁶ Many temporins only have activity against Gram-positive bacteria, although there are exceptions that have broad-spectrum activity.^{454,457,458} Several members of the temporin family have shown synergistic interactions against Gram-negative bacteria. Temporin A and B from *Rana temporaria* showed little to no activity against Gram-negative bacteria, which was hypothesized to be due to oligomerization of the peptide in the presence of LPS on the cell membrane of Gram-negative bacteria.⁴⁵⁹ However, if either peptide was in the presence of temporin 1, there were synergistic interactions that allowed the peptides to have potent activity

against Gram-negative bacteria.⁴⁵⁹ This activity was likely a result of temporin 1 assisting temporin A and B across the membrane and avoiding oligomerization due to contact with LPS.^{459,460} In addition, it has been shown that temporin A and temporin B with two Lys substitutions are also synergistic against both Gram-negative and -positive bacteria.⁴⁶¹ Recently, four temporins were derived from *Hylarana guentheri*, named temporin-GHa-d, where temporin-GHb (FIHHIIGALGHLF) has an ATCUN motif that is reminiscent of the highly conserved N-terminus of piscidin AMPs.²⁹³ The other three temporins all have His residues in the fourth position rather than the third, and have a conserved N-terminus with the sequence FLQHIIIGAL. All four AMPs are neutrally charged at physiological pH and all were α -helical, with the exception of temporin-GHb which was a random coil based on secondary structure predictions.²⁹³ Antimicrobial testing revealed that temporin-GHa-d were active against several Gram-positive and -negative bacteria, and *C. albicans*, where temporin-GHb was one of the most active, including against a MRSA strain.²⁹³ This activity was resilient in the presence of *S. aureus* V8 protease, 2 M NaCl, and in the presence of human serum.²⁹³ Scanning electron microscopy images revealed that the mode of action was likely membrane disruption for Gram-negative and -positive bacteria due to the change in morphology of the tested cells.²⁹³ The effect of metal ions on this set of temporins was not tested. However, temporin-GHb was more active than the other temporins, which may be explainable through metal-mediated activity. The N-terminus of temporin-GHb is very similar to that of the piscidin peptides, where there is a “hydrophobic fence” to stabilize metal binding. Curiously, both temporins and piscidins act as chemoattractants for FPRs.^{355,453} The sequence of temporin-GHb is different from most other temporins and is the only one that is currently known to have an ATCUN motif. This raises the question of if the major function of temporin-GHb is related to chemoattractant activity, and why it is advantageous for this peptide to utilize metal ions.

3.6.5 Other amphibian ATCUN-peptides

Several other ATCUN-peptides have been derived from amphibians; however, their activity or purpose has not been well studied. Six peptides were discovered from the skin of *Odorrana schmackeri* and were named schmackerin-A to F.²⁸⁸ Schmackerin-F1 (VDHLWQVWLPR) is an 11 residue ATCUN-peptide, rich in Trp residues.²⁸⁸ Only schmackerin-C1 was tested for antimicrobial activity, which is broad-spectrum, but its sequence is not homologous to schmackerin-F1, which is shorter and less cationic.²⁸⁸ In short peptides, Trp helps with internalization, and that may be the case with schmackerin-F1.⁴⁶² Electrin 3 (FVHPM) is another short ATCUN-peptide that was isolated as a minor product from *Litoria electrica* skin.²⁸⁷ It is in the tryptophillin group of peptides, which usually have myotropic behavior and are short, Trp- and Pro-containing peptides.⁴⁶³ Electrin 3 is different from other tryptophyllin peptides due to its non-amidated C-terminus, no Trp residue, and the inclusion of an ATCUN motif. Although electrin 3 was a minor product of the skin secretions and was not tested for either antimicrobial activity or ability to cause muscle contractions, electrin 1 and 2.1 did not have any antimicrobial activity below 100 µg/mL and did not behave as neuropeptides or have antioxidant activity.²⁸⁷ The role of these peptides in *L. electrica* skin secretions are not currently known and have not been investigated since their discovery in 1999. Overall, amphibian peptides serve many diverse roles that include antimicrobial, antioxidant, myotropic, and signal transmitting activities. There are examples of amphibian ATCUN-peptides that can act as either potent AMPs via the generation of ROS or that have a neuroprotective role by sequestering metal ions that may produce ROS-mediated damage.

3.7 Mussel AMPs

The Mollusca phylum is comprised of bivalves including clams, mussels, and oysters. As filter feeders, bivalve organisms are constantly taking in bacteria and other pathogens, including parasites.⁴⁶⁴ In order to stay healthy, bivalves have protective barriers of both a shell and mucus membranes. They mainly rely on the innate immune response because mollusks do not have immunological memory.^{464,465} The immune system of invertebrates differs from that of vertebrates in regards to their phagocytic cells. Invertebrate circulating hemocytes are equivalent to macrophages and phagocytic cells in vertebrates.^{464,465} In addition to phagocytic hemocytes, there are lectins, AMPs, lysozymes, peroxidases, agglutinins, and hydrolytic enzymes in the serum of the hemolymph that can kill invading pathogens.^{464,465} Pathogen recognition is most likely mediated by lectins found in hemolymph that have opsonic roles in phagocytosis.⁴⁶⁴ Agglutination can also be triggered by lectin recognition and may lead to bacterial death.⁴⁶⁴ AMPs may be used in conjunction with ROS in hemocytes to detoxify filter feeders. However, some species do not produce ROS and may need to rely heavily on AMPs.⁴⁶⁶ Mussel AMPs are one of the most studied systems in this phylum, and eight different AMP families have been reported: myticusins, myticins, mytilins, defensins, mytimacins, big defensins, mytichitins, and mytimycins. Mussel AMPs are large, rich in Cys residues, and commonly found in hemocytes. Although only members

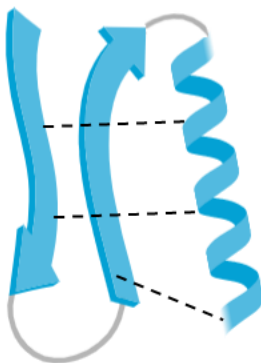


Figure 24. CS α β motif that is found in many of the mollusca family AMPs, where the dashed lines represent typical positions for disulfide bridges.

of the myticin, myticusin, and mytimycin groups have ATCUN motifs, all groups of mussel AMPs have similar disulfide bonds and many have Cys-stabilized α -helix and β -sheet (CS α β) structures (Figure 24).

3.7.1 Myticins

Mytilus galloprovincialis hemocytes and plasma yielded two 40 residue AMPs, myticin A and myticin B.³⁰¹ These two isoforms have four intramolecular disulfide bonds and both have ATCUN motifs, although their metal binding activity has not been investigated.³⁰¹ Both peptides are characterized by Cys-X₄-Cys-X₃-Cys-X₄-Cys-X₄-Cys-X₈-Cys-X₁-Cys-X₂-Cys spacing and a conserved 20 residue signal peptide.³⁰¹ Although myticin AMPs were found in high concentrations in hemocytes and blood plasma, they are also expressed in gill, digestive gland, intestine, and adductor muscle cells.⁴⁶⁷ Myticin A and B were tested against fungi, Gram-positive, and -negative bacteria. Both peptides were active against Gram-positive bacteria, but only myticin B had activity against *E. coli* and the fungus *Fusarium oxysporum*.³⁰¹ Myticin C was identified later in *M. galloprovincialis* as another isoform, but had a 43 residue sequence (QEAQSVACTSYYCSKFCGSAGCSLYGCYLLHPGKICYCLHCSR) and an immunomodulatory role as a chemokine.^{468,469} Although the Cys residues of myticin C are spaced as the other myticins, there is only 48% and 70% homology between it and myticin A and B, respectively, where the N-terminus of myticin C is more variable. After a BLAST search, we found eight other myticins. The new myticins all have ATCUN motifs except for myticin 5, which is more similar to myticin C than A or B (Figure 25). The consensus sequence reveals a highly conserved signal peptide and N-terminal region amongst all of the myticins (Figure 25). The

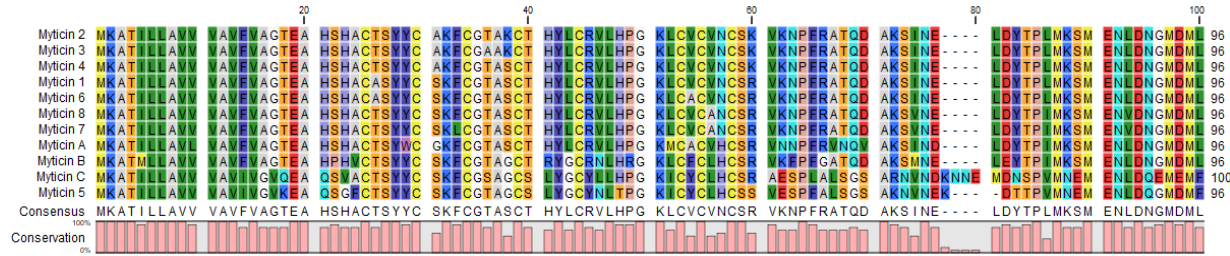


Figure 25. Myticin sequence alignment showing highly conserved signal peptide and N-terminal regions of the myticin family.

sequence similarity of this family of peptides raises the question of why all 11 related AMPs are expressed and whether they act synergistically with one another or target specific pathogens.

3.7.2 Mytilins

Mytilins have been isolated from both *Mytilus edulis* and *M. galloprovincialis* hemocytes, and have six conserved Cys residues that form three disulfide bonds.^{470,471} Two 34 residue isoforms named mytilin A and B were found in *M. edulis* and were found in concentrations of up to 2 μ M in hemocytes.⁴⁷⁰ Mytilin A is more active against Gram-positive bacteria, but was active against some Gram-negative bacteria as well.⁴⁷⁰ The amount of peptide found in these hemocytes is comparable to the MIC values of these peptides against many of the tested Gram-positive bacteria.⁴⁷⁰ Moreover, the expression of mytilin B is reduced upon bacterial challenge rather than being upregulated, which may mean that the peptide is specifically transported to the infection site rather than upregulated.⁴⁷² A mytilin B isoform, along with mytilin C, D, and G1, was isolated by Mitta *et al.* from *M. galloprovincialis* hemocytes.⁴⁷¹ Mytilin G1 is 36 residues and mytilin C is 31 residues long, but all others are 34 residues long, consistent with the originally isolated mytilins.⁴⁷¹ These peptides ranged in activity, but mytilin G1 was only active against Gram-positive bacteria, while mytilin B and D were the only antifungal mytilins.⁴⁷¹ Upon bacterial injection, mytilin-containing hemocytes accumulated at the injection site and these hemocytes were able to

phagocytose bacteria.⁴⁷¹ Co-localization of mytilins and bacteria in hemocytes, in addition to previous evidence that mytilin B is downregulated after bacterial challenge, may suggest that mytilins are transported or recruited to the site of infection to specifically kill pathogens.⁴⁷¹ In addition to intracellular killing, it is likely that mytilins can kill pathogens extracellularly because they were also released from hemocyte granules.⁴⁷¹ This activity is similar to piscidin peptides that can kill intracellularly in macrophages or extracellularly after being released from granules.³⁴³

3.7.3 Mytimycins and Mytichitins

Mytimycins were first isolated in *Mytilus edulis*.⁴⁷⁰ The two mytimycin isoforms have 34 residues, 12 of which are Cys residues that form six intramolecular disulfide bonds.⁴⁷⁰ Their antimicrobial activity was exclusive to fungi.⁴⁷⁰ Since the initial isolation of mytimycin, several other isoforms have been discovered, specifically from *M. galloprovincialis*.⁴⁷³ Mytimycin J does have an ATUCN motif, but it has not been well studied and was only recently identified.⁴⁷⁴ The ATCUN motif is comprised of CCH, where the ATCUN binding would be within disulfide bonds, similar to nigroain AMPs.⁴⁷⁴ Moreover, several chitin binding peptides have been isolated from marine animals, including crabs and shrimp.⁴⁷⁵⁻⁴⁷⁷ Mytichitin peptides from mussels are unique AMPs that have chitin binding regions and that are typically more active against fungi due to binding to chitin in the fungal cell wall. The first was isolated from the gonads of *Mytilus coruscus* and was named mytichitin-1.⁴⁷⁸ A C-terminally active AMP fragment from mytichitin-1 called mytichitin-CB was discovered to be strongly active against fungi, Gram-positive bacteria, and to some extent Gram-negative bacteria.⁴⁷⁸ Mytichitin-CB has 55 residues, with six Cys residues, and the structure was predicted to be a β -sheet.⁴⁷⁸ Mytichitin-1 was upregulated 9-fold after bacterial challenge, and it was suggested that the cleavage of the active mytichitin-CB may occur in the hemolymph where mytichitin-CB was found upon bacterial infection.⁴⁷⁸ Another mytichitin with

broad-spectrum antimicrobial activity has been isolated from the foot of *M. coruscus* and called mytichitin-CBD.⁴⁷⁹ These mytichitin peptides display the advantages of targeted or activatable peptide cleavage upon pathogen infection.

3.7.5 Myticusins

Similar to other mussel AMPs, myticusin peptides have several Cys pairs that form disulfide bonds. Myticusins are characterized by their 104-amino acid length, including 10 Cys residues with a conserved Cys-X₁₆-Cys-X₅-Cys-X₃-Cys-X₂₁-Cys-X₄-CysCysCys motif that has a unique Cys triplicate towards the end of the sequence.⁴⁸⁰ It may be argued that myticusins are not actually AMPs due to their large size (>10 kDa). To date, two myticusin peptides have been identified in *M. coruscus*, where the ATCUN motif varies, being either TDH or SDH.^{303,480} Myticusin-1 was identified in 2013 and was highly expressed in hemocytes.⁴⁸⁰ After a bacterial challenge, the expression of myticusin-1 was upregulated up to 20-fold, indicating the necessity of this peptide to fight bacterial infections.⁴⁸⁰ Broad-spectrum activity was revealed against fungi, Gram-negative, and Gram-positive bacteria, including *Vibrio* spp. that infect marine life.⁴⁸⁰ It was shown that myticusin-1 has better activity against Gram-positive bacteria. Transmission electron microscopy (TEM) was used to show that the mode of action of the peptide is likely cell membrane disruption.⁴⁸⁰ Interestingly, myticusin is a large AMP and has nine positively and nine negatively charged residues, making it neutrally charged, which is uncommon among AMPs. In 2020, a second myticusin AMP, myticusin-beta, was found in mantle tissue of *M. coruscus*.³⁰³ Myticusin-beta has two other isoforms, both with only one residue change near the C-terminus of the peptide. The isoforms are 78% homologous to the sequence of myticusin-1 and the signal peptides are 66% homologous.³⁰³ Although the sequence of myticusin-beta was homologous to myticusin-1, its antimicrobial activity varied because, unlike myticusin-1, it was not active against *C. albicans*.³⁰³

A disk-diffusion assay revealed antimicrobial activity against Gram-negative and -positive bacteria, with essentially no lysis of flounder erythrocytes up to 100 µg/mL.³⁰³ Myticusin-beta was able to kill 50% of scuticociliates, a marine parasite, within 24 hours, where the parasites appeared to have burst or been damaged under microscopic observation.³⁰³ It seems that at least part of the mode of action of the myticusin family of AMPs acts on the membrane of pathogens. However, additional biophysical and biological studies of these peptides are necessary to establish their mechanism of action.

3.7.5 Defensins and Big Defensins

Another important family of Cys-rich AMPs from the Mollusca phylum are the defensins. Mollusca defensins have six conserved Cys residues that form three disulfide bonds. Two isoforms, MGD1 and MGD2, were first isolated in granules of *M. galloprovincialis*.⁴⁸¹ The peptides are both 39 residues with 85% homology with a highly hydrophobic N-terminus.⁴⁸¹ MGD1 and MGD2 have 21 residue C-terminal extension peptides that are highly acidic and have up to eight Asp or Glu residues.⁴⁸¹ Upon bacterial challenge, MGD1 is released from hemocyte granules and is upregulated by 18 times, suggesting an antimicrobial role.⁴⁸¹ Curiously, MGD2 expression was decreased after bacterial infection, but it was upregulated during other stress events such as shell damage and heat shock.⁴⁷² Although the two defensin isoforms have high homology, they may serve different roles when the mussel is under stress. Similarly to mytichitin peptides, it is possible that there is a cleavage of the anionic C-terminal portion of the peptide that could stabilize the peptide in hemocytes but that activates the cationic C-terminus upon bacterial infection.⁴⁸¹

A closely related group are big defensins that have a highly hydrophobic N-terminus with a charged C-terminus that resembles β-defensins.⁷² The structure of big defensins has three

intracellular disulfide bonds that typically form a CS α β motif (Figure 24).^{481,482} The first big defensin isolated was from the hemocyte granules of *T. tridentatus*, a horseshoe crab, and has 79 residues, six of which are Cys that form three intracellular disulfide bonds at the C-terminus of the peptide.⁴⁸³ The peptide, termed limulus (horseshoe crab) big defensin, has broad-spectrum antimicrobial activity and LPS binding activity. Secretion of limulus big defensin from hemocytes is triggered by LPS stimulation of hemocytes. There is a protease cleavage at Arg37 to yield two differently active peptide fragments. The N-terminal fragment forms an α -helix that is more active against Gram-positive bacteria. However, the C-terminal portion is active against Gram-negative bacteria and forms a β -sheet as a fragment.⁴⁸⁴ The N-terminus portion in the full length peptide forms two α -helical and one β -sheet portions with a break between Leu21 and Ala23.⁴⁸⁴ NMR revealed that in micellar solution the N-terminal fragment forms an α -helix and penetrates micelles at the N-terminal end, while the C-terminal end of the fragment is solvent exposed.⁴⁸⁵ Several big defensins from bivalves including clams, scallops, mussels, and oysters have been isolated since the initial discovery. The scallop *Argopecten irradians*, the mussel *Hyriopsis cumingii*, and the clams *Chlamys nobilis* and *Venerupis philippinarum* all have big defensins that are highly expressed in hemocytes.⁴⁸⁶⁻⁴⁸⁹ *A. irradians*, *C. nobilis*, and *V. philippinarum* big defensins were upregulated in hemocytes after bacterial challenge.^{486,487,489} The *A. irradians* big defensin was highly active against Gram-positive bacteria but only active against the Gram-negative *Vibrio* spp. and not *E. coli*.⁴⁸⁶ It is likely that, based on the upregulation of big defensins in the hemocytes after bacterial challenge, the role of hemocyte expression is to circulate the AMP through the tissue. Further, eight big defensins from *M. galloprovincialis* (MgB) were isolated and their expression was studied. Their abundance and presence varied and, unlike all other big defensins, the three tested peptides were not found in the hemolymph.⁴⁹⁰ MgB1 was expressed exclusively in the

digestive gland, while MgB3 and MgB6 were found in the gills and mantel of the mussel.⁴⁹⁰ Another big defensin named ApBD1 from the scallop *Argopecten purpuratus* is not found in hemocytes but is constitutively expressed in gills, muscle, gonads, digestive glands, and the mantle.⁴⁹¹ After bacterial challenge, there was a 7-fold increase of expression in the gills but seemingly no change in hemocytes. Using an immunostaining method, however, it was shown that there was an increased expression in hemocytes. It is unclear why there was this discrepancy, but these big defensins may be for localized protection or there may be a transport mechanism from tissue through hemocytes upon bacterial challenge.⁴⁹¹ Specifically, localized protection may be needed in the mantle, as it is highly exposed and on the outer edge of the mussel or scallop.

The oyster *Crassostrea gigas* big defensins Cg-BigDef1, 2, and 3 were isolated from hemocytes and are 87-94 residues in length.⁴⁹² These three big defensins are encoded by distinct genomic sequences and the N- and C-terminus are encoded by different exons.⁴⁹² The C-terminal regions of Cg-BigDef1, 2, and 3 resemble vertebrate β -defensins. Cg-BigDef1 and 2 are both upregulated upon bacterial challenge but not upon tissue damage, while Cg-BigDef3 is non-regulated, suggesting potential differences in their roles in hemocytes.⁴⁹² Their mode of action has not been well elucidated for big defensins, but it was recently shown that big defensins can kill bacteria not through membrane permeabilization, but through the triggering of nanonets.⁷² Nanonets can entrap bacteria in nanofibrils and cause bacterial aggregation.⁷¹ Cg-BigDef1 from *C. gigas* induced nanonet formation with as little as 5 μ M peptide in the presence of *S. aureus*, and effectively killed without manipulation of the cell membrane.⁷² Intriguingly, the N-terminal domain, but not the C-terminal domain was able to trigger nanonet formation, although the bacteria were not killed with only the N-terminus present.⁷² It was previously seen that in horseshoe crab big defensins, the N-terminal fragment was more active against Gram-positive bacteria.⁴⁸³

Formation of nanonets has also been recently reported in the big defensin peptide ApBD1 from scallops.⁷³ Nanonet formation may be a major mode of action for big defensin peptides.

3.7.6 Mytimacins

Unlike other mussel peptides, members of the mytimacin family are not found in hemocytes of both *Achatina fulica* the land-living snail and *M. galloprovincialis*, but are found in mucus and other tissues.^{490,493} They typically have eight Cys residues, but can have up to 10 in certain cases.⁴⁹⁰ Five cationic mytimacin isoforms in *M. galloprovincialis* were termed mytimacin-1 to -5. Mytimacin-2 and -3 are different from the others and have eight Cys residues, where the three others have 10 Cys residues and a C-terminal extension.⁴⁹⁰ Mytimacin-3 has a flexible, Gly-rich N-terminus region and has a similar structure to hydramacin-1.⁴⁹⁰ Mytimacin-1 was expressed in all tissues that were tested, although there was low expression in hemocytes.⁴⁹⁰ Mytimacin-2 and -3 were not expressed in hemocytes and were more selectively expressed in the gills and mantle, respectively.⁴⁹⁰ Mytimacin-3 was similar to mytimacins from the mussel *Mytilus californianus*.⁴⁹⁰ The signal peptide of the mussel mytimacins was conserved when compared to mytimacin-AF from *A. fulica*.⁴⁹³ Mytimacin-AF is a non-hemolytic, 80-amino acid peptide with 10 Cys-residues that is more similar to mytimacin-1, -4, and -5.⁴⁹³ Mytimacin-AF had broad-spectrum activity, with greatest activity against Gram-positive bacteria.⁴⁹³ Clearly, the AMPs in the Mollusca phylum have many similarities in that they all contain Cys residues and form several intramolecular disulfide bonds. The mode of action and importance of Cys and disulfide bond formation of these AMPs should be further studied to examine whether nanonet formation may a major mode of action for mollusk AMPs.

3.8 AMPs from Bacteria: Bacteriocins

The AMPs that were described above are produced by organisms as part of their innate immune system against bacterial pathogens. Bacteria themselves produce AMPs, known as bacteriocins, to kill other competing bacteria to have a heightened growth advantage (Table 5).^{494,495} Most of the bacteria found in the literature that produce bacteriocins are lactic acid (LA) bacteria, which have bacteriostatic and/or bactericidal effects against other bacteria of usually closely related species.⁴⁹⁶⁻⁵⁰⁰ These peptides are synthesized from ribosomes before being extracellularly released to potentiate their activity.⁴⁹⁶ LA bacteria are known as biopreservative organisms for food preservation, and production of bacteriocins from LA bacteria are potentially responsible for the preservation effects by killing microorganisms that can contaminate food products.^{496,500} Potentially, industrial scale production of bacteriocins can be harnessed for food preservation, leading to the high research interest in these AMPs. Bacteriocins are generally classified into three classes: post-translationally modified peptides are in class I, small (less than 10 kDa) unmodified peptides are in class II, and large (greater than 21.5 kDa), heat-labile peptides are in class III.⁵⁰¹

Table 5. Examples of naturally-occurring bacteriocins.

Peptide	Sequence
Pediocin PA-1 ⁵⁰²	KYYGN GVTcyclo[CG KHSC]S VDWGK ATTcyclo[CI INNGA MAWAT GGHQG NHKC]
Sakacin P ⁵⁰²	KYYGN GVHcyclo[CG KHSC]T VDWGT AIGNI GNNAANWAT GGNAG WNK
Enterocin A ⁵⁰³	TTHSG KYYGN GVYCT KNKCT VDWAK ATTCAAGMSI GGFLG GAIPG KC
GarQ ³⁰⁵	EYHLM NGANG YLTRV NGKYV YRVTK DPVSA VFGVI SNGWG SAGAG FGPQH
GarML ⁵⁰⁴	<u>cyclo</u> [LVATG MAAGV AKTIV NAVSA GMDIA TALSL FSGAF TAAGG IMALI KKYAQ KKLWK QLIAA]
GarA ⁵⁰⁵	IGGAL GNALN GLGTW ANMMN GGGFV NQWQV YANKG KINQY RPY

Lantibiotics are class I bacteriocins that contains lanthionine and/or methyllanthionine post-translationally modified residues.⁵⁰⁶ The lanthionine moiety is formed by dimerization of two Cys residues. It can also be seen as two Ala residues wherein the side chains are connected by a thioether bond (Figure 26). They have broad-spectrum antimicrobial activity against both Gram-negative and -positive bacteria, including drug-resistant strains of the genus *Helicobacter* and genus *Staphylococcus*.⁵⁰⁷ These are further sub-classified into linear, linear and globular, and globular conformations. Nisin, from *Lactococcus lactis*, is an example of a linear lantibiotic. It binds to lipid II, a precursor required for peptidoglycan polymerization during cell wall biosynthesis, inhibiting the process and killing the target bacteria.⁵⁰⁸ Mersacidin, from *Bacillus* spp., is a globular lantibiotic that also inhibits the cell wall biosynthesis by binding to lipid II.⁵⁰⁹ Despite the differences in their structure, it is interesting that they both target lipid II. What seems to be common in the bound states of these bacteriocins to lipid II is that they both have a flexible hinge that is crucial in their mode of action. In nisin, once the N-terminus is bound to lipid II, the hinge allows insertion of the remaining regions of the peptide to form pores that will span the lipid

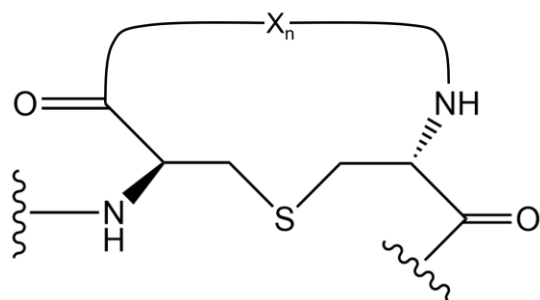


Figure 26. Structure of the lanthionine moiety in lantibiotics. X_n indicates the residues that are cyclized.

bilayer of the target bacteria.⁵⁰⁸ In mersacidin, the hinge allows easier conformational changes to provide accessibility of lipid II to the charged N-terminus and Glu17.⁵⁰⁹

Class II bacteriocins are described as small bacteriocins with no post-translational modifications. There is no clear definition in the literature of what is considered to be small bacteriocin, but for the purposes of this review, we will classify bacteriocins having a molecular weight of less than 10 kDa to be class II bacteriocins. Pediocins, sakacins, and enterocins all belong to class IIa bacteriocins, a subclass of class II bacteriocins, which all contain the YGNG motif.⁵⁰¹ They are also known as pediocin-like bacteriocins due to their shared structural characteristics with pediocin PA-1, the most studied and first characterized bacteriocin in the group.⁵⁰³ Pediocin-like bacteriocins contain at least one disulfide bridge, amphipathic α -helix, and net positive charge, but they have low sequence homology at the C-terminus region.⁵¹⁰ They fold into an S-shape at the N-terminus, consisting of three stranded β -sheet with disulfide bridge after the YGNG motif to form a five-residue hairpin that stabilizes the structure (Figure 27).⁵⁰¹ It was suggested that the disulfide bridge in the N-terminus is for structure stabilization,⁵⁰¹ while having an additional disulfide bridge in the C-terminus gives bacteriocins a greater target cell specificity and a less temperature-dependent activity.⁵⁰² Class IIb bacteriocins are two linear peptides that form pores in their target cell as the mechanism of action.⁵⁰¹ Despite the two peptides having low sequence homology, they have a common GXXXG or GXXXG-like motifs.⁵¹¹ These Gly residues allow the peptides to have a flat surface for interactions between the α -helices.⁵¹¹ Class IIc bacteriocins are AMPs that are produced from precursors with no N-terminal extensions (or leader sequences); thus, they are called leaderless bacteriocins.⁵¹² The formylation of Met at the N-terminus in some of these bacteriocins increase the antimicrobial activity of the AMP.⁵¹³ Class IId bacteriocins are single peptides and non-pediocin-like, such as some plantaricins and garviecins. Due to their small

similarities in their structural characteristics, they have diverse antimicrobial activities, gene cluster organization, secretion mechanisms, and modes of action.⁵⁰¹

Two variants of sakacin AMPs (sakacin P and sakacin A) and pediocin PA-1 have antimicrobial activities against 200 different strains of *Listeria monocytogenes*, which are common foodborne pathogens.⁵¹⁴ Similar to class I bacteriocins, disulfide bridges are formed in class II bacteriocins that decreases their flexibility and enhances their antimicrobial activity. Wild-type pediocin PA-1 and wild-type sakacin P have high sequence homology, differing in their number of disulfide bridges.⁵⁰² The wild-type pediocin PA-1 has an extra disulfide bridge at the C-terminal

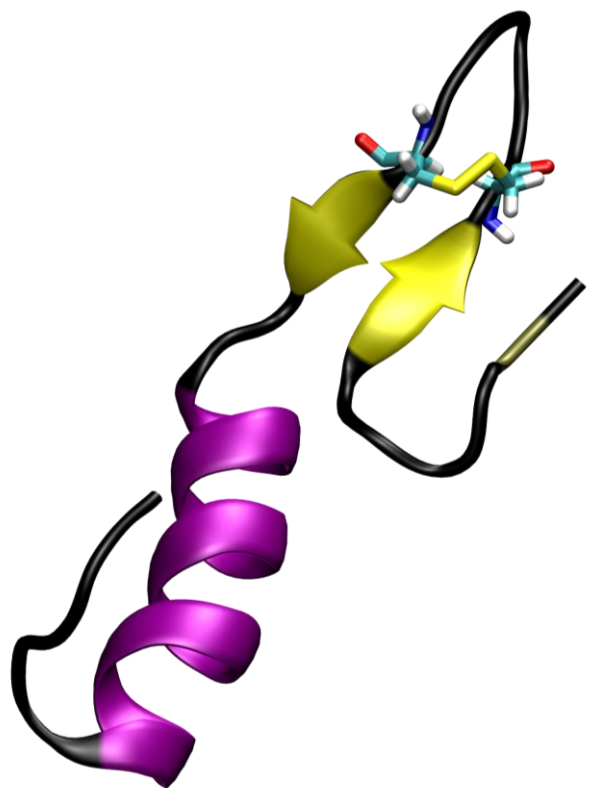


Figure 27. Unique S-shaped fold of YGNG-motif containing class II bacteriocins. The Cys residues on the N-terminal region of the peptide form a disulfide bond that stabilizes strands of β -sheets.

formed by Cys24 and Cys44.⁵⁰² Cys24Ser + Cys44Ser mutants of PA-1 exhibited loss of activity against *Pediococcus acidilactici* and *Pediococcus pentosaceus*.⁵⁰² This similar activity is seen in wild-type sakacin P, which does not have the C-terminal disulfide bridge.⁵⁰² It has been shown that the presence of the C-terminal disulfide bridges in pediocin-like bacteriocins widens their antimicrobial spectrum at lower temperatures (around 20°C) with increased antimicrobial activity at a higher temperature of 37°C.⁵⁰² Eight resistant mutants of *L. monocytogenes* have been identified by exposing wild-type strains of the bacteria to four class IIa bacteriocin-producing LA bacteria, including those that produce pediocin PA-1.⁵¹⁵ A common mechanism of resistance against class IIa bacteriocins was reported for *L. monocytogenes*, where expression of genes involved in β-glucoside phosphotransferase systems was increased.⁵¹⁵ This is an effect of the MptA subunit from a mannose phosphotransferase system (mPTS) being no longer expressed.⁵¹⁵ This suggests that the general mechanism of action for class IIa bacteriocins is by targeting the mPTS.

Enterocin A is a pediocin-like bacteriocin that is isolated from an *Enterococcus faecium* strain. It has 54.6% sequence homology with pediocin PA-1 and it also contains the conserved YGNGV sequence found in pediocin-like bacteriocins.⁵⁰³ This motif is part of a unique S-shaped fold, which may form three strands of β-sheets (Figure 27).⁵⁰¹ It is capable of forming a disulfide bridge between two Cys residues at the N-terminal region of the peptide, stabilizing the S-shaped fold.⁵⁰¹ This motif does not have any known role in the mechanism of action of the AMPs, but rather it only stabilizes the active peptide conformation.⁵⁰¹ The major difference between enterocin A and some pediocin-like bacteriocins is the presence of an additional five residues preceding the YGNGV motif at its N-terminal region.⁵⁰³ These residues contain the ATCUN motif, giving it the possibility of binding Cu²⁺ or Ni²⁺ ions. Enterocin A has a broad-spectrum activity against different species of *Lactobacillus*, *Listeria*, *Enterococcus*, and *Pediococcus*.⁵⁰³ It was hypothesized by

Casaus *et al.* that enterocin A and enterocin B, another bacteriocin isolated from *E. faecium*, have different targets that lead to their synergy. This is another example of an ATCUN-containing AMP that has synergy with another AMP.⁵¹⁶ It was predicted that a transmembrane helix is formed in enterocin A between residues 26 to 43, suggesting a pore formation mechanism as with other pediocin-like bacteriocins.⁵⁰³

Garviecins are class II^d bacteriocins that are produced by *Lactococcus garvieae*.^{305,504,517–519} *L. garvieae* is phenotypically related to *L. lactis*, which is a bacterial strain known for fermentation of dairy products. It is still not known whether *L. garvieae* can be used for the same purpose. The first garviecin that was detected and characterized from *L. garvieae* isolated from raw cow's milk is garviecin L1-5.⁵¹⁷ Its antimicrobial activity was measured from its crude extract using the agar-well diffusion method, and it was found to be active against *L. monocytogenes* and three strains of *Clostridium*.⁵¹⁷ To our knowledge, the sequence of this garviecin has not yet been identified and it has not yet been described at a molecular level.⁵⁰⁵ Another strain of *L. garvieae* was isolated from mallard ducks (*Anas platyrhynchos*) and produces a circular garvicin, garvicin ML (GarML).⁵⁰⁴ It has high resistance to pH and temperature changes, and is suggested to have a tight conformation, making sites for digestion inaccessible and making it more resistant to proteolytic degradation.⁵⁰⁴ Similarly, lactocyclin Q, a cyclic bacteriocin isolated from the *Lactococcus* spp. strain Q12,⁵²⁰ has high resistance to pH, temperature, and proteolytic degradation, suggesting that cyclization of bacteriocins increases their stability. However, it does not have any activity against Gram-negative bacteria, unlike lactocyclin Q, suggesting that they have different mechanisms of action.⁵²⁰

Garviecin Q (GarQ) contains the ATCUN motif and belongs to the class II bacteriocins.³⁰⁵ It was isolated from the culture supernatant of *L. garvieae* BCC 43578.³⁰⁵ GarQ has antimicrobial

activity against different species of *Listeria*, including *L. monocytogenes* and *Listeria ivanovii*, *Enterococcus* spp., and *P. pentosaceus*.^{305,519} These bacterial strains can cause listeriosis, gastroenteritis, and bacteremia.⁵¹⁹ It has also shown no cytotoxicity against human liver hepatocarcinoma and human colon adenocarcinoma cell lines.³⁰⁵ Bacterial resistance against GarQ was seen in bacterial strains that have non-functioning mannose phosphotransferase system, similar to the general resistance mechanism of pediocin- and leucocin-resistant bacteria described earlier.^{515,519} Despite the presence of the ATCUN motif, the ability of this motif to bind metal ions was never studied, making it a potential area of research.

Different strains of *L. garvieae* have been identified to be the causative agents of lactococcosis, a disease that causes hyperacute and hemorrhagic septicemia in fishes.⁵²¹⁻⁵²³ In Iran, 38 strains of *L. garvieae* were isolated from rainbow trout grown via aquaculture.⁵²² The microbiota in rainbow trout is an interesting example of how closely related species of *L. garvieae* can produce bacteriocins that inhibit the growth of *L. garvieae*. Strains of *Lactobacillus*, *Lactococcus*, and *Leuconostoc* were identified as antagonistic strains of the pathogenic bacteria.⁵²⁴ This is due to proteinaceous compounds released extracellularly by these strains.⁵²⁴ However, they were not able to identify and characterize the specific bacteriocins that caused the antagonistic effect.⁵²⁴ Interestingly, a garviecin isolated from human patients, GarA, has antimicrobial activity against the fish pathogen *L. garvieae* 8831, isolated from diseased rainbow trout in Spain.^{505,523} Its mature peptide sequence is not homologous to GarQ, but its leader peptide sequence is nearly identical to that of GarQ.⁵⁰⁵ This explains the high level of similarity between the proteins involved in the secretion and processing of the two bacteriocins.⁵⁰⁵ Currently, it is known to be active only against other *L. garvieae* strains, unlike garviecin L1-5, GarML, and GarQ, which have broad-spectrum antimicrobial activity.^{305,504,505,517} It acts by inhibiting cell wall biosynthesis, particularly

by inhibiting septum formation, as its bactericidal effect is greater during the exponential growth of *L. garvieae* 8831.⁵⁰⁵ However, it is not yet known whether it inhibits septum formation by interacting with lipid II, as described earlier for the lantibiotics.⁵⁰⁵

AMPs isolated from *Lactobacillus plantarum* have also gained interest, as it belongs to a group of microorganisms that is classified as generally recognized as safe.⁵²⁵ It is used to ferment dairy products, meat products, vegetables, and beverages.⁵²⁵ A number of AMPs known as plantaricins were extracted from various strains of *L. plantarum* isolated from fermented products.^{306,526–529} An interesting ATCUN-containing plantaricin, plantaricin 163, was isolated from *L. plantarum* 163, traditionally used in China to ferment vegetables.³⁰⁶ Using the agar well diffusion assay, plantaricin 163 was found to be strongly active against the Gram-positive bacteria *S. aureus*, *Bacillus cereus*, *Bacillus pumilus*, *L. monocytogenes*, and the Gram-negative bacteria *E. coli*, and *Pseudomonas fluorescens*.³⁰⁶ Plantaricin F (PlnF) is another ATCUN-containing plantaricin, and has antimicrobial activity against different Gram-positive strains of *Pediococcus* and *Lactobacillus*.³⁰⁷ However, unlike plantaricin 163, PlnF is a member of the class IIb bacteriocins, also known as the two-peptide bacteriocins, and requires interaction with plantaricin E to act as one unit and become active.^{307,501,530} The majority of the secondary structure of both peptides are α -helical, with PlnF having a Pro kink in its central region.⁵³⁰ Upon binding of the two peptides, the polar residues are buried, allowing the two-peptides to cross the lipid bilayer in a perpendicular fashion.⁵³⁰ Both peptides contain the GXXXG motif, which is hypothesized to be responsible for the helix-helix interactions, as demonstrated in membrane proteins.^{530,531} Strikingly, both plantaricin 163 and PlnF have the same VFH sequence in the N-terminus as clavanin C (*vide supra*).

While there is no strong evidence of metal binding to bacteriocins, particularly those that contain the ATCUN motif, a recent study shows that the presence of Ca^{2+} and Mg^{2+} ions in the culture medium induce antimicrobial activities in some LA bacterial strains.⁵³² There were a variety of suggestions made on how these ions were able to induce activity. Proteolytic activity in some LA bacterial strains is increased in the presence of Ca^{2+} , suggesting that there may be antimicrobial components produced after proteolysis,⁵³² some of which may be AMPs. However, the study did not mention the possibility that metal ions binding to the bacteriocins produced by these LA bacterial strains could potentially explain the antimicrobial activity. This raises the question of what other roles do Ca^{2+} and Mg^{2+} ions play in the enhancement of antimicrobial activity of these LA bacterial strains. Is it possible that once bacteriocins are extracellularly released, they can bind these ions and direct the bacteriocins to a different mechanism of action that is more suitable for killing? Is the presence of the ATCUN motif in some of the class II bacteriocins beneficial for the antimicrobial activity? This interesting area of research should be explored further.

4. Designing ATCUN-AMPs

The ATCUN motif has been exploited in the field of catalytic metallodrugs for at least two decades thanks to the pioneering work by Cowan and co-workers.^{197,212,213,323,533,534} These ATCUN-containing metallodrugs can selectively cleave DNA, RNA, or proteins, depending on the molecules attached to the ATCUN motif. Likewise, adding an ATCUN motif to a peptide sequence turns the latter into a catalytic metallodrug.^{146,214,324,325,535} Studies show that the peptide sequence acts as a guidance system to the ATCUN- Cu^{2+} payload. If the guidance peptide sequence has high affinity for the bacterial cellular membrane, then, the synthetic ATCUN-AMP still has high affinity for the lipid membrane and acts by forming pores, oxidizing lipids or a combination

of both mechanisms.^{214,324,325,535} Some examples of these peptides in natural systems are p1 and ixosin. Sequences belonging to intracellular peptides, *i.e.* peptides that cross the membrane and reach the cytosolic space, can also benefit from the addition of an ATCUN motif, as the resulting peptide can find an intracellular target.^{212,214} For example, the peptides VIH RAGLQFPVGRVHRLRK-NH₂ and RTH RAGLQFPVGRVHRLRK-NH₂, formed by the attachment of the ATCUN sequences VIH and RTH to the intracellular targeting short-buforin II (sh-buferin),⁵³⁶ have been shown to damage *E. coli* DNA in *in cellulo* assays.¹⁹³ The TUNEL assay was used for this purpose. Measuring the TUNEL fluorescence of 100,000 cells, it was shown that these two peptides were capable of cleaving DNA strand breaks in *E. coli* at their MIC. Moreover, the ATCUN-sh-buferin conjugates exhibited greater TUNEL fluorescence compared to sh-buferin alone, and the fluorescence correlated with the observed trend in MIC. This study also showed that ATCUN-peptides formed using D-amino acids (D-ATCUN-peptides) were more active than their L counterparts. The D-ATCUN-D-sh-buferin analogs also had a higher nuclease activity *in cellulo*,¹⁹³ consistent with the higher ROS production observed for ATCUN motifs formed by D-amino acids.²¹¹ An important example of an intracellular peptide bound to an ATCUN motif is that of WRWYCR, a peptide known to enter cells and bind to Holliday Junctions. Upon conjugation to the GGH ATCUN motif the peptide was able to produce ROS and cleave DNA and RNA.²¹² The *in cellulo* nuclease activity of this ATCUN-AMP has not yet been reported.

ATCUN-AMPs are compatible with lipidation, an important posttranslational modification and a common conjugation strategy to deliver drugs to cellular membranes. *N*-palmitoylation of short cationic di- and tri-peptides have been shown to be active against *S. aureus* *in vitro* and against *C. albicans* in mouse models.⁵³⁷ The S-palmitoylation of cationic intrinsically disordered antimicrobial peptides (CIDAMPs), peptides containing a high percentage of disorder-promoting

amino acids and a low percentage of order-promoting amino acids, revealed that potent antimicrobial agents result from this strategy (Figure 28).⁵³⁸ TEM images of cells treated with one of the palmitoylated peptides in this study, although not one containing the ATCUN motif, showed extensive membrane and ribosome damage, hinting at possible targets for *S*-palmitoylated peptides. Although it was suggested that the improved antimicrobial activity could be related to the presence of the ATCUN motif, the specific role of metal binding remains to be determined. Based on these results, it was hypothesized that palmitoylated CIDAMPs, depending on the assay conditions, use two plausible mechanisms: (1) an energy-dependent transportation, and (2) a lipid-directed pathway that involves strong interaction with phospholipid membranes.

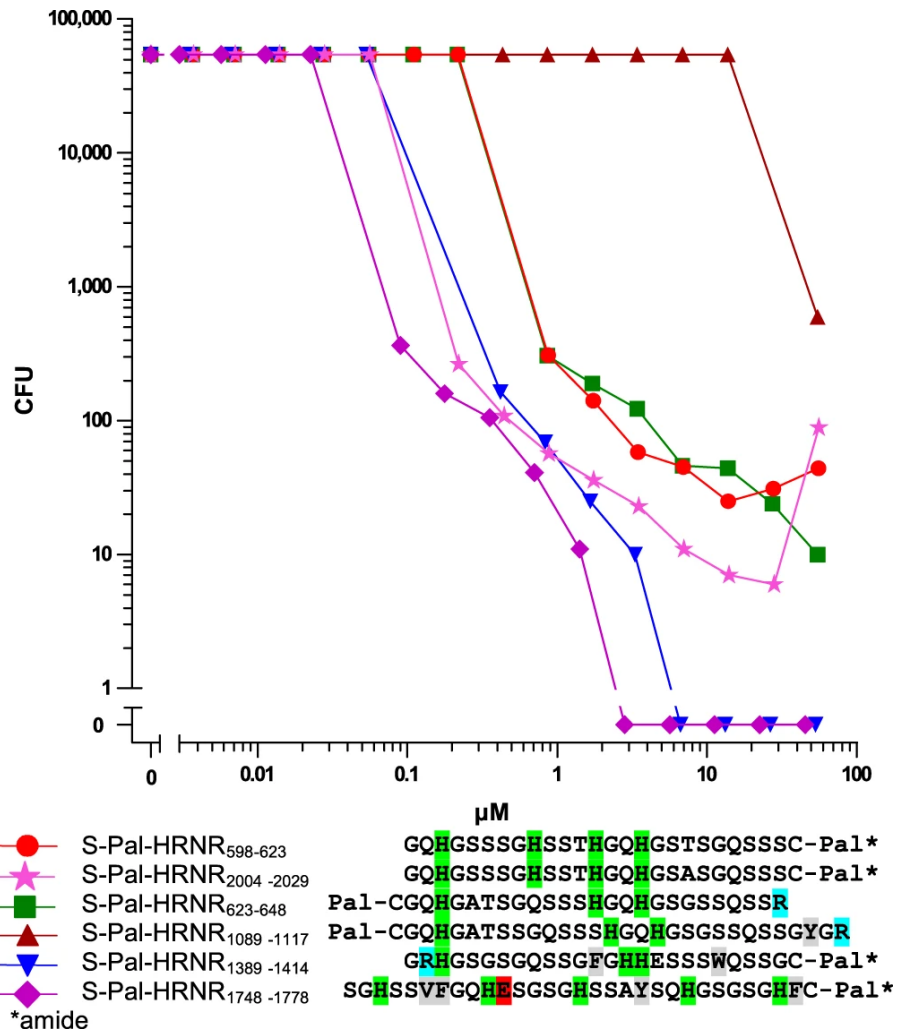


Figure 28. Susceptibility of *S. aureus* (ATCC 6538) towards selected S-palmitoylated peptides. Sensitivity of *S. a.* ATCC 6538 towards peptides was tested in 10 mM NaP/pH 5.5/0.25% glucose. Residues cationic at pH 7, cationic only at acidic pH, anionic at pH 7 and hydrophobic are highlighted in blue, green, magenta and grey. Pal-C and S-Pal means an S-palmitoyl-Cys-residue. All data shown are representatives ($n=2$). Figure was taken from reference 538 without modifications.

An *in silico* approach to select AMPs suitable for conjugation to the GGH and VIH ATCUN motifs was recently reported.¹⁴⁶ An initial selection of 14 cationic α -helical AMPs from the Antimicrobial Peptide Database⁵³⁹ was modified in the N-terminal region of the GGH VIH motifs. Two antimicrobial activity prediction modules were used to rank the resulting peptides based on their likelihood of having antimicrobial activity, and I-TASSER was used to determine

whether the peptides would favor an α -helical conformation in the presence of membranes. CM15 (WKKLFKKIGAVLKVL-NH₂) and citropin1.1 (GLFDVIKKVASVIGGL-NH₂) were the top-ranked peptides. Not only were the resulting ATCUN-AMPs active against ESKAPE pathogens, they were also effective at eradicating carbapenem-resistant strains of *E. coli* and *K. pneumoniae*. The activity was not the same against all bacteria tested and depended on the bacterial strain. Microbial biofilms are surface-associated communities of microorganisms surrounded by an extracellular polymeric matrix that are resistant to many antimicrobial agents including a number of AMPs.⁵⁴⁰ The ATCUN-AMPs selected in this study were active against biofilms either alone or in combination with antibiotics. For instance, CM15, GGH-CM15, and VIH-CM15 synergized with meropenem to inhibit *E. coli* (KpC+ 1812446) biofilm formation with FIC values of 0.33, 0.27, and 0.185, respectively.¹⁴⁶ Of particular interest is the observation that the ATCUN motifs influence the antibiofilm activity of the ATCUN-AMPs and that the activity depended on the bacterial strain producing the biofilm. The effect of the ATCUN motif is also reflected in the *in vivo* activity of ATCUN-AMPs. While CM15 and GGH-CM15 show high toxicity in mice with a systemic *E. coli* KpC+ 1812446 infection, VIH-CM15 decreased the toxicity of CM15 and protected 40% of the animals at the sixth and seventh day of infection. Overall, this study highlights the fact that attaching an ATCUN motif to a peptide does not always result in a more active AMP, as the result depends on the sequence, the pathogen, and whether the pathogen is its planktonic state or forming a biofilm. It must be mentioned, that AMPs, just like other classes of antimicrobial agents, have an efficacy that depends on the biological matrices in which they are tested.⁵⁴¹

Nanoparticles are materials in the nanometer scale range that has a number of uses that range from catalysis to drug delivery. Moreover, nanoparticles may find applications in treating

bacterial infections, from biofilms to systemic chronic infections and bacterial sensors.⁵⁴² A proof-of-concept study has shown that the click reaction can be used to attach the ATCUN peptide VIHGW to a silver nanoparticle (AgNP) containing thiol-polyethylene glycol-azide chains.⁵⁴³ The ATCUN nanocomposite was more active against planktonic *E. coli* than the AgPEG parent nanoparticle or the ATCUN sequence alone, demonstrating that AgNP-ATCUN combinations have the potential for practical applications.

5. Outlook and Future Prospects

In recent decades, AMPs have received a great deal of attention and many of them have entered clinical trials. However, despite the discovery of AMPs with promising *in vitro* and *in vivo* activities, few have been approved for use in the clinic. We speculate that the discovery of novel mechanisms of action associated with the interaction between AMPs and metal ions represents an interesting strategy to develop new antimicrobials designed to control pathogens. Initial focus for application of metalloAMPs could have ectopic applications (where bacitracin is successfully used already^{544,545}), target intracellular pathogens that hide in macrophages where there are elevated metal levels, treat urinary tract infections (where Cu²⁺ concentrations are already high¹⁰⁸), and sanitize medical devices (since a few metalloAMPs have been shown to successfully eradicate biofilms).¹¹⁹ Another application is to take advantage of disease conditions that have elevated metal concentration (Wilson's disease, Alzheimer's Disease, cystic fibrosis (CF), and *M. tuberculosis* infections), where metalloAMPs can readily bind metal ions, that are typically tightly regulated due to redox properties. A recent example from our lab used the metalloAMP Gad-1 to combat CF related *P. aeruginosa* biofilms.⁵⁴⁶ Gad-1 in the presence of Cu²⁺ was able to cleave extracellular DNA *in vitro* and *in vivo* in mature *P. aeruginosa* biofilms under CF lung conditions,

where there is excess exogenous DNA that has been shown to limit the potency of AMPs.^{546,547} Gad-1 was able to efficiently clear mature *P. aeruginosa* biofilms even in the presence of DNA, showing that the strong, metal-mediated nuclease activity confers an advantage in a biofilm environment.⁵⁴⁶ In addition to eradicating biofilms, Gad-1 in the presence of Cu²⁺ was able to limit the adhesion of new biofilms, which not only has utility to limit biofilm spread but may have potential as a coating on medical devices that can readily grow biofilms.⁵⁴⁶ It is likely that these metalloAMPs will need to be optimized to become therapeutically useful. Although metal binding makes metalloAMPs more resistant to proteolytic degradation,⁵⁴⁸ further modifications will be needed. Cyclization could lead to increased bioavailability and slower degradation within cells. Kritzer and coworkers have demonstrated that cyclization of the ATCUN motif, as well as the simultaneous introduction of non-natural amino acids, is possible while keeping its ROS formation activity.⁵⁴⁹

Concomitantly, it is important to obtain a better understanding of the mechanism of action for ATCUN-AMPs. We have catalogued almost 200 AMPs that can potentially use metal ions to potentiate their activity. Since the AMP database contains less than 4000 AMPs, it is clear that the metalloAMPs are highly represented. Computational strategies could also be utilized and improved to gain information about their mechanisms. The importance of having force fields parametrized specifically for metals involved in metalloAMPs (especially Cu²⁺ and Zn²⁺) are emphasized by this growing interest in metalloAMPs. Transition metal ions are best modeled when parametrized with quantum mechanical methods. However, there is a large number of methods to choose from, making it difficult to really determine which is the best method. Simple unpolarized force field models such as CHARMM and AMBER have parameters for transition metal ions, but care must be exercised when interpreting simulations that use these force fields. The electronic

properties of transition metal ions depend on their chemical environment. Thus, there are efforts to develop fluctuating charge models for transition metal ions such as OPLS-AA-FQ,⁵⁵⁰ CHARMM-FQ,^{551,552} and ABEEM/MM⁵⁵³ models. Another approach is by doing QM/MM, which models the transition metal ion and the atoms that are in its local environment, defined by a certain area, using a quantum mechanical model, while modeling the remaining bulk of the system using molecular mechanics. This approach aims to balance the electronic property fluctuations of the transition metal ion and the atoms around it, while keeping the feasibility of running the simulations. With these approaches that can better capture the properties of transition metal ions and their binding sites on peptides and proteins, we hope that simulation studies on metalloAMPs will continue to provide important mechanistic insights on an atomic level. Machine learning methods can also be explored to design synthetic metalloAMPs with better efficacy. Besides the realm of applications, there is also room for some basic inorganic chemistry research. Very little is known about the active species of Cu-ATCUN that leads to the production of ROS.³²² The elucidation of these intermediates is of utmost relevance, as ROS production activity of ATCUN-Cu²⁺ is sequence dependent. Moreover, it might be possible to tune the redox properties of Cu²⁺–ATCUN sequences by changing the amino acids after the His residue as postulated recently by Faller and coworkers.⁵⁵⁴

AUTHOR INFORMATION

Corresponding Author

Email: alfredo.angeles-boza@uconn.edu

Email: jonathan.klassen@uconn.edu

Biographies

Jasmin Portelinha earned two bachelor's degrees from University of New Haven in Biology and Chemistry, along with a Master's degree and PhD in Chemistry from the University of Connecticut. Her doctoral work focused on studying the advantages of metal-binding antimicrobial peptides and peptoids for their use as potential therapeutic agents. She is currently working at PhagePro Inc developing a prophylactic to treat *Vibrio cholerae* infections.

Searle S. Duay obtained his Bachelor of Science in Chemistry from University of the Philippines, Diliman, Quezon City. He worked as an instructor for one year in the same university before going to University of Connecticut for his PhD. He finished his doctorate degree in August 2020 under the tutelage of Prof. Alfredo Angeles-Boza and Prof. Eric May, with his work focusing on mechanistic studies of interaction between the antimicrobial peptide Clavanin A and different models of lipid bilayer. He is currently in the Philippines to begin his academic career in Adamson University.

Seung I. Yu is an undergraduate student at the University of Connecticut working toward her Bachelor of Science degree in Molecular and Cellular Biology. She studies in Dr. Jonathan Klassen's lab, with her current project characterizing abaecin antimicrobial peptides in fungus-growing ants.

Kara Heilemann is currently a Master's student at the University of Connecticut in Dr. Janine Caira's lab. She earned two bachelor's degrees from the University of Connecticut in Pathobiology and Nutritional Sciences. During this time, she worked in the Angeles-Boza lab on antimicrobial peptides. Her Master's work focuses on resolving phylogenetic relationships within the cestode order *Tetraphyllidea*.

M. Daben J. Libardo was born in Manila, Philippines in 1990. He obtained his PhD in Chemistry in 2017 at the University of Connecticut under the supervision of Dr. Alfredo Angeles-Boza studying mechanisms of action and synergy between copper and copper-binding host-defense peptides. He later joined the group of Dr. Clifton E. Barry III in the Tuberculosis Research Section of the National Institute of Allergy and Infectious Disease at the National Institutes of Health to study pathogenic mechanisms in *Mycobacterium tuberculosis*. In 2019, he joined Merck Research Laboratories as a Senior Scientist in Infectious Diseases & Vaccines working to develop small molecule therapeutics for Gram-negative pathogens.

Samuel A. Juliano attended the University of Scranton from 2009 to 2013 where he obtained his Bachelor of Science in Biochemistry and Philosophy. He later obtained his PhD from the University of Connecticut while studying the effect of zinc on the activity of tunicate antimicrobial peptides under the supervision of Dr. Alfredo Angeles-Boza. He has worked as an adjunct professor of chemistry and biochemistry at several institutions in Connecticut including Sacred Heart University, the University of Hartford, and the University of Connecticut. Samuel currently works in medical education, promoting education on COVID-19 and influenza vaccines as well as biological therapies for atopic conditions.

Jonathan Klassen is an Associate Professor at the University of Connecticut in the Department of Molecular and Cell Biology, which he joined in 2013. He received his B.Sc. (Hon.) in Biochemistry from the University of Victoria, and a PhD in Microbiology and Biotechnology from the University of Alberta, studying the chemical diversity and evolution of carotenoid pigments in Antarctic bacteria under Dr. Julia Foght. After a year studying the microbiology of oil sands tailings as a postdoctoral researcher at the University of Alberta, he was awarded a National Science and Engineering Research Council of Canada Postdoctoral Fellowship to study the

ecology and evolution of antibiotics at the University of Wisconsin-Madison under Dr. Cameron Currie, research that especially focused on the antibiotics produced by *Pseudonocardia* symbionts of fungus-growing ants. His current research at the University of Connecticut studies various aspects of microbiome function, particularly the natural roles and evolution of secondary metabolites and primarily using fungus-growing ants as a model experimental system.

Alfredo M. Angeles-Boza obtained his B.S. Degree in Chemistry from the Pontificia Universidad Catolica del Peru, Peru. After a short research stint at Texas Christian University under the supervision of Prof. Tracy Hanna, he pursued his Ph.D. studies in Inorganic Chemistry at Texas A&M University (TAMU) (2007), working under the direction of Kim R. Dunbar. After two postdoctoral stints at TAMU (with Prof. Jean-Philippe Pellois) and Johns Hopkins University (with Prof. Justine Roth), he joined the faculty at UConn in 2012 as an Assistant Professor. He was promoted to Associate Professor of Chemistry in 2018. His current research focuses on elucidating the role of metal ions in the antimicrobial activity of host defense peptides and the use of heavy atom kinetic isotope effects to study mechanisms of reactions in small molecule activation.

Supporting Information

Supporting information includes: Figure S1, Sequence similarity network showing the homology relationships between ATCUN-containing AMPs.; Figure S2, The largest cluster, Cluster 1, displaying the sequence of hepcidin AMPs from a multitude of organisms.; Figure S3, Cluster 2 is made up of His-rich piscidin AMPs with a highly conserved N-terminus region.; Figure S4, Cluster 3 showing the conserved **DSHH** ATCUN motif in histatin AMPs.; Figure S5, Beta-defensin AMPs

(Cluster 4).; Figure S6, Cluster 5 shows the highly conserved N- and C-terminus of a group of AMPs derived from ants.; Figure S7, Myticin family of AMPs (Cluster 6).; Figure S8, AMPs from human Furin-prodomain (Cluster 7).; Figure S9, Wasp (*Nasonia vitripennis*) AMPs (Cluster 8).; Figure S10, Cluster 9 is made up of amphibian AMPs.; Figure S11, Cluster 10 that displays the conserved KVHGSL N-terminus region of 40S ribosomal proteins.; Figure S12, LEAP-2 AMPs make up Cluster 11.; Figure S13, α -defensin AMPs (Cluster 12).; Figure S14, Defensins from the Arthropoda phyla make up Cluster 13.; Figure S15, Myticusin AMPs from the Molluska phylum make up Cluster 14.; Figure S16, Beta-defensin AMPs with a highly conserved N-terminus and ATCUN sequence (Cluster 15).; Figure S17, His-rich AMPs from *Lucilia sericata* (Cluster 16).; Figure S18, Cluster 17 is a small cluster that consists of two amphibian peptides from *Pseudophryne giintheri*.; Figure S19, Cluster 18 is made up of AMPs from *Gallus gallus* or wild chicken.; Figure S20, Cluster 19 consists of two Attacin AMPs from *Hyalophora cecropia*.; Figure S21, AMPs from *Solenopsis invicta* (Cluster 20).; Figure S22, Cluster 21 displays the cystatin AMPs from goats or *Capra hircus*. (PDF)

Notes

The authors declare no competing financial interests.

ACKNOWLEDGEMENTS

J.L.K. and A.M.A.-B. acknowledge funding from the UConn Microbiome Research Seed Grant program. A.M.A.-B. also thanks the National Science Foundation (grant MCB-1715494) for its support.

References

(1) Fleming, A. *Penicillin*; 1945. <https://doi.org/10.1016/B978-0-12-386454-3.00764-8>.

(2) Barlow, G. Clinical Challenges in Antimicrobial Resistance. *Nat. Microbiol.* **2018**, *3*, 258–260. <https://doi.org/10.1038/s41564-018-0121-y>.

(3) O’Neil, J. *Tackling Drug-Resistant Infections Globally: Final Report and Recommendations*; 2016. <https://doi.org/10.4103/2045-080x.186181>.

(4) Ventola, C. L. The Antibiotic Resistance Crisis: Part 1: Causes and Threats. *P T A peer-reviewed J. Formul. Manag.* **2015**, *40* (4), 277–283. <https://doi.org/Article>.

(5) O’Neill, J. Antimicrobial Resistance: Tackling a Crisis for the Health and Wealth of Nations. *Rev. Antimicrob. Resist.* **2016**, 1–16.

(6) Fox, J. L. Antimicrobial Peptides Stage a Comeback. *Nat. Biotechnol.* **2013**, *31*, 379–382. <https://doi.org/10.1038/nbt.2572>.

(7) Tonk, M.; Vilcinskas, A. The Medical Potential of Antimicrobial Peptides from Insects. *Curr. Top. Med. Chem.* **2017**, *17* (5), 554–575. <https://doi.org/10.2174/1568026616666160713123654>.

(8) Hancock, R. E. W.; Lehrer, R. Cationic Peptides: A New Source of Antibiotics. *Trends Biotechnol.* **1998**, *16* (2), 82–88. [https://doi.org/10.1016/S0167-7799\(97\)01156-6](https://doi.org/10.1016/S0167-7799(97)01156-6).

(9) Patil, A.; Hughes, A. L.; Zhang, G. Rapid Evolution and Diversification of Mammalian α -Defensins as Revealed by Comparative Analysis of Rodent and Primate Genes. *Physiol. Genomics* **2004**, *20* (1), 1–11. <https://doi.org/10.1152/physiolgenomics.00150.2004>.

(10) Tassanakajon, A.; Somboonwiwat, K.; Amparyup, P. Sequence Diversity and Evolution of Antimicrobial Peptides in Invertebrates. *Dev. Comp. Immunol.* **2015**, *48* (2), 324–341.

<https://doi.org/10.1016/j.dci.2014.05.020>.

(11) Faye, I.; Lindberg, B. G. Towards a Paradigm Shift in Innate Immunity—Seminal Work by Hans G. Boman and Co-Workers. *Philos. Trans. R. Soc. B Biol. Sci.* **2016**, *371* (1695), 1–8. <https://doi.org/10.1098/rstb.2015.0303>.

(12) Hultmark, D.; Steiner, H.; Rasmussen, T.; Boman, H. G. Insect Immunity. Purification and Properties of Three Inducible Bactericidal Proteins from Hemolymph of Immunized Pupae of *Hyalophora Cecropia*. *Eur. J. Biochem.* **1980**, *106* (1), 7–16. <https://doi.org/10.1111/j.1432-1033.1980.tb05991.x>.

(13) Steiner, H.; Hultmark, D.; Engström, Å.; Bennich, H.; Boman, H. G. Sequence and Specificity of Two Antibacterial Proteins Involved in Insect Immunity. *Nature* **1981**, *292*, 246–248. <https://doi.org/10.1038/292246a0>.

(14) Selsted, M. E.; Brown, D. M.; DeLange, R. J.; Lehrer, R. I. Primary Structures of MCP-1 and MCP-2, Natural Peptide Antibiotics of Rabbit Lung Macrophages. *J. Biol. Chem.* **1983**, *258* (23), 14485–14489.

(15) Selsted, M. E.; Szklarek, D.; Lehrer, R. I. Purification and Antibacterial Activity of Antimicrobial Peptides of Rabbit Granulocytes. *Infect. Immun.* **1984**, *45* (1), 150–154. [https://doi.org/Selsted ME, Szklarek D, Lehrer RI. Purification and antibacterial activity of antimicrobial peptides of rabbit granulocytes. Infect Immun. 1984;45\(1\):150-154. doi:10.1128/IAI.45.1.150-154.1984](https://doi.org/Selsted ME, Szklarek D, Lehrer RI. Purification and antibacterial activity of antimicrobial peptides of rabbit granulocytes. Infect Immun. 1984;45(1):150-154. doi:10.1128/IAI.45.1.150-154.1984).

(16) Selsted, M. E.; Harwig, S. S. L.; Ganz, T.; Schilling, J. W.; Lehrer, R. I. Primary Structures of Three Human Neutrophil Defensins. *J. Clin. Invest.* **1985**, *76* (4), 1436–1439. <https://doi.org/10.1172/JCI112121>.

(17) Zasloff, M. Magainins, a Class of Antimicrobial Peptides from *Xenopus* Skin: Isolation, Characterization of Two Active Forms, and Partial CDNA Sequence of a Precursor. *Proc Natl Acad Sci USA* **1987**, *84*, 5459–5453. <https://doi.org/10.1097/00043764-198806000-00004>.

(18) Ge, Y.; MacDonald, D. L.; Holroyd, K. J.; Thornsberry, C.; Wexler, H.; Zasloff, M. In Vitro Antibacterial Properties of Pexiganan, an Analog of Magainin. *Antimicrob. Agents Chemother.* **1999**, *43* (4), 782–788. <https://doi.org/10.1128/aac.43.4.782>.

(19) Matsuzaki, K.; Murase, O.; Fujii, N.; Miyajima, K. An Antimicrobial Peptide, Magainin 2, Induced Rapid Flip-Flop of Phospholipids Coupled with Pore Formation and Peptide Translocation. *Biochemistry* **1996**, *35* (35), 11361–11368. <https://doi.org/10.1021/bi960016v>.

(20) Tamba, Y.; Ariyama, H.; Levadny, V.; Yamazaki, M. Kinetic Pathway of Antimicrobial Peptide Magainin 2-Induced Pore Formation in Lipid Membranes. *J. Phys. Chem. B* **2010**, *114* (37), 12018–12026. <https://doi.org/10.1021/jp104527y>.

(21) Hasan, M.; Karal, M. A. S.; Levadnyy, V.; Yamazaki, M. Mechanism of Initial Stage of Pore Formation Induced by Antimicrobial Peptide Magainin 2. *Langmuir* **2018**, *34* (10), 3349–3362. <https://doi.org/10.1021/acs.langmuir.7b04219>.

(22) Tamba, Y.; Yamazaki, M. Single Giant Unilamellar Vesicle Method Reveals Effect of Antimicrobial Peptide Magainin 2 on Membrane Permeability. *Biochemistry* **2005**, *44* (48), 15823–15833. <https://doi.org/10.1021/bi051684w>.

(23) Matsuzaki, K.; Sugishita, K. I.; Miyajima, K. Interactions of an Antimicrobial Peptide, Magainin 2, with Lipopolysaccharide-Containing Liposomes as a Model for Outer

Membranes of Gram-Negative Bacteria. *FEBS Lett.* **1999**, *449* (2–3), 221–224.
[https://doi.org/10.1016/S0014-5793\(99\)00443-3](https://doi.org/10.1016/S0014-5793(99)00443-3).

(24) Bechinger, B.; Zasloff, M.; Opella, S. J. Structure and Orientation of the Antibiotic Peptide Magainin in Membranes by Solid-state Nuclear Magnetic Resonance Spectroscopy. *Protein Sci.* **1993**, *2* (12), 2077–2084.
<https://doi.org/10.1002/pro.5560021208>.

(25) Nakamura, T.; Furunaka, H.; Miyata, T.; Tokunaga, F.; Muta, T.; Iwanaga, S.; Niwa, M.; Takao, T.; Shimonishi, Y. Tachyplesin, a Class of Antimicrobial Peptide from the Hemocytes of the Horseshoe Crab (*Tachypleus Tridentatus*). Isolation and Chemical Structure. *J. Biol. Chem.* **1988**, *263* (32), 16709–16713.

(26) Kawano, K.; Yoneya, T.; Miyata, T.; Yoshikawa, K.; Tokunaga, F.; Terada, Y.; Iwanaga, S. Antimicrobial Tachyplesin I, Isolated from Hemocytes of the Horseshoe Crab (*Tachypleus Tridentatus*). NMR Determination of the Beta-Sheet Structure. *J. Biol. Chem.* **1990**, *265* (26), 15365–15367.

(27) Yu, D.; Sheng, Z.; Xu, X.; Li, J.; Yang, H.; Liu, Z.; Rees, H. H.; Lai, R. A Novel Antimicrobial Peptide from Salivary Glands of the Hard Tick, *Ixodes Sinensis*. *Peptides* **2006**, *27* (1), 31–35. <https://doi.org/10.1016/j.peptides.2005.06.020>.

(28) Juliano, S. A.; Pierce, S.; Demayo, J. A.; Balunas, M. J.; Angeles-Boza, A. M. Exploration of the Innate Immune System of *Styela Clava*: Zn²⁺ Binding Enhances the Antimicrobial Activity of the Tunicate Peptide Clavanin A. *Biochemistry* **2017**, *56* (10), 1403–1414.
<https://doi.org/10.1021/acs.biochem.6b01046>.

(29) Selsted, M. E.; Novotny, M. J.; Morris, W. L.; Tang, Y. Q.; Smith, W.; Cullor, J. S.

Indolicidin, a Novel Bactericidal Tridecapeptide Amide from Neutrophils. *J. Biol. Chem.* **1992**, *267* (7), 4292–4295.

(30) Yang, D.; Biragyn, A.; Kwak, L. W.; Oppenheim, J. J. Mammalian Defensins in Immunity: More than Just Microbicidal. *Trends Immunol.* **2002**, *23* (6), 291–296. [https://doi.org/10.1016/S1471-4906\(02\)02246-9](https://doi.org/10.1016/S1471-4906(02)02246-9).

(31) Cohn, M.; Townsend, J. Gramicidin S: Relationship of Cyclic Structure to Antibiotic Activity. *Nature* **1954**, *174*, 840–841. [https://doi.org/https://doi.org/10.1038/174840a0](https://doi.org/10.1038/174840a0).

(32) Fehlbaum, P.; Bulet, P.; Chernysh, S.; Briand, J.; Roueisl, J.; Letellierii, L.; Hetru, C.; Hoffmann, J. A. Structure-Activity Analysis of Thanatin, a 21-Residue Inducible Insect Defense Peptide with Sequence Homology to Frog Skin Antimicrobial Peptides. *Proc Natl Acad Sci USA* **1996**, *93* (3), 1221–1225. <https://doi.org/10.1073/pnas.93.3.1221>.

(33) Wu, M.; Hancock, R. E. W. Interaction of the Cyclic Antimicrobial Cationic Peptide Bactenecin with the Outer and Cytoplasmic Membrane. *J. Biol. Chem.* **1999**, *274* (1), 29–35. <https://doi.org/10.1074/jbc.274.1.29>.

(34) Sung, W. S.; Lee, J.; Lee, D. G. Fungicidal Effect of Piscidin on *Candida Albicans*: Pore Formation in Lipid Vesicles and Activity in Fungal Membranes. *Biol. Pharm. Bull.* **2008**, *31* (10), 1906–1910. <https://doi.org/10.1248/bpb.31.1906>.

(35) Wimley, W. C. Describing the Mechanism of Antimicrobial Peptide Action with the Interfacial Activity Model. *ACS Chem Biol* **2010**, *5* (10), 905–917. <https://doi.org/10.1021/cb1001558>.

(36) Shai, Y. Mode of Action of Membrane Active Antimicrobial Peptides. *Biopolymers* **2002**,

66 (4), 236–248. <https://doi.org/doi: 10.1002/bip.10260>.

(37) Brogden, K. A. Antimicrobial Peptides: Pore Formers or Metabolic Inhibitors in Bacteria? *Nat. Rev. Microbiol.* **2005**, 3, 238–250. <https://doi.org/10.1038/nrmicro1098>.

(38) Dempsey, C. E. The Actions of Melittin on Membranes. *BBA - Rev. Biomembr.* **1990**, 1031 (2), 143–161. [https://doi.org/10.1016/0304-4157\(90\)90006-X](https://doi.org/10.1016/0304-4157(90)90006-X).

(39) Rangarajan, N.; Bakshi, S.; Weisshaar, J. C. Localized Permeabilization of E. Coli Membranes by the Antimicrobial Peptide Cecropin A. *Biochemistry* **2013**, 52 (38), 6584–6594. <https://doi.org/10.1021/bi400785j>.

(40) Sochacki, K. A.; Barns, K. J.; Bucki, R.; Weisshaar, J. C. Real-Time Attack on Single Escherichia Coli Cells by the Human Antimicrobial Peptide LL-37. *Proc. Natl. Acad. Sci.* **2011**, 108 (16), E77–E81. <https://doi.org/10.1073/pnas.1101130108>.

(41) El Khoury, M.; Swain, J.; Sautrey, G.; Zimmermann, L.; Van Der Smissen, P.; Décout, J. L.; Mingeot-Leclercq, M. P. Targeting Bacterial Cardiolipin Enriched Microdomains: An Antimicrobial Strategy Used by Amphiphilic Aminoglycoside Antibiotics. *Sci. Rep.* **2017**, 7, 1–12. <https://doi.org/10.1038/s41598-017-10543-3>.

(42) Cruciani, R. A.; Barker, J. L.; Durell, S. R.; Raghunathan, G.; Guy, H. R.; Zasloff, M.; Stanley, E. F. Magainin 2, a Natural Antibiotic from Frog Skin, Forms Ion Channels in Lipid Bilayer Membranes. *Eur. J. Pharmacol. Mol. Pharmacol.* **1992**, 226 (4), 287–296. [https://doi.org/10.1016/0922-4106\(92\)90045-w](https://doi.org/10.1016/0922-4106(92)90045-w).

(43) Matsuzaki, K.; Sugishita, K. I.; Harada, M.; Fujii, N.; Miyajima, K. Interactions of an Antimicrobial Peptide, Magainin 2, with Outer and Inner Membranes of Gram-Negative

Bacteria. *Biochim. Biophys. Acta* **1997**, *1327* (1), 119–130. [https://doi.org/10.1016/s0005-2736\(97\)00051-5](https://doi.org/10.1016/s0005-2736(97)00051-5).

(44) Mihailescu, M.; Sorci, M.; Seckute, J.; Silin, V. I.; Hammer, J.; Perrin, B. S.; Hernandez, J. I.; Smajic, N.; Shrestha, A.; Bogardus, K. A.; Greenwood, A. I.; Fu, R.; Blazyk, J.; Pastor, R. W.; Nicholson, L. K.; Belfort, G.; Cotten, M. L. Structure and Function in Antimicrobial Piscidins: Histidine Position, Directionality of Membrane Insertion, and PH-Dependent Permeabilization. *J. Am. Chem. Soc.* **2019**, *141* (25), 9837–9853. <https://doi.org/10.1021/jacs.9b00440>.

(45) Comert, F.; Greenwood, A.; Maramba, J.; Acevedo, R.; Lucas, L.; Kulasinghe, T.; Cairns, L. S.; Wen, Y.; Fu, R.; Hammer, J.; Blazyk, J.; Sukharev, S.; Cotten, M. L.; Mihailescu, M. The Host-Defense Peptide Piscidin P1 Reorganizes Lipid Domains in Membranes and Decreases Activation Energies in Mechanosensitive Ion Channels. *J. Biol. Chem.* **2019**, *294* (49), 18557–18570. <https://doi.org/10.1074/jbc.RA119.010232>.

(46) Pouny, Y.; Rapaport, D.; Shai, Y.; Mor, A.; Nicolas, P. Interaction of Antimicrobial Dermaseptin and Its Fluorescently Labeled Analogs with Phospholipid Membranes. *Biochemistry* **1992**, *31* (49), 12416–12423. <https://doi.org/10.1021/bi00164a017>.

(47) Gazit, E.; Miller, I. R.; Biggin, P. C.; Sansom, M. S. P.; Shai, Y. Structure and Orientation of the Mammalian Antibacterial Peptide Cecropin P1 within Phospholipid Membranes. *J. Mol. Biol.* **1996**, *258* (5), 860–870. <https://doi.org/10.1006/jmbi.1996.0293>.

(48) Ambroggio, E. E.; Separovic, F.; Bowie, J. H.; Fidelio, G. D.; Bagatolli, L. A. Direct Visualization of Membrane Leakage Induced by the Antibiotic Peptides: Maculatin, Citropin, and Aurein. *Biophys. J.* **2005**, *89* (3), 1874–1881.

<https://doi.org/10.1529/biophysj.105.066589>.

(49) Gehman, J. D.; Luc, F.; Hall, K.; Lee, T. H.; Boland, M. P.; Pukala, T. L.; Bowie, J. H.; Aguilar, M. I.; Separovic, F. Effect of Antimicrobial Peptides from Australian Tree Frogs on Anionic Phospholipid Membranes. *Biochemistry* **2008**, *47* (33), 8557–8565. <https://doi.org/10.1021/bi800320v>.

(50) Fernandez, D. I.; Le Brun, A. P.; Whitwell, T. C.; Sani, M. A.; James, M.; Separovic, F. The Antimicrobial Peptide Aurein 1.2 Disrupts Model Membranes via the Carpet Mechanism. *Phys. Chem. Chem. Phys.* **2012**, *14* (45), 15739–15751. <https://doi.org/10.1039/c2cp43099a>.

(51) Park, C. B. C.; Kim, M. M. S.; Kim, S. C. S. A Novel Antimicrobial Peptide from Bufo Bufo Gargarizans. *Biochem. Biophys. Res. Commun.* **1996**, *218* (1), 408–413. <https://doi.org/10.1006/bbrc.1996.0071>.

(52) Falla, T. J.; Karunaratne, D. N.; Hancock, R. E. W. Mode of Action of the Antimicrobial Peptide Indolicidin Mode of Action of the Antimicrobial Peptide Indolicidin. *J Biol Chem* **1996**, *271* (32), 19298–19303. <https://doi.org/10.1074/jbc.271.32.19298>.

(53) Subbalakshmi, C.; Sitaran, N. Mechanism of Antimicrobial Action of Indolicidin. *FEMS Microbiol Lett* **1998**, *160* (1), 91–96. <https://doi.org/10.1111/j.1574-6968.1998.tb12896.x>.

(54) Yonezawa, A.; Kuwahara, J.; Fujii, N.; Sugiura, Y. Binding of Tachyplesin I to DNA Revealed by Footprinting Analysis: Significant Contribution of Secondary Structure to DNA Binding and Implication for Biological Action. *Biochemistry* **1992**, *31* (11), 2998–3004. <https://doi.org/10.1021/bi00126a022>.

(55) Castle, M.; Nazarian, A.; Yi, S. S.; Tempst, P. Lethal Effects of Apidaecin on Escherichia Coli Involve Sequential Molecular Interactions with Diverse Targets. *Lethal Effects of Apidaecin on Escherichia Coli Involve Sequential Molecular Interactions with Diverse Targets. J. Biol. Chem.* **1999**, *274* (46), 32555–32564.
<https://doi.org/10.1074/jbc.274.46.32555>.

(56) Boman, H. G.; Agerberth, B.; Boman, A. Mechanisms of Action on Escherichia Coli of Cecropin-P1 and PR-39, Two Antibacterial Peptides from Pig Intestine. *Infect. Immun.* **1993**, *61* (7), 2978–2984. <https://doi.org/10.1128/IAI.61.7.2978-2984.1993>.

(57) Juliano, S. A.; Serafim, L. F.; Duay, S. S.; Heredia Chavez, M.; Sharma, G.; Rooney, M.; Comert, F.; Pierce, S.; Radulescu, A.; Cotten, M. L.; Mihailescu, M.; May, E. R.; Greenwood, A. I.; Prabhakar, R.; Angeles-Boza, A. M. A Potent Host Defense Peptide Triggers DNA Damage and Is Active against Multidrug-Resistant Gram-Negative Pathogens. *ACS Infect. Dis.* **2020**, *6* (5), 1250–1263.
<https://doi.org/10.1021/acsinfecdis.0c00051>.

(58) Cruz, J.; Mihailescu, M.; Wiedman, G.; Herman, K.; Searson, P. C.; Wimley, W. C.; Hristova, K. A Membrane-Translocating Peptide Penetrates into Bilayers without Significant Bilayer Perturbations. *Biophys. J.* **2013**, *104* (11), 2419–2428.
<https://doi.org/10.1016/j.bpj.2013.04.043>.

(59) Wang, T. Y.; Sun, Y.; Muthukrishnan, N.; Erazo-Oliveras, A.; Najjar, K.; Pellois, J. P. Membrane Oxidation Enables the Cytosolic Entry of Polyarginine Cell-Penetrating Peptides. *J. Biol. Chem.* **2016**, *291* (15), 7902–7914.
<https://doi.org/10.1074/jbc.M115.711564>.

(60) Robison, A. D.; Sun, S.; Poyton, M. F.; Johnson, G. A.; Pellois, J. P.; Jungwirth, P.; Vazdar, M.; Cremer, P. S. Polyarginine Interacts More Strongly and Cooperatively than Polylysine with Phospholipid Bilayers. *J. Phys. Chem. B* **2016**, *120* (35), 9287–9296. <https://doi.org/10.1021/acs.jpcb.6b05604>.

(61) Mattiuzzo, M.; Bandiera, A.; Gennaro, R.; Benincasa, M.; Pacor, S.; Antcheva, N.; Scocchi, M. Role of the Escherichia Coli SbmA in the Antimicrobial Activity of Proline-Rich Peptides. *Mol. Microbiol.* **2007**, *66* (1), 151–163. <https://doi.org/10.1111/j.1365-2958.2007.05903.x>.

(62) Otvos, L.; O, I.; Rogers, M. E.; Consolvo, P. J.; Condie, B. A.; Lovas, S.; Bulet, P.; Blaszczyk-Thurin, M. Interaction between Heat Shock Proteins and Antimicrobial Peptides. *Biochemistry* **2000**, *39* (46), 14150–14159. <https://doi.org/10.1021/bi0012843>.

(63) Casteels, P.; Tempst, P. Apidaecin-Type Peptide Antibiotics Function through a Nonporeforming Mechanism Involving Stereospecificity. *Biochem. Biophys. Res. Commun.* **1994**, *199* (1), 339–345. <https://doi.org/10.1006/bbrc.1994.1234>.

(64) Park, C. B.; Kim, H. S.; Kim, S. C. Mechanism of Action of the Antimicrobial Peptide Buforin II: Buforin II Kills Microorganisms by Penetrating the Cell Membrane and Inhibiting Cellular Functions. *Biochem. Biophys. Res. Commun.* **1998**, *244* (1), 253–257. <https://doi.org/10.1006/bbrc.1998.8159>.

(65) Yi, G. S.; Park, C. B.; Kim, S. C.; Cheong, C. Solution Structure of an Antimicrobial Peptide Buforin II. *FEBS Lett.* **1996**, *398* (1), 87–90. [https://doi.org/10.1016/S0014-5793\(96\)01193-3](https://doi.org/10.1016/S0014-5793(96)01193-3).

(66) Hsu, C. H.; Chen, C.; Jou, M. L.; Lee, A. Y. L.; Lin, Y. C.; Yu, Y. P.; Huang, W. T.; Wu,

S. H. Structural and DNA-Binding Studies on the Bovine Antimicrobial Peptide, Indolicidin: Evidence for Multiple Conformations Involved in Binding to Membranes and DNA. *Nucleic Acids Res.* **2005**, *33* (13), 4053–4064. <https://doi.org/10.1093/nar/gki725>.

(67) Marchand, C.; Krajewski, K.; Lee, H. F.; Antony, S.; Johnson, A. A.; Amin, R.; Roller, P.; Kvaratskhelia, M.; Pommier, Y. Covalent Binding of the Natural Antimicrobial Peptide Indolicidin to DNA Abasic Sites. *Nucleic Acids Res.* **2006**, *34* (18), 5157–5165. <https://doi.org/10.1093/nar/gkl667>.

(68) Ohta, M.; Ito, H.; Masuda, K.; Tanaka, S.; Arakawa, Y.; Wacharotayankun, R.; Kato, N. Mechanisms of Antibacterial Action of Tachyplesins and Polyphemusins, a Group of Antimicrobial Peptides Isolated from Horseshoe Crab Hemocytes. *Antimicrob. Agents Chemother.* **1992**, *36* (7), 1460–1465. <https://doi.org/10.1128/AAC.36.7.1460>.

(69) Hong, J.; Guan, W.; Jin, G.; Zhao, H.; Jiang, X.; Dai, J. Mechanism of Tachyplesin I Injury to Bacterial Membranes and Intracellular Enzymes, Determined by Laser Confocal Scanning Microscopy and Flow Cytometry. *Microbiol. Res.* **2015**, *170*, 69–77. <https://doi.org/10.1016/j.micres.2014.08.012>.

(70) Groves, J. T.; Oison, J. R. Models of Zinc-Containing Proteases. Rapid Amide Hydrolysis by an Unusually Acidic Zn²⁺-OH₂ Complex. *Inorg. Chem.* **1985**, *24* (18), 2715–2717. <https://doi.org/10.1021/ic00212a001>.

(71) Chu, H.; Pazgier, M.; Jung, G.; Nuccio, S. P.; Castillo, P. A.; De Jong, M. F.; Winter, M. G.; Winter, S. E.; Wehkamp, J.; Shen, B.; Salzman, N. H.; Underwood, M. A.; Tsolis, R. M.; Young, G. M.; Lu, W.; Lehrer, R. I.; Bäumler, A. J.; Bevins, C. L. Human α -Defensin 6 Promotes Mucosal Innate Immunity through Self-Assembled Peptide Nanonets. *Science*

(80-.). **2012**, *337* (6093), 477–481. <https://doi.org/10.1126/science.1218831>.

(72) Loth, K.; Vergnes, A.; Barreto, C.; Voisin, S. N.; Meudal, H.; Silva, D.; Bressan, A.; Bulet, P.; Touqui, L.; Delmas, A. F.; Destoumieux-Garzón, D. The Ancestral N-Terminal Domain of Big Defensins Drives Bacterially Triggered Assembly into Antimicrobial Nanonets. *MBio* **2019**, *10* (5), 1–15. <https://doi.org/10.1128/mBio.01821-19>.

(73) Stambuk, F.; Ojeda, C.; Schmitt, P. Big Defensin ApBD1 from the Scallop *Argopecten Purpuratus* Is an Antimicrobial Peptide Which Entraps Bacteria through Nanonets Formation. *bioRxiv* **2020**. <https://doi.org/10.1101/2020.02.25.965327>.

(74) Hanson, M. A.; Dostálová, A.; Ceroni, C.; Poidevin, M.; Kondo, S.; Lemaitre, B. Synergy and Remarkable Specificity of Antimicrobial Peptides in Vivo Using a Systematic Knockout Approach. *Elife* **2019**, *8* (e44341), 1–24. <https://doi.org/10.7554/elife.44341>.

(75) Yu, G.; Baeder, D. Y.; Regoes, R. R.; Rolff, J. Combination Effects of Antimicrobial Peptides. *Antimicrob. Agents Chemother.* **2016**, *60* (3), 1717–1724. <https://doi.org/10.1128/AAC.02434-15>.

(76) Baeder, D. Y.; Yu, G.; Hozé, N.; Rolff, J.; Regoes, R. R. Antimicrobial Combinations: Bliss Independence and Loewe Additivity Derived from Mechanistic Multi-Hit Models. *Philos. Trans. R. Soc. B Biol. Sci.* **2016**, *371* (1695), 1–11. <https://doi.org/10.1098/rstb.2015.0294>.

(77) Yan, H.; Hancock, R. E. W. Synergistic Interactions between Mammalian Antimicrobial Defense Peptides. *Antimicrob. Agents Chemother.* **2001**, *45* (5), 1558–1560. <https://doi.org/10.1128/AAC.45.5.1558-1560.2001>.

(78) Westerhoff, H. V.; Zasloff, M.; Rosner, J. L.; Helder, R. W.; DE Waal, A.; Gomes, A. V.; Jongsma, A. P. M.; Riethorst, A.; Juretić, D. Functional Synergism of the Magainins PGLa and Magainin-2 in Escherichia Coli, Tumor Cells and Liposomes. *Eur. J. Biochem.* **1995**, 228 (2), 257–264. <https://doi.org/10.1111/j.1432-1033.1995.00257.x>.

(79) Da Silva, A.; Teschke, O. Effects of the Antimicrobial Peptide PGLa on Live Escherichia Coli. *Biochim. Biophys. Acta* **2003**, 1643 (1–3), 95–103. <https://doi.org/10.1016/j.bbamcr.2003.10.001>.

(80) Zasloff, M. Magainins, a Class of Antimicrobial Peptides from Xenopus Skin: Isolation, Characterization of Two Active Forms, and Partial CDNA Sequence of a Precursor. *Proc Natl Acad Sci USA* **1987**, 84, 5499–5453. <https://doi.org/10.1097/00043764-198806000-00004>.

(81) Matsuzaki, K.; Mitani, Y.; Akada, K. Y.; Murase, O.; Yoneyama, S.; Zasloff, M.; Miyajima, K. Mechanism of Synergism between Antimicrobial Peptides Magainin 2 and PGLa. *Biochemistry* **1998**, 37 (43), 15144–15153. <https://doi.org/10.1021/bi9811617>.

(82) Hara, T.; Mitani, Y.; Tanaka, K.; Uematsu, N.; Takakura, A.; Tachi, T.; Kodama, H.; Kondo, M.; Mori, H.; Otaka, A.; Nobutaka, F.; Matsuzaki, K. Heterodimer Formation between the Antimicrobial Peptides Magainin 2 and PGLa in Lipid Bilayers: A Cross-Linking Study. *Biochemistry* **2001**, 40 (41), 12395–12399. <https://doi.org/10.1021/bi011413v>.

(83) Strandberg, E.; Tremouilhac, P.; Wadhwani, P.; Ulrich, A. S. Synergistic Transmembrane Insertion of the Heterodimeric PGLa/Magainin 2 Complex Studied by Solid-State NMR. *Biochim. Biophys. Acta - Biomembr.* **2009**, 1788 (8), 1667–1679.

<https://doi.org/10.1016/j.bbamem.2008.12.018>.

(84) Lemaitre, B.; Reichhart, J. M.; Hoffmann, J. A. Drosophila Host Defense: Differential Induction of Antimicrobial Peptide Genes after Infection by Various Classes of Microorganisms. *Proc. Natl. Acad. Sci. U. S. A.* **1997**, *94* (26), 14614–14619. <https://doi.org/10.1073/pnas.94.26.14614>.

(85) Nuding, S.; Frasch, T.; Schaller, M.; Stange, E. F.; Zabel, L. T. Synergistic Effects of Antimicrobial Peptides and Antibiotics against Clostridium Difficile. *Antimicrob. Agents Chemother.* **2014**, *58* (10), 5719–5725. <https://doi.org/10.1128/AAC.02542-14>.

(86) Kampshoff, F.; Willcox, M. D. P.; Dutta, D. A Pilot Study of the Synergy between Two Antimicrobial Peptides and Two Common Antibiotics. *Antibiotics* **2019**, *8* (2). <https://doi.org/10.3390/antibiotics8020060>.

(87) Shang, D.; Liu, Y.; Jiang, F.; Ji, F.; Wang, H.; Han, X. Synergistic Antibacterial Activity of Designed Trp-Containing Antibacterial Peptides in Combination With Antibiotics Against Multidrug-Resistant Staphylococcus Epidermidis. *Front. Microbiol.* **2019**, *10*, 1–15. <https://doi.org/10.3389/fmicb.2019.02719>.

(88) Zygiel, E. M.; Nolan, E. M. Transition Metal Sequestration by the Host-Defense Protein Calprotectin. *Annu. Rev. Biochem.* **2018**, *87*, 621–643. <https://doi.org/10.1146/annurev-biochem-062917-012312>.

(89) Silva, F. D.; Rossi, D. C. P.; Martinez, L. R.; Frases, S.; Fonseca, F. L.; Campos, C. B. L.; Rodrigues, M. L.; Nosanchuk, J. D.; Daffre, S. Effects of Microplusin, a Copper-Chelating Antimicrobial Peptide, against Cryptococcus Neoformans. *FEMS Microbiol. Lett.* **2011**, *324* (1), 64–72. <https://doi.org/10.1111/j.1574-6968.2011.02386.x>.

(90) Silva, F. D.; Rezende, C. A.; Rossi, D. C. P.; Esteves, E.; Dyszy, F. H.; Schreier, S.; Gueiros-Filho, F.; Campos, C. B.; Pires, J. R.; Daffre, S. Structure and Mode of Action of Microplusin, a Copper II-Chelating Antimicrobial Peptide from the Cattle Tick *Rhipicephalus (Boophilus) Microplus*. *J. Biol. Chem.* **2009**, *284* (50), 34735–34746. <https://doi.org/10.1074/jbc.M109.016410>.

(91) Besold, A. N.; Gilston, B. A.; Radin, J. N.; Ramsoomair, C.; Culbertson, E. M.; Li, C. X.; Cormack, B. P.; Chazin, W. J.; Kehl-Fie, T. E.; Culotta, V. C. Role of Calprotectin in Withholding Zinc and Copper from *Candida Albicans*. *Infect. Immun.* **2018**, *86* (2), 1–16. <https://doi.org/10.1128/IAI.00779-17>.

(92) Clohessy, P. A.; Golden, B. E. Calprotectin-Mediated Zinc Chelation as a Biostatic Mechanism in Host Defence. *Scand. J. Immunol.* **1995**, *42* (5), 551–556. <https://doi.org/10.1111/j.1365-3083.1995.tb03695.x>.

(93) Brophy, M. B.; Hayden, J. A.; Nolan, E. M. Calcium Ion Gradients Modulate the Zinc Affinity and Antibacterial Activity of Human Calprotectin. *J Am Chem Soc* **2012**, *134* (43), 18089–18100. <https://doi.org/10.1021/ja307974e>.

(94) Cunden, L. S.; Gaillard, A.; Nolan, E. M. Calcium Ions Tune the Zinc-Sequestering Properties and Antimicrobial Activity of Human S100A12. *Chem. Sci.* **2016**, *7* (2), 1338–1348. <https://doi.org/10.1039/C5SC03655K>.

(95) Gagnon, D. M.; Brophy, M. B.; Bowman, S. E. J.; Stich, T. A.; Drennan, C. L.; Britt, R. D.; Nolan, E. M. Manganese Binding Properties of Human Calprotectin under Conditions of High and Low Calcium: X-Ray Crystallographic and Advanced Electron Paramagnetic Resonance Spectroscopic Analysis. *J. Am. Chem. Soc.* **2015**, *137* (8), 3004–3016.

<https://doi.org/10.1021/ja512204s>.

(96) Hayden, J. A.; Brophy, M. B.; Cunden, L. S.; Nolan, E. M. High-Affinity Manganese Coordination by Human Calprotectin Is Calcium-Dependent and Requires the Histidine-Rich Site Formed at the Dimer Interface. *J Am Chem Soc* **2013**, *135* (2), 775–787.
<https://doi.org/10.1021/ja3096416>.

(97) Nakashige, T. G.; Zhang, B.; Krebs, C.; Nolan, E. M. Human Calprotectin Is an Iron-Sequestering Host-Defense Protein. *Nat Chem Biol* **2015**, *11* (10), 765–771.
<https://doi.org/10.1038/nchembio.1891>.

(98) Nakashige, T. G.; Zygiel, E. M.; Drennan, C. L.; Nolan, E. M. Nickel Sequestration by the Host-Defense Protein Human Calprotectin. *J. Am. Chem. Soc.* **2017**, *139* (26), 8828–8836.
<https://doi.org/10.1021/jacs.7b01212>.

(99) Zygiel, E. M.; Nelson, C. E.; Brewer, L. K.; Oglesby-Sherrouse, A. G.; Nolan, E. M. The Human Innate Immune Protein Calprotectin Induces Iron Starvation Responses in *Pseudomonas Aeruginosa*. *J. Biol. Chem.* **2019**, *294* (10), 3549–3562.
<https://doi.org/10.1074/jbc.RA118.006819>.

(100) Harford, C.; Sarkar, B. Amino Terminal Cu(II)- and Ni(II)-Binding (ATCUN) Motif of Proteins and Peptides: Metal Binding, DNA Cleavage, and Other Properties. *Acc. Chem. Res.* **1997**, *30* (3), 123–130. <https://doi.org/10.1021/ar9501535>.

(101) Andreini, C.; Bertini, I.; Cavallaro, G.; Holliday, G. L.; Thornton, J. M. Metal Ions in Biological Catalysis: From Enzyme Databases to General Principles. *J. Biol. Inorg. Chem.* **2008**, *13* (8), 1205–1218. <https://doi.org/10.1007/s00775-008-0404-5>.

(102) Chang, C. J. Searching for Harmony in Transition-Metal Signaling. *Nat. Chem. Biol.* **2015**, *11* (10), 744–747. <https://doi.org/10.1038/nchembio.1913>.

(103) Hood, M. I.; Skaar, E. P. Nutritional Immunity: Transition Metals at the Pathogen-Host Interface. *Nat. Rev. Microbiol.* **2012**, *10* (8), 525–537. <https://doi.org/10.1038/nrmicro2836>.

(104) Kehl-Fie, T. E.; Skaar, E. P. Nutritional Immunity beyond Iron: A Role for Manganese and Zinc. *Curr. Opin. Chem. Biol.* **2010**, *14* (2), 218–224. <https://doi.org/10.1016/j.cbpa.2009.11.008>.

(105) Skaar, E. P.; Raffatellu, M. Metals in Infectious Diseases and Nutritional Immunity. *Metallomics* **2015**, *7* (6), 926–928. <https://doi.org/10.1039/c5mt90021b>.

(106) Djoko, K. Y.; Ong, C. Y.; Walker, M. J.; McEwan, A. G. The Role of Copper and Zinc Toxicity in Innate Immune Defense against Bacterial Pathogens. *J. Biol. Chem.* **2015**, *290* (31), 18954–18961. <https://doi.org/10.1074/jbc.R115.647099>.

(107) Lemire, J. A.; Harrison, J. J.; Turner, R. J. Antimicrobial Activity of Metals: Mechanisms, Molecular Targets and Applications. *Nat. Rev. Microbiol.* **2013**, *11* (6), 371–384. <https://doi.org/10.1038/nrmicro3028>.

(108) Hyre, A. N.; Kavanagh, K.; Kock, N. D.; Donati, G. L.; Subashchandrabose, S. Copper Is a Host Effector Mobilized to Urine during Urinary Tract Infection to Impair Bacterial Colonization. *Infect. Immun.* **2017**, *85* (3), 1–14. <https://doi.org/10.1128/IAI.01041-16>.

(109) Samanovic, M. I.; Ding, C.; Thiele, D. J.; Darwin, K. H. Copper in Microbial Pathogenesis: Meddling with the Metal. *Cell Host Microbe* **2012**, *11* (2), 106–115.

<https://doi.org/10.1016/j.chom.2012.01.009>.

(110) Besold, A. N.; Culbertson, E. M.; Cullota, V. C. The Yin and Yang of Copper During Infection. *J Biol Inorg Chem.* **2016**, *21* (2), 137–144. <https://doi.org/10.1007/s00775-016-1335-1>.

(111) White, C.; Lee, J.; Kambe, T.; Fritsche, K.; Petris, M. J. A Role for the ATP7A Copper-Transporting ATPase in Macrophage Bactericidal Activity. *J. Biol. Chem.* **2009**, *284* (49), 33949–33956. <https://doi.org/10.1074/jbc.M109.070201>.

(112) Wagner, D.; Maser, J.; Lai, B.; Cai, Z.; Barry, C. E.; Höner, K.; David, G.; Bermudez, L. E.; Iii, C. E. B. Elemental Analysis of *Mycobacterium Avium*-, *Mycobacterium Tuberculosis*-, and *Mycobacterium Smegmatis*-Containing Phagosomes Indicates Pathogen-Induced Microenvironments within the Host Cell's Endosomal System. *J. Immunol.* **2005**, *174* (3), 1491–1500. <https://doi.org/10.4049/jimmunol.174.3.1491>.

(113) Cernat, R.; Mihaescu, T.; Vornicu, M.; Vione, D.; Olariu, R.; Arsene, C. Serum Trace Metal and Ceruloplasmin Variability in Individuals Treated for Pulmonary Tuberculosis. *Int. J. Tuberc. Lung Dis.* **2011**, *15* (9), 1239–1245. <https://doi.org/10.5588/ijtld.10.0445>.

(114) Kocyigit, A.; Erel, O.; Gurel, M. S.; Avci, S.; Aktepe, N. Alterations of Serum Selenium, Zinc, Copper, and Iron Concentrations and Some Related Antioxidant Enzyme Activities in Patients with Cutaneous Leishmaniasis. *Biol. Trace Elem. Res.* **1998**, *65* (3), 271–281. <https://doi.org/10.1007/bf02789102>.

(115) Wolschendorf, F.; Ackart, D.; Shrestha, T. B.; Hascall-Dove, L.; Nolan, S.; Lamichhane, G.; Wang, Y.; Bossmann, S. H.; Basaraba, R. J.; Niederweis, M. Copper Resistance Is Essential for Virulence of *Mycobacterium Tuberculosis*. *Proc. Natl. Acad. Sci. U. S. A.*

2011, *108* (4), 1621–1626. <https://doi.org/10.1073/pnas.1009261108>.

(116) Subashchandrabose, S.; Hazen, T. H.; Brumbaugh, A. R.; Himpel, S. D.; Smith, S. N.; Ernst, R. D.; Rasko, D. A.; Mobley, H. L. T. Host-Specific Induction of *Escherichia Coli* Fitness Genes during Human Urinary Tract Infection. *Proc. Natl. Acad. Sci. U. S. A.* **2014**, *111* (51), 18327–18332. <https://doi.org/10.1073/pnas.1415959112>.

(117) Duggal, M. S.; Chawla, H. S.; Curzon, M. E. J. A Study of the Relationship between Trace Elements in Saliva and Dental Caries in Children. *Arch. Oral Biol.* **1991**, *36* (12), 881–884. [https://doi.org/10.1016/0003-9969\(91\)90118-E](https://doi.org/10.1016/0003-9969(91)90118-E).

(118) Libardo, M. D. J.; Gorbatyuk, V. Y.; Angeles-Boza, A. M. Central Role of the Copper-Binding Motif in the Complex Mechanism of Action of Ixosin: Enhancing Oxidative Damage and Promoting Synergy with Ixosin B. *ACS Infect. Dis.* **2016**, *2* (1), 71–81. <https://doi.org/10.1021/acsinfecdis.5b00140>.

(119) Libardo, M. D. J.; Bahar, A. A.; Ma, B.; Fu, R.; McCormick, L. E.; Zhao, J.; McCallum, S. A.; Nussinov, R.; Ren, D.; Angeles-Boza, A. M.; Cotten, M. L. Nuclease Activity Gives an Edge to Host-Defense Peptide Piscidin 3 over Piscidin 1, Rendering It More Effective against Persisters and Biofilms. *FEBS J.* **2017**, *284* (21), 3662–3683. <https://doi.org/10.1111/febs.14263>.

(120) Zahran, E.; Noga, E. J. Evidence for Synergism of the Antimicrobial Peptide Piscidin 2 with Antiparasitic and Antioomycete Drugs. *J. Fish Dis.* **2010**, *33* (12), 995–1003. <https://doi.org/10.1111/j.1365-2761.2010.01205.x>.

(121) Fu, Y.; Chang, F.-M. J.; Giedroc, D. P. Copper Transport and Trafficking at the Host–Bacterial Pathogen Interface. *Acc. Chem. Res.* **2014**, *47* (12), 3605–3613.

<https://doi.org/10.1021/ar500300n>.

(122) Wayne Outten, F.; Munson, G. P. Lability and Liability of Endogenous Copper Pools. *J. Bacteriol.* **2013**, *195* (20), 4553–4555. <https://doi.org/10.1128/JB.00891-13>.

(123) Macomber, L.; Imlay, J. A. The Iron-Sulfur Clusters of Dehydratases Are Primary Intracellular Targets of Copper Toxicity. *Proc. Natl. Acad. Sci. U. S. A.* **2009**, *106* (20), 8344–8349. <https://doi.org/10.1073/pnas.0812808106>.

(124) Irving, B. H.; Williams, R. J. P. The Stability of Transition-Metal Complexes. *J. Chem. Soc.* **1953**, 3192–3210. <https://doi.org/10.1039/JR9530003192>.

(125) Varadwaj, P. R.; Varadwaj, A.; Jin, B. Y. Ligand(s)-to-Metal Charge Transfer as a Factor Controlling the Equilibrium Constants of Late First-Row Transition Metal Complexes: Revealing the Irving-Williams Thermodynamical Series. *Phys. Chem. Chem. Phys.* **2015**, *17* (2), 805–811. <https://doi.org/10.1039/c4cp03953j>.

(126) Hong, R.; Kang, T. Y.; Michels, C. A.; Gadura, N. Membrane Lipid Peroxidation in Copper Alloy-Mediated Contact Killing of Escherichia Coli. *Appl. Environ. Microbiol.* **2012**, *78* (6), 1776–1784. <https://doi.org/10.1128/AEM.07068-11>.

(127) Argüello, J. M.; Raimunda, D.; Padilla-Benavides, T. Mechanisms of Copper Homeostasis in Bacteria. *Front. Cell. Infect. Microbiol.* **2013**, *3*, 1–14.
<https://doi.org/10.3389/fcimb.2013.00073>.

(128) Finney, L. A.; O'Halloran, T. V. Transition Metal Speciation in the Cell: Insights from the Chemistry of Metal Ion Receptors. *Science (80-).* **2003**, *300* (5621), 931–936.
<https://doi.org/10.1126/science.1085049>.

(129) Gold, B.; Deng, H.; Bryk, R.; Vargas, D.; Eliezer, D.; Roberts, J.; Jiang, X.; Nathan, C. Identification of a Copper-Binding Metallothionein in Pathogenic Mycobacteria. *Nat Chem Biol* **2008**, *4* (10), 609–616. <https://doi.org/10.1038/nchembio.109>.

(130) Chaturvedi, Kaveri S.; Hung, Chia S.; Crowley Jan R.; Stapleton, Ann E.; Henderson, J. P. The Siderophore Yersiniabactin Binds Copper to Protect Pathogens during Infection. *Nat. Chem. Biol.* **2012**, *8* (8), 731–736. <https://doi.org/10.1038/nchembio.1020>.

(131) Chaturvedi, K. S.; Hung, C. S.; Giblin, D. E.; Urushidani, S.; Austin, A. M.; Dinauer, M. C.; Henderson, J. P. Cupric Yersiniabactin Is a Virulence-Associated Superoxide Dismutase Mimic. *ACS Chem. Biol.* **2014**, *9* (2), 551–561.
<https://doi.org/10.1021/cb400658k>.

(132) Rowland, J. L.; Niederweis, M. A Multicopper Oxidase Is Required for Copper Resistance in *Mycobacterium Tuberculosis*. *J. Bacteriol.* **2013**, *195* (16), 3724–3733.
<https://doi.org/10.1128/JB.00546-13>.

(133) Huffman, D. L.; Huyett, J.; Outten, F. W.; Doan, P. E.; Finney, L. A.; Hoffman, B. M.; O'Halloran, T. V. Spectroscopy of Cu(II)-PcoC and the Multicopper Oxidase Function of PcoA, Two Essential Components of *Escherichia Coli* Pco Copper Resistance Operon. *Biochemistry* **2002**, *41* (31), 10046–10055. <https://doi.org/10.1021/bi0259960>.

(134) Rae, T. D.; Schmidt, P. J.; Pufahl, R. A.; Culotta, V. C.; O'Halloran, T. V. Undetectable Intracellular Free Copper: The Requirement of a Copper Chaperone for Superoxide Dismutase. *Science (80-.).* **1999**, *284* (5415), 805–808.
<https://doi.org/10.1126/science.284.5415.805>.

(135) Duay, S. S.; Sharma, G.; Prabhakar, R.; Angeles-Boza, A. M.; May, E. R. Molecular

Dynamics Investigation into the Effect of Zinc(II) on the Structure and Membrane Interactions of the Antimicrobial Peptide Clavanin A. *J Phys Chem B* **2019**, *123* (15), 3163–3176. <https://doi.org/10.1021/acs.jpcb.8b11496>.

(136) Gong, Z.; Ikonomova, S. P.; Karlsson, A. J. Secondary Structure of Cell-Penetrating Peptides during Interaction with Fungal Cells. *Protein Sci.* **2018**, *27* (3), 702–713. <https://doi.org/10.1002/pro.3364>.

(137) Wang, W.; Smith, D. K.; Moulding, K.; Chen, H. M. The Dependence of Membrane Permeability by the Antibacterial Peptide Cecropin B and Its Analogs, CB-1 and CB-3, on Liposomes of Different Composition. *J. Biol. Chem.* **1998**, *273* (42), 27438–27448. <https://doi.org/10.1074/jbc.273.42.27438>.

(138) Nymeyer, H.; Woolf, T. B.; Garcia, A. E. Folding Is Not Required for Bilayer Insertion: Replica Exchange Simulations of an α -Helical Peptide with an Explicit Lipid Bilayer. *Proteins* **2005**, *59* (4), 783–790. <https://doi.org/10.1002/prot.20460>.

(139) Abu-Shummays, A.; Dufield, J. J. Circular Dichroism-Theory and Instrumentation. *Anal. Chem.* **1966**, *38* (7), 29A-58A. <https://doi.org/10.1021/ac60239a726>.

(140) Holzwarth, G.; Doty, P. The Ultraviolet Circular Dichroism of Polypeptides. *J. Am. Chem. Soc.* **1965**, *87* (2), 218–228. <https://doi.org/10.1021/ja01080a015>.

(141) Greenfield, N.; Fasman, G. D. Computed Circular Dichroism Spectra for the Evaluation of Protein Conformation. *Biochemistry* **1969**, *8* (10), 4108–4116. <https://doi.org/10.1021/bi00838a031>.

(142) Venyaminov, S. Y.; Baikalov, I. A.; Shen, Z. M.; Wu, C.-S. C.; Yang, J. T. Circular

Dichroic Analysis of Denatured Proteins: Inclusion of Denatured Proteins in the Reference Set. *Anal. Biochem.* **1993**, *214* (1), 17–24.
<https://doi.org/10.1006/abio.1993.1450>.

(143) Avitabile, C.; D'Andrea, L. D.; Romanelli, A. Circular Dichroism Studies on the Interactions of Antimicrobial Peptides with Bacterial Cells. *Sci. Rep.* **2014**, *4* (4293), 1–7.
<https://doi.org/10.1038/srep04293>.

(144) Yorita, H.; Otomo, K.; Hiramatsu, H.; Toyama, A.; Miura, T.; Takeuchi, H. Evidence for the Cation- π Interaction between Cu²⁺ and Tryptophan. *J. Am. Chem. Soc.* **2008**, *130* (46), 15266–15267. <https://doi.org/10.1021/ja807010f>.

(145) Brewer, D.; Lajoie, G. Evaluation of the Metal Binding Properties of the Histidine-Rich Antimicrobial Peptides Histatin 3 and 5 by Electrospray Ionization Mass Spectrometry. *Rapid Commun. mass Spectrom.* **2000**, *14* (19), 1736–1745. [https://doi.org/10.1002/1097-0231\(20001015\)14:19<1736::AID-RCM86>3.0.CO;2-2](https://doi.org/10.1002/1097-0231(20001015)14:19<1736::AID-RCM86>3.0.CO;2-2).

(146) Agbale, C. M.; Sarfo, J. K.; Galyuon, I. K.; Juliano, S. A.; Silva, G. G. O.; Buccini, D. F.; Cardoso, M. H.; Torres, M. D. T.; Angeles-Boza, A. M.; De La Fuente-Nunez, C.; Franco, O. L. Antimicrobial and Antibiofilm Activities of Helical Antimicrobial Peptide Sequences Incorporating Metal-Binding Motifs. *Biochemistry* **2019**, *58* (36), 3802–3812.
<https://doi.org/10.1021/acs.biochem.9b00440>.

(147) Portelinha, J.; Heilemann, K.; Jin, J.; Angeles-Boza, A. M. Unraveling the Implications of Multiple Histidine Residues in the Potent Antimicrobial Peptide Gaduscidin-1. *Submitt. Manuscr.* **2020**.

(148) Płonka, D.; Bal, W. The N-Terminus of Hepcidin Is a Strong and Potentially Biologically

Relevant Cu(II) Chelator. *Inorganica Chim. Acta* **2018**, *472*, 76–81.
<https://doi.org/10.1016/j.ica.2017.06.051>.

(149) Gusman, H.; Lendenmann, U.; Grogan, J.; Troxler, R. F.; Oppenheim, F. G. Is Salivary Histatin 5 a Metallopeptide? *Biochim. Biophys. Acta - Protein Struct. Mol. Enzymol.* **2001**, *1545* (1–2), 86–95. [https://doi.org/10.1016/S0167-4838\(00\)00265-X](https://doi.org/10.1016/S0167-4838(00)00265-X).

(150) Conklin, S. E.; Bridgman, E. C.; Su, Q.; Riggs-Gelasco, P.; Haas, K. L.; Franz, K. J. Specific Histidine Residues Confer Histatin Peptides with Copper-Dependent Activity against *Candida Albicans*. *Biochemistry* **2017**, *56* (32), 4244–4255.
<https://doi.org/10.1021/acs.biochem.7b00348>.

(151) Xiao, Z.; Wedd, A. G. The Challenges of Determining Metal-Protein Affinities. *Nat. Prod. Rep.* **2010**, *27* (5), 768–789. <https://doi.org/10.1039/b906690j>.

(152) Henriksen, J. R.; Andresen, T. L. Thermodynamic Profiling of Peptide Membrane Interactions by Isothermal Titration Calorimetry: A Search for Pores and Micelles. *Biophys. J.* **2011**, *101* (1), 100–109. <https://doi.org/10.1016/j.bpj.2011.05.047>.

(153) Wenk, M. R.; Seelig, J. Magainin 2 Amide Interaction with Lipid Membranes: Calorimetric Detection of Peptide Binding and Pore Formation. *Biochemistry* **1998**, *37* (11), 3909–3916. <https://doi.org/10.1021/bi972615n>.

(154) Bringezu, F.; Wen, S.; Dante, S.; Hauss, T.; Majerowicz, M.; Waring, A. The Insertion of the Antimicrobial Peptide Dicynthaurin Monomer in Model Membranes: Thermodynamics and Structural Characterization. *Biochemistry* **2007**, *46* (19), 5678–5686. <https://doi.org/10.1021/bi7001295>.

(155) Quinn, C. F.; Carpenter, M. C.; Croteau, M. L.; Wilcox, D. E. *Isothermal Titration Calorimetry Measurements of Metal Ions Binding to Proteins*, 1st ed.; Elsevier Inc., 2016; Vol. 567. <https://doi.org/10.1016/bs.mie.2015.08.021>.

(156) Wiseman, T.; Williston, S.; Brandts, J. F.; Lin, L. N. Rapid Measurement of Binding Constants and Heats of Binding Using a New Titration Calorimeter. *Anal. Biochem.* **1989**, *179* (1), 131–137. [https://doi.org/10.1016/0003-2697\(89\)90213-3](https://doi.org/10.1016/0003-2697(89)90213-3).

(157) Velazquez-Campoy, A.; Freire, E. Isothermal Titration Calorimetry to Determine Association Constants for High-Affinity Ligands. *Nat. Protoc.* **2006**, *1* (1), 186–191. <https://doi.org/10.1038/nprot.2006.28>.

(158) Krainer, G.; Keller, S. Single-Experiment Displacement Assay for Quantifying High-Affinity Binding by Isothermal Titration Calorimetry. *Methods* **2015**, *76*, 116–123. <https://doi.org/10.1016/j.ymeth.2014.10.034>.

(159) Trapaidze, A.; Hureau, C.; Bal, W.; Winterhalter, M.; Faller, P. Thermodynamic Study of Cu²⁺ Binding to the DAHK and GHK Peptides by Isothermal Titration Calorimetry (ITC) with the Weaker Competitor Glycine. *J Biol Inorg Chem* **2012**, *17* (1), 37–47. <https://doi.org/10.1007/s00775-011-0824-5>.

(160) Arias, M.; Prenner, E. J.; Vogel, H. J. Calorimetry Methods to Study Membrane Interactions and Perturbations Induced by Antimicrobial Host Defense Peptides. In *Antimicrobial Peptides*; 2017; pp 119–140.

(161) Epand, R. F.; Umezawa, N.; Porter, E. A.; Gellman, S. H.; Epand, R. M. Interactions of the Antimicrobial β -Peptide β -17 with Phospholipid Vesicles Differ from Membrane Interactions of Magainins. *Eur. J. Biochem.* **2003**, *270* (6), 1240–1248.

<https://doi.org/10.1046/j.1432-1033.2003.03484.x>.

(162) Karmakar, S.; Maity, P.; Halder, A. Charge-Driven Interaction of Antimicrobial Peptide NK-2 with Phospholipid Membranes. *ACS Omega* **2017**, *2* (12), 8859–8867.
<https://doi.org/10.1021/acsomega.7b01222>.

(163) Wei, L.; LaBouyer, M. A.; Darling, L. E. O.; Elmore, D. E. Bacterial Spheroplasts as a Model for Visualizing Membrane Translocation of Antimicrobial Peptides. *Antimicrob. Agents Chemother.* **2016**, *60* (10), 6350–6352. <https://doi.org/10.1128/AAC.01008-16>.

(164) Choi, H.; Yang, Z.; Weisshaar, J. C. Single-Cell, Real-Time Detection of Oxidative Stress Induced in Escherichia Coli by the Antimicrobial Peptide CM15. *Proc. Natl. Acad. Sci. U. S. A.* **2015**, *112* (3), E303–E310. <https://doi.org/10.1073/pnas.1417703112>.

(165) Choi, H.; Rangarajan, N.; Weisshaar, J. C. Lights, Camera, Action! Antimicrobial Peptide Mechanisms Imaged in Space and Time Mechanistic Studies of Antimicrobial Peptides. *Trends Microbiol* **2016**, *24* (2), 111–122. <https://doi.org/10.1016/j.tim.2015.11.004>.

(166) Agrawal, A.; Rangarajan, N.; Weisshaar, J. C. Resistance of Early Stationary Phase E. Coli to Membrane Permeabilization by the Antimicrobial Peptide Cecropin A. *Biochim. Biophys. Acta - Biomembr.* **2019**, *1861* (10), 1–10.
<https://doi.org/10.1016/j.bbamem.2019.05.012>.

(167) Buck, A. K.; Elmore, D. E.; Darling, L. E. Using Fluorescence Microscopy to Shed Light on the Mechanisms of Antimicrobial Peptides. *Future Med. Chem.* **2019**, *11* (18), 2447–2460. <https://doi.org/10.4155/fmc-2019-0095>.

(168) Haas, K. L.; Puttermann, A. B.; White, D. R.; Thiele, D. J.; Franz, K. J. Model Peptides

Provide New Insights into the Role of Histidine Residues as Potential Ligands in Human Cellular Copper Acquisition via Ctr1. *J Am Chem Soc* **2011**, *113* (12), 4427–4437.
<https://doi.org/10.1021/ja108890c>.

(169) Rahimi, Y.; Goulding, A.; Shrestha, S.; Mirpuri, S.; Deo, S. K. Mechanism of Copper Induced Fluorescence Quenching of Red Fluorescent Protein, DsRed. *Biochem Biophys Res Commun* **2008**, *370* (1), 57–61. <https://doi.org/10.1016/j.bbrc.2008.03.034>.

(170) Liu, Z. C.; Yang, Z. Y.; Li, T. R.; Wang, B. D.; Li, Y.; Qin, D. D.; Wang, M. F.; Yan, M. H. An Effective Cu(II) Quenching Fluorescence Sensor in Aqueous Solution and 1D Chain Coordination Polymer Framework. *Dalt. Trans.* **2011**, *40* (37), 9370–9373.
<https://doi.org/10.1039/c1dt10987a>.

(171) Torrado, A.; Walkup, G. K.; Imperiali, B. Exploiting Polypeptide Motifs for the Design of Selective Cu(II) Ion Chemosensors. *J. Am. Chem. Soc.* **1998**, *120* (3), 609–610.
<https://doi.org/10.1021/ja973357k>.

(172) Wende, C.; Kulak, N. Fluorophore ATCUN Complexes: Combining Agent and Probe for Oxidative DNA Cleavage. *Chem. Commun.* **2015**, *51* (62), 12395–12398.
<https://doi.org/10.1039/C5CC04508H>.

(173) Deng, D.; Hao, Y.; Yang, P.; Xia, N.; Yu, W.; Liu, X.; Liu, L. Single-Labeled Peptide Substrates for Detection of Protease Activity Based on the Inherent Fluorescence Quenching Ability of Cu²⁺. *Anal. Methods* **2019**, *11* (9), 1264–1269.
<https://doi.org/10.1039/c8ay02650e>.

(174) Libardo, M. D. J.; De La Fuente-Nuñez, C.; Anand, K.; Krishnamoorthy, G.; Kaiser, P.; Pringle, S. C.; Dietz, C.; Pierce, S.; Smith, M. B.; Barczak, A.; Kaufmann, S. H. E.; Singh,

A.; Angeles-Boza, A. M. Phagosomal Copper-Promoted Oxidative Attack on Intracellular Mycobacterium Tuberculosis. *ACS Infect. Dis.* **2018**, *4* (11), 1623–1634.
<https://doi.org/10.1021/acsinfecdis.8b00171>.

(175) Hedegaard, S. F.; Derbas, M. S.; Lind, T. K.; Kasimova, M. R.; Christensen, M. V.; Michaelsen, M. H.; Campbell, R. A.; Jorgensen, L.; Franzyk, H.; Cárdenas, M.; Nielsen, H. M. Fluorophore Labeling of a Cell-Penetrating Peptide Significantly Alters the Mode and Degree of Biomembrane Interaction. *Sci. Rep.* **2018**, *8* (1), 1–14.

<https://doi.org/10.1038/s41598-018-24154-z>.

(176) Birch, D.; Christensen, M. V.; Staerk, D.; Franzyk, H.; Nielsen, H. M. Fluorophore Labeling of a Cell-Penetrating Peptide Induces Differential Effects on Its Cellular Distribution and Affects Cell Viability. *Biochim. Biophys. Acta - Biomembr.* **2017**, *1859* (12), 2483–2494. <https://doi.org/10.1016/j.bbamem.2017.09.015>.

(177) Cavaco, M.; Pérez-Peinado, C.; Valle, J.; Silva, R. D. M.; Correia, J. D. G.; Andreu, D.; Castanho, M. A. R. B.; Neves, V. To What Extent Do Fluorophores Bias the Biological Activity of Peptides? A Practical Approach Using Membrane-Active Peptides as Models. *Front. Bioeng. Biotechnol.* **2020**, *8*, 1–13. <https://doi.org/10.3389/fbioe.2020.552035>.

(178) Marion, D.; Zasloff, M.; Bax, A. A Two-Dimensional NMR Study of the Antimicrobial Peptide Magainin 2. *FEBS Lett.* **1988**, *227* (1), 21–26. [https://doi.org/10.1016/0014-5793\(88\)81405-4](https://doi.org/10.1016/0014-5793(88)81405-4).

(179) Rai, R. K.; De Angelis, A.; Greenwood, A. I.; Opella, S. J.; Cotten, M. Metal-Ion Binding to Host Defense Peptide Piscidin 3 Observed in Phospholipid Bilayers by Magic Angle Spinning Solid-State NMR. *ChemPhysChem* **2019**, *20* (2), 295–301.

<https://doi.org/10.1002/cphc.201800855>.

(180) Abbas, I. M.; Vranic, M.; Hoffmann, H.; El-Khatib, A. H.; Montes-Bayón, M.; Möller, H. M.; Weller, M. G. Investigations of the Copper Peptide Hepcidin-25 by LC-MS/MS and NMR. *Int. J. Mol. Sci.* **2018**, *19* (8), 1–16. <https://doi.org/10.3390/ijms19082271>.

(181) Song, C.; Weichbrodt, C.; Salnikov, E. S.; Dynowski, M.; Forsberg, B. O.; Bechinger, B.; Steinem, C.; De Groot, B. L.; Zachariae, U.; Zeth, K. Crystal Structure and Functional Mechanism of a Human Antimicrobial Membrane Channel. *Proc. Natl. Acad. Sci. U. S. A.* **2013**, *110* (12), 4586–4591. <https://doi.org/10.1073/pnas.1214739110>.

(182) Terwilliger, T. C.; Weissman, L.; Eisenberg, D. The Structure of Melittin in the Form I Crystals and Its Implication for Melittin’s Lytic and Surface Activities. *Biophys. J.* **1982**, *37* (1), 353–361. [https://doi.org/10.1016/S0006-3495\(82\)84683-3](https://doi.org/10.1016/S0006-3495(82)84683-3).

(183) Dawson, C. R.; Drake, A. F.; Helliwell, J.; Hider, R. C. The Interaction of Bee Melittin with Lipid Bilayer Membranes. *Biochim. Biophys. Acta* **1978**, *510* (1), 75–86. [https://doi.org/10.1016/0006-2736\(78\)90131-1](https://doi.org/10.1016/0006-2736(78)90131-1).

(184) Socarras, K. M.; Theophilus, P. A.; Torres, J. P.; Gupta, K.; Sapi, E. Antimicrobial Activity of Bee Venom and Melittin against Borrelia Burgdorferi. *Antibiotics* **2017**, *6* (4), 31. <https://doi.org/10.3390/antibiotics6040031>.

(185) Ratcliffe, N. A.; Mello, C. B.; Garcia, E. S.; Butt, T. M.; Azambuja, P. Insect Natural Products and Processes: New Treatments for Human Disease. *Insect Biochem. Mol. Biol.* **2011**, *41* (10), 747–769. <https://doi.org/10.1016/j.ibmb.2011.05.007>.

(186) Berneche, S.; Nina, M.; Roux; Benoit. Molecular Dynamics Simulation of Melittin in a

Dimyristoylphosphatidylcholine Bilayer Membrane. *Biophys. J.* **1998**, *75* (4), 1603–1618.
[https://doi.org/10.1016/S0006-3495\(98\)77604-0](https://doi.org/10.1016/S0006-3495(98)77604-0).

(187) Bachar, M.; Becker, O. M. Protein-Induced Membrane Disorder: A Molecular Dynamics Study of Melittin in a Dipalmitoylphosphatidylcholine Bilayer. *Biophys. J.* **2000**, *78* (3), 1359–1375. [https://doi.org/10.1016/S0006-3495\(00\)76690-2](https://doi.org/10.1016/S0006-3495(00)76690-2).

(188) Bachar, M.; Becker, O. M. Melittin at a Membrane/Water Interface: Effects on Water Orientation and Water Penetration. *J. Chem. Phys.* **1999**, *111* (18), 8672–8685.
<https://doi.org/10.1063/1.480207>.

(189) Sun, D.; Forsman, J.; Woodward, C. E. Molecular Simulations of Melittin-Induced Membrane Pores. *J. Phys. Chem. B* **2017**, *121* (44), 10209–10214.
<https://doi.org/10.1021/acs.jpcb.7b07126>.

(190) Vidossich, P.; Magistrato, A. QM/MM Molecular Dynamics Studies of Metal Binding Proteins. *Biomolecules* **2014**, *4* (3), 616–645. <https://doi.org/10.3390/biom4030616>.

(191) Lai, R.; Tang, W. J.; Li, H. Catalytic Mechanism of Amyloid- β Peptide Degradation by Insulin Degrading Enzyme: Insights from Quantum Mechanics and Molecular Mechanics Style Møller-Plesset Second Order Perturbation Theory Calculation. *J. Chem. Inf. Model.* **2018**, *58* (9), 1926–1934. <https://doi.org/10.1021/acs.jcim.8b00406>.

(192) Hermann, J. C.; Hensen, C.; Ridder, L.; Mulholland, A. J.; Höltje, H. D. Mechanisms of Antibiotic Resistance: QM/MM Modeling of the Acylation Reaction of a Class A β -Lactamase with Benzylpenicillin. *J. Am. Chem. Soc.* **2005**, *127* (12), 4454–4465.
<https://doi.org/10.1021/ja044210d>.

(193) Libardo, M. D. J.; Paul, T. J.; Prabhakar, R.; Angeles-Boza, A. M. Hybrid Peptide ATCUN-Sh-Buforin: Influence of the ATCUN Charge and Stereochemistry on Antimicrobial Activity. *Biochimie* **2015**, *113*, 143–155.
<https://doi.org/10.1016/j.biochi.2015.04.008>.

(194) Baker, N.; Holst, M.; Wang, F. Adaptive Multilevel Finite Element Solution of the Poisson-Boltzmann Equation II. Refinement at Solvent-Accessible Surfaces in Biomolecular Systems. *J. Comput. Chem.* **2000**, *21* (15), 1343–1352.
[https://doi.org/10.1002/1096-987X\(20001130\)21:15<1343::AID-JCC2>3.0.CO;2-K](https://doi.org/10.1002/1096-987X(20001130)21:15<1343::AID-JCC2>3.0.CO;2-K).

(195) Baker, N. A.; Sept, D.; Joesph, S.; Holst, M. J.; McCammon, J. A. Electrostatics of Nanosystems: Application to Microtubules and the Ribosome. *PNAS* **2001**, *98* (18), 10037–10041. <https://doi.org/10.1073/pnas.181342398>.

(196) Gonzalez, P.; Bossak, K.; Stefaniak, E.; Hureau, C.; Raibaut, L.; Bal, W.; Faller, P. N-Terminal Cu-Binding Motifs (Xxx-Zzz-His, Xxx-His) and Their Derivatives: Chemistry, Biology and Medicinal Applications. *Chem. - A Eur. J.* **2018**, *24* (32), 8029–8041.
<https://doi.org/10.1002/chem.201705398>.

(197) Jin, Y.; Cowan, J. A. DNA Cleavage by Copper-ATCUN Complexes. Factors Influencing Cleavage Mechanism and Linearization of DsDNA. *J. Am. Chem. Soc.* **2005**, *127* (23), 8408–8415. <https://doi.org/10.1021/ja0503985>.

(198) Kotuniak, R.; Strampraad, M. J. F.; Bossak-Ahmad, K.; Wawrzyniak, U. E.; Ufnalska, I.; Hagedoorn, P.-L.; Bal, W. Key Intermediate Species Reveal the Cu(II) Exchange Pathway in Biorelevant ATCUN/NTS Complexes. *Angew. Chemie Int. Ed.* **2020**, *59*, 11234–11239.
<https://doi.org/10.1002/anie.202004264>.

(199) Sokolowska, M.; Krezel, A.; Dyba, M.; Szewczuk, Z.; Bal, W. Short Peptides Are Not Reliable Models of Thermodynamic and Kinetic Properties of the N-Terminal Metal Binding Site in Serum Albumin. *Eur. J. Biochem.* **2002**, *269* (4), 1323–1331.
<https://doi.org/10.1046/j.1432-1033.2002.02772.x>.

(200) Zhang, Y.; Akilesh, S.; Wilcox, D. E. Isothermal Titration Calorimetry Measurements of Ni(II) and Cu(II) Binding to His, GlyGlyHis, HisGlyHis, and Bovine Serum Albumin: A Critical Evaluation. *Inorg. Chem.* **2000**, *39* (14), 3057–3064.
<https://doi.org/10.1021/ic000036s>.

(201) Mlynarz, P.; Gaggelli, N.; Panek, J.; Stasiak, M.; Valensin, G.; Kowalik-Jankowska, T.; Leplawy, M. L.; Latajka, Z.; Koziowski, H. How the α -Hydroxymethylserine Residue Stabilizes Oligopeptide Complexes with Nickel(II) and Copper(II) Ions. *J. Chem. Soc., Dalt. Trans.* **2000**, No. 7, 1033–1038. <https://doi.org/10.1039/a909354k>.

(202) Miyamoto, T.; Fukino, Y.; Kamino, S.; Ueda, M.; Enomoto, S. Enhanced Stability of Cu²⁺–ATCUN Complexes under Physiologically Relevant Conditions by Insertion of Structurally Bulky and Hydrophobic Amino Acid Residues into the ATCUN Motif. *Dalt. Trans.* **2016**, *45* (23), 9436–9445. <https://doi.org/10.1039/C6DT01387B>.

(203) Bal, W.; Chmurny, G. N.; Hilton, B. D.; Sadler, P. J.; Tucker, A. Axial Hydrophobic Fence in Highly-Stable Ni(II) Complex of Des-Angiotensinogen N-Terminal Peptide. *J. Am. Chem. Soc.* **1996**, *118* (19), 4727–4728. <https://doi.org/10.1021/ja953988j>.

(204) Miyamoto, T.; Kamino, S.; Odani, A.; Hiromura, M.; Enomoto, S. Basicity of N-Terminal Amine in ATCUN Peptide Regulates Stability Constant of Albumin-like Cu²⁺ Complex. *Chem. Lett.* **2013**, *42* (9), 1099–1101. <https://doi.org/10.1246/cl.130405>.

(205) Sóvágó, I.; Osz, K. Metal Ion Selectivity of Oligopeptides. *Dalt. Trans.* **2006**, No. 32, 3841–3854. <https://doi.org/10.1039/b607515k>.

(206) Heinrich, J.; König, N. F.; Sobottka, S.; Sarkar, B.; Kulak, N. Flexible vs. Rigid Bis(2-Benzimidazolyl) Ligands in Cu(II) Complexes: Impact on Redox Chemistry and Oxidative DNA Cleavage Activity. *J. Inorg. Biochem.* **2019**, *194* (August 2018), 223–232. <https://doi.org/10.1016/j.jinorgbio.2019.01.016>.

(207) Fernandes, A. S.; Flôrido, A.; Saraiva, N.; Cerqueira, S.; Ramalhete, S.; Cipriano, M.; Cabral, M. F.; Miranda, J. P.; Castro, M.; Costa, J.; Oliveira, N. G. Role of the Copper(II) Complex Cu[15]PyN5 in Intracellular ROS and Breast Cancer Cell Motility and Invasion. *Chem. Biol. Drug Des.* **2015**, *86* (4), 578–588. <https://doi.org/10.1111/cbdd.12521>.

(208) Hureau, C.; Faller, P. A β -Mediated ROS Production by Cu Ions: Structural Insights, Mechanisms and Relevance to Alzheimer's Disease. *Biochimie* **2009**, *91* (10), 1212–1217. <https://doi.org/10.1016/j.biochi.2009.03.013>.

(209) Ng, C. H.; Kong, S. M.; Tiong, Y. L.; Maah, M. J.; Sukram, N.; Ahmad, M.; Khoo, A. S. B. Selective Anticancer Copper(Ii)-Mixed Ligand Complexes: Targeting of ROS and Proteasomes. *Metallomics* **2014**, *6* (4), 892–906. <https://doi.org/10.1039/c3mt00276d>.

(210) Cowan, J. A. Chemical Nucleases. *Curr. Opin. Chem. Biol.* **2001**, *5* (6), 634–642. [https://doi.org/10.1016/S1367-5931\(01\)00259-9](https://doi.org/10.1016/S1367-5931(01)00259-9).

(211) Jin, Y.; Lewis, M. A.; Gokhale, N. H.; Long, E. C.; Cowan, J. A. Influence of Stereochemistry and Redox Potentials on the Single- and Double-Strand DNA Cleavage Efficiency of Cu(II) and Ni(II) Lys-Gly-His-Derived ATCUN Metallopeptides. *J. Am. Chem. Soc.* **2007**, *129* (26), 8353–8361. <https://doi.org/10.1021/ja0705083>.

(212) Joyner, J. C.; Hodnick, W. F.; Cowan, A. S.; Tamuly, D.; Boyd, R.; Cowan, J. A. Antimicrobial Metallopeptides with Broad Nuclease and Ribonuclease Activity. *Chem. Commun.* **2013**, *49* (21), 2118–2120. <https://doi.org/10.1039/c3cc38977d>.

(213) Joyner, J.; Reichfield, J.; Cowan, J.; Manuscript, A.; Chelates, C. Factors Influencing the DNA Nuclease Activity of Iron, Cobalt, Nickel, and Copper Chelates. *J. Am. Chem. Soc.* **2011**, *133* (39), 15613–15626. <https://doi.org/10.1021/ja2052599>.

(214) Libardo, M. D.; Cervantes, J. L.; Salazar, J. C.; Angeles-Boza, A. M. Improved Bioactivity of Antimicrobial Peptides by Addition of Amino-Terminal Copper and Nickel (ATCUN) Binding Motifs. *ChemMedChem* **2014**, *9* (8), 1892–1901. <https://doi.org/10.1002/cmdc.201402033>.

(215) Kim, D. H.; Lee, Y. T.; Lee, Y. J.; Chung, J. H.; Lee, B. L.; Choi, B. S.; Lee, Y. Bacterial Expression of Tenecin 3, an Insect Antifungal Protein Isolated from *Tenebrio Molitor*, and Its Efficient Purification. *Mol. Cells* **1998**, *8* (6), 786–789.

(216) Pöppel, A.-K.; Vogel, H.; Wiesner, J.; Vilcinskas, A. Antimicrobial Peptides Expressed in Medicinal Maggots of the Blow Fly *Lucilia Sericata* Show Combinatorial Activity against Bacteria. *Antimicrob. Agents Chemother.* **2015**, *59* (5), 2508–2514. <https://doi.org/10.1128/aac.05180-14>.

(217) Levashina, E. A.; Ohresser, S.; Bulet, P.; Reichhart, J. -M; Hetru, C.; Hoffmann, J. A. Metchnikowin, a Novel Immune-Inducible Proline-Rich Peptide from *Drosophila* with Antibacterial and Antifungal Properties. *Eur. J. Biochem.* **1995**, *233* (2), 694–700. https://doi.org/10.1111/j.1432-1033.1995.694_2.x.

(218) Zhou, J.; Ueda, M.; Umamiya, R.; Battsetseg, B.; Boldbaatar, D.; Xuan, X.; Fujisaki, K. A

Secreted Cystatin from the Tick *Haemaphysalis Longicornis* and Its Distinct Expression Patterns in Relation to Innate Immunity. *Insect Biochem. Mol. Biol.* **2006**, *36* (7), 527–535. <https://doi.org/10.1016/j.ibmb.2006.03.003>.

(219) Lee, H.; Hwang, J. S.; Lee, D. G. Periplanetasin-4, a Novel Antimicrobial Peptide from the Cockroach, Inhibits Communications between Mitochondria and Vacuoles. *Biochem. J.* **2019**, *476* (8), 1267–1284. <https://doi.org/10.1042/bcj20180933>.

(220) Kim, I. W.; Lee, J. H.; Subramaniyam, S.; Yun, E. Y.; Kim, I.; Park, J.; Hwang, J. S. De Novo Transcriptome Analysis and Detection of Antimicrobial Peptides of the American Cockroach *Periplaneta Americana* (Linnaeus). *PLoS One* **2016**, *11* (5), 1–16. <https://doi.org/10.1371/journal.pone.0155304>.

(221) Zhou, J.; Liao, M.; Ueda, M.; Gong, H.; Xuan, X.; Fujisaki, K. Sequence Characterization and Expression Patterns of Two Defensin-like Antimicrobial Peptides from the Tick *Haemaphysalis Longicornis*. *Peptides* **2007**, *28* (6), 1304–1310. <https://doi.org/10.1016/j.peptides.2007.04.019>.

(222) Ratzka, C.; Förster, F.; Liang, C.; Kupper, M.; Dandekar, T.; Feldhaar, H.; Gross, R. Molecular Characterization of Antimicrobial Peptide Genes of the Carpenter Ant *Camponotus Floridanus*. *PLoS One* **2012**, *7* (8), 1–10. <https://doi.org/10.1371/journal.pone.0043036>.

(223) Ishikawa, M.; Kubo, T.; Natori, S. Purification and Characterization of a Diptericin Homologue from *Sarcophaga Peregrina* (Flesh Fly). *Biochem. J.* **1992**, *287* (2), 573–578. <https://doi.org/10.1042/bj2870573>.

(224) Tian, C.; Gao, B.; Fang, Q.; Ye, G.; Zhu, S. Antimicrobial Peptide-like Genes in *Nasonia*

Vitripennis: A Genomic Perspective. *BMC Genomics* **2010**, *11* (187), 1–19.

<https://doi.org/10.1186/1471-2164-11-187>.

(225) Gokudan, S.; Muta, T.; Tsuda, R.; Koori, K.; Kawahara, T.; Seki, N.; Mizunoe, Y.; Wai, S. N.; Iwanaga, S.; Kawabata, S. Horseshoe Crab Acetyl Group-Recognizing Lectins Involved in Innate Immunity Are Structurally Related to Fibrinogen. *Proc. Natl. Acad. Sci.* **2002**, *96* (18), 10086–10091. <https://doi.org/10.1073/pnas.96.18.10086>.

(226) Zhang, Z.; Zhu, S. Comparative Genomics Analysis of Five Families of Antimicrobial Peptide-like Genes in Seven Ant Species. *Dev. Comp. Immunol.* **2012**, *38* (2), 262–274. <https://doi.org/10.1016/j.dci.2012.05.003>.

(227) Hultmark, D.; Engström, A.; Andersson, K.; Steiner, H.; Bennich, H.; Boman, H. G. Insect Immunity. Attacins, a Family of Antibacterial Proteins from *Hyalophora Cecropia*. *EMBO J.* **1983**, *2* (4), 571–576. <https://doi.org/10.1002/j.1460-2075.1983.tb01465.x>.

(228) Lauth, X.; Shike, H.; Burns, J. C.; Westerman, M. E.; Ostland, V. E.; Carlberg, J. M.; Van Olst, J. C.; Nizet, V.; Taylor, S. W.; Shimizu, C.; Bulet, P. Discovery and Characterization of Two Isoforms of Moronecidin, a Novel Antimicrobial Peptide from Hybrid Striped Bass. *J. Biol. Chem.* **2002**, *277* (7), 5030–5039. <https://doi.org/10.1074/jbc.M109173200>.

(229) Muncaster, S.; Kraakman, K.; Gibbons, O.; Mensink, K.; Forlenza, M.; Jacobson, G.; Bird, S. Antimicrobial Peptides within the Yellowtail Kingfish (*Seriola Lalandi*). *Dev. Comp. Immunol.* **2018**, *80*, 67–80. <https://doi.org/10.1016/j.dci.2017.04.014>.

(230) Sun, B. J.; Xie, H. X.; Song, Y.; Nie, P. Gene Structure of an Antimicrobial Peptide from Mandarin Fish, *Siniperca Chuatsi* (Basilewsky), Suggests That Moronecidins and Pleurocidins Belong in One Family: The Piscidins. *J. Fish Dis.* **2007**, *30* (6), 335–343.

<https://doi.org/10.1111/j.1365-2761.2007.00789.x>.

(231) Browne, M. J.; Feng, C. Y.; Booth, V.; Rise, M. L. Characterization and Expression Studies of Gaduscidin-1 and Gaduscidin-2; Paralogous Antimicrobial Peptide-like Transcripts from Atlantic Cod (Gadus Morhua). *Dev. Comp. Immunol.* **2011**, *35* (3), 399–408. <https://doi.org/10.1016/j.dci.2010.11.010>.

(232) Ruangsri, J.; Salger, S. A.; Caipang, C. M. A.; Kiron, V.; Fernandes, J. M. O. Differential Expression and Biological Activity of Two Piscidin Paralogues and a Novel Splice Variant in Atlantic Cod (Gadus Morhua L.). *Fish Shellfish Immunol.* **2012**, *32* (3), 396–406. <https://doi.org/10.1016/j.fsi.2011.11.022>.

(233) Houyvet, B.; Bouchon-Navaro, Y.; Bouchon, C.; Goux, D.; Bernay, B.; Corre, E.; Zatylny-Gaudin, C. Identification of a Moronecidin-like Antimicrobial Peptide in the Venomous Fish Pterois Volitans: Functional and Structural Study of Pteroicidin- α . *Fish Shellfish Immunol.* **2018**, *72* (November 2017), 318–324. <https://doi.org/10.1016/j.fsi.2017.11.003>.

(234) Subramanian, S.; Ross, N. W.; MacKinnon, S. L. Myxinidin, a Novel Antimicrobial Peptide from the Epidermal Mucus of Hagfish, Myxine Glutinosa L. *Mar. Biotechnol.* **2009**, *11* (6), 748–757. <https://doi.org/10.1007/s10126-009-9189-y>.

(235) Salerno, G.; Parrinello, N.; Roch, P.; Cammarata, M. CDNA Sequence and Tissue Expression of an Antimicrobial Peptide, Dicentracin; a New Component of the Moronecidin Family Isolated from Head Kidney Leukocytes of Sea Bass, Dicentrarchus Labrax. *Comp. Biochem. Physiol. - B Biochem. Mol. Biol.* **2007**, *146* (4), 521–529. <https://doi.org/10.1016/j.cbpb.2006.12.007>.

(236) Acosta, J.; Montero, V.; Carpio, Y.; Velázquez, J.; Garay, H. E.; Reyes, O.; Cabrales, A.; Masforrol, Y.; Morales, A.; Estrada, M. P. Cloning and Functional Characterization of Three Novel Antimicrobial Peptides from Tilapia (*Oreochromis Niloticus*). *Aquaculture* **2013**, *372–375*, 9–18. <https://doi.org/10.1016/j.aquaculture.2012.07.032>.

(237) Peng, K. C.; Lee, S. H.; Hour, A. L.; Pan, C. Y.; Lee, L. H.; Chen, J. Y. Five Different Piscidins from Nile Tilapia, *Oreochromis Niloticus*: Analysis of Their Expressions and Biological Functions. *PLoS One* **2012**, *7* (11), 1–12. <https://doi.org/10.1371/journal.pone.0050263>.

(238) Zhang, D. L.; Guan, R. Z.; Huang, W. S.; Xiong, J. Isolation and Characterization of a Novel Antibacterial Peptide Derived from Hemoglobin Alpha in the Liver of Japanese Eel, *Anguilla Japonica*. *Fish Shellfish Immunol.* **2013**, *35* (3), 625–631. <https://doi.org/10.1016/j.fsi.2012.08.022>.

(239) Lee, I. H.; Zhao, C.; Cho, Y.; Harwig, S. S. L.; Cooper, E. L.; Lehrer, R. I. Clavanins, α -Helical Antimicrobial Peptides from Tunicate Hemocytes. *FEBS Lett.* **1997**, *400* (2), 158–162. [https://doi.org/10.1016/S0014-5793\(96\)01374-9](https://doi.org/10.1016/S0014-5793(96)01374-9).

(240) Tincu, J. A.; Menzel, L. P.; Azimov, R.; Sands, J.; Hong, T.; Waring, A. J.; Taylor, S. W.; Lehrer, R. I. Plicatamide, an Antimicrobial Octapeptide from *Styela Plicata* Hemocytes. *J. Biol. Chem.* **2003**, *278* (15), 13546–13553. <https://doi.org/10.1074/jbc.M211332200>.

(241) Li, H.; Guo, H.; Shan, S.; Qi, C.; An, L.; Yang, G. Characterization and Expression Pattern of a Novel β -Defensin in Common Carp (*Cyprinus Carpio L.*): Implications for Its Role in Mucosal Immunity. *Biosci. Biotechnol. Biochem.* **2014**, *78* (3), 430–437. <https://doi.org/10.1080/09168451.2014.885830>.

(242) Gui, L.; Zhang, P.; Zhang, Q.; Zhang, J. Two Hepcidins from Spotted Scat (*Scatophagus Argus*) Possess Antibacterial and Antiviral Functions in Vitro. *Fish Shellfish Immunol.* **2016**, *50*, 191–199. <https://doi.org/10.1016/j.fsi.2016.01.038>.

(243) Nam, Y. K.; Cho, Y. S.; Lee, S. Y.; Kim, B. S.; Kim, D. S. Molecular Characterization of Hepcidin Gene from Mud Loach (*Misgurnus Mizolepis*; Cypriniformes). *Fish Shellfish Immunol.* **2011**, *31* (6), 1251–1258. <https://doi.org/10.1016/j.fsi.2011.09.007>.

(244) Liang, T.; Ji, W.; Zhang, G. R.; Wei, K. J.; Feng, K.; Wang, W. M.; Zou, G. W. Molecular Cloning and Expression Analysis of Liver-Expressed Antimicrobial Peptide 1 (LEAP-1) and LEAP-2 Genes in the Blunt Snout Bream (*Megalobrama Amblycephala*). *Fish Shellfish Immunol.* **2013**, *35* (2), 553–563. <https://doi.org/10.1016/j.fsi.2013.05.021>.

(245) Gong, L. cai; Wang, H.; Deng, L. Molecular Characterization, Phylogeny and Expression of a Hepcidin Gene in the Blotched Snakehead *Channa Maculata*. *Dev. Comp. Immunol.* **2014**, *44* (1), 1–11. <https://doi.org/10.1016/j.dci.2013.11.007>.

(246) Ke, F.; Wang, Y.; Yang, C. S.; Xu, C. Molecular Cloning and Antibacterial Activity of Hepcidin Fromchinese Rare Minnow (*Gobiocypris Rarus*). *Electron. J. Biotechnol.* **2015**, *18* (3), 169–174. <https://doi.org/10.1016/j.ejbt.2015.03.003>.

(247) Cai, L.; Cai, J. J.; Liu, H. P.; Fan, D. Q.; Peng, H.; Wang, K. J. Recombinant Medaka (*Oryzias Melastigma*) pro-Hepcidin: Multifunctional Characterization. *Comp. Biochem. Physiol. - B Biochem. Mol. Biol.* **2012**, *161* (2), 140–147. <https://doi.org/10.1016/j.cbpb.2011.10.006>.

(248) Solstad, T.; Larsen, A. N.; Seppola, M.; Jørgensen, T. Identification, Cloning and Expression Analysis of a Hepcidin CDNA of the Atlantic Cod (*Gadus Morhua L.*). *Fish*

Shellfish Immunol. **2008**, *25* (3), 298–310. <https://doi.org/10.1016/j.fsi.2008.05.013>.

(249) Krause, A.; Neitz, S.; Schulz, A.; Forssmann, W.; Schulz-knappe, P.; Adermann, K. LEAP-1, a Novel Highly Disulfide-Bonded Human Peptide, Exhibits Antimicrobial Activity. *FEBS Lett.* **2000**, *480* (2–3), 147–150. [https://doi.org/10.1016/S0014-5793\(00\)01920-7](https://doi.org/10.1016/S0014-5793(00)01920-7).

(250) Chen, J. Y.; Lin, W. J.; Lin, T. L. A Fish Antimicrobial Peptide, Tilapia Hepcidin TH2-3, Shows Potent Antitumor Activity against Human Fibrosarcoma Cells. *Peptides* **2009**, *30* (9), 1636–1642. <https://doi.org/10.1016/j.peptides.2009.06.009>.

(251) Badial, P. R.; Oliveira Filho, J. P.; Cunha, P. H. J.; Cagnini, D. Q.; Araújo, J. P.; Winand, N. J.; Borges, A. S. Identification, Characterization and Expression Analysis of Hepcidin Gene in Sheep. *Res. Vet. Sci.* **2011**, *90* (3), 443–450. <https://doi.org/10.1016/j.rvsc.2010.07.017>.

(252) Kulprachakarn, K.; Chen, Y. L.; Kong, X.; Arno, M. C.; Hider, R. C.; Srichairatanakool, S.; Bansal, S. S. Copper(II) Binding Properties of Hepcidin. *J. Biol. Inorg. Chem.* **2016**, *21* (3), 329–338. <https://doi.org/10.1007/s00775-016-1342-2>.

(253) Sang, C.; Lin, Y.; Jiang, K.; Zhang, F.; Song, W. Molecular Cloning and mRNA Expression of a Hepcidin Gene from the Spinyhead Croaker, *Collichthys Lucidus*. *Genet. Mol. Res.* **2015**, *14* (4), 16050–16059. <https://doi.org/10.4238/2015.December.7.18>.

(254) Fry, M. M.; Liggett, J. L.; Baek, S. J. Molecular Cloning and Expression of Canine Hepcidin. *J. Biol. Chem.* **2004**, *33* (4), 223–227. <https://doi.org/10.1111/j.1939-165x.2004.tb00377.x>.

(255) Segat, L.; Pontillo, A.; Milanese, M.; Tossi, A.; Crovella, S. Evolution of the Hepcidin Gene in Primates. *BMC Genomics* **2008**, *9* (120), 1–7. <https://doi.org/10.1186/1471-2164-9-120>.

(256) Neves, J. V.; Caldas, C.; Vieira, I.; Ramos, M. F.; Rodrigues, P. N. S. Multiple Hepcidins in a Teleost Fish, *Dicentrarchus Labrax* : Different Hepcidins for Different Roles. *J. Immunol.* **2015**, *195* (6), 2696–2709. <https://doi.org/10.4049/jimmunol.1501153>.

(257) Khangembam, V. C.; Kumar, A. Buffalo Hepcidin: Characterization of CDNA and Study of Antimicrobial Property. *Vet. Res. Commun.* **2011**, *35* (2), 79–87. <https://doi.org/10.1007/s11259-010-9452-8>.

(258) Editor, R. M. E. *Host Defense Peptides and Their Potential as Therapeutic Agents*; Springer, 2016.

(259) Boumaiza, M.; Abidi, S. Hepcidin CDNA Evolution in Vertebrates. *Vitam. Horm.* **2019**, *110*, 1–16. <https://doi.org/10.1016/bs.vh.2019.01.001>.

(260) Mu, Y.; Huo, J.; Guan, Y.; Fan, D.; Mu, P.; Ao, J.; Chen, X. An Improved Genome Assembly for Larimichthys Crocea Reveals Hepcidin Gene Expansion with Diversified Regulation and Function. *Commun. Biol.* **2018**, *195* (1), 1–12. <https://doi.org/10.1038/s42003-018-0207-3>.

(261) Park, C. H.; Valore, E. V.; Waring, A. J.; Ganz, T. Hepcidin, a Urinary Antimicrobial Peptide Synthesized in the Liver. *J. Biol. Chem.* **2001**, *276* (11), 7806–7810. <https://doi.org/10.1074/jbc.M008922200>.

(262) Xu, Q.; Cheng, C. H. C.; Hu, P.; Ye, H.; Chen, Z.; Cao, L.; Chen, L.; Shen, Y.; Chen, L.

Adaptive Evolution of Hepcidin Genes in Antarctic Notothenioid Fishes. *Mol. Biol. Evol.* **2008**, *25* (6), 1099–1112. <https://doi.org/10.1093/molbev/msn056>.

(263) Hilton, K. B.; Lambert, L. A. Molecular Evolution and Characterization of Hepcidin Gene Products in Vertebrates. *Gene* **2008**, *415* (1–2), 40–48. <https://doi.org/10.1016/j.gene.2008.02.016>.

(264) Zhang, J.; Yu, L.; Li, M.; Sun, L. Turbot (*Scophthalmus Maximus*) Hepcidin-1 and Hepcidin-2 Possess Antimicrobial Activity and Promote Resistance against Bacterial and Viral Infection. *Fish Shellfish Immunol.* **2014**, *38* (1), 127–134. <https://doi.org/10.1016/j.fsi.2014.03.011>.

(265) Howard, A.; Townes, C.; Milona, P.; Nile, C. J.; Michailidis, G.; Hall, J. Expression and Functional Analyses of Liver Expressed Antimicrobial Peptide-2 (LEAP-2) Variant Forms in Human Tissues. *Cell. Immunol.* **2010**, *261* (2), 128–133. <https://doi.org/10.1016/j.cellimm.2009.11.010>.

(266) Ke, F.; Wang, Y.; Yang, C. S.; Xu, C. Molecular Cloning and Antibacterial Activity of Hepcidin from Chinese Rare Minnow (*Gobiocypris Rarus*). *Electron. J. Biotechnol.* **2015**, *18* (3), 169–174. <https://doi.org/10.1016/j.ejbt.2015.03.003>.

(267) Bao, B.; Peatman, E.; Li, P.; He, C.; Liu, Z. Catfish Hepcidin Gene Is Expressed in a Wide Range of Tissues and Exhibits Tissue-Specific Upregulation after Bacterial Infection. *Dev. Comp. Immunol.* **2005**, *29* (11), 939–950. <https://doi.org/10.1016/j.dci.2005.03.006>.

(268) Huang, T.; Gu, W.; Wang, B.; Zhang, Y.; Cui, L.; Yao, Z.; Zhao, C.; Xu, G. Identification and Expression of the Hepcidin Gene from Brown Trout (*Salmo Trutta*) and Functional

Analysis of Its Synthetic Peptide. *Fish Shellfish Immunol.* **2019**, *87* (232), 243–253.

<https://doi.org/10.1016/j.fsi.2019.01.020>.

(269) Li, H.; Zhang, F.; Guo, H.; Zhu, Y.; Yuan, J.; Yang, G.; An, L. Molecular Characterization of Hepcidin Gene in Common Carp (*Cyprinus Carpio L.*) and Its Expression Pattern Responding to Bacterial Challenge. *Fish Shellfish Immunol.* **2013**, *35* (3), 1030–1038. <https://doi.org/10.1016/j.fsi.2013.07.001>.

(270) Krause, A. Isolation and Biochemical Characterization of LEAP-2, a Novel Blood Peptide Expressed in the Liver. *Protein Sci.* **2003**, *12* (1), 143–152.
<https://doi.org/10.1110/ps.0213603>.

(271) Melino, S.; Gallo, M.; Trotta, E.; Mondello, F.; Paci, M.; Petruzzelli, R. Metal-Binding and Nuclease Activity of an Antimicrobial Peptide Analogue of the Salivary Histatin 5. *Biochemistry* **2006**, *45* (51), 15373–15383. <https://doi.org/10.1021/bi0615137>.

(272) Brouwer, C. P. J. M.; Bogaards, S. J. P.; Wulferink, M.; Velders, M. P.; Welling, M. M. Synthetic Peptides Derived from Human Antimicrobial Peptide Ubiquicidin Accumulate at Sites of Infection and Eradicate (Multi-Drug Resistant) *Staphylococcus Aureus* in Mice. *Peptides* **2006**, *27* (11), 2585–2591. <https://doi.org/10.1016/j.peptides.2006.05.022>.

(273) Padovan, L.; Segat, L.; Pontillo, A.; Antcheva, N.; Tossi, A.; Crovella, S. Histatins In Non-Human Primates: Gene Variations and Functional Effects. *Protein Pept. Lett.* **2010**, *17* (7), 909–918. <https://doi.org/10.2174/092986610791306715>.

(274) Xu, T.; Tesler, E.; Troxler, R. F.; Oppenheim, F. G. Primary Structure and Anticandidal Activity of the Major Histatin from Parotid Secretion of the Subhuman Primate, *Macaca Fascicularis*. *J. Dent. Res.* **1990**, *69* (11), 1717–1723.

<https://doi.org/10.1177/00220345900690110301>.

(275) Bobek, L. A.; Situ, H. MUC7 20-Mer: Investigation of Antimicrobial Activity, Secondary Structure, and Possible Mechanism of Antifungal Action. *Antimicrob Agents Chemother* **2003**, *47* (2), 643–652. <https://doi.org/10.1128/AAC.47.2.643-652.2003>.

(276) Oppenheim, F. G.; Xu, T.; McMillian, F. M.; Levitz, S. M.; Diamond, R. D.; Offner, G. D.; Troxler, R. F. Histatins, a Novel Family of Histidine-Rich Proteins in Human Parotid Secretion. Isolation, Characterization, Primary Structure, and Fungistatic Effects on *Candida Albicans*. *J. Biol. Chem.* **1988**, *263* (16), 7472–7477.

(277) Khurshid, Z.; Najeeb, S.; Mali, M.; Moin, S. F.; Raza, S. Q.; Zohaib, S.; Sefat, F.; Zafar, M. S. Histatin Peptides: Pharmacological Functions and Their Applications in Dentistry. *Saudi Pharm. J.* **2017**, *25* (1), 25–31. <https://doi.org/10.1016/j.jsp.2016.04.027>.

(278) Hong, W.; Zhang, R.; Di, Z.; He, Y.; Zhao, Z.; Hu, J.; Wu, Y.; Li, W.; Cao, Z. Design of Histidine-Rich Peptides with Enhanced Bioavailability and Inhibitory Activity against Hepatitis C Virus. *Biomaterials* **2013**, *34* (13), 3511–3522. <https://doi.org/10.1016/j.biomaterials.2013.01.075>.

(279) Ooi, C. E.; Weiss, J.; Levy, O.; Elsbach, P. Isolation of Two Isoforms of a Novel 15-KDa Protein from Rabbit Polymorphonuclear Leukocytes That Modulate the Antibacterial Actions of Other Leukocyte Proteins. *J. Biol. Chem.* **1990**, *265* (26), 15956–15962.

(280) Fernandes, J. M. O.; Smith, V. J. A Novel Antimicrobial Function for a Ribosomal Peptide from Rainbow Trout Skin. *Biochem. Biophys. Res. Commun.* **2002**, *296* (1), 167–171. [https://doi.org/10.1016/S0006-291X\(02\)00837-9](https://doi.org/10.1016/S0006-291X(02)00837-9).

(281) Duits, L. A.; Langermans, J. A. M.; Paltansing, S.; Van der Straaten, T.; Vervenne, R. A. W.; Frost, P. A.; Hiemstra, P. S.; Thomas, A. W.; Nibbering, P. H. Expression of β -Defensin-1 in Chimpanzee (Pan Troglodytes) Airways. *J. Med. Primatol.* **2000**, *29* (5), 318–323. <https://doi.org/10.1034/j.1600-0684.2000.290502.x>.

(282) Semple, C.; Rolfe, M.; Dorin, J. Duplication and Selection in the Evolution of Primate Beta-Defensin Genes. *Genome Biol.* **2003**, *4* (5). <https://doi.org/10.1186/gb-2003-4-5-r31>.

(283) Yang, M.; Zhang, C.; Zhang, M. Z.; Zhang, S. Beta-Defensin Derived Cationic Antimicrobial Peptides with Potent Killing Activity against Gram-Negative and Gram-Positive Bacteria. *BMC Microbiol.* **2018**, *18* (54), 1–14. <https://doi.org/10.1186/s12866-018-1190-z>.

(284) Das, S.; Nikolaidis, N.; Goto, H.; McCallister, C.; Li, J.; Hirano, M.; Cooper, M. D. Comparative Genomics and Evolution of the Alpha-Defensin Multigene Family in Primates. *Mol. Biol. Evol.* **2010**, *27* (10), 2333–2343. <https://doi.org/10.1093/molbev/msq118>.

(285) Sinha, S.; Harioudh, M. K.; Dewangan, R. P.; Ng, W. J.; Ghosh, J. K.; Bhattacharjya, S. Cell-Selective Pore Forming Antimicrobial Peptides of the Prodomain of Human Furin: A Conserved Aromatic/Cationic Sequence Mapping, Membrane Disruption, and Atomic-Resolution Structure and Dynamics. *ACS Omega* **2018**, *3* (11), 14650–14664. <https://doi.org/10.1021/acsomega.8b01876>.

(286) Simmaco, M.; Severini, C.; De Biase, D.; Barra, D.; Bossa, F.; Roberts, J. D.; Melchiorri, P.; Erspamer, V. Six Novel Tachykinin- and Bombesin-Related Peptides from the Skin of the Australian Frog Pseudophryne Güntheri. *Peptides* **1990**, *11* (2), 299–304.

[https://doi.org/10.1016/0196-9781\(90\)90086-K](https://doi.org/10.1016/0196-9781(90)90086-K).

(287) Wabnitz, P. A.; Bowie, J. H.; Wallace, J. C.; Tyler, M. J. Peptides from the Skin Glands of the Australian Buzzing Tree Frog *Litoria Electrica*. Comparison with the Skin Peptides of the Red Tree Frog *Litoria Rubella*. *Aust. J. Chem.* **1999**, *52* (7), 639–645.

<https://doi.org/https://doi.org/10.1071/CH98171>.

(288) Yang, X.; Lee, W. H.; Zhang, Y. Extremely Abundant Antimicrobial Peptides Existed in the Skins of Nine Kinds of Chinese Odorous Frogs. *J. Proteome Res.* **2012**, *11* (1), 306–319. <https://doi.org/10.1021/pr200782u>.

(289) Wu, Y.; Wang, L.; Zhou, M.; Ma, C.; Chen, X.; Bai, B.; Chen, T.; Shaw, C. Limnonectins: A New Class of Antimicrobial Peptides from the Skin Secretion of the Fujian Large-Headed Frog (*Limnonectes Fujianensis*). *Biochimie* **2011**, *93* (6), 981–987. <https://doi.org/10.1016/j.biochi.2011.03.003>.

(290) Ma, Y.; Liu, C.; Liu, X.; Wu, J.; Yang, H.; Wang, Y.; Li, J.; Yu, H.; Lai, R. Peptidomics and Genomics Analysis of Novel Antimicrobial Peptides from the Frog, *Rana Nigrovittata*. *Genomics* **2010**, *95* (1), 66–71. <https://doi.org/10.1016/j.ygeno.2009.09.004>.

(291) Xu, X.; Lai, R. The Chemistry and Biological Activities of Peptides from Amphibian Skin Secretions. *Chem. Rev.* **2015**, *115* (4), 1760–1846. <https://doi.org/10.1021/cr4006704>.

(292) Yang, H.; Wang, X.; Liu, X.; Wu, J.; Liu, C.; Gong, W.; Zhao, Z.; Hong, J.; Lin, D.; Wang, Y.; Lai, R. Antioxidant Peptidomics Reveals Novel Skin Antioxidant System. *Mol. Cell. Proteomics* **2008**, *8* (3), 571–583. <https://doi.org/10.1074/mcp.m800297-mcp200>.

(293) Dong, Z.; Luo, W.; Zhong, H.; Wang, M.; Song, Y.; Deng, S.; Zhang, Y. Molecular

Cloning and Characterization of Antimicrobial Peptides from Skin of *Hylarana Guentheri*.
Acta Biochim. Biophys. Sin. (Shanghai). **2017**, *49* (5), 450–457.
<https://doi.org/10.1093/abbs/gmx023>.

(294) Lynn, D. J.; Higgs, R.; Gaines, S.; Tierney, J.; James, T.; Lloyd, A. T.; Fares, M. A.; Mulcahy, G.; O'Farrelly, C. Bioinformatic Discovery and Initial Characterisation of Nine Novel Antimicrobial Peptide Genes in the Chicken. *Immunogenetics* **2004**, *56* (3), 170–177. <https://doi.org/10.1007/s00251-004-0675-0>.

(295) Zanutto-Elgui, M. R.; Vieira, J. C. S.; Prado, D. Z. do; Buzalaf, M. A. R.; Padilha, P. de M.; Elgui de Oliveira, D.; Fleuri, L. F. Production of Milk Peptides with Antimicrobial and Antioxidant Properties through Fungal Proteases. *Food Chem.* **2019**, *278* (25), 823–831. <https://doi.org/10.1016/j.foodchem.2018.11.119>.

(296) Lee, M. O.; Jang, H. J.; Rengaraj, D.; Yang, S. Y.; Han, J. Y.; Lamont, S. J.; Womack, J. E. Tissue Expression and Antibacterial Activity of Host Defense Peptides in Chicken. *BMC Vet. Res.* **2016**, *12* (231), 1–9. <https://doi.org/10.1186/s12917-016-0866-6>.

(297) Rydengard, V.; Olsson, A. K.; Morgelin, M.; Schmidtchen, A. Histidine-Rich Glycoprotein Exerts Antibacterial Activity. *FEBS J* **2007**, *274* (2), 377–389. <https://doi.org/10.1111/j.1742-4658.2006.05586.x>.

(298) Pasupuleti, M.; Roupe, M.; Rydengård, V.; Surewicz, K.; Surewicz, W. K.; Chalupka, A.; Malmsten, M.; Soörensen, O. E.; Schmidtchen, A. Antimicrobial Activity of Human Prion Protein Is Mediated by Its N-Terminal Region. *PLoS One* **2009**, *4* (10). <https://doi.org/10.1371/journal.pone.0007358>.

(299) Ringstad, L.; Kacprzyk, L.; Schmidtchen, A.; Malmsten, M. Effects of Topology, Length,

and Charge on the Activity of a Kininogen-Derived Peptide on Lipid Membranes and Bacteria. *Biochim. Biophys. Acta - Biomembr.* **2007**, *1768* (3), 715–727.
<https://doi.org/10.1016/j.bbamem.2006.11.016>.

(300) Sadaf, Z.; Shahid, P. B.; Bilqees, B. Isolation, Characterization and Kinetics of Goat Cystatins. *Comp. Biochem. Physiol. - B Biochem. Mol. Biol.* **2005**, *142* (4), 361–368.
<https://doi.org/10.1016/j.cbpb.2005.08.007>.

(301) Mitta, G.; Hubert, F.; Noël, T.; Roch, P. Myticin, a Novel Cysteine-Rich Antimicrobial Peptide Isolated from Haemocytes and Plasma of the Mussel *Mytilus galloprovincialis*. *Eur. J. Biochem.* **1999**, *265* (1), 71–78. <https://doi.org/10.1046/j.1432-1327.1999.00654.x>.

(302) Liao, Z.; Wang, X.; Liu, H.; Fan, M.; Sun, J.; Shen, W. Molecular Characterization of a Novel Antimicrobial Peptide from *Mytilus coruscus*. *Fish Shellfish Immunol.* **2013**, *34* (2), 610–616. <https://doi.org/10.1016/j.fsi.2012.11.030>.

(303) Oh, R.; Lee, M. J.; Kim, Y. O.; Nam, B. H.; Kong, H. J.; Kim, J. W.; Park, J. yeon; Seo, J. K.; Kim, D. G. Myticusin-Beta, Antimicrobial Peptide from the Marine Bivalve, *Mytilus coruscus*. *Fish Shellfish Immunol.* **2020**, *99*, 342–352.
<https://doi.org/10.1016/j.fsi.2020.02.020>.

(304) McClintock, M. K.; Kaznessis, Y. N.; Hackel, B. J. Enterocin A Mutants Identified by Saturation Mutagenesis Enhance Potency Towards Vancomycin-Resistant Enterococci. *Biotechnol Bioeng.* **2016**, *113* (2), 414–423. <https://doi.org/10.1002/bit.25710>.

(305) Tosukhowong, A.; Zendo, T.; Visessanguan, W.; Roytrakul, S.; Pumpuang, L.; Jaresitthikunchai, J.; Sonomoto, K. Garvieacin Q, a Novel Class II Bacteriocin from *Lactococcus Garvieae* BCC 43578. *Appl. Environ. Microbiol.* **2012**, *78* (5), 1619–1623.

<https://doi.org/10.1128/aem.06891-11>.

(306) Hu, M.; Zhao, H.; Zhang, C.; Yu, J.; Lu, Z. Purification and Characterization of Plantaricin 163, a Novel Bacteriocin Produced by *Lactobacillus Plantarum* 163 Isolated from Traditional Chinese Fermented Vegetables. *J. Agric. Food Chem.* **2013**, *61* (47), 11676–11682. <https://doi.org/10.1021/jf403370y>.

(307) Anderssen, E. L.; Diep, D. B.; Nes, I. F.; Eijsink, V. G. H.; Nissen-Meyer, J. Antagonistic Activity of *Lactobacillus Plantarum* C11: Two New Two- Peptide Bacteriocins, Plantaricins EF and JK, and the Induction Factor Plantaricin A. *Appl. Environ. Microbiol.* **1998**, *64* (6), 2269–2272. <https://doi.org/10.1128/aem.64.6.2269-2272.1998>.

(308) Kanatani, K.; Tahara, T.; Oshimura, M.; Sano, K.; Umezawa, C. Cloning and Nucleotide Sequence of the Gene for Acidocin 8912, a Bacteriocin from *Lactobacillus Acidophilus* TK8912. *Lett. Appl. Microbiol.* **1995**, *21* (6), 384–386. <https://doi.org/10.1111/j.1472-765x.1995.tb01087.x>.

(309) Tasiemski, A.; Vandenbulcke, F.; Mitta, G.; Lemoine, J.; Lefebvre, C.; Sautière, P. E.; Salzet, M. Molecular Characterization of Two Novel Antibacterial Peptides Inducible upon Bacterial Challenge in an Annelid, the Leech *Theromyzon Tessulatum*. *J. Biol. Chem.* **2004**, *279* (30), 30973–30982. <https://doi.org/10.1074/jbc.M312156200>.

(310) Cui, P.; Dong, Y.; Li, Z.; Zhang, Y.; Zhang, S. Identification and Functional Characterization of an Uncharacterized Antimicrobial Peptide from a Ciliate *Paramecium Caudatum*. *Dev. Comp. Immunol.* **2016**, *60*, 53–65.
<https://doi.org/10.1016/j.dci.2016.02.016>.

(311) Jabrane, A.; Sabri, A.; Compere, P.; Jacques, P.; Vandenberghe, I.; Beeumen, J. Van;

Thornart, P. Characterization of Serracin P, a Phage-Tail-Like Bacteriocin, and Its Activity against *Erwinia Amylovora*, the Fire Blight Pathogen. *Appl. Environ. Microbiol.* **2002**, *68* (11), 5704–5710. <https://doi.org/10.1128/AEM.68.11.5704-5710.2002>.

(312) Park, C. J.; Park, C. B.; Hong, S. S.; Lee, H. S.; Lee, S. Y.; Kim, S. C. Characterization and CDNA Cloning of Two Glycine- and Histidine-Rich Antimicrobial Peptides from the Roots of Shepherd's Purse, *Capsella Bursa-Pastoris*. *Plant Mol. Biol.* **2000**, *44* (2), 187–197. <https://doi.org/10.1023/A:1006431320677>.

(313) Hoeckendorf, A.; Stanisak, M.; Leippe, M. The Saposin-like Protein SPP-12 Is an Antimicrobial Polypeptide in the Pharyngeal Neurons of *Caenorhabditis Elegans* and Participates in Defence against a Natural Bacterial Pathogen. *Biochem. J.* **2012**, *445* (2), 205–212. <https://doi.org/10.1042/BJ20112102>.

(314) Cusimano, M. G.; Spinello, A.; Barone, G.; Schillaci, D.; Cascioferro, S.; Magistrato, A.; Parrino, B.; Arizza, V.; Vitale, M. A Synthetic Derivative of Antimicrobial Peptide Holothuroidin 2 from Mediterranean Sea Cucumber (*Holothuria Tubulosa*) in the Control of *Listeria Monocytogenes*. *Mar. Drugs* **2019**, *17* (3), 1–11.
<https://doi.org/10.3390/md17030159>.

(315) Solstad, R. G.; Li, C.; Isaksson, J.; Johansen, J.; Svenson, J.; Stensvåg, K.; Haug, T. Novel Antimicrobial Peptides EeCentrocins 1, 2 and EeStrongylocin 2 from the Edible Sea Urchin *Echinus Esculentus* Have 6-Br-Trp Post-Translational Modifications. *PLoS One* **2016**, *11* (3), 1–25. <https://doi.org/10.1371/journal.pone.0151820>.

(316) Oyama, L. B.; Girdwood, S. E.; Cookson, A. R.; Fernandez-fuentes, N.; Privé, F.; Vallin, H. E.; Wilkinson, T. J.; Golyshin, P. N.; Golyshina, O. V; Mikut, R.; Hilpert, K.;

Richards, J.; Wooton, M.; Edwards, J. E.; Maresca, M.; Perrier, J.; Lundy, F. T.; Luo, Y.; Zhou, M.; Hess, M.; Mantovani, H. C.; Creevey, C. J.; Huws, S. A. The Rumen Microbiome: An Underexplored Resource for Novel Antimicrobial Discovery. *Nat. Biofilms Microbiomes* **2017**, *3* (33), 1–9. [https://doi.org/https://doi.org/10.1038/s41522-017-0042-1](https://doi.org/10.1038/s41522-017-0042-1).

(317) Sudmoon, R.; Sattayasai, N.; Bunyatratchata, W.; Chaveerach, A. Thermostable Mannose-Binding Lectin from *Dendrobium* *Findleyanum* with Activities Dependent on Sulfhydryl Content. *Acta Biochim. Biophys. Sin. (Shanghai)*. **2008**, *40* (9), 811–818. <https://doi.org/https://doi.org/10.1093/abbs/40.9.811>.

(318) Hodgkinson, V.; Petris, M. J. Copper Homeostasis at the Host-Pathogen Interface. *J. Biol. Chem.* **2012**, *287* (17), 13549–13555. <https://doi.org/10.1074/jbc.R111.316406>.

(319) Aruoma, O. I.; Reilly, T.; MacLaren, D.; Halliwell, B. Iron, Copper and Zinc Concentrations in Human Sweat and Plasma; the Effect of Exercise. *Clin. Chim. Acta* **1988**, *177* (1), 81–88. [https://doi.org/10.1016/0009-8981\(88\)90310-5](https://doi.org/10.1016/0009-8981(88)90310-5).

(320) Chinevere, T. D.; McClung, J. P.; Cheuvront, S. N. Trace Mineral Losses in Sweat. *Curr. Nutr. Food Sci.* **2007**, *3* (3), 236–241. <https://doi.org/10.2174/157340107781369215>.

(321) Walsh, G.; Jefferis, R. Post-Translational Modifications in the Context of Therapeutic Proteins. *Nat. Biotechnol.* **2006**, *24* (10), 1241–1252. <https://doi.org/10.1038/nbt1252>.

(322) Elwell, C. E.; Gagnon, N. L.; Neisen, B. D.; Dhar, D.; Spaeth, A. D.; Yee, G. M.; Tolman, W. B. Copper–Oxygen Complexes Revisited: Structures, Spectroscopy, and Reactivity. *Chem Rev.* **2017**, *117* (3), 2059–2107. <https://doi.org/10.1021/acs.chemrev.6b00636>.

(323) Bradford, S.; Cowan, J. A. Catalytic Metallocdrugs Targeting HCV IRES RNA. *Chem. Commun.* **2012**, *48* (25), 3118–3120. <https://doi.org/10.1039/c2cc17377h>.

(324) Alexander, J. L.; Yu, Z.; Cowan, J. A. Amino Terminal Copper and Nickel Binding Motif Derivatives of Ovispirin-3 Display Increased Antimicrobial Activity via Lipid Oxidation. *J. Med. Chem.* **2017**, *60* (24), 10047–10055. <https://doi.org/10.1021/acs.jmedchem.7b01117>.

(325) Alexander, J. L.; Thompson, Z.; Yu, Z.; Cowan, J. A. Cu-ATCUN Derivatives of Sub5 Exhibit Enhanced Antimicrobial Activity via Multiple Modes of Action. *ACS Chem. Biol.* **2019**, *14* (3), 449–458. <https://doi.org/10.1021/acschembio.8b01087>.

(326) Atkinson, H. J.; Morris, J. H.; Ferrin, T. E.; Babbitt, P. C. Using Sequence Similarity Networks for Visualization of Relationships across Diverse Protein Superfamilies. *PLoS One* **2009**, *4* (2), 1–14. <https://doi.org/10.1371/journal.pone.0004345>.

(327) Camacho, C.; Coulouris, G.; Avagyan, V.; Ma, N.; Papadopoulos, J.; Bealer, K.; Madden, T. L. BLAST+: Architecture and Applications. *BMC Bioinformatics* **2009**, *10* (421), 1–9. <https://doi.org/10.1186/1471-2105-10-421>.

(328) Sievers, F.; Wilm, A.; Dineen, D.; Gibson, T. J.; Karplus, K.; Li, W.; Lopez, R.; McWilliam, H.; Remmert, M.; Söding, J.; Thompson, J. D.; Higgins, D. G. Fast, Scalable Generation of High-Quality Protein Multiple Sequence Alignments Using Clustal Omega. *Mol. Syst. Biol.* **2011**, *7* (539), 1–6. <https://doi.org/10.1038/msb.2011.75>.

(329) Radulovic, Z. M.; Kim, T. K.; Porter, L. M.; Sze, S.-H.; Lewis, L.; Mulenga, A. A 24-48 h Fed Amblyomma Americanum Tick Saliva Immuno-Proteome. *BMC Genomics* **2014**, *15* (518), 1–30. <https://doi.org/10.1186/1471-2164-15-518>.

(330) Libardo, M. D. J.; Wang, T. Y.; Pellois, J. P.; Angeles-Boza, A. M. How Does Membrane Oxidation Affect Cell Delivery and Cell Killing? *Trends Biotechnol.* **2017**, *35* (8), 686–690. <https://doi.org/10.1016/j.tibtech.2017.03.015>.

(331) Wang, T.-Y.; Libardo, M. D. J.; Angeles-Boza, A. M.; Pellois, J.-P. Membrane Oxidation in Cell Delivery and Cell Killing Applications. *ACS Chem. Biol.* **2017**, *12* (5), 1170–1182. <https://doi.org/10.1021/acscchembio.7b00237>.

(332) Boylan, J. A.; Lawrence, K. A.; Downey, J. S.; Gherardini, F. C. Borrelia Burgdorferi Membranes Are the Primary Targets of Reactive Oxygen Species. *Mol. Microbiol.* **2008**, *68* (3), 786–799. <https://doi.org/10.1111/j.1365-2958.2008.06204.x>.

(333) Ledin, K. E.; Zeidner, N. S.; Ribeiro, J. M. C.; Biggerstaff, B. J.; Dolan, M. C.; Dietrich, G.; Vredevoe, L.; Piesman, J. Borreliacidal Activity of Saliva of the Tick Amblyomma Americanum. *Med. Vet. Entomol.* **2005**, *19* (1), 90–95. <https://doi.org/10.1111/j.0269-283X.2005.00546.x>.

(334) Unckless, R. L.; Howick, V. M.; Lazzaro, B. P. Convergent Balancing Selection on an Antimicrobial Peptide in Drosophila. *Curr Biol.* **2016**, *26* (2), 257–262. <https://doi.org/10.1016/j.cub.2015.11.063>.

(335) Unckless, R. L.; Lazzaro, B. P. The Potential for Adaptive Maintenance of Diversity in Insect Antimicrobial Peptides. *Philos. Trans. R. Soc. B Biol. Sci.* **2016**, *371* (1695). <https://doi.org/10.1098/rstb.2015.0291>.

(336) Rahnamaeian, M.; Cytrynska, M.; Zdybicka-Barabas, A.; Dobslaff, K.; Wiesner, J.; Twyman, R. M.; Zuchner, T.; Sadd, B. M.; Regoes, R. R.; Schmid-Hempel, P.; Vilcinskas, A. Insect Antimicrobial Peptides Show Potentiating Functional Interactions

against Gram-Negative Bacteria. *Proc Biol Sci* **2015**, *282* (1806), 1–10.

<https://doi.org/10.1098/rspb.2015.0293>.

(337) Rahnamaeian, M.; Cytrynska, M.; Zdybicka-Barabas, A.; Vilcinskas, A. The Functional Interaction between Abaecin and Pore-Forming Peptides Indicates a General Mechanism of Antibacterial Potentiation. *Peptides* **2016**, *78*, 17–23.

<https://doi.org/10.1016/j.peptides.2016.01.016>.

(338) Nygaard, S.; Zhang, G.; Schiøtt, M.; Li, C.; Wurm, Y.; Hu, H.; Zhou, J.; Ji, L.; Qiu, F.; Rasmussen, M.; Pan, H.; Hauser, F.; Krogh, A.; Grimmelikhuijen, C. J. P.; Wang, J.; Boomsma, J. J. The Genome of the Leaf-Cutting Ant *Acromyrmex echinatior* Suggests Key Adaptations to Advanced Social Life and Fungus Farming. *Genome Res.* **2011**, *21* (8), 1339–1348. <https://doi.org/10.1101/gr.121392.111>.

(339) Weber, N. A. Fungus-Growing Ants and Their Fungi: *Cyphomyrmex costatus*. *Ecology* **1957**, *38* (3), 480–494. <https://doi.org/10.2307/1929893>.

(340) Shrestha, B. Cordyceps Species Parasitizing Hymenopteran and Hemipteran Insects. *Mycosphere* **2018**, *8* (9), 1424–1442. <https://doi.org/10.5943/mycosphere/8/9/8>.

(341) Wurm, Y.; Wang, J.; Riba-Grognuz, O.; Corona, M.; Nygaard, S.; Hunt, B. G.; Ingram, K.; Falquet, L.; Nipitwattanaphon, M.; Gotzek, D.; Dijkstra, M. B.; Oettler, J.; Comtesse, F.; Shih, C.-J.; Wu, W.-J.; Yang, C.-C.; Thomas, J.; Beaudoin, E.; Pradervand, S.; Flegel, V.; Cook, E. D.; Fabbretti, R.; Stockinger, H.; Long, L.; Farmerie, W. G.; Oakey, J.; Boomsma, J. J.; Pamilo, P.; Yi, S. V.; Heinze, J.; Goodisman, M. A. D.; Farinelli, L.; Harshman, K.; Hulo, N.; Cerutti, L.; Xenarios, I.; Shoemaker, D.; Keller, L. The Genome of the Fire Ant *Solenopsis invicta*. *Proc. Natl. Acad. Sci.* **2011**, *108* (14), 5679–5684.

<https://doi.org/10.1073/pnas.1009690108>.

(342) Smith, C. R.; Smith, C. D.; Robertson, H. M.; Helmkampf, M.; Zimin, A.; Yandell, M.; Holt, C.; Hu, H.; Abouheif, E.; Benton, R.; Cash, E.; Croset, V.; Currie, C. R.; Elhaik, E.; Elsik, C. G.; Fave, M.-J.; Fernandes, V.; Gibson, J. D.; Graur, D.; Gronenberg, W.; Grubbs, K. J.; Hagen, D. E.; Viniegra, A. S. I.; Johnson, B. R.; Johnson, R. M.; Khila, A.; Kim, J. W.; Mathis, K. A.; Munoz-Torres, M. C.; Murphy, M. C.; Mustard, J. A.; Nakamura, R.; Niehuis, O.; Nigam, S.; Overson, R. P.; Placek, J. E.; Rajakumar, R.; Reese, J. T.; Suen, G.; Tao, S.; Torres, C. W.; Tsutsui, N. D.; Viljakainen, L.; Wolschin, F.; Gadau, J. Draft Genome of the Red Harvester Ant *Pogonomyrmex barbatus*. *Proc. Natl. Acad. Sci.* **2011**, *108* (14), 5667–5672. <https://doi.org/10.1073/pnas.1007901108>.

(343) Mulero, I.; Noga, E. J.; Meseguer, J.; García-Ayala, A.; Mulero, V. The Antimicrobial Peptides Piscidins Are Stored in the Granules of Professional Phagocytic Granulocytes of Fish and Are Delivered to the Bacteria-Containing Phagosome upon Phagocytosis. *Dev. Comp. Immunol.* **2008**, *32* (12), 1531–1538. <https://doi.org/10.1016/j.dci.2008.05.015>.

(344) Silphaduang, U.; Noga, E. J. Peptide Antibiotics in Mast Cells of Fish. *Nature* **2001**, *414* (6861), 268–269. <https://doi.org/10.1038/35104690>.

(345) Silphaduang, U.; Colorni, A.; Noga, E. J. Evidence for Widespread Distribution of Piscidin Antimicrobial Peptides in Teleost Fish. *Dis. Aquat. Organ.* **2006**, *72* (3), 241–252. <https://doi.org/10.3354/dao072241>.

(346) Chekmenev, E. Y.; Vollmar, B. S.; Forseth, K. T.; Manion, M. N.; Jones, S. M.; Wagner, T. J.; Endicott, R. L. M.; Kyriss, B. P.; Homem, L. M.; Pate, M.; He, J.; Raines, J.; Gor'kov, P. L.; Brey, W. W.; Mitchell, D. J.; Auman, A. J.; Ellard-Ivey, M. J.; Blazyk, J.;

Cotten, M. Investigating Molecular Recognition and Biological Function at Interfaces Using Piscidins, Antimicrobial Peptides from Fish. *Biochim. Biophys. Acta - Biomembr.* **2006**, *1758* (9), 1359–1372. <https://doi.org/10.1016/j.bbamem.2006.03.034>.

(347) McDonald, M.; Mannion, M.; Pike, D.; Lewis, K.; Flynn, A.; Brannan, A. M.; Browne, M. J.; Jackman, D.; Madera, L.; Power Coombs, M. R.; Hoskin, D. W.; Rise, M. L.; Booth, V. Structure-Function Relationships in Histidine-Rich Antimicrobial Peptides from Atlantic Cod. *Biochim. Biophys. Acta - Biomembr.* **2015**, *1848* (7), 1451–1461. <https://doi.org/10.1016/j.bbamem.2015.03.030>.

(348) Ruangsri, J.; Fernandes, J. M. O.; Rombout, J. H. W. M.; Brinchmann, M. F.; Kiron, V. Ubiquitous Presence of Piscidin-1 in Atlantic Cod as Evidenced by Immunolocalisation. *BMC Vet. Res.* **2012**, *8* (46), 1–13. <https://doi.org/10.1186/1746-6148-8-46>.

(349) Colorni, A.; Ullal, A.; Heinisch, G.; Noga, E. J. Activity of the Antimicrobial Polypeptide Piscidin 2 against Fish Ectoparasites. *J. Fish Dis.* **2008**, *31* (6), 423–432. <https://doi.org/10.1111/j.1365-2761.2008.00922.x>.

(350) Hayden, R. M.; Goldberg, G. K.; Ferguson, B. M.; Schoeneck, M. W.; Libardo, M. D. J.; Mayeux, S. E.; Shrestha, A.; Bogardus, K. A.; Hammer, J.; Pryshchep, S.; Lehman, H. K.; McCormick, M. L.; Blazyk, J.; Angeles-Boza, A. M.; Fu, R.; Cotten, M. L. Complementary Effects of Host Defense Peptides Piscidin 1 and Piscidin 3 on DNA and Lipid Membranes: Biophysical Insights into Contrasting Biological Activities. *J. Phys. Chem. B* **2015**, *119* (49), 15235–15246. <https://doi.org/10.1021/acs.jpcb.5b09685>.

(351) Sung, W. S.; Lee, J.; Lee, D. G. Fungicidal Effect and the Mode of Action of Piscidin 2 Derived from Hybrid Striped Bass. *Biochem. Biophys. Res. Commun.* **2008**, *371* (3), 551–

555. <https://doi.org/10.1016/j.bbrc.2008.04.107>.

(352) Chinchar, V. G.; Bryan, L.; Silphadaung, U.; Noga, E.; Wade, D.; Rollins-Smith, L.

Inactivation of Viruses Infecting Ectothermic Animals by Amphibian and Piscine Antimicrobial Peptides. *Virology* **2004**, *323* (2), 268–275.

<https://doi.org/10.1016/j.virol.2004.02.029>.

(353) Perrin, B. S.; Fu, R.; Cotten, M. L.; Pastor, R. W. Simulations of Membrane-Disrupting Peptides II: AMP Piscidin 1 Favors Surface Defects over Pores. *Biophys. J.* **2016**, *111* (6),

1258–1266. <https://doi.org/10.1016/j.bpj.2016.08.015>.

(354) Perrin, B. S.; Tian, Y.; Fu, R.; Grant, C. V.; Chekmenev, E. Y.; Wieczorek, W. E.; Dao, A. E.; Hayden, R. M.; Burzynski, C. M.; Venable, R. M.; Sharma, M.; Opella, S. J.; Pastor, R. W.; Cotten, M. L. High-Resolution Structures and Orientations of

Antimicrobial Peptides Piscidin 1 and Piscidin 3 in Fluid Bilayers Reveal Tilting, Kinking, and Bilayer Immersion. *J. Am. Chem. Soc.* **2014**, *136* (9), 3491–3504.

<https://doi.org/10.1021/ja411119m>.

(355) Kim, S. Y.; Zhang, F.; Gong, W.; Chen, K.; Xia, K.; Liu, F.; Gross, R. A.; Wang, J. M.; Linhardt, R. J.; Cotten, M. L. Copper Regulates the Interactions of Antimicrobial Piscidin Peptides from Fish Mast Cells with Formyl Peptide Receptors and Heparin. *J. Biol. Chem.*

2018, *293* (40), 15381–15396. <https://doi.org/10.1074/jbc.RA118.001904>.

(356) Dorward, D. A.; Lucas, C. D.; Chapman, G. B.; Haslett, C.; Dhaliwal, K.; Rossi, A. G.

The Role of Formylated Peptides and Formyl Peptide Receptor 1 in Governing Neutrophil Function during Acute Inflammation. *Am. J. Pathol.* **2015**, *185* (5), 1172–1184.

<https://doi.org/10.1016/j.ajpath.2015.01.020>.

(357) Lieke, T.; Meinelt, T.; Hoseinifar, S. H.; Pan, B.; Straus, D. L.; Steinberg, C. E. W. Sustainable Aquaculture Requires Environmental-Friendly Treatment Strategies for Fish Diseases. *Rev. Aquac.* **2019**, *12* (2), 943–965. <https://doi.org/10.1111/raq.12365>.

(358) Chang, T. W.; Wei, S. Y.; Wang, S. H.; Wei, H. M.; Wang, Y. J.; Wang, C. F.; Chen, C.; Liao, Y. Di. Hydrophobic Residues Are Critical for the Helix-Forming, Hemolytic and Bactericidal Activities of Amphipathic Antimicrobial Peptide TP4. *PLoS One* **2017**, *12* (10), 1–22. <https://doi.org/10.1371/journal.pone.0186442>.

(359) Terova, G.; Cattaneo, A. G.; Preziosa, E.; Bernardini, G.; Saroglia, M. Impact of Acute Stress on Antimicrobial Polypeptides mRNA Copy Number in Several Tissues of Marine Sea Bass (*Dicentrarchus Labrax*). *BMC Immunol.* **2011**, *12* (1), 69. <https://doi.org/10.1186/1471-2172-12-69>.

(360) Portelinha, J. Examining the Role of Histidine in the Antimicrobial Peptide Gaduscidin-1, 2018.

(361) Khatami, M. H.; Bromberek, M.; Saika-Voivod, I.; Booth, V. Molecular Dynamics Simulations of Histidine-Containing Cod Antimicrobial Peptide Paralogs in Self-Assembled Bilayers. *Biochim. Biophys. Acta - Biomembr.* **2014**, *1838* (11), 2778–2787. <https://doi.org/10.1016/j.bbamem.2014.07.013>.

(362) Esteban-Martín, S.; Salgado, J. Self-Assembling of Peptide/Membrane Complexes by Atomistic Molecular Dynamics Simulations. *Biophys. J.* **2007**, *92* (3), 903–912. <https://doi.org/10.1529/biophysj.106.093013>.

(363) Cantisani, M.; Leone, M.; Mignogna, E.; Kampanaraki, K.; Falanga, A.; Morelli, G.; Galdiero, M.; Galdiero, S. Structure-Activity Relations of Myxinidin, an Antibacterial

Peptide Derived from the Epidermal Mucus of Hagfish. *Antimicrob. Agents Chemother.* **2013**, *57* (11), 5665–5673. <https://doi.org/10.1128/AAC.01341-13>.

(364) Cantisani, M.; Finamore, E.; Mignogna, E.; Falanga, A.; Nicoletti, G. F.; Pedone, C.; Morelli, G.; Leone, M.; Galdiero, M.; Galdiero, S. Structural Insights into and Activity Analysis of the Antimicrobial Peptide Myxinidin. *Antimicrob. Agents Chemother.* **2014**, *58* (9), 5280–5290. <https://doi.org/10.1128/AAC.02395-14>.

(365) Hancock, R. E. Peptide Antibiotics. *Lancet* **1997**, *349* (9049), 418–422. [https://doi.org/10.1016/S0140-6736\(97\)80051-7](https://doi.org/10.1016/S0140-6736(97)80051-7).

(366) Imai, Y.; Meyer, K. J.; Iinishi, A.; Favre-Godal, Q.; Green, R.; Manuse, S.; Caboni, M.; Mori, M.; Niles, S.; Ghiglieri, M.; Honrao, C.; Ma, X.; Guo, J. J.; Makriyannis, A.; Linares-Otoya, L.; Böhringer, N.; Wuisan, Z. G.; Kaur, H.; Wu, R.; Mateus, A.; Typas, A.; Savitski, M. M.; Espinoza, J. L.; O'Rourke, A.; Nelson, K. E.; Hiller, S.; Noinaj, N.; Schäberle, T. F.; D'Onofrio, A.; Lewis, K. A New Antibiotic Selectively Kills Gram-Negative Pathogens. *Nature* **2019**, *576* (7787), 459–464. <https://doi.org/10.1038/s41586-019-1791-1>.

(367) Chen, W. C.; Sud, I. J.; Chou, D.-L.; Feingold, D. S. Selective Toxicity of the Polyene Antibiotics and Their Methyl Ester Derivatives. *Biochem. Biophys. Res. Commun.* **1977**, *74* (2), 480–487. [https://doi.org/10.1016/0006-291X\(77\)90329-1](https://doi.org/10.1016/0006-291X(77)90329-1).

(368) Tran, K. K.; Jayawardena, B. M.; Elphick, M. R.; Jones, C. E. A Gonadotropin-Releasing Hormone Type Neuropeptide with a High Affinity Binding Site for Copper(II) and Nickel(II). *Metallomics* **2019**, *11* (2), 404–414. <https://doi.org/10.1039/c8mt00279g>.

(369) Nakamura, K.; Kodaka, M.; El-Mehasseb, I. M.; Gajewska, A.; Okuno, H.;

Ochwanowska, E.; Witek, B.; Kozłowski, H.; Kochman, K. Further Structural Analysis of GnRH Complexes with Metal Ions. *Neuroendocrinol. Lett.* **2005**, *26* (3), 247–252.

(370) Fernandes, J. M. O.; Ruangsri, J.; Kiron, V. Atlantic Cod Piscidin and Its Diversification through Positive Selection. *PLoS One* **2010**, *5* (3), 1–7.
<https://doi.org/10.1371/journal.pone.0009501>.

(371) Holland, L. Z. Tunicates. *Curr. Biol.* **2016**, *26* (4), R146–R152.
<https://doi.org/10.1016/j.cub.2015.12.024>.

(372) Rinkevich, B. Primitive Immune Systems: Are Your Ways My Ways? *Immunol. Rev.* **2004**, *198* (1), 25–35. <https://doi.org/10.1111/j.0105-2896.2004.0114.x>.

(373) Dishaw, L. J.; Flores-Torres, J. A.; Mueller, M. G.; Karrer, C. R.; Skapura, D. P.; Melillo, D.; Zucchetti, I.; De Santis, R.; Pinto, M. R.; Litman, G. W. A Basal Chordate Model for Studies of Gut Microbial Immune Interactions. *Front. Immunol.* **2012**, *3* (96), 1–10.
<https://doi.org/10.3389/fimmu.2012.00096>.

(374) Menna, M.; Aiello, A. The Chemistry of Marine Tunicates. In *Handbook of Marine Natural Products*; 2012; pp 295–385.

(375) Fenical, W. Geranyl Hydroquinone, a Cancer-Protective Agent from the Tunicate Aplidium Species. *Food-Drugs Sea Proc* **1976**, *4*, 388–394.

(376) Sings, H. L.; Rinehart, K. L. Compounds Produced from Potential Tunicate-Blue-Green Algal Symbiosis: A Review. *J. Ind. Microbiol.* **1996**, *17*, 385–396.
<https://doi.org/https://doi.org/10.1007/BF01574769>.

(377) Fu, X.; Do, T.; Schmitz, F. J.; Andrusevich, V.; Engel, M. H. New Cyclic Peptides from

the Ascidian *Lissoclinum Patella*. *J. Nat. Prod.* **1998**, *61* (12), 1547–1551.
<https://doi.org/10.1021/np9802872>.

(378) Schmidt, E. W.; Nelson, J. T.; Rasko, D. A.; Sudek, S.; Eisen, J. A.; Haygood, M. G.; Ravel, J. Patellamide A and C Biosynthesis by a Microcin-like Pathway in Prochloron Didemni, the Cyanobacterial Symbiont of *Lissoclinum Patella*. *Proc. Natl. Acad. Sci. U. S. A.* **2005**, *102* (20), 7315–7320. <https://doi.org/10.1073/pnas.0501424102>.

(379) Long, P. F.; Dunlap, W. C.; Battershill, C. N.; Jaspars, M. Shotgun Cloning and Heterologous Expression of the Patellamide Gene Cluster as a Strategy to Achieving Sustained Metabolite Production. *ChemBioChem* **2005**, *6* (10), 1760–1765.
<https://doi.org/10.1002/cbic.200500210>.

(380) Nganga, J. K.; Samanamu, C. R.; Tanski, J. M.; Pacheco, C.; Saucedo, C.; Batista, V. S.; Grice, K. A.; Ertem, M. Z.; Angeles-Boza, A. M. Electrochemical Reduction of CO₂ Catalyzed by Re(Pyridine-Oxazoline)(CO)3Cl Complexes. *Inorg. Chem.* **2017**, *56* (6), 3214–3226. <https://doi.org/10.1021/acs.inorgchem.6b02384>.

(381) Koehnke, J.; Bent, A. F.; Houssen, W. E.; Mann, G.; Jaspars, M.; Naismith, J. H. The Structural Biology of Patellamide Biosynthesis. *Curr. Opin. Struct. Biol.* **2014**, *29*, 112–121. <https://doi.org/10.1016/j.sbi.2014.10.006>.

(382) Freeman, D. J.; Pattenden, G.; Drake, A. F.; Siligardi, G. Marine Metabolites and Metal Ion Chelation. Circular Dichroism Studies of Metal Binding to *Lissoclinum Cyclopeptides*. *J. Chem. Soc. Perkin Trans. 2* **1998**, No. 1, 129–135.
<https://doi.org/10.1039/a703530f>.

(383) van den Brenk, A. L.; Byriel, K. A.; Fairlie, D. P.; Gahan, L. R.; Hanson, G. R.; Hawkins,

C. J.; Jones, A.; Kennard, C. H. L.; Moubaraki, B.; Murray, K. S. Crystal Structure and Electrospray Ionization Mass Spectrometry, Electron Paramagnetic Resonance, and Magnetic Susceptibility Study of $[\text{Cu}_2(\text{AscidH}_2)(1,2-\mu\text{-CO}_3)(\text{H}_2\text{O})_2] \cdot 2\text{H}_2\text{O}$, the Bis(Copper(II)) Complex of Ascidiacyclamide (AscidH4), a Cyclic Peptide Isolat. *Inorg. Chem.* **1994**, *33* (16), 3549–3557. <https://doi.org/10.1021/ic00094a019>.

(384) Macara, I. G.; McLeod, G. C.; Kustin, K. Tunichromes and Metal Ion Accumulation in Tunicate Blood Cells. *Comp. Biochem. Physiol. -- Part B Biochem.* **1979**, *63* (3), 299–302. [https://doi.org/10.1016/0305-0491\(79\)90252-9](https://doi.org/10.1016/0305-0491(79)90252-9).

(385) Lee, I. H.; Cho, Y.; Lehrer, R. I. Styelins, Broad-Spectrum Antimicrobial Peptides from the Solitary Tunicate, *Styela Clava*. *Comp. Biochem. Physiol. - B Biochem. Mol. Biol.* **1997**, *118* (3), 515–521. [https://doi.org/10.1016/S0305-0491\(97\)00109-0](https://doi.org/10.1016/S0305-0491(97)00109-0).

(386) Lehrer, R. I.; Tincu, J. A.; Taylor, S. W.; Menzel, L. P.; Waring, A. J. Natural Peptide Antibiotics from Tunicates: Structures, Functions and Potential Uses. *Integr. Comp. Biol.* **2003**, *43* (2), 313–322. <https://doi.org/10.1093/icb/43.2.313>.

(387) Azumi, K.; Yokosawa, H.; Ishii, S. I. Halocyamines: Novel Antimicrobial Tetrapeptide-like Substances Isolated from the Hemocytes of the Solitary Ascidian *Halocynthia Roretzi*. *Biochemistry* **1990**, *29* (1), 159–165. <https://doi.org/10.1021/bi00453a021>.

(388) Andy Tincu, J.; Taylor, S. W. Tunichrome Sp-1: New Pentapeptide Tunichrome from the Hemocytes of *Styela Plicata*. *J. Nat. Prod.* **2002**, *65* (3), 377–378. <https://doi.org/10.1021/np010352z>.

(389) Kato, Y.; Nishikawa, T.; Kawakishi, S. Formation of Protein-Bound 3,4-Dihydroxyphenylalanine in Collagen Types I and Iv Exposed To Ultraviolet Light.

Photochem. Photobiol. **1995**, *61* (4), 367–372. <https://doi.org/10.1111/j.1751-1097.1995.tb08624.x>.

(390) Nelson, M. J. Catecholate Complexes of Ferric Soybean Lipoxygenase 1. *Biochemistry* **1988**, *27* (12), 4273–4278. <https://doi.org/10.1021/bi00412a011>.

(391) Liu, Y.; Mukherjee, A.; Nahumi, N.; Ozbil, M.; Brown, D.; Angeles-Boza, A. M.; Dooley, D. M.; Prabhakar, R.; Roth, J. P. Experimental and Computational Evidence of Metal-O₂ Activation and Rate-Limiting Proton-Coupled Electron Transfer in a Copper Amine Oxidase. *J. Phys. Chem. B* **2013**, *117* (1), 218–229. <https://doi.org/10.1021/jp3121484>.

(392) Andersson, K. K.; Cox, D. D.; Que, L.; Flatmark, T.; Haavik, J. Resonance Raman Studies on the Blue-Green-Colored Bovine Adrenal Tyrosine 3-Monooxygenase (Tyrosine Hydroxylase). Evidence That the Feedback Inhibitors Adrenaline and Noradrenaline Are Coordinated to Iron. *J. Biol. Chem.* **1988**, *263* (35), 18621–18626.

(393) Taylor, S. W.; Bruce Chase, D.; Emptage, M. H.; Nelson, M. J.; Herbert Waite, J. Ferric Ion Complexes of a DOPA-Containing Adhesive Protein from *Mytilus Edulis*. *Inorg. Chem.* **1996**, *35* (26), 7572–7577. <https://doi.org/10.1021/ic960514s>.

(394) Gieseg, S.; Simpson, J.; Charlton, T.; Duncan, M.; Dean, R. Protein-Bound 3,4-Dihydroxyphenylalanine Is a Major Reductant Formed During Hydroxyl Radical Damage to Proteins. *Biochemistry* **1993**, *32* (18), 4780–4786. <https://doi.org/10.1021/bi00069a012>.

(395) Que Jr., L. Metalloproteins with Phenolate Coordination. *Coord. Chem. Rev.* **1983**, *50* (1–2), 73–108. [https://doi.org/10.1016/0010-8545\(83\)85027-9](https://doi.org/10.1016/0010-8545(83)85027-9).

(396) Zhao, C.; Liaw, L.; Hee Lee, I.; Lehrer, R. I. CDNA Cloning of Clavanins: Antimicrobial

Peptides of Tunicate Hemocytes. *FEBS Lett.* **1997**, *410* (2–3), 490–492.

[https://doi.org/10.1016/S0014-5793\(97\)00646-7](https://doi.org/10.1016/S0014-5793(97)00646-7).

(397) Sherman, M. A.; Lehrer, R. I.; Waring, A. J.; Menzel, L.; Nguyen, T.; Zhao, C.; In, I. Clavaspirin, an Antibacterial and Haemolytic Peptide from *Styela Clava*. *J. Pept. Res.* **2001**, *58* (6), 445–456. <https://doi.org/10.1034/j.1399-3011.2001.10975.x>.

(398) Lehrer, R. I.; Lee, I. H.; Menzel, L.; Waring, A.; Zhao, C. Clavanins and Styelins, α -Helical Antimicrobial Peptides from The Hemocytes of *Styela Clava*. In *Phylogenetic Perspectives on the Vertebrate Immune System. Advances in Experimental Medicine and Biology*; 2001; pp 71–76.

(399) Ribeiro, K. L.; Frías, I. A. M.; Franco, O. L.; Dias, S. C.; Sousa-Junior, A. A.; Silva, O. N.; Bakuzis, A. F.; Oliveira, M. D. L.; Andrade, C. A. S. Clavanin A-Bioconjugated Fe₃O₄/Silane Core-Shell Nanoparticles for Thermal Ablation of Bacterial Biofilms. *Colloids Surfaces B Biointerfaces* **2018**, *169*, 72–81.
<https://doi.org/10.1016/j.colsurfb.2018.04.055>.

(400) Silva, O. N.; Fensterseifer, I. C. M.; Rodrigues, E. A.; Holanda, H. H. S.; Novaes, N. R. F.; Cunha, J. P. A.; Rezende, T. M. B.; Magalhães, K. G.; Moreno, S. E.; Jerônimo, M. S.; Bocca, A. L.; Franco, O. L. Clavanin A Improves Outcome of Complications from Different Bacterial Infections. *Antimicrob. Agents Chemother.* **2015**, *59* (3), 1620–1626.
<https://doi.org/10.1128/AAC.03732-14>.

(401) van Kan, E. J. M.; van Der Bent, A.; Demel, R. A.; De Kruijff, B. Membrane Activity of the Peptide Antibiotic Clavanin and the Importance of Its Glycine Residues. *Biochemistry* **2001**, *40* (21), 6398–6405. <https://doi.org/10.1021/bi0028136>.

(402) Saúde, A. C. M.; Ombredane, A. S.; Silva, O. N.; Barbosa, J. A. R. G.; Moreno, S. E.; Araujo, A. C. G.; Falcão, R.; Silva, L. P.; Dias, S. C.; Franco, O. L. Clavanin Bacterial Sepsis Control Using a Novel Methacrylate Nanocarrier. *Int. J. Nanomedicine* **2014**, *9* (1), 5055–5069. <https://doi.org/10.2147/IJN.S66300>.

(403) van Kan, E. J. M.; Demel, R. A.; Breukink, E.; van der Bent, A.; de Kruijff, B. Clavanin Permeabilizes Target Membranes via Two Distinctly Different PH-Dependent Mechanisms. *Biochemistry* **2002**, *41* (24), 7529–7539. <https://doi.org/10.1021/bi012162t>.

(404) Lee, I. H.; Cho, Y.; Lehrer, R. Effects of PH and Salinity on the Antimicrobial Properties of Clavanins. *Infect. Immun.* **1997**, *65* (7), 2898–2903. <https://doi.org/10.1128/IAI.65.7.2898-2903.1997>.

(405) Silva, O. N.; Alves, E. S. F.; de la Fuente-Núñez, C.; Ribeiro, S. M.; Mandal, S. M.; Gaspar, D.; Veiga, A. S.; Castanho, M. A. R. B.; Andrade, C. A. S.; Nascimento, J. M.; Fensterseifer, I. C. M.; Porto, W. F.; Correa, J. R.; Hancock, R. E. W.; Korpole, S.; Oliveria, A. L.; Liao, L. M.; Franco, O. L. Structural Studies of a Lipid Binding Peptide from Tunicate Hemocytes with Anti-Biofilm Activity. *Sci. Rep.* **2016**, *6*. <https://doi.org/10.1038/srep27128>.

(406) Marrink, S. J.; Corradi, V.; Souza, P. C. T.; Ingólfsson, H. I.; Tielemans, D. P.; Sansom, M. S. P. Computational Modeling of Realistic Cell Membranes. *Chem. Rev.* **2019**, *119* (9), 6184–6226. <https://doi.org/10.1021/acs.chemrev.8b00460>.

(407) Howe, J.; Andrä, J.; Conde, R.; Iriarte, M.; Garidel, P.; Koch, M. H. J.; Gutsmann, T.; Moriyón, I.; Brandenburg, K. Thermodynamic Analysis of the Lipopolysaccharide-Dependent Resistance of Gram-Negative Bacteria against Polymyxin B. *Biophys. J.* **2007**,

92 (8), 2796–2805. <https://doi.org/10.1529/biophysj.106.095711>.

(408) Zhao, L.; Cao, Z.; Bian, Y.; Hu, G.; Wang, J.; Zhou, Y. Molecular Dynamics Simulations of Human Antimicrobial Peptide LL-37 in Model POPC and POPG Lipid Bilayers. *Int. J. Mol. Sci.* **2018**, *19* (4), 1–13. <https://doi.org/10.3390/ijms19041186>.

(409) Jordan, J. B.; Poppe, L.; Haniu, M.; Arvedson, T.; Syed, R.; Li, V.; Kohno, H.; Kim, H.; Schnier, P. D.; Harvey, T. S.; Miranda, L. P.; Cheetham, J.; Sasu, B. J. Hepcidin Revisited, Disulfide Connectivity, Dynamics, and Structure. *J. Biol. Chem.* **2009**, *284* (36), 24155–24167. <https://doi.org/10.1074/jbc.M109.017764>.

(410) Nemeth, E.; Tuttle, M. S.; Powelson, J.; Vaughn, M. D.; Donovan, A.; Ward, D. M. V.; Ganz, T.; Kaplan, J. Hepcidin Regulates Cellular Iron Efflux by Binding to Ferroportin and Inducing Its Internalization. *Science (80-.).* **2004**, *306* (5704), 2090–2093. <https://doi.org/10.1126/science.1104742>.

(411) Nemeth, E.; Ganz, T. Regulation of Iron Metabolism by Hepcidin. *Annu. Rev. Nutr.* **2006**, *26* (1), 323–342. <https://doi.org/10.1146/annurev.nutr.26.061505.111303>.

(412) Laussac, J. P.; Sarkar, B. Characterization of the Copper(II)- and Nickel(II)-Transport Site of Human Serum Albumin. Studies of Copper(II) and Nickel(II) Binding to Peptide 1-24 of Human Serum Albumin by ¹³C and ¹H NMR Spectroscopy. *Biochemistry* **1984**, *23* (12), 2832–2838. <https://doi.org/10.1021/bi00307a046>.

(413) Campopiano, D. J.; Clarke, D. J.; Polfer, N. C.; Barran, P. E.; Langley, R. J.; Govan, J. R. W.; Maxwell, A.; Dorin, J. R. Structure-Activity Relationships in Defensin Dimers: A Novel Link between β -Defensin Tertiary Structure and Antimicrobial Activity. *J. Biol. Chem.* **2004**, *279* (47), 48671–48679. <https://doi.org/10.1074/jbc.M404690200>.

(414) Maisetta, G.; Petruzzelli, R.; Brancatisano, F. L.; Esin, S.; Vitali, A.; Campa, M.; Batoni, G. Antimicrobial Activity of Human Hepcidin 20 and 25 against Clinically Relevant Bacterial Strains: Effect of Copper and Acidic PH. *Peptides* **2010**, *31* (11), 1995–2002. <https://doi.org/10.1016/j.peptides.2010.08.007>.

(415) Tselepis, C.; Ford, S. J.; McKie, A. T.; Vogel, W.; Zoller, H.; Simpson, R. J.; Diaz Castro, J.; Iqbal, T. H.; Ward, D. G. Characterization of the Transition-Metal-Binding Properties of Hepcidin. *Biochem. J.* **2010**, *427* (2), 289–296. <https://doi.org/10.1042/bj20091521>.

(416) Nemeth, E.; Preza, G. C.; Jung, C. L.; Kaplan, J.; Waring, A. J.; Ganz, T. The N-Terminus of Hepcidin Is Essential for Its Interaction with Ferroportin: Structure-Function Study. *Blood* **2006**, *107* (1), 328–333. <https://doi.org/10.1182/blood-2005-05-2049>.

(417) Maisetta, G.; Petruzzelli, R.; Brancatisano, F. L.; Esin, S.; Vitali, A.; Campa, M.; Batoni, G. Antimicrobial Activity of Human Hepcidin 20 and 25 against Clinically Relevant Bacterial Strains: Effect of Copper and Acidic PH. *Peptides* **2010**, *31* (11), 1995–2002. <https://doi.org/10.1016/j.peptides.2010.08.007>.

(418) Lobado, D.; Kozlowski, H.; Rowinska-Zyrek, M. Antimicrobial Peptide–Metal Ion Interactions—a Potential Way of Activity Enhancement. *New J. Chem* **2018**, *42*, 7560–7568. <https://doi.org/10.1039/c7nj04709f>.

(419) Puri, S.; Edgerton, M. How Does It Kill?: Understanding the Candidacidal Mechanism of Salivary Histatin 5. *Eukaryot. Cell* **2014**, *13* (8), 958–964. <https://doi.org/10.1128/EC.00095-14>.

(420) Oudhoff, M. J.; Bolscher, J. G. M.; Nazmi, K.; Kalay, H.; van 't Hof, W.; Amerongen, A. V. N.; Veerman, E. C. I. Histatins Are the Major Wound-Closure Stimulating Factors in

Human Saliva as Identified in a Cell Culture Assay. *FASEB J.* **2008**, *22* (11), 3805–3812.
<https://doi.org/10.1096/fj.08-112003>.

(421) Houghton, E. A.; Nicholas, K. M. In Vitro Reactive Oxygen Species Production by Histatins and Copper (I,II). *J Biol Inorg Chem* **2009**, *14*, 243–251.
<https://doi.org/10.1007/s00775-008-0444-x>.

(422) Demori, I.; Rashed, Z. El; Corradino, V.; Catalano, A.; Rovegno, L.; Queirolo, L.; Salvidio, S.; Biggi, E.; Zanotti-Russo, M.; Canesi, L.; Catenazzi, A.; Grasselli, E. Peptides for Skin Protection and Healing in Amphibians. *Molecules* **2019**, *24* (2).
<https://doi.org/10.3390/molecules24020347>.

(423) Clarke, B. T. The Natural History of Amphibian Skin Secretions, Their Normal Functioning and Potential Medical Applications. *Biol. Rev.* **1997**, *72* (3), 365–379.
<https://doi.org/10.1017/s0006323197005045>.

(424) Daly, J. W.; Spande, T. F.; Garraffo, H. M. Alkaloids from Amphibian Skin: A Tabulation of over Eight-Hundred Compounds. *J. Nat. Prod.* **2005**, *68* (10), 1556–1575.
<https://doi.org/10.1021/np0580560>.

(425) Daly, J. W.; Garraffo, H. M.; Spande, T. F.; Decker, M. W.; Sullivan, J. P.; Williams, M. Alkaloids from Frog Skin: The Discovery of Epibatidine and the Potential for Developing Novel Non-Opioid Analgesics. *Nat. Prod. Rep.* **2000**, *17* (2), 131–135.
<https://doi.org/10.1039/a900728h>.

(426) Marenah, L.; Flatt, P. R.; Orr, D. F.; Shaw, C.; Abdel-Wahab, Y. H. A. Skin Secretions of *Rana Saharica* Frogs Reveal Antimicrobial Peptides Esculetins-1 and -1B and Brevinins-1E and -2EC with Novel Insulin Releasing Activity. *J. Endocrinol.* **2006**, *188* (1), 1–9.

<https://doi.org/10.1677/joe.1.06293>.

(427) Maggio, J. E. “Kassinin” in Mammals: The Newest Tachykinins. *Peptides* **1985**, *6* (3), 237–243. [https://doi.org/10.1016/0196-9781\(85\)90380-8](https://doi.org/10.1016/0196-9781(85)90380-8).

(428) Wade, A. M.; Tucker, H. N. Antioxidant Characteristics of L-Histidine. *J. Nutr. Biochem.* **1998**, *9* (6), 308–315. [https://doi.org/10.1016/s0955-2863\(98\)00022-9](https://doi.org/10.1016/s0955-2863(98)00022-9).

(429) Papadimitriou, E. A.; Loumbourdis, N. S. Copper Kinetics and Hepatic Metallothionein Levels in the Frog *Rana Ridibunda*, after Exposure to CuCl₂. *BioMetals* **2003**, *16* (2), 271–277. <https://doi.org/10.1023/A:1020683404803>.

(430) Domingues, T. M.; Perez, K. R.; Miranda, A.; Riske, K. A. Comparative Study of the Mechanism of Action of the Antimicrobial Peptide Gomesin and Its Linear Analogue: The Role of the β-Hairpin Structure. *Biochim. Biophys. Acta - Biomembr.* **2015**, *1848* (10), 2414–2421. <https://doi.org/10.1016/j.bbamem.2015.07.012>.

(431) Busby, W. H.; Quackenbush, G. E.; Humm, J.; Youngblood, W. W.; Kizers, J. S. An Enzyme(s) That Converts Glutaminyl-Peptides into Pyroglutamyl-Peptides. *J. Biol. Chem.* **1987**, *262* (18), 8532–8536.

(432) Garden, R. W.; Moroz, T. P.; Gleeson, J. M.; Floyd, P. D.; Li, L.; Rubakhin, S. S.; Sweedler, J. V. Formation of N-Pyroglutamyl Peptides from N-Glu and N-Gln Precursors in Aplysia Neurons. *J. Neurochem.* **1999**, *72* (2), 676–681. <https://doi.org/10.1046/j.1471-4159.1999.0720676.x>.

(433) Blombäck, B. Derivatives of Glutamine in Peptides. *Methods Enzymol.* **1967**, *11*, 398–411. [https://doi.org/10.1016/S0076-6879\(67\)11046-X](https://doi.org/10.1016/S0076-6879(67)11046-X).

(434) Saido, T. C.; Iwatsubo, T.; Mann, D. M. A.; Shimada, H.; Ihara, Y.; Kawashima, S. Dominant and Differential Deposition of Distinct β -Amyloid Peptide Species, A β N3(PE), in Senile Plaques. *Neuron* **1995**, *14* (2), 457–466. [https://doi.org/10.1016/0896-6273\(95\)90301-1](https://doi.org/10.1016/0896-6273(95)90301-1).

(435) Kowalik-Jankowska, T.; Jankowska, E.; Szewczuk, Z.; Kasprzykowski, F. Coordination Abilities of Neurokinin A and Its Derivative and Products of Metal-Catalyzed Oxidation. *J. Inorg. Biochem.* **2010**, *104* (8), 831–842. <https://doi.org/10.1016/j.jinorgbio.2010.03.016>.

(436) Harford, C.; Sarkar, B. Neuromedin C Binds Cu(II) and Ni(II) via the ATCUN Motif: Implications for the CNS and Cancer Growth. *Biochem. Biophys. Res. Commun.* **1995**, *209* (3), 877–882. [https://doi.org/https://doi.org/10.1006/bbrc.1995.1580](https://doi.org/10.1006/bbrc.1995.1580).

(437) Russino, D.; McDonald, E.; Hejazi, L.; Hanson, G. R.; Jones, C. E. The Tachykinin Peptide Neurokinin b Binds Copper Forming an Unusual [CuII(NKB)2] Complex and Inhibits Copper Uptake into 1321N1 Astrocytoma Cells. *ACS Chem. Neurosci.* **2013**, *4* (10), 1371–1381. <https://doi.org/10.1021/cn4000988>.

(438) Grosas, A. B.; Kalimuthu, P.; Smith, A. C.; Williams, P. A.; Millar, T. J.; Bernhardt, P. V.; Jones, C. E. The Tachykinin Peptide Neurokinin B Binds Copper(I) and Silver(I) and Undergoes Quasi-Reversible Electrochemistry: Towards a New Function for the Peptide in the Brain. *Neurochem. Int.* **2014**, *70*, 1–9. <https://doi.org/10.1016/j.neuint.2014.03.002>.

(439) Pietruszka, M.; Jankowska, E.; Kowalik-Jankowska, T.; Szewczuk, Z.; Smużyńska, M. Complexation Abilities of Neuropeptide Gamma toward Copper(II) Ions and Products of Metal-Catalyzed Oxidation. *Inorg. Chem.* **2011**, *50* (16), 7489–7499.

<https://doi.org/10.1021/ic2002942>.

(440) Park, J. M.; Jung, J. E.; Lee, B. J. Antimicrobial Peptides from the Skin of a Korean Frog, *Rana Rugosa*. *Biochem. Biophys. Res. Commun.* **1994**, *205* (1), 948–954.

<https://doi.org/10.1006/bbrc.1994.2757>.

(441) Parvin, A.; Anand, S.; Asha, R.; Reshmy, V.; Sanil, G.; Kumar, K. S. Structure-Activity Relationship and Mode of Action of a Frog Secreted Antibacterial Peptide B1CTcu5 Using Synthetically and Modularly Modified or Deleted (SMMD) Peptides. *PLoS One* **2015**, *10* (5), 1–14. <https://doi.org/10.1371/journal.pone.0124210>.

(442) Zhang, F.; Guo, Z. L.; Chen, Y.; Li, L.; Yu, H. N.; Wang, Y. P. Effects of C-Terminal Amidation and Heptapeptide Ring on the Biological Activities and Advanced Structure of Amurin-9KY, a Novel Antimicrobial Peptide Identified from the Brown Frog, *Rana Kunyuensis*. *Zool. Res.* **2019**, *40* (3), 198–204. <https://doi.org/10.24272/j.issn.2095-8137.2018.070>.

(443) Kwon, M. Y.; Hong, S. Y.; Lee, K. H. Structure-Activity Analysis of Brevinin 1E Amide, an Antimicrobial Peptide from *Rana Esculenta*. *Biochim. Biophys. Acta - Protein Struct. Mol. Enzymol.* **1998**, *1387* (1–2), 239–248. [https://doi.org/10.1016/S0167-4838\(98\)00123-X](https://doi.org/10.1016/S0167-4838(98)00123-X).

(444) Bao, K.; Yuan, W.; Ma, C.; Yu, X.; Wang, L.; Hong, M.; Xi, X.; Zhou, M.; Chen, T. Modification Targeting the “Rana Box” Motif of a Novel Nigrocin Peptide from *Hyalarana Latouchii* Enhances and Broadens Its Potency against Multiple Bacteria. *Front. Microbiol.* **2018**, *9*, 1–11. <https://doi.org/10.3389/fmicb.2018.02846>.

(445) Park, S. H.; Kim, Y. K.; Park, J. W.; Lee, B. J.; Lee, B. J. Solution Structure of the

Antimicrobial Peptide Gaegurin 4 by ¹H and ¹⁵N Nuclear Magnetic Resonance Spectroscopy. *Eur. J. Biochem.* **2000**, *267* (9), 2695–2704. <https://doi.org/10.1046/j.1432-1327.2000.01287.x>.

(446) Kim, H. J.; Kim, S. S.; Lee, M. H.; Lee, B. J.; Ryu, P. D. Role of C-Terminal Heptapeptide in Pore-Forming Activity of Antimicrobial Agent, Gaegurin 4. *J. Pept. Res.* **2004**, *64* (4), 151–158. <https://doi.org/10.1111/j.1399-3011.2004.00183.x>.

(447) Mangoni, M. L.; Fiocco, D.; Mignogna, G.; Barra, D.; Simmaco, M. Functional Characterisation of the 1-18 Fragment of Esculentin-1b, an Antimicrobial Peptide from *Rana Esculenta*. *Peptides* **2003**, *24* (11), 1771–1777.
<https://doi.org/10.1016/j.peptides.2003.07.029>.

(448) Fernández-Mazarrasa, C.; Mazarrasa, O.; Calvo, J.; Del Arco, A.; Martínez-Martínez, L. High Concentrations of Manganese in Mueller-Hinton Agar Increase MICs of Tigecycline Determined by Etest. *J. Clin. Microbiol.* **2009**, *47* (3), 827–829.
<https://doi.org/10.1128/JCM.02464-08>.

(449) Sai, K. P.; Jagannadham, M. V.; Vairamani, M.; Raju, N. P.; Devi, A. S.; Nagaraj, R.; Sitaram, N. Tigerinins: Novel Antimicrobial Peptides from the Indian Frog *Rana Tigerina*. *J. Biol. Chem.* **2001**, *276* (4), 2701–2707. <https://doi.org/10.1074/jbc.M006615200>.

(450) Li, J.; Xu, X.; Xu, C.; Zhou, W.; Zhang, K.; Yu, H.; Zhang, Y.; Zheng, Y.; Rees, H. H.; Lai, R.; Yang, D.; Wu, J. Anti-Infection Peptidomics of Amphibian Skin. *Mol. Cell. Proteomics* **2007**, *6* (5), 882–894. <https://doi.org/10.1074/mcp.M600334-MCP200>.

(451) Yang, X.; Hu, Y.; Xu, S.; Hu, Y.; Meng, H.; Guo, C.; Liu, Y.; Liu, J.; Yu, Z.; Wang, H. Identification of Multiple Antimicrobial Peptides from the Skin of Fine-Spined Frog,

Hylarana Spinulosa (Ranidae). *Biochimie* **2013**, *95* (12), 2429–2436.

<https://doi.org/10.1016/j.biochi.2013.09.002>.

(452) Neupane, K. P.; Aldous, A. R.; Kritzer, J. A. Macrocyclization of the ATCUN Motif Controls Metal Binding and Catalysis. *Inorg. Chem.* **2013**, *52* (5), 2729–2735.

<https://doi.org/10.1021/ic302820z>.

(453) Chen, Q.; Wade, D.; Kurosaka, K.; Wang, Z. Y.; Oppenheim, J. J.; Yang, D. Temporin A and Related Frog Antimicrobial Peptides Use Formyl Peptide Receptor-like 1 as a Receptor to Chemoattract Phagocytes. *J. Immunol.* **2004**, *173* (4), 2652–2659.

<https://doi.org/10.4049/jimmunol.173.4.2652>.

(454) Simmaco, M.; Mignogna, G.; Canofeni, S.; Miele, R.; Mangoni, M. L.; Barra, D. Temporins, Antimicrobial Peptides from the European Red Frog *Rana Temporaria*. *Eur. J. Biochem.* **1996**, *242* (3), 788–792. <https://doi.org/10.1111/j.1432-1033.1996.0788r.x>.

(455) Mechkarska, M.; Ojo, O. O.; Meetani, M. A.; Coquet, L.; Jouenne, T.; Abdel-Wahab, Y. H. A.; Flatt, P. R.; King, J. D.; Conlon, J. M. Peptidomic Analysis of Skin Secretions from the Bullfrog *Lithobates Catesbeianus* (Ranidae) Identifies Multiple Peptides with Potent Insulin-Releasing Activity. *Peptides* **2011**, *32* (2), 203–208.

<https://doi.org/10.1016/j.peptides.2010.11.002>.

(456) Mangoni, M. L. Temporins, Anti-Infective Peptides with Expanding Properties. *Cell. Mol. Life Sci.* **2006**, *63* (9), 1060–1069. <https://doi.org/10.1007/s00018-005-5536-y>.

(457) Wade, D.; Silberring, J.; Soliymani, R.; Heikkinen, S.; Kilpeläinen, I.; Lankinen, H.; Kuusela, P. Antibacterial Activities of Temporin A Analogs. *FEBS Lett.* **2000**, *479* (1–2), 6–9. [https://doi.org/10.1016/S0014-5793\(00\)01754-3](https://doi.org/10.1016/S0014-5793(00)01754-3).

(458) Raja, Z.; AndreA, S.; Abbassi, F.; Humblot, V.; Lequin, O.; Bouceba, T.; Correia, I.; Casale, S.; Foulon, T.; Sereno, D.; Oury, B.; Ladram, A. Insight into the Mechanism of Action of Temporin-SHa, a New Broad-Spectrum Antiparasitic and Antibacterial Agent. *PLoS One* **2017**, *12* (3), 1–41. <https://doi.org/10.1371/journal.pone.0174024>.

(459) Rosenfeld, Y.; Barra, D.; Simmaco, M.; Shai, Y.; Mangoni, M. L. A Synergism between Temporins toward Gram-Negative Bacteria Overcomes Resistance Imposed by the Lipopolysaccharide Protective Layer. *J. Biol. Chem.* **2006**, *281* (39), 28565–28574. <https://doi.org/10.1074/jbc.M606031200>.

(460) Mangoni, M. L.; Shai, Y. Temporins and Their Synergism against Gram-Negative Bacteria and in Lipopolysaccharide Detoxification. *Biochim. Biophys. Acta - Biomembr.* **2009**, *1788* (8), 1610–1619. <https://doi.org/10.1016/j.bbamem.2009.04.021>.

(461) Capparelli, R.; Romanelli, A.; Iannaccone, M.; Nocerino, N.; Ripa, R.; Pensato, S.; Pedone, C.; Iannelli, D. Synergistic Antibacterial and Anti-Inflammatory Activity of Temporin A and Modified Temporin B in Vivo. *PLoS One* **2009**, *4* (9), 1–11. <https://doi.org/10.1371/journal.pone.0007191>.

(462) Jobin, M. L.; Blanchet, M.; Henry, S.; Chaignepain, S.; Manigand, C.; Castano, S.; Lecomte, S.; Burlina, F.; Sagan, S.; Alves, I. D. The Role of Tryptophans on the Cellular Uptake and Membrane Interaction of Arginine-Rich Cell Penetrating Peptides. *Biochim. Biophys. Acta - Biomembr.* **2015**, *1848* (2), 593–602. <https://doi.org/10.1016/j.bbamem.2014.11.013>.

(463) Montecucchi, P. C. Isolation and Primary Structure Determination of Amphibian Skin Tryptophyllins. *Peptides* **1985**, *6* (SUPPL. 3), 187–195. <https://doi.org/10.1016/0196->

9781(85)90373-0.

(464) Canesi, L.; Gallo, G.; Gavioli, M.; Pruzzo, C. Bacteria-Hemocyte Interactions and Phagocytosis in Marine Bivalves. *Microsc. Res. Tech.* **2002**, *57* (6), 469–476.
<https://doi.org/10.1002/jemt.10100>.

(465) Gestal, C.; Roch, P.; Renault, T.; Pallavicini, A.; Paillard, C.; Novoa, B.; Oubella, R.; Venier, P.; Figueras, A. Study of Diseases and the Immune System of Bivalves Using Molecular Biology and Genomics. *Rev. Fish. Sci.* **2008**, *16* (S1), 133–156.
<https://doi.org/10.1080/10641260802325518>.

(466) Nguyen, T. V.; Alfaro, A. C.; Merien, F.; Lulijwa, R.; Young, T. Copper-Induced Immunomodulation in Mussel (*Perna Canaliculus*) Haemocytes. *Metallomics* **2018**, *10* (7), 965–978. <https://doi.org/10.1039/c8mt00092a>.

(467) Mitta, G.; Vandenbulcke, F.; Noel, T.; Romestand, B.; Beauvillain, J. C.; Salzet, M.; Roch, P. Differential Distribution and Defence Involvement of Antimicrobial Peptides in Mussel. *J. Cell Sci.* **2000**, *113* (15), 2759–2769.

(468) Pallavicini, A.; del Mar Costa, M.; Gestal, C.; Dreos, R.; Figueras, A.; Venier, P.; Novoa, B. High Sequence Variability of Myticin Transcripts in Hemocytes of Immune-Stimulated Mussels Suggests Ancient Host-Pathogen Interactions. *Dev. Comp. Immunol.* **2008**, *32* (3), 213–226. <https://doi.org/10.1016/j.dci.2007.05.008>.

(469) Balseiro, P.; Falcó, A.; Romero, A.; Dios, S.; Martínez-López, A.; Figueras, A.; Estepa, A.; Novoa, B. *Mytilus Galloprovincialis* Myticin C: A Chemotactic Molecule with Antiviral Activity and Immunoregulatory Properties. *PLoS One* **2011**, *6* (8), 1–14.
<https://doi.org/10.1371/journal.pone.0023140>.

(470) Charlet, M.; Chernysh, S.; Hetru, C.; Hoffmann, J. A.; Bulet, P. Innate Immunity: Isolation of Several Cysteine-Rich Antimicrobial Peptides From The Blood of a Mollusc, *Mytilus Edulis*. *J. Biol. Chem.* **1996**, *271* (36), 21808–21813.
<https://doi.org/10.1074/jbc.271.36.21808>.

(471) Mitta, G.; Vandenbulcke, F.; Hubert, F.; Salzet, M.; Roch, P. Involvement of Mytilins in Mussel Antimicrobial Defense. *J. Biol. Chem.* **2000**, *275* (17), 12954–12962.
<https://doi.org/10.1074/jbc.275.17.12954>.

(472) Mitta, G.; Hubert, F.; Dyrynda, E. A.; Boudry, P.; Roch, P. Mytilin B and MGD2, Two Antimicrobial Peptides of Marine Mussels: Gene Structure and Expression Analysis. *Dev. Comp. Immunol.* **2000**, *24* (4), 381–393. [https://doi.org/10.1016/S0145-305X\(99\)00084-1](https://doi.org/10.1016/S0145-305X(99)00084-1).

(473) Venier, P.; Varotto, L.; Rosani, U.; Millino, C.; Celegato, B.; Bernante, F.; Lanfranchi, G.; Novoa, B.; Roch, P.; Figueras, A.; Pallavicini, A. Insights into the Innate Immunity of the Mediterranean Mussel *Mytilus Galloprovincialis*. *BMC Genomics* **2011**, *12* (69), 1–19.
<https://doi.org/10.1186/1471-2164-12-69>.

(474) Gerdol, M.; Venier, P. An Updated Molecular Basis for Mussel Immunity. *Fish Shellfish Immunol.* **2015**, *46* (1), 17–38. <https://doi.org/10.1016/j.fsi.2015.02.013>.

(475) Destoumieux, D.; Muñoz, M.; Cosseau, C.; Rodriguez, J.; Bulet, P.; Comps, M.; Bachère, E. Penaeidins, Antimicrobial Peptides with Chitin-Binding Activity, Are Produced and Stored in Shrimp Granulocytes and Released after Microbial Challenge. *J. Cell Sci.* **2000**, *113* (3), 461–469.

(476) Shan, Z.; Zhu, K.; Peng, H.; Chen, B.; Liu, J.; Chen, F.; Ma, X.; Wang, S.; Qiao, K.; Wang, K. The New Antimicrobial Peptide Sphyastatin from the Mud Crab *Scylla*

Paramamosain with Multiple Antimicrobial Mechanisms and High Effect on Bacterial Infection. *Front. Microbiol.* **2016**, *7* (1140), 1–14.

<https://doi.org/10.3389/fmicb.2016.01140>.

(477) Osaki, T.; Omotezako, M.; Nagayama, R.; Hirata, M.; Iwanaga, S.; Kasahara, J.; Hattori, J.; Ito, I.; Sugiyama, H.; Kawabata, S. I. Horseshoe Crab Hemocyte-Derived Antimicrobial Polypeptides, Tachystatins, with Sequence Similarity to Spider Neurotoxins. *J. Biol. Chem.* **1999**, *274* (37), 26172–26178.

<https://doi.org/10.1074/jbc.274.37.26172>.

(478) Qin, C. L.; Huang, W.; Zhou, S. Q.; Wang, X. C.; Liu, H. H.; Fan, M. H.; Wang, R. X.; Gao, P.; Liao, Z. Characterization of a Novel Antimicrobial Peptide with Chiting-Biding Domain from *Mytilus Coruscus*. *Fish Shellfish Immunol.* **2014**, *41* (2), 362–370.

<https://doi.org/10.1016/j.fsi.2014.09.019>.

(479) Oh, R.; Lee, M. J.; Kim, Y. O.; Nam, B. H.; Kong, H. J.; Kim, J. W.; Park, J. Y.; Seo, J. K.; Kim, D. G. Purification and Characterization of an Antimicrobial Peptide Mytichitin-Chitin Binding Domain from the Hard-Shelled Mussel, *Mytilus Coruscus*. *Fish Shellfish Immunol.* **2018**, *83*, 425–435. <https://doi.org/10.1016/j.fsi.2018.09.009>.

(480) Liao, Z.; Wang, X.; Liu, H.; Fan, M.; Sun, J.; Shen, W. Molecular Characterization of a Novel Antimicrobial Peptide from *Mytilus Coruscus*. *Fish Shellfish Immunol.* **2013**, *34* (2), 610–616. <https://doi.org/10.1016/j.fsi.2012.11.030>.

(481) Mitta, G.; Vandenbulcke, F.; Hubert, F.; Roch, P. Mussel Defensins Are Synthesised and Processed in Granulocytes Then Released into the Plasma after Bacterial Challenge. *J. Cell Sci.* **1999**, *112* (23), 4233–4242.

(482) Zhu, S.; Gao, B.; Tytgat, J. Phylogenetic Distribution, Functional Epitopes and Evolution of the CS α β Superfamily. *Cell. Mol. Life Sci.* **2005**, *62* (19–20), 2257–2269.
<https://doi.org/10.1007/s00018-005-5200-6>.

(483) Saito, T.; Kawabata, S. I.; Shigenaga, T.; Takayenoki, Y.; Cho, J.; Nakajima, H.; Hirata, M.; Iwanaga, S. A Novel Big Defensin Identified in Horseshoe Crab Hemocytes: Isolation, Amino Acid Sequence, and Antibacterial Activity. *J. Biochem.* **1995**, *117* (5), 1131–1137. <https://doi.org/10.1093/oxfordjournals.jbchem.a124818>.

(484) Kouno, T.; Fujitani, N.; Mizuguchi, M.; Osaki, T.; Nishimura, S. I.; Kawabata, S. I.; Aizawa, T.; Demura, M.; Nitta, K.; Kawano, K. A Novel β -Defensin Structure: A Potential Strategy of Big Defensin for Overcoming Resistance by Gram-Positive Bacteria. *Biochemistry* **2008**, *47* (40), 10611–10619. <https://doi.org/10.1021/bi800957n>.

(485) Kouno, T.; Mizuguchi, M.; Aizawa, T.; Shinoda, H.; Demura, M.; Kawabata, S. I.; Kawano, K. A Novel β -Defensin Structure: Big Defensin Changes Its N-Terminal Structure to Associate with the Target Membrane. *Biochemistry* **2009**, *48* (32), 7629–7635. <https://doi.org/10.1021/bi900756y>.

(486) Zhao, J.; Song, L.; Li, C.; Ni, D.; Wu, L.; Zhu, L.; Wang, H.; Xu, W. Molecular Cloning, Expression of a Big Defensin Gene from Bay Scallop *Argopecten irradians* and the Antimicrobial Activity of Its Recombinant Protein. *Mol. Immunol.* **2007**, *44* (4), 360–368.
<https://doi.org/10.1016/j.molimm.2006.02.025>.

(487) Yang, J.; Luo, J.; Zheng, H.; Lu, Y.; Zhang, H. Cloning of a Big Defensin Gene and Its Response to *Vibrio parahaemolyticus* Challenge in the Noble Scallop *Chlamys nobilis* (Bivalve: Pectinidae). *Fish Shellfish Immunol.* **2016**, *56*, 445–449.

[https://doi.org/10.1016/j.fsi.2016.07.030.](https://doi.org/10.1016/j.fsi.2016.07.030)

(488) Wang, G. L.; Xia, X. L.; Li, X. L.; Dong, S. J.; Li, J. L. Molecular Characterization and Expression Patterns of the Big Defensin Gene in Freshwater Mussel (*Hyriopsis Cummingii*). *Genet. Mol. Res.* **2014**, *13* (1), 704–715. <https://doi.org/10.4238/2014.January.29.1>.

(489) Zhao, J.; Li, C.; Chen, A.; Li, L.; Su, X.; Li, T. Molecular Characterization of a Novel Big Defensin from Clam *Venerupis Philippinarum*. *PLoS One* **2010**, *5* (10), 1–6. <https://doi.org/10.1371/journal.pone.0013480>.

(490) Gerdol, M.; De Moro, G.; Manfrin, C.; Venier, P.; Pallavicini, A. Big Defensins and Mytimacins, New AMP Families of the Mediterranean Mussel *Mytilus Galloprovincialis*. *Dev. Comp. Immunol.* **2012**, *36* (2), 390–399. <https://doi.org/10.1016/j.dci.2011.08.003>.

(491) González, R.; Brokordt, K.; Cárcamo, C. B.; Coba de la Peña, T.; Oyanedel, D.; Mercado, L.; Schmitt, P. Molecular Characterization and Protein Localization of the Antimicrobial Peptide Big Defensin from the Scallop *Argopecten Purpuratus* after *Vibrio Splendidus* Challenge. *Fish Shellfish Immunol.* **2017**, *68*, 173–179. <https://doi.org/10.1016/j.fsi.2017.07.010>.

(492) Rosa, R. D.; Santini, A.; Fievet, J.; Bulet, P.; Destoumieux-Garzón, D.; Bachère, E. Big Defensins, a Diverse Family of Antimicrobial Peptides That Follows Different Patterns of Expression in Hemocytes of the Oyster *Crassostrea Gigas*. *PLoS One* **2011**, *6* (9), 1–11. <https://doi.org/10.1371/journal.pone.0025594>.

(493) Zhong, J.; Wang, W.; Yang, X.; Yan, X.; Liu, R. A Novel Cysteine-Rich Antimicrobial Peptide from the Mucus of the Snail of *Achatina Fulica*. *Peptides* **2013**, *39* (1), 1–5. <https://doi.org/10.1016/j.peptides.2012.09.001>.

(494) Sassone-Corsi, M.; Nuccio, S. P.; Liu, H.; Hernandez, D.; Vu, C. T.; Takahashi, A. A.; Edwards, R. A.; Raffatellu, M. Microcins Mediate Competition among Enterobacteriaceae in the Inflamed Gut. *Nature* **2016**, *540* (7632), 280–283. <https://doi.org/10.1038/nature20557>.

(495) Kommineni, S.; Bretl, D. J.; Lam, V.; Chakraborty, R.; Hayward, M.; Simpson, P.; Cao, Y.; Bousounis, P.; Kristich, C. J.; Salzman, N. H. Bacteriocin Production Augments Niche Competition by Enterococci in the Mammalian Gastrointestinal Tract. *Nature* **2015**, *526* (7575), 719–722. <https://doi.org/10.1038/nature15524>.

(496) Vaughan, A.; Eijsink, V. G.; Sinderen, D. van. Functional Characterization of a Composite Bacteriocin Locus from Malt Isolate *Lactobacillus Sakei* 5. *Appl. Environ. Microbiol.* **2003**, *69* (12), 7194–7203. <https://doi.org/10.1128/AEM.69.12.7194-7203.2003>.

(497) Eijsink, V. G. H.; Skeie, M.; Middelhoven, P. H.; Brurberg, M. B.; Nes, I. F. Comparative Studies of Class IIa Bacteriocins of Lactic Acid Bacteria. *Appl. Environ. Microbiol.* **1998**, *64* (9), 3275–3281. <https://doi.org/10.1128/aem.64.9.3275-3281.1998>.

(498) Klaenhammer, T. R. Genetics of Bacteriocins Produced by Lactic Acid Bacteria. *FEMS Microbiol. Rev.* **1993**, *12* (1–3), 39–85. <https://doi.org/10.1111/j.1574-6976.1993.tb00012.x>.

(499) Jack, R. W.; Tagg, J. R.; Ray, B. Bacteriocins of Gram-Positive Bacteria. *Microbiol. Rev.* **1995**, *59* (2), 171–200.

(500) Eijsink, V. G. H.; Axelsson, L.; Diep, D. B.; Håvarstein, L. S.; Holo, H.; Nes, I. F. Production of Class II Bacteriocins by Lactic Acid Bacteria; an Example of Biological

Warfare and Communication. *Antonie van Leeuwenhoek, Int. J. Gen. Mol. Microbiol.* **2002**, *81* (1–4), 639–654. <https://doi.org/10.1023/A:1020582211262>.

(501) Acedo, J. Z.; Chiorean, S.; Vederas, J. C.; van Belkum, M. J. The Expanding Structural Variety among Bacteriocins from Gram-Positive Bacteria. *FEMS Microbiol. Rev.* **2018**, *42* (6), 805–828. <https://doi.org/10.1093/femsre/fuy033>.

(502) Fimland, G.; Johnsen, L.; Axelsson, L.; Brurberg, M. B.; Nes, I. F.; Eijsink, V. G. H.; Nissen-Meyer, J. A C-Terminal Disulfide Bridge in Pediocin-like Bacteriocins Renders Bacteriocin Activity Less Temperature Dependent and Is a Major Determinant of the Antimicrobial Spectrum. *J. Bacteriol.* **2000**, *182* (9), 2643–2648. <https://doi.org/10.1128/JB.182.9.2643-2648.2000>.

(503) Aymerich, T.; Holo, H.; Håavarstein, L. S.; Hugas, M.; Garriga, M.; Nes, I. F. Biochemical and Genetic Characterization of Enterocin A from Enterococcus Faecium, a New Antilisterial Bacteriocin in the Pediocin Family of Bacteriocins. *Appl. Environ. Microbiol.* **1996**, *62* (5), 1676–1682. <https://doi.org/10.1128/aem.62.5.1676-1682.1996>.

(504) Borrero, J.; Brede, D. A.; Skaugen, M.; Diep, D. B.; Herranz, C.; Nes, I. F.; Cintas, L. M.; Hernández, P. E. Characterization of Garvicin ML, a Novel Circular Bacteriocin Produced by Lactococcus Garvieae DCC43, Isolated from Mallard Ducks (*Anas Platyrhynchos*). *Appl. Environ. Microbiol.* **2011**, *77* (1), 369–373. <https://doi.org/10.1128/AEM.01173-10>.

(505) Maldonado-Barragán, A.; Cárdenas, N.; Martínez, B.; Ruiz-Barba, J. L.; Fernández-Garayzábal, J. F.; Rodríguez, J. M.; Gibello, A. Garvicin A, a Novel Class IIId Bacteriocin from Lactococcus Garvieae That Inhibits Septum Formation in *L. Garvieae* Strains. *Appl. Environ. Microbiol.* **2013**, *79* (14), 4336–4346. <https://doi.org/10.1128/AEM.00830-13>.

(506) Knerr, P. J.; van der Donk, W. A. Discovery, Biosynthesis, and Engineering of Lantipeptides. *Annu. Rev. Biochem.* **2012**, *81* (1), 479–505.
<https://doi.org/10.1146/annurev-biochem-060110-113521>.

(507) Piper, C.; Cotter, P.; Ross, R.; Hill, C. Discovery of Medically Significant Lantibiotics. *Curr. Drug Discov. Technol.* **2009**, *6* (1), 1–18.
<https://doi.org/10.2174/157016309787581075>.

(508) Hsu, S. T. D.; Breukink, E.; Tischenko, E.; Lutters, M. A. G.; De Kruijff, B.; Kaptein, R.; Bonvin, A. M. J. J.; Van Nuland, N. A. J. The Nisin-Lipid II Complex Reveals a Pyrophosphate Cage That Provides a Blueprint for Novel Antibiotics. *Nat. Struct. Mol. Biol.* **2004**, *11* (10), 963–967. <https://doi.org/10.1038/nsmb830>.

(509) Hsu, S. T. D.; Breukink, E.; Bierbaum, G.; Sahl, H. G.; De Kruijff, B.; Kaptein, R.; Van Nuland, N. A. J.; Bonvin, A. M. J. J. NMR Study of Mersacidin and Lipid II Interaction in Dodecylphosphocholine Micelles: Conformational Changes Are a Key to Antimicrobial Activity. *J. Biol. Chem.* **2003**, *278* (15), 13110–13117.
<https://doi.org/10.1074/jbc.M211144200>.

(510) Drider, D.; Fimland, G.; Héchard, Y.; McMullen, L. M.; Prévost, H. The Continuing Story of Class IIa Bacteriocins. *Microbiol. Mol. Biol. Rev.* **2006**, *70* (2), 564–582.
<https://doi.org/10.1128/mmbr.00016-05>.

(511) Nissen-Meyer, J.; Oppegård, C.; Rogne, P.; Haugen, H. S.; Kristiansen, P. E. Structure and Mode-of-Action of the Two-Peptide (Class-IIb) Bacteriocins. *Probiotics Antimicrob. Proteins* **2010**, *2* (1), 52–60. <https://doi.org/10.1007/s12602-009-9021-z>.

(512) Perez, R. H.; Zendo, T.; Sonomoto, K. Circular and Leaderless Bacteriocins: Biosynthesis,

Mode of Action, Applications, and Prospects. *Front. Microbiol.* **2018**, *9* (2085), 1–18.

<https://doi.org/10.3389/fmicb.2018.02085>.

(513) Hanchi, H.; Hammami, R.; Fernandez, B.; Kourda, R.; Ben Hamida, J.; Fliss, I. Simultaneous Production of Formylated and Nonformylated Enterocins L50A and L50B as Well as 61A, a New Glycosylated Durancin, by Enterococcus Durans 61A, a Strain Isolated from Artisanal Fermented Milk in Tunisia. *J. Agric. Food Chem.* **2016**, *64* (18), 3584–3590. <https://doi.org/10.1021/acs.jafc.6b00700>.

(514) Katla, T.; Naterstad, K.; Vancanneyt, M.; Swings, J.; Axelsson, L. Differences in Susceptibility of Listeria Monocytogenes Strains to Sakacin P, Sakacin A, Pediocin PA-1, and Nisin. *Appl. Environ. Microbiol.* **2003**, *69* (8), 4431–4437. <https://doi.org/10.1128/AEM.69.8.4431-4437.2003>.

(515) Gravesen, A.; Ramnath, M.; Rechinger, K. B.; Andersen, N.; Jänsch, L.; Héchard, Y.; Hastings, J. W.; Knøchel, S. High-Level Resistance to Class IIa Bacteriocins Is Associated with One General Mechanism in Listeria Monocytogenes. *Microbiology* **2002**, *148* (8), 2361–2369. <https://doi.org/10.1099/00221287-148-8-2361>.

(516) Casaus, P.; Nilsen, T.; Cintas, L. M.; Nes, I. F.; Hernández, P. E.; Holo, H. Enterocin B, a New Bacteriocin from Enterococcus Faecium T136 Which Can Act Synergistically with Enterocin A. *Microbiology* **1997**, *143* (7), 2287–2294. <https://doi.org/10.1099/00221287-143-7-2287>.

(517) Villani, F.; Aponte, M.; Blaiotta, G.; Mauriello, G.; Pepe, O.; Moschetti, G. Detection and Characterization of a Bacteriocin, Garviecin L1-5, Produced by Lactococcus Garvieae Isolated from Raw Cow's Milk. *J. Appl. Microbiol.* **2001**, *90* (3), 430–439.

<https://doi.org/10.1046/j.1365-2672.2001.01261.x>.

(518) Sánchez, J.; Basanta, A.; Gómez-Sala, B.; Herranz, C.; Cintas, L. M.; Hernández, P. E. Antimicrobial and Safety Aspects, and Biotechnological Potential of Bacteriocinogenic Enterococci Isolated from Mallard Ducks (*Anas Platyrhynchos*). *Int. J. Food Microbiol.* **2007**, *117* (3), 295–305. <https://doi.org/10.1016/j.ijfoodmicro.2007.04.012>.

(519) Tymoszewska, A.; Dlep, D. B.; Wirtek, P.; Aleksandrak-Piekarczyk, T. The Non-Lantibiotic Bacteriocin Garvicin Q Targets Man-PTS in a Broad Spectrum of Sensitive Bacterial Genera. *Sci. Rep.* **2017**, *7* (1), 1–14. <https://doi.org/10.1038/s41598-017-09102-7>.

(520) Sawa, N.; Zendo, T.; Kiyofuji, J.; Fujita, K.; Himeno, K.; Nakayama, J.; Sonomoto, K. Identification and Characterization of Lactocyclicin Q, a Novel Cyclic Bacteriocin Produced by *Lactococcus* Sp. Strain QU 12. *Appl. Environ. Microbiol.* **2009**, *75* (6), 1552–1558. <https://doi.org/10.1128/AEM.02299-08>.

(521) Vendrell, D.; Balcázar, J. L.; Ruiz-Zarzuela, I.; de Blas, I.; Gironés, O.; Múzquiz, J. L. *Lactococcus* Garvieae in Fish: A Review. *Comp. Immunol. Microbiol. Infect. Dis.* **2006**, *29* (4), 177–198. <https://doi.org/10.1016/j.cimid.2006.06.003>.

(522) Haghghi Karsidani, S.; Soltani, M.; Nikbakhat-Brojeni, G.; Ghasemi, M.; Skall, H. F. Molecular Epidemiology of Zoonotic Streptococcosis/Lactococcosis in Rainbow Trout (*Oncorhynchus Mykiss*) Aquaculture in Iran. *Iran. J. Microbiol.* **2010**, *2* (4), 198–209.

(523) Aguado-Urda, M.; López-Campos, G. H.; Gibello, A.; Cutuli, M. T.; López-Alonso, V.; Fernández-Garayzábal, J. F.; Blanco, M. M. Genome Sequence of *Lactococcus* Garvieae 8831, Isolated from Rainbow Trout Lactococcosis Outbreaks in Spain. *J. Bacteriol.* **2011**,

193 (16), 4263–4264. <https://doi.org/10.1128/JB.05326-11>.

(524) Pérez-Sánchez, T.; Balcázar, J. L.; García, Y.; Halaihel, N.; Vendrell, D.; de Blas, I.; Merrifield, D. L.; Ruiz-Zarzuela, I. Identification and Characterization of Lactic Acid Bacteria Isolated from Rainbow Trout, *Oncorhynchus Mykiss* (Walbaum), with Inhibitory Activity against *Lactococcus Garvieae*. *J. Fish Dis.* **2011**, *34* (7), 499–507. <https://doi.org/10.1111/j.1365-2761.2011.01260.x>.

(525) Seddik, H. A.; Bendali, F.; Gancel, F.; Fliss, I.; Spano, G.; Drider, D. *Lactobacillus Plantarum* and Its Probiotic and Food Potentialities. *Probiotics Antimicrob. Proteins* **2017**, *9* (2), 111–122. <https://doi.org/10.1007/s12602-017-9264-z>.

(526) Abdulhussain Kareem, R.; Razavi, S. H. Plantaricin Bacteriocins: As Safe Alternative Antimicrobial Peptides in Food Preservation—A Review. *J. Food Saf.* **2020**, *40* (1), 1–12. <https://doi.org/10.1111/jfs.12735>.

(527) Wen, L. S.; Philip, K.; Ajam, N. Purification, Characterization and Mode of Action of Plantaricin K25 Produced by *Lactobacillus Plantarum*. *Food Control* **2016**, *60*, 430–439. <https://doi.org/10.1016/j.foodcont.2015.08.010>.

(528) Kanatani, K.; Oshimura, M. Plasmid-Associated Bacteriocin Production by a *Lactobacillus Plantarum* Strain. *Biosci. Biotechnol. Biochem.* **1994**, *58* (11), 2084–2086. <https://doi.org/10.1271/bbb.58.2084>.

(529) Wang, Y.; Qin, Y.; Xie, Q.; Zhang, Y.; Hu, J.; Li, P. Purification and Characterization of Plantaricin LPL-1, a Novel Class IIa Bacteriocin Produced by *Lactobacillus Plantarum* LPL-1 Isolated From Fermented Fish. *Front. Microbiol.* **2018**, *9* (2276), 1–12. <https://doi.org/10.3389/fmicb.2018.02276>.

(530) Fimland, N.; Rogne, P.; Fimland, G.; Nissen-Meyer, J.; Kristiansen, P. E. Three-Dimensional Structure of the Two Peptides That Constitute the Two-Peptide Bacteriocin Plantaricin EF. *Biochim. Biophys. Acta - Proteins Proteomics* **2008**, *1784* (11), 1711–1719. <https://doi.org/10.1016/j.bbapap.2008.05.003>.

(531) Senes, A.; Engel, D. E.; Degrado, W. F. Folding of Helical Membrane Proteins: The Role of Polar, GxxxG-like and Proline Motifs. *Curr. Opin. Struct. Biol.* **2004**, *14* (4), 465–479. <https://doi.org/10.1016/j.sbi.2004.07.007>.

(532) Matevosyan, L.; Bazukyan, I.; Trchounian, A. Comparative Analysis of the Effect of Ca and Mg Ions on Antibacterial Activity of Lactic Acid Bacteria Isolates and Their Associations Depending on Cultivation Conditions. *AMB Express* **2019**, *9* (32), 1–11. <https://doi.org/10.1186/s13568-019-0758-9>.

(533) Fidai, I.; Hocharoen, L.; Bradford, S.; Wachnowsky, C.; Cowan, J. A. Inactivation of Sortase A Mediated by Metal ATCUN Complexes. *J. Biol. Inorg. Chem.* **2014**, *19* (8), 1327–1339. <https://doi.org/10.1007/s00775-014-1190-x>.

(534) Joyner, J. C.; Cowan, J. A. Targeted Cleavage of HIV RRE RNA by Rev-Coupled Transition Metal Chelates. *J. Am. Chem. Soc.* **2011**, *133* (25), 9912–9922. <https://doi.org/10.1021/ja203057z>.

(535) Libardo, M. D. J.; Nagella, S.; Lugo, A.; Pierce, S.; Angeles-Boza, A. M. Copper-Binding Tripeptide Motif Increases Potency of the Antimicrobial Peptide Anoplin via Reactive Oxygen Species Generation. *Biochem. Biophys. Res. Commun.* **2015**, *456* (1), 446–451. <https://doi.org/10.1016/j.bbrc.2014.11.104>.

(536) Park, C. B.; Yi, K. S.; Matsuzaki, K.; Kim, M. S.; Kim, S. C. Structure-Activity Analysis

of Buforin II, a Histone H2A-Derived Antimicrobial Peptide: The Proline Hinge Is Responsible for the Cell-Penetrating Ability of Buforin II. *Proc. Natl. Acad. Sci. U. S. A.* **2000**, *97* (15), 8245–8250. <https://doi.org/10.1073/pnas.150518097>.

(537) Makovitzki, A.; Baram, J.; Shai, Y. Antimicrobial Lipopolypeptides Composed of Palmitoyl Di- and Tricationic Peptides: In Vitro and in Vivo Activities, Self-Assembly to Nanostructures, and a Plausible Mode of Action. *Biochemistry* **2008**, *47* (40), 10630–10636. <https://doi.org/10.1021/bi8011675>.

(538) Latendorf, T.; Gerstel, U.; Wu, Z.; Bartels, J.; Becker, A.; Tholey, A.; Schröder, J. M. Cationic Intrinsically Disordered Antimicrobial Peptides (CIDAMPs) Represent a New Paradigm of Innate Defense with a Potential for Novel Anti-Infectives. *Sci. Rep.* **2019**, *9* (3331), 1–25. <https://doi.org/10.1038/s41598-019-39219-w>.

(539) Wang, G.; Li, X.; Wang, Z. APD3: The Antimicrobial Peptide Database as a Tool for Research and Education. *Nucleic Acids Res.* **2016**, *44* (D1), D1087–D1093. <https://doi.org/10.1093/nar/gkv1278>.

(540) Römling, U.; Balsalobre, C. Biofilm Infections, Their Resilience to Therapy and Innovative Treatment Strategies. *J. Intern. Med.* **2012**, *272* (6), 541–561. <https://doi.org/10.1111/joim.12004>.

(541) Mercer, D. K.; Torres, M. D. T.; Duay, S. S.; Lovie, E.; Simpson, L.; von Köckritz-Blickwede, M.; de la Fuente-Nunez, C.; O’Neil, D. A.; Angeles-Boza, A. M. Antimicrobial Susceptibility Testing of Antimicrobial Peptides to Better Predict Efficacy. *Front. Cell. Infect. Microbiol.* **2020**, *10*, 1–34. <https://doi.org/10.3389/fcimb.2020.00326>.

(542) Huh, A. J.; Kwon, Y. J. “Nanoantibiotics”: A New Paradigm for Treating Infectious

Diseases Using Nanomaterials in the Antibiotics Resistant Era. *J. Control. Release* **2011**, *156* (2), 128–145. <https://doi.org/10.1016/j.jconrel.2011.07.002>.

(543) Gakiya-Teruya, M.; Palomino-Marcelo, L.; Pierce, S.; Angeles-Boza, A. M.; Krishna, V.; Rodriguez-Reyes, J. C. F. Enhanced Antimicrobial Activity of Silver Nanoparticles Conjugated with Synthetic Peptide by Click Chemistry. *J. Nanoparticle Res.* **2020**, *22* (90), 1–11. <https://doi.org/10.1007/s11051-020-04799-6>.

(544) Saryan, J. A.; Dammin, T. C.; Bouras, A. E. Anaphylaxis to Topical Bacitracin Zinc Ointment. *Am. J. Emerg. Med.* **1998**, *16* (5), 512–513. [https://doi.org/10.1016/S0735-6757\(98\)90005-5](https://doi.org/10.1016/S0735-6757(98)90005-5).

(545) Alexander, J. L.; Thompson, Z.; Cowan, J. A. Antimicrobial Metallopeptides. *ACS Chem. Biol.* **2018**, *13* (4), 844–853. <https://doi.org/10.1021/acschembio.7b00989>.

(546) Portelinha, J.; Angeles-Boza, A. M. The Antimicrobial Peptide Gad-1 Clears *Pseudomonas Aeruginosa* Biofilms under Cystic Fibrosis Conditions. *ChemBioChem* **2021**. <https://doi.org/10.1002/cbic.202000816>.

(547) Lewenza, S. Extracellular DNA-Induced Antimicrobial Peptide Resistance Mechanisms in *Pseudomonas Aeruginosa*. *Front. Microbiol.* **2013**, *4*, 1–6. <https://doi.org/10.3389/fmicb.2013.00021>.

(548) Peng, J.; Yang, Y.; Zhao, P.; Qiu, S.; Jia, F.; Wang, J.; Liang, X.; Chaudhry, A. S.; Xu, P.; Yan, W.; Xu, Z.; Wang, K. Cu²⁺ Reduces Hemolytic Activity of the Antimicrobial Peptide HMPI and Enhances Its Trypsin Resistance. *Acta Biochim. Biophys. Sin. (Shanghai)* **2020**, *52* (6), 603–611. <https://doi.org/10.1093/abbs/gmaa043>.

(549) Neupane, K. P.; Aldous, A. R.; Kritzer, J. A. Metal-Binding and Redox Properties of Substituted Linear and Cyclic ATCUN Motifs. *J Inorg Biochem* **2014**, *139*, 65–76. <https://doi.org/10.1016/j.jinorgbio.2014.06.004>.

(550) Banks, J. L.; Kaminski, G. A.; Zhou, R.; Mainz, D. T.; Berne, B. J.; Friesner, R. A. Parametrizing a Polarizable Force Field from Ab Initio Data. I. The Fluctuating Point Charge Model. *J. Chem. Phys.* **1999**, *110* (2), 741–754. <https://doi.org/10.1063/1.478043>.

(551) Patel, S.; Brooks, C. L. CHARMM Fluctuating Charge Force Field for Proteins: I Parameterization and Application to Bulk Organic Liquid Simulations. *J. Comput. Chem.* **2004**, *25* (1), 1–15. <https://doi.org/10.1002/jcc.10355>.

(552) Patel, S.; Mackerell, A. D.; Brooks, C. L. CHARMM Fluctuating Charge Force Field for Proteins: II Protein/Solvent Properties from Molecular Dynamics Simulations Using a Nonadditive Electrostatic Model. *J. Comput. Chem.* **2004**, *25* (12), 1504–1514. <https://doi.org/10.1002/jcc.20077>.

(553) Yang, Z. Z.; Wang, J. J.; Zhao, D. X. Valence State Parameters of All Transition Metal Atoms in Metalloproteins - Development of ABEM $\sigma\pi$ Fluctuating Charge Force Field. *J. Comput. Chem.* **2014**, *35* (23), 1690–1706. <https://doi.org/10.1002/jcc.23676>.

(554) Santoro, A.; Walke, G.; Vilen, B.; Kulkarni, P. P.; Raibaut, L.; Faller, P. Low Catalytic Activity of the Cu(II)-Binding Motif (Xxx-Zzz-His; ATCUN) in Reactive Oxygen Species Production and Inhibition by the Cu(I)-Chelator BCS. *Chem. Commun.* **2018**, *54* (84), 11945–11948. <https://doi.org/10.1039/c8cc06040a>.

FOR TOC ONLY

